

2.10.8 Quarter-Scale Model Drop Test Program for the NAC-LWT Cask

2.10.8.1 Introduction

This appendix provides a detailed presentation of the Quarter-Scale Model Drop Test Program, which was carried out for confirmatory support of the analysis and licensing effort for the design qualification of the NAC-LWT cask. The analyses presented elsewhere in this report demonstrate that the NAC-LWT cask design meets all of the requirements for use in the packaging and transportation of radioactive material (10 CFR 71), especially PWR, BWR, and metallic spent-fuel rods. The test results presented in this appendix confirm the analyses and provide additional confidence that the cask design provides for the safe transport of radioactive material. This test program considered the 30-foot (9-meter) Free Drop and the 1-meter (40-in) Puncture events of the 10 CFR 71 Hypothetical Accident Conditions, but the test results also lend credence to the analyses performed for the 10 CFR 71 Normal Conditions of Transport.

2.10.8.2 Purpose

The purpose of the Quarter-Scale Model Drop Test Program was to verify that the NAC-LWT cask design satisfies the Free Drop and the Puncture requirements of 10 CFR 71.73, Hypothetical Accident Conditions; each test simulated a specific load condition. The tests verified the structural adequacy of the NAC-LWT cask packaging in: (1) the performance of its containment function, (2) the performance of the impact limiters, (3) reacting dynamic loadings, and (4) resisting puncture by a pin.

2.10.8.3 Summary

The detailed quarter-scale model of the body of the NAC-LWT cask, which was fabricated for use in this test program, is presented in NAC drawings: 315-40-30, 315-40-31 (sheets 1 through 3), and 315-40-32 (Figure 2.10.8-1 through Figure 2.10.8-3).

The details of the impact limiters, which were fabricated for this test program, are presented in NAC drawings 315-40-33 and 315-40-34 (Figure 2.10.8-4 and Figure 2.10.8-5). The full-scale cask cavity contents weight (4000 lbs) is simulated in the quarter-scale model by the steel cylinder, shown on Drawing 315-40-35 (Figure 2.10.8-6), whose weight is appropriately scaled, $W_s = (4000)/(4)^3 = 62.5$ lbs.

The model of the body of the NAC-LWT cask, which was used in the Drop Test Program, was a quarter-scale duplication of the full-scale cask in all aspects, except as described in subsequent paragraphs of this appendix. The model was fabricated of Type 304 stainless steel inner and

outer shells, upper and lower end forgings, and closure lid; the port cover was Type 17-4PH stainless steel; and the gamma shield was chemical copper lead per ASTM B29. The impact limiters were fabricated of 5052 aluminum honeycomb enclosed in 6061-T6 aluminum alloy shells. The closure lid bolts were SA-453, Grade 660 high strength alloy steel bolting material. A carbon steel tube was used to simulate the fuel basket and payload in the cask cavity.

The quarter-scale model lead gamma shield forms an annulus 1.438 inches thick and 43.75 inches long. The lead was enclosed between the 0.1875 inch thick, 3.344-inch inside diameter inner shell and the 0.28-inch thick, 7.155-inch outer diameter outer shell. The ends of the inner shell include 0.75-inch long by 0.314-inch thick transition regions. The bottom end forging of the quarter-scale model cask was 1.0 inch thick. The bottom also included a 0.75-inch thick, 5.19-inch diameter lead disk enclosed by a 0.875-inch thick end cover. The upper ring forging was 3.5625 inches thick with a machined interior to accept the closure lid. The model closure lid was 5.625 inches in diameter and 2.81 inches thick. The 12 closure lid bolts were 1/4-32 UNEF-2B \times 2 1/4 long socket head cap screws, which were selected to provide a tensile stress area equal to $1/(4)^2$ times that of the full-scale closure bolts. Since the applied impact load on the model is four times that applied to the full-scale cask, the proper bolt stress results. The port cover was a 0.748-inch outer diameter, 0.406-inch inner diameter, piston-type cylinder with an integral 0.25-inch thick, 1.125-inch diameter cover plate. The model impact limiters were quarter-size replicas of the full-scale limiters with full-strength aluminum honeycomb energy absorption material to produce the properly scaled impact loads on the model cask (3500 psi multidirectional and 1200 psi unidirectional crush strengths). The honeycomb sections' pie-shapes, joints, and bonds duplicated those of the full-scale limiters. The aluminum honeycomb of the model limiters was enclosed in 0.062-inch thick aluminum shells with epoxy-bonded joints; the model limiter attachment lugs were 0.062-inch thick aluminum alloy sheet. The model upper impact limiter had an outside diameter of 16.25 inches, a depth of 7.06 inches, an inner cup diameter of 7.22 inches, a cup depth of 3.00 inches, and four 0.75-inch \times 1.28-inch trunnion cutouts. The model lower impact limiter had an outside diameter of 15.00 inches, a depth of 7.09 inches, an inner cup diameter of 7.22 inches, and a cup depth of 3.00 inches. The model load was a steel tube 43.75 inches long with a 3.22-inch outside diameter, a 2.00-inch inside diameter, and 0.25-inch thick end plates.

The inner shell, end forgings, and the closure lid establish a model cask cavity of 44.50 inches in length and 3.344 inches in diameter. The weight of the quarter-scale model cask with impact limiters and cavity load was 860 lbs (approximately 6 percent heavier than the design weight).

Three significant differences do exist between the quarter-scale model cask body and the full-scale cask body: (1) the model does not include the neutron shield and expansion tanks; the weight of these tanks and their contents are simulated on the model by segmented steel bars

welded on the exterior surface of the outer shell; (2) the inner and outer shells of the model are Type 304 stainless steel, with a yield strength of $S_y = 30$ ksi and an ultimate strength of $S_u = 75$ ksi, while the inner and outer shells of the full-scale cask are Type XM-19 stainless steel with $S_y = 55$ ksi and $S_u = 100$ ksi; and (3) the outer shell of the model did not include the transition regions at each end, which are present on the full-scale Type XM-19 stainless steel outer shell. The use of segmented weights to simulate the neutron shield prevents the weights from contributing to the strength of the cask, and conservatively neglects the effect of the neutron shell. The impact limiter attachment lugs were 0.062-inch thick on the impact limiters and 0.037-inch thick on the cask body, while the full-scale lugs are 0.50-inch thick on both components. The quarter-scale model impact limiter joints were riveted and/or epoxied; whereas, on the full-scale model, the joints are all welded. Some other minor differences do exist between the quarter-scale model and the full-scale cask, but based on the absence of the shield/expansion tanks and the reduced strength of the inner and outer shells, the model is a conservative, fully representative replica of the full-scale cask. The differences, which do exist, are considered in detail in Section 2.10.8.4.

Prior to the start of testing, the model was instrumented with tri-axial accelerometers (one near each end of the cask body) and rosette strain gauges (a set of four, located at 90-degree intervals near the upper end, near the lower end, and at the midpoint of the body), so that a record of the model's response to the various tests could be obtained. The tests were performed at Oak Ridge National Laboratory (ORNL) in Oak Ridge, Tennessee. A detailed description of the test facility can be found in the Drop Test Facility's Information Brochure (Shappert and Box). A description of the test procedures and instrumentation is presented in Section 2.10.8.5 of this report. The test sequence followed at ORNL is summarized as follows:

- Inspect cask model.
- Perform pretest weight and geometry measurements.
- Assemble packaging for the 30-foot End Drop Test (install simulated cavity load, cask closure lid, and port cover, and attach upper impact limiter).
- Pressurize and leak test the cask cavity.
- Perform 30-foot Top End Drop (impact on lid end).
- Observe cask condition and perform leak test.
- Repeat packaging assembly and leak test for each drop.
- Perform 30-foot Top Corner Drop (15.7° from vertical).
- Perform 30-foot Side Drop (cask axis horizontal).
- Perform 30-foot Oblique Drop (cask axis 60° from vertical).
- Perform 40-inch Side Drop on puncture pin (impact at midpoint of side of cask).
- Disassemble cask model and perform final geometry measurement inspection.

This test sequence is summarized in the photographs presented in Figure 2.10.8-7 through Figure 2.10.8-31. The significant results obtained from the LWT Cask Quarter-Scale Drop Test Program are presented in Section 2.10.8.6.

The test program was very successful in confirming the structural adequacy of the NAC-LWT Spent Fuel Shipping Cask for the Hypothetical Accident Condition Free Drop and Puncture events. Based on the pre-test and post-test dimensional measurements, nearly all permanent deformation of the packaging model was limited to the impact limiters, as expected and desired. The only significant deformation of the cask body model occurred in the side puncture test, where local deformation of the outer shell and the lead shielding did occur; as designed, the outer shell was not punctured. This local deformation was fully expected and produced a very slight, local dimple in the inner shell wall (0.05 in) of the model. These local puncture deformations are of no consequence since the containment vessel and its contents are protected.

Because no deformation to the package was observed, except as previously discussed, and the containment vessel sustained essentially no deformation, leakage was not expected and did not occur. As noted in the detailed test results in Section 2.10.8.6, some experimental problems precluded actual “contained” pressure measurements before and after each test; however, leaktightness of the cavity was verified before and after each test. The test results were as expected. The results correlated well with the assumptions made and the analyses performed elsewhere in this report. An accurate detailed analysis of the cask body in the local region of the impact for the side drop puncture test is very difficult, even with state-of-the-art finite element analysis computer programs, but the observed test results confirm the adequacy of the NAC-LWT cask design. The test conservatively did not include the neutron shield shell or the higher strength Type XM-19 stainless steel inner and outer shells. Although the quarter-scaled attachment lugs were significantly undersized through a manufacturing error, the impact limiters remained in position on the cask body and performed their energy absorption function as designed for the entirety of each test. On the basis of the good agreement shown between the test results and those expected (based on analyses), and on the observed physical condition of the test model, it is concluded that this test program has confirmed the adequacy of the NAC-LWT cask design to meet the requirements of the Free Drop (30-ft) and the Puncture (40-in) events specified by 10 CFR 71.73.

2.10.8.4 Description of Quarter-Scale LWT Cask Model

Quarter-scale modeling was achieved by reducing dimensions to precisely one-fourth of the full-scale dimensions. The scaling relations are defined in Table 2.10.8-1. With the exceptions noted below, the quarter-scale model was a duplicate of the full-scale design.

1. Deviations

The items/components omitted from the quarter-scale model included the neutron shield and expansion tank shells and their contents, the rotation trunnions, and the valve ports. It was determined that omission of these items/components would have either a conservative effect, or no effect, on the test results.

2. Differences

Some modifications were made to the quarter-scale model to eliminate complex operations, to allow installation of instrumentation, and to meet scheduler concerns based on material availability. These modifications included a single external pressure port valve, a single closure lid O-ring (O-ring cross sections and thicknesses do not scale), Type 304 stainless steel inner and outer shells (Type XM19 stainless steel is not commonly available), and lifting trunnions that were not final machined. All of the bolts used in the quarter-scale model - closure lid, port cover, and impact limiter attachment - were chosen with a minimum tensile area equal (as near as practical) to $1/(4)^2 = 1/16$ of the minimum tensile area of the corresponding full-scale bolt. The cask cavity contents, the fuel basket and payload, were simulated in the quarter-scale model by an appropriately scaled steel cylinder. The weights of the rotation trunnions, the neutron shield and expansion tanks, and the shield fluid were simulated by segments of steel bar welded on the exterior surface of the outer shell. These 4.25-inch \times 2.5-inch \times 1.0-inch steel bars were spaced along the length of the model body to represent the distribution of the shield/expansion tanks and fluid, but away from the cask midpoint (Puncture Test region). The steel bars were also spaced circumferentially for load distribution and to preclude strengthening the outer shell in that direction.

In summary, the NAC-LWT cask quarter-scale model that was tested reflects all of the significant structural characteristics of the full-scale cask design, which is defined and analyzed elsewhere in this report. The quarter-scale model weight of 860 lbs, corresponding to a full-scale cask weight of $860 \times 43 = 55,040$ lbs, provided a 5.8 percent conservative margin over the 52,000-lb cask design weight used in the analyses of this report. With only one impact limiter attached for the top end and top corner drops, the model weight was 840 lbs, providing a 3.4 percent conservative margin.

2.10.8.5 Description of Test Procedures and Instrumentation

The test program for the quarter-scale model consisted of the following five drop tests:

Test No. 1	Vertical top end drop of 30 feet.
Test No. 2	Top corner drop of 30 feet at an angle of 15.7 degrees from the vertical. (At this angle, the center of gravity of the cask is directly over the edge of the cask body, which prohibits rotation of the cask on initial impact.)
Test No. 3	Side drop from a height of 30 feet.
Test No. 4	Bottom oblique drop of 30 feet at an angle of 60 degrees from the vertical.
Test No. 5	A 40-inch drop onto a pin at the mid-point side of the cask.

The tests were performed in this order so as to make the puncture test more severe. All cask drops employed an impact pad located at the ORNL facilities. The impact pad was a 600-metric-ton, reinforced concrete structure (2-inch diameter rebar). The concrete structure is a stepped pyramid arrangement with a large base and a 70-metric-ton armor plate surface (24 inches thick). The massive structure was considered to be unyielding so as to minimize any significant energy absorption by the impact surface.

2.10.8.5.1 Equipment

The ancillary equipment for drop testing the quarter-scale model included the following:

- still and normal speed photography (30 frames/second)
- high speed photography (500 frames/second)
- video recorders
- strain gauge recorders
- computerized drop test timing sequencer (DTTS).

The DTTS is a small computer, which receives a feedback message that stops the sequence leading to the drop of the cask if predetermined messages are not received from each component. When all systems are functional, the computer advances the program to the next step and will automatically fire the release mechanism that drops the cask model. One of the important checks performed by the DTTS is the continuity check of the firing circuits of the explosive release mechanism.

2.10.8.5.2 Instrumentation

The primary data to be used in the assessment of cask integrity is the strain gauge time history data obtained during the cask impact event. Nine rosette strain gauges (each rosette allowed unidirectional strains to be measured in 0/45/90 degree directions) were bonded to the cask. The locations of the strain gauges are shown in Figure 2.10.8-32. The nine rosettes were attached at three longitudinal locations. At each longitudinal location, three rosettes were placed 120 degrees apart around the circumference of the outer surface of the cask model. Such an arrangement permitted the maximum bending stresses to be determined, as well as, the

maximum plastic strains observed during the tests. The strain gauges employed in the test had a rise time of 50 kHz, which would enable the strain gauge to track the high strain rates accompanying the impact. To ensure proper operation of the strain gauges, positive and negative calibrations of the strain gauges were performed prior to the drop. These calibrations are retained with the strain time histories on FM tape.

2.10.8.5.3 Drop Test Sequence

This section describes the test procedures used for each time the cask was dropped. ORNL personnel performed all tasks related to instrumentation and the actual sequence leading up to the drop.

1. Cask Preparation

- Install the model cask lid using a new cask lid O-ring. The O-ring is inspected for defects prior to installation.
- Install the port cover on the model cask using a new O-ring for the port cover lid. The O-ring is inspected for defects prior to installation.
- Verify the lid and port cover seals by pressurizing the cavity to 30 (+5/-0) psig. Observe the cavity pressure over a 10-minute period to ensure leaktightness.
- Attach limiters to the model cask.

2. Performing the Drop Test

- Check umbilical cord connection to data recorders.
- Ensure safety of cask hook assembly prior to lift and correct angle of orientation of the cask.
- Final check to ascertain if all systems are ready for the drop.
- Turn on the recorders for the strain gauges.
- Initiate the 10-second countdown in preparation of the drop.
- At the 5-second mark, start high speed (500 frames/second) photography and normal speed photography.
- When the countdown reaches zero, energize the explosive mechanism.

When the explosive mechanism fragments, the nut and bolt assembly restraining the cask in the hook allows the hook to open, which allows the cask to initiate the fall unimpeded.

2.10.8.6 Detailed Test Results

Data obtained from the tests consists of both qualitative information with respect to observations about the cask and the limiter and quantitative data obtained from the recorders. The data for each test to be presented consists of:

- Impact limiter deformation.
- Strain gauge results and stress calculations (for the end drop and side drop only).
- Observations of the cask and attachments.

The strain gauge data is only presented for the end drop and the side drop since the loads developed in those tests are the most severe from an overall structural consideration. The end drop corresponds to the maximum axial loading condition, while the side drop developed the maximum lateral loading on the overall cask body. The puncture test involves larger strains, but only on a localized area at the point of impact. The amount of energy available for the puncture impact is one-ninth of the energy for the 30-foot drop, which limits the amount of the lateral load that can be generated.

2.10.8.6.1 Top End Drop Test

Impact Limiter Deformation Data

Essentially all deformation of the impact limiter occurred at the interface of the cask body outside diameter and the limiter inside diameter (Figure 2.10.8-11 and Figure 2.10.8-12). The cask body moved into the limiter shearing and crushing the aluminum honeycomb at the 7.2-inch diameter to an average depth of 1.2 inches. There was some slight variation of the crush depth around the perimeter of the cask body. This is confirmed by the slight tilt of the cask body after the impact as shown in Figure 2.10.8-10. There was some hoop expansion of the top limiter near the surface of impact, but it was minimal since the limiter shell did not show any signs of tearing (Figure 2.10.8-12). The 1.2-inch crush corresponded to an overall crush strain of 33 percent. The soft pad of the 1200 psi crush strength material compressed completely and became solid as expected, since it is designed for the 1-foot drop (Note that the soft pad was changed to 250 psi material since the tests showed that the soft pad is backed up by the harder impact limiter material over its entire diameter). It was also observed that the attachment lugs for the limiter failed; however, once the limiter is engaged in the crushing action, the lugs do not provide additional functionality in the end drop condition.

Strain Gauge Data

Strain gauge time histories for the end drop at the midpoint locations are shown in Figure 2.10.8-33 through Figure 2.10.8-35. The corresponding location on the circumference is shown in Figure 2.10.8-32. The maximum axial strain observed in the test was 560 microstrains. This value is approximately 25 percent larger than the maximums (450 microstrains) recorded on the other two channels, indicating some amount of unequal loading due to variation of the axial stress wave propagation in the cask body. Because of the orientation of the gauges, a positive value in the graphs is associated with a compressive strain. This was as expected. By using elastic properties for the cask body from NUREG/CR-0481, the corresponding axial stress is E (modulus of elasticity) times the strain value, which gives:

$$\begin{aligned}\sigma &= (28.3 \times 10^3)(560 \times 10^{-6}) \\ &= 15.8 \text{ ksi} < \text{yield strength.}\end{aligned}$$

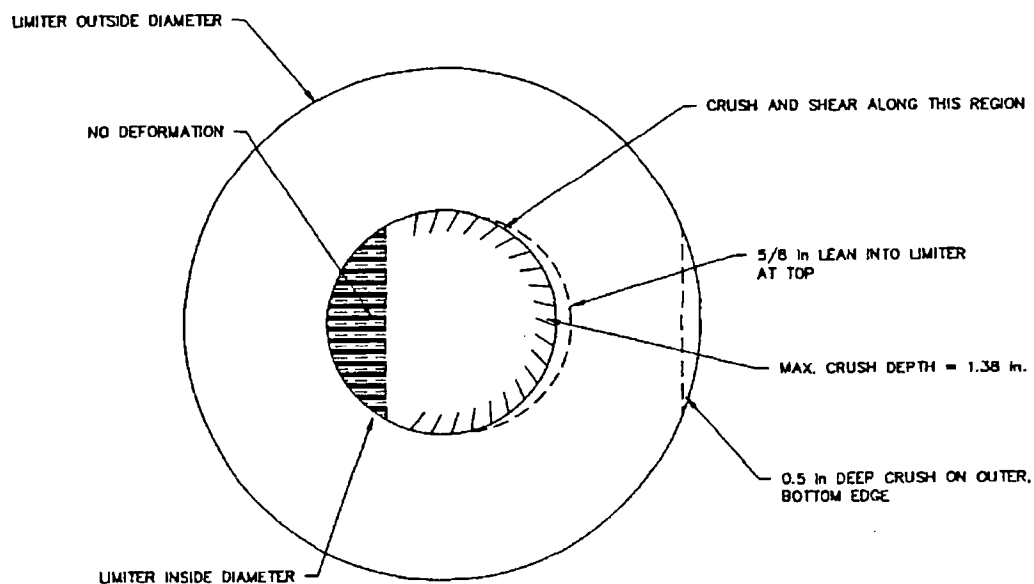
Test Observations

As the limiter was driven onto the cask, the test valve used to pressurize the interior was broken off, which prevented the pressure from being measured after the test. A new valve was installed and the cavity was pressurized to 30 psig and was maintained to determine if the cask containment boundary was damaged. There was no measurable pressure loss. The loss of this valve has no implications for the full-scale cask, since the full-scale version does not have this valve.

2.10.8.6.2 Top Corner Drop Test

Impact Limiter Deformation

The corner drop did not produce any significant rotation of the cask about the surface of impact as observed in the high speed photography and by the final upright position of the cask. The final position of the cask after the drop is shown in Figure 2.10.8-15. The crushing of the limiter occurred as in the end drop. The shearing at the outer diameter of the cask is supported by Figure 2.10.8-16. The amount of crush and the distribution of the crush are shown as follows.



Limiter Deformation for the Top Corner Drop

The maximum amount of crush was determined to be 1.38 inches, which is a strain of 38 percent. It was also observed that the attachment lugs for the limiter failed; however, once the limiter is engaged in the crushing action, the lugs do not provide additional functionality in the corner drop condition.

Test Observations

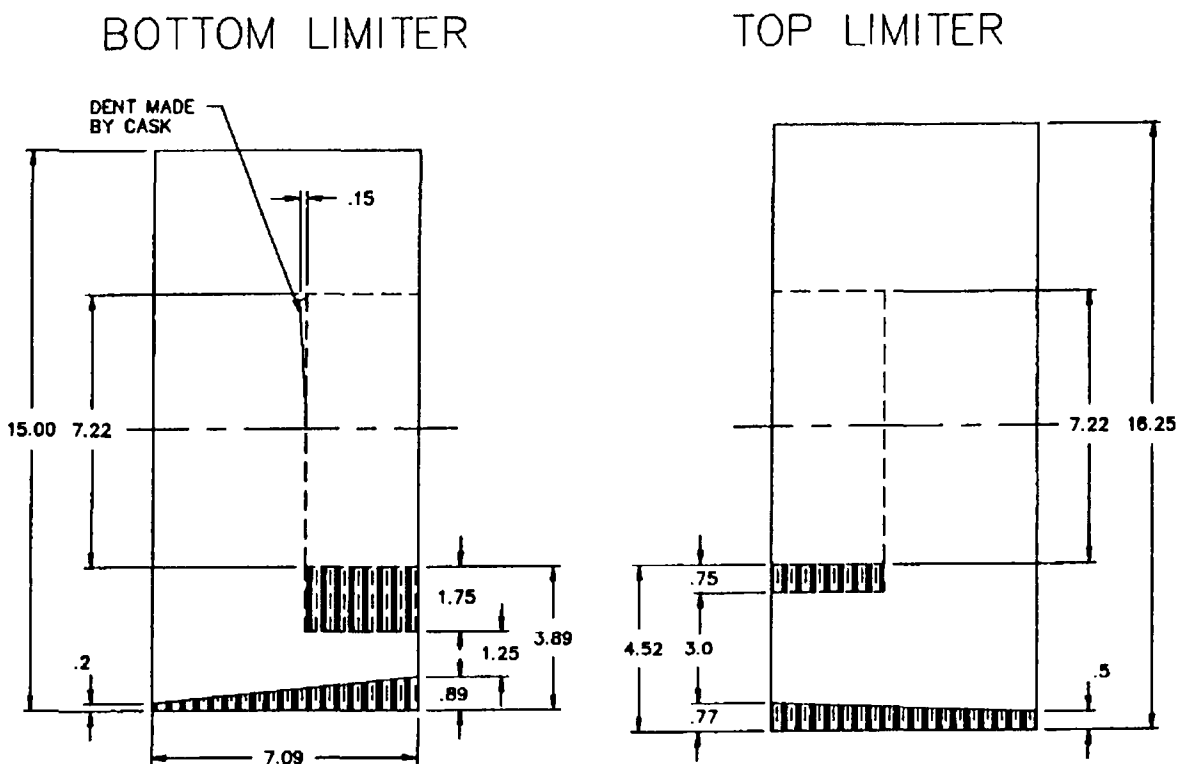
During the impact event, the coupling connected to the valve used to pressurize the interior was loosened, which prevented the pressure from being measured after the test. The coupling was tightened and the cavity was pressurized to 29.2 psig and was maintained to determine if the cask containment boundary was damaged. There was no measurable pressure loss.

Tethers were attached to the cask to prevent a tip-over after the impact event. In observing the photographic results, the tethers also responded to the fall by vibrating in an oscillatory manner. This additional oscillating load allowed the cask to incur a secondary impact, which would not occur for an untethered cask with an impact limiter attached over each end.

2.10.8.6.3 Side Drop Test

Impact Limiter Deformation

Limiters in the side drop condition were crushed only in regions that are backed by the cask body. The amount of crush and the variation of the crush for the top and bottom limiters for the side drop are described as follows.



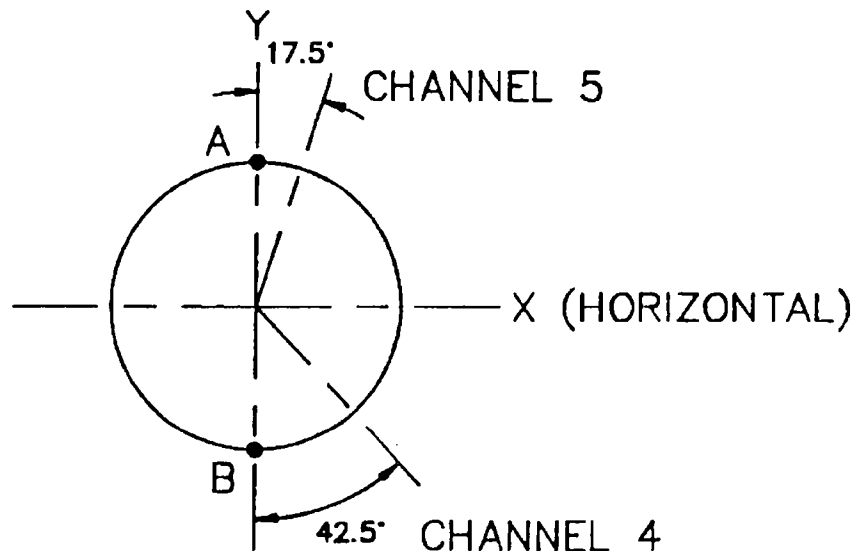
ALL DIMENSIONS ARE IN INCHES
Limiter Deformation for the Side Drop

The uniform crushed surface of the limiters resulting from the side drop can be seen in Figure 2.10.8-19, Figure 2.10.8-20 and Figure 2.10.8-21. Note that the surface is uniform in both the axial direction and the lateral direction. The maximum strain for the side drop was 68 percent for the bottom limiter and 34 percent for the top limiter. The average strains under the backed areas were 30 percent for the top limiter and 59 percent for the bottom limiter. The larger strains correspond to the bottom limiter, since it was significantly smaller than the top limiter.

As shown in the previous sketch, both limiters showed evidence of a small rotation relative to the cask (Figure 2.10.8-17). This accounts for the greater deformation of the circumferential surface along the inner face of the impact limiter and the smaller compression on the outer diameter of the cask. The limiter shell also experienced large deformations that had no effect on the limiter performance.

Strain Gauge Data

Strain gauge time histories for the side drop at the midpoint locations are shown in Figure 2.10.8-36 through Figure 2.10.8-38. The corresponding locations on the circumference are shown in Figure 2.10.8-32. The maximum axial strain observed in the test was 2500 microstrains, which also resulted in a permanent set of 750 microstrains. Due to the manner in which the cask is loaded, the maximum strains occurred at the midpoint. The strains from channels 4 and 5 can be used to estimate the maximum stresses and strains in the side drop test.



Definition of Channel Orientation for the Side Drop

The maximum strains are expected to occur at points A and B as shown above. Assuming that the cask cross-section remains plane, the values for the maximum strain and plastic strain at

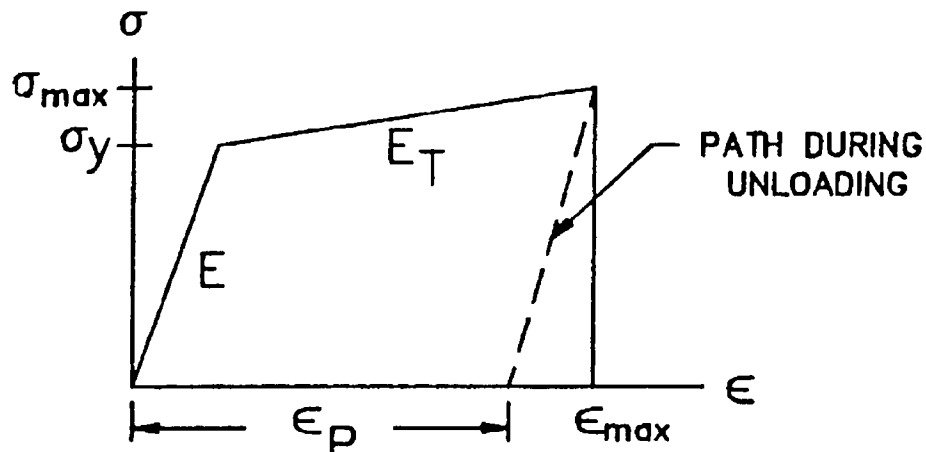
locations A and B can be obtained by factoring the test data by $1/\cos(17.5^\circ)$ and $1/\cos(42.5^\circ)$, respectively.

To estimate the σ_y and σ_{max} , the stress strain curve for Type 304 stainless steel is required. The static values for Type 304 stainless steel were extracted from NUREG/CR-0481 as:

$$E = 28.3 \times 10^3 \text{ ksi} \quad (75^\circ)$$

$$E_T = 370 \text{ ksi}$$

This assumes that the stress strain curve takes the form shown as follows.



Typical Stress Strain Curve for Type 304 Stainless Steel

The plastic strain recorded from the strain gauge corresponds to ϵ_p . The relations for the stress and strain can be written as:

$$\epsilon_{max} = \frac{\sigma_y}{E} + \epsilon_p \quad (1)$$

$$\sigma_{max} = \sigma_y + E_T (\epsilon_p) \quad (2)$$

By equation (1)

$$\sigma_y = (\epsilon_{max} - \epsilon_p)E \quad (3)$$

The calculated maximum strains from the strain gauge data are as follows.

Channel	Strain Gauge		Extrapolated		σ_Y (ksi)	σ_{max} (ksi)
	ϵ_{max}	ϵ_p	ϵ_{max}	ϵ_p		
	(microstrain)		(microstrain)			
4	2200	1000	2984	1356	46.1	46.6
5	2500	750	2621	786	51.9	52.2

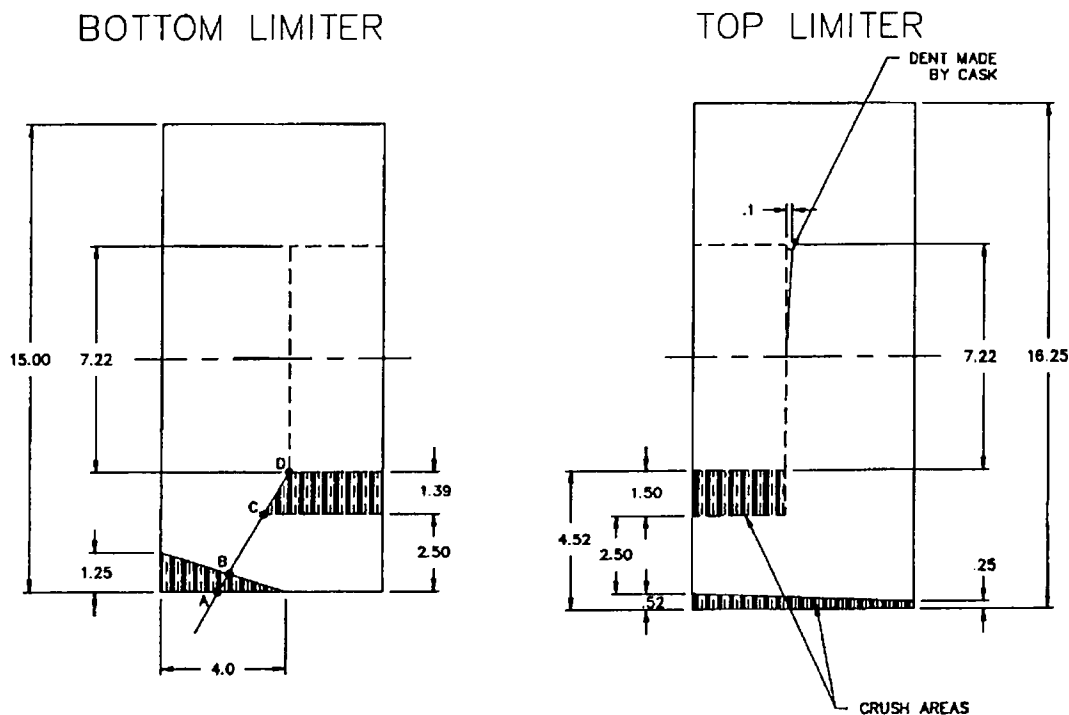
Test Observations

In reviewing the high speed photographic results, the side drop actually represents a drop angle that is the most conducive to the slapdown effect. The drop is actually estimated to be 80 degrees rather than 90 degrees. The pressure in the cask was checked prior to the test and afterwards. It was found to be 30.4 psig. This indicates that pressure containment was maintained during the impact.

2.10.8.6.4 Bottom Oblique Drop Test

Impact Limiter Deformation

In the 60-degree oblique drop test, the bottom impact limiter is initially crushed at the corner as shown below. During the deceleration, the cask body also initiates crushing at the inner surface of the limiter. The upper limiter results in a pattern similar to the side drop in which crushing occurs at both the inner surface of the limiter and at the plane of impact. The maximum crush strains for the bottom and top limiters were 60.7 percent and 45 percent, respectively. The strain direction for the 60.7 percent strain is shown as follows.



ALL DIMENSIONS ARE IN INCHES
Limiter Deformation for Oblique (60°) Drop

The following equation was used to determine the crush strain for the impact limiter as shown.

$$\text{Crush strain} + \frac{AB + CD}{AD} = 60.7 \text{ percent}$$

where:

$$CD = 1.39/\cos(30) = 1.605 \text{ inches}$$

$$AD = (1.39 + 2.50)/\cos(30) = 4.492 \text{ inches}$$

$$AB - AD[\sin(30)][\sin(30)] = 1.123 \text{ inches}$$

Test Observations

The pressure measurement indicated that the cavity pressure did not change as a result of the oblique drop test. Cavity pressure was measured to be 30.2 psig before and after the test.

2.10.8.6.5 One-Meter Puncture Test

As a result of dropping the cask body onto the steel pin, the containment of the cask body was not violated. This was confirmed by the pressure measurements before and after the test. All permanent strain was local to the region of impact of the pin. The resulting shape of the pin impact is shown in Figure 2.10.8-30 and Figure 2.10.8-31. The maximum deformation of the outer shell was 0.5 inch deep and a localized depression of 0.05 inch occurred in the inner shell. Note that the pin puncture impact was directed against the portion of the outer shell that was stressed most severely in the 30-foot drop tests to show that the outer shell retained its puncture capability after the dynamic stress of the 30-foot fall impact.

2.10.8.7 Metrology Results

Prior to the drop tests, the NAC-LWT cask was submitted to the ORNL Plant and Equipment Division to obtain metrology data that would be compared after completion of the drop tests. The cask model was placed on a certified flat surface. The inner diameter was measured in a vertical direction and in a horizontal direction at seven locations starting at the front of the cask cavity and proceeding to the rear of the cavity. The casks' outer diameter measurements were taken at three different locations starting just inside the circumferential welds at either end and in the middle. In addition, external longitudinal measurements were made starting at the open end of the cask and ending at the back end of the external blocks used to simulate the weight of the neutron shield. These measurements, taken before the tests, are given in inches and are shown in Table 2.10.8-2 through Table 2.10.8-4. The same measurements were taken after the last drop test was completed. These values are given in Table 2.10.8-5 through Table 2.10.8-7.

Changes to the inner diameter as a result of the four 30-foot drops onto a solid surface and one 1-meter drop onto a punch can be determined by comparing Table 2.10.8-2 and Table 2.10.8-5. The changes are very small, less than about 0.005 inch at every measured location except in the

cask middle. At the midpoint, some 26 inches from the closure, the changes to the vertical and horizontal diameters were -0.0568 inch and +0.0490 inch, respectively, due to the action of the punch in the 1-meter puncture drop. The change in vertical diameter measurement is equivalent to less than a quarter inch on the full-scale cask.

Changes to the outer diameter measurements as a result of the tests can be determined by comparing Table 2.10.8-3 and Table 2.10.8-6. As before, these dimensions changed little, less than about 0.006 inch at every measured location except in the cask middle. At the midpoint, the vertical change was approximately -0.5 inch, equivalent to 2 inches in a full-scale cask. The change in the horizontal diameter at that location was +0.02 inch, equivalent to less than 0.1 inch in a full-scale cask. These changes were again due to the action of the punch on the outer cask shell in the 1-meter puncture drop.

Changes to the cask length measurements as a result of the tests can be determined by comparing Table 2.10.8-4 and Table 2.10.8-7. With the exception of two data points, all after-drop measurements were within 0.031 (1/32) inch of the beginning data points. This is less than a quarter inch deviation on the full-scale cask. The two exceptions include a 0.14 inch change in length measured at the 180-degree point on the first block set, and at the 270 degree point on the second block set. These exceptions are attributed to error in replicating the exact measuring locations as opposed to a real change in length, since other measurements, even at that block set, showed little or no change.

2.10.8.8 Discussion of Test Results

As previously noted, pre- and post-test measurements showed that nearly all permanent deformation of the packaging model was limited to the impact limiters. The only significant exception to this occurred for the side puncture test, where local deformation of the outer shell and the lead shielding did occur, but the outer shell was not punctured. The local deformation was as expected and produced only a very slight, local dimple in the inner shell wall (0.05 inch).

Before each test, the model closure lid was installed with a new O-ring and with a bolt torque of 44 inch-pounds, which was calculated to produce a bolt tensile stress equal to one-half the yield strength of the bolt material (same as full-scale criteria). This bolt load exceeds the calculated maximum bolt load for the accident conditions. The model cavity was pressurized to 30 psig and held with a gauge reading verifying that leakage was not occurring. After each test, the leaktightness of the cavity was checked. For the side drop, the oblique drop, and the side puncture drop, the pressure gauge provided this verification; for the end drop and the corner drop, verification was provided by repressurizing the cavity and maintaining a gauge reading after repairing the external pressure test valve. The unprotected external pressure test valve was sheared off during the end drop as the model body moved into the upper impact limiter during

the impact. During the corner drop, the valve piping loosened due to shock loading. These occurrences are not a concern in the full-scale cask because the valve ports are protectively recessed in the upper ring forging, where containment is provided by double O-rings in the port covers. Thus, it is concluded that the structural adequacy of the containment vessel is confirmed.

The aluminum honeycomb materials of the model impact limiters were identical in all aspects to those of the full-scale cask. Since the crush area of the limiters and the stress area of the body of the model are reduced by the $(\text{scale factor})^2 = 1/16$, the impact acceleration is $1/(\text{scale factor}) = 4$ times that of the full-scale cask and the crush deformation is the $(\text{scale factor}) = (1/4)$ times that of the full-scale cask. The measured crush deformations of the model limiters were essentially the same as the values scaled from the full-size impact limiter analyses of this report. Visual observation of the model impact limiter deformations confirmed that for every cask drop orientation, only the “backed” areas of the limiters are effective in absorbing the impact energy. This result supports the “backed” area principle established by previous testing programs and confirms the impact limiter analyses performed elsewhere in this report. As previously described, the model impact limiter attachment lugs were undersized and failed. The four 30-foot drop tests confirmed the analysis results for each cask orientation, which determined that the impact limiters will remain in position on the cask during the impact(s), whether or not there are attachment lugs present; the attachment lugs retain the impact limiters on the cask body until an impact occurs. Thus, it is concluded that the structural and functional adequacy of the NAC-LWT cask impact limiters is confirmed.

The report analyses were confirmed, as the cask body sustained a 30-foot drop test for each of the four drop orientations without incurring any measurable permanent deformation. Since the model did not include the neutron shield and expansion tank shells, the model is conservative. Additionally, the model inner and outer shells are Type 304 stainless steel ($S_u = 75$ ksi, $S_y = 30$ ksi), while the full-scale inner and outer shells are Type XM-19 stainless steel ($S_u = 100$ ksi, $S_y = 55$ ksi). Therefore, it is concluded that the structural adequacy of the NAC-LWT cask body is confirmed for the 30-foot Free Drop Hypothetical Accident Condition.

Based on visual observation of the model tests; i.e., the side drop and the 60-degree oblique drop, and inspection of the crushed region of the model limiters, no “slapdown”/rebound effects were apparent. This confirms the results of the “slapdown” evaluation analysis found in Section 2.10.4.

The side puncture test was performed last in the testing sequence because some local deformation of the outer shell was expected. Since an accurate, reliable analysis of the local puncture region of the cask body is very difficult, an empirical relationship based on testing of lead-backed shells was used to establish the outer shell thickness. The outer shell of the model cask body incurred significant permanent deformation in a very local region around the point of

impact during the side puncture test. As expected, the outer shell was not penetrated. Based on post-test measurements, a very slight, local deformation (0.05 inch) of the inner shell occurred at the midpoint. Since the full-scale cask will include a well-supported 0.25-inch thick neutron shield tank and the stronger, Type XM-19 stainless steel inner and outer shells, the deformation of the outer shell will be substantially reduced and the deformation of the inner shell will be eliminated. Furthermore, the isolation of the inner shell provided by the lead, as it diffuses the shock of a pin puncture, will be enhanced by the factor of four increase in lead thickness of the full-size cask. It is concluded that the side puncture test has confirmed the adequacy of the puncture protection of the NAC-LWT cask and the design criteria and methodology of this report.

In summary, the detailed results of the Quarter-Scale Model Drop Test Program for the NAC-LWT cask described in this appendix, confirm the analyses found elsewhere in this report and the structural adequacy of the cask design for the Free Drop and Puncture events specified by the Hypothetical Accident Conditions of 10 CFR 71.73.

2.10.8.9 Post-Test Revisions

As discussed in prior paragraphs of this appendix, the impact limiter attachment lugs and bolts (cask and limiter) failed during some of the 30-foot drop tests without any effect on the protection of the cask provided by the impact limiters. The attachment lug thickness on the quarter-scale model impact limiters was 0.062 inch (0.25/4). The actual thickness of the impact limiter attachment lugs on the model cask body was 0.037 inch due to a fabrication error (the lug thickness was designed to be $0.25/4 = 0.062$ inch). The model limiter attachment bolts, No. 4-40 NC, were selected to have a cross-sectional area equal to one-fourth that of the full-scale bolts. After the initial drop test (30-foot end drop), the 0.037-inch thick limiter attachment lugs on the model cask body were replaced with 0.125-inch thick lugs and no subsequent failures of those lugs occurred during the ensuing drop tests. Thus, the full-scale impact limiter attachment lug design was revised to include 0.50-inch (0.125×4) thick lugs on both the cask body and the impact limiters along with 0.50-inch diameter attachment pins to alleviate concerns about their adequacy.

The purpose of the aluminum impact limiter shell is to provide a sealed container unit for the aluminum honeycomb energy absorbing material since the energy absorption capability of the shell is negligible; a 0.062-inch thickness was selected for the shell of the model impact limiters as the minimum thickness desirable for fabrication. Overlapped and epoxyed joints were used in the model impact limiters, since long-term sealing was not a concern. Because some of the model impact limiters split open at one or more joints during the crushing phase of some of the

drop tests, the full-scale impact limiter design was revised to include 0.125-inch thick aluminum shells with groove-welded joints all around (same as the NLI 1/2 cask.)

Examination of the model impact limiter following the 30-foot top end drop test showed that the 0.38-inch thick layer of lower strength (1,200 psi crush strength) unidirectional honeycomb located at the outer end of the impact limiter was crushed over the full diameter of the model impact limiter. This crushing resulted because the lower strength layer of honeycomb was effectively “backed” by the 3,500 psi crush strength multidirectional honeycomb, which makes up the remainder of the model impact limiter. The 3,500 psi crush strength honeycomb was not crushed over the full model impact limiter diameter; it only crushed over the diameter of the model cask body on the inside of the impact limiter directly under the model cask body. Thus, the calculated maximum design impact force for the 30-foot end drop is not affected by the crushing behavior of the lower strength layer of honeycomb, since that force was calculated based on the “backed” area of the cask body diameter. The purpose of the lower strength layer of honeycomb in the impact limiter is to control the g load applied to the cask during a 1-foot drop. Since the 1,200 psi crush strength of the lower strength honeycomb layer was designed based on the “backed” area of the cask body only, the design crush strength of that honeycomb layer was revised to 250 psi to account for the effective “backed” area of the full diameter of the impact limiter: average $P_{\text{new}} = (1200)(D_{\text{body}}^2 / D_{\text{Limiter}}^2) = 250$ psi, where $D_{\text{body}} = 7.155$ inches and $D_{\text{Limiter}} = 16.25$ inches for the quarter-scale model upper limiter and $D_{\text{Limiter}} = 15.00$ inches for the quarter-scale model lower limiter. Thus, the design impact forces for the 1-foot end drops that are used in this report remain unchanged.

Figure 2.10.8-1 Drawing of Quarter-Scale Model

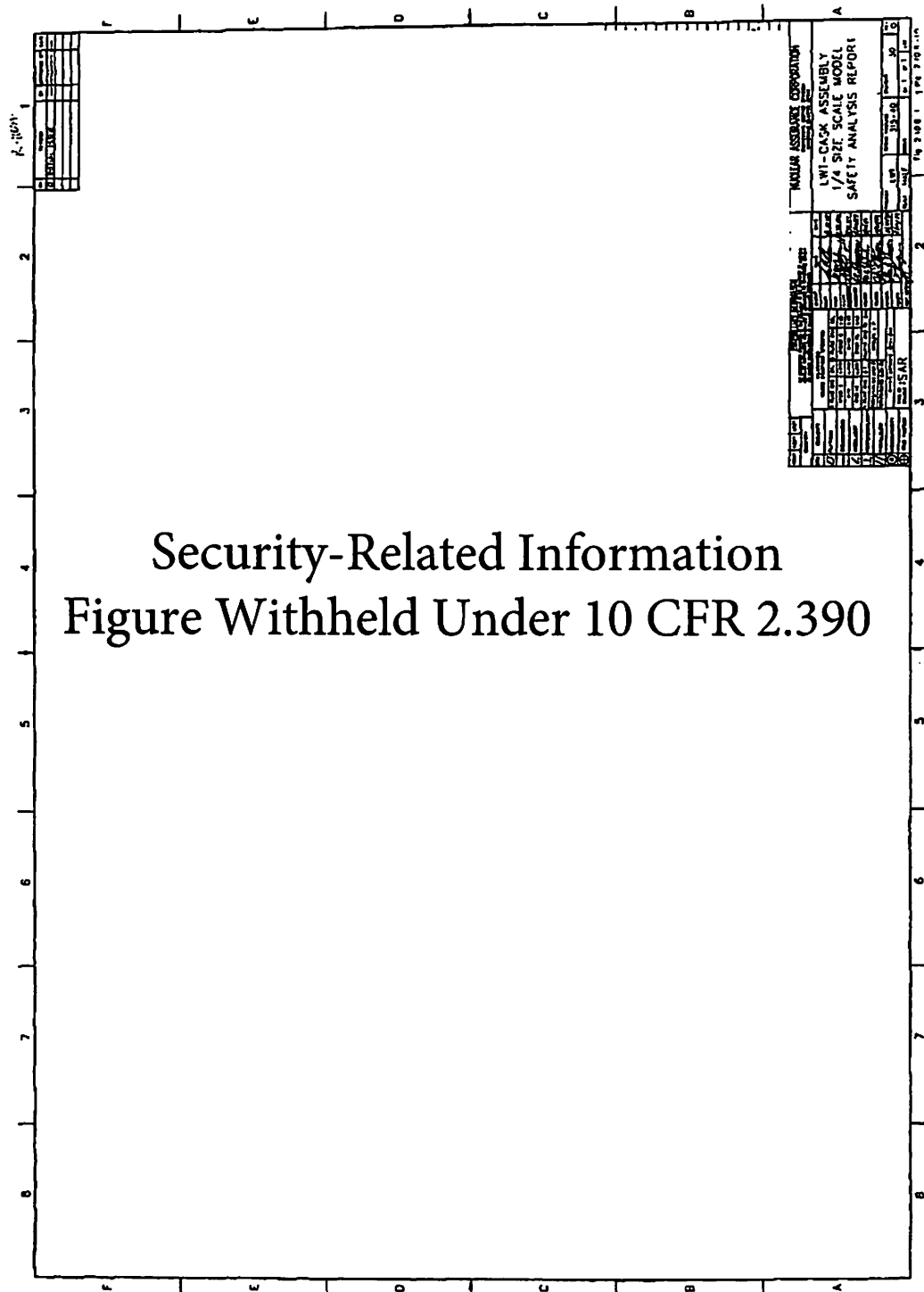


Figure 2.10.8-2 Drawing of Model Body

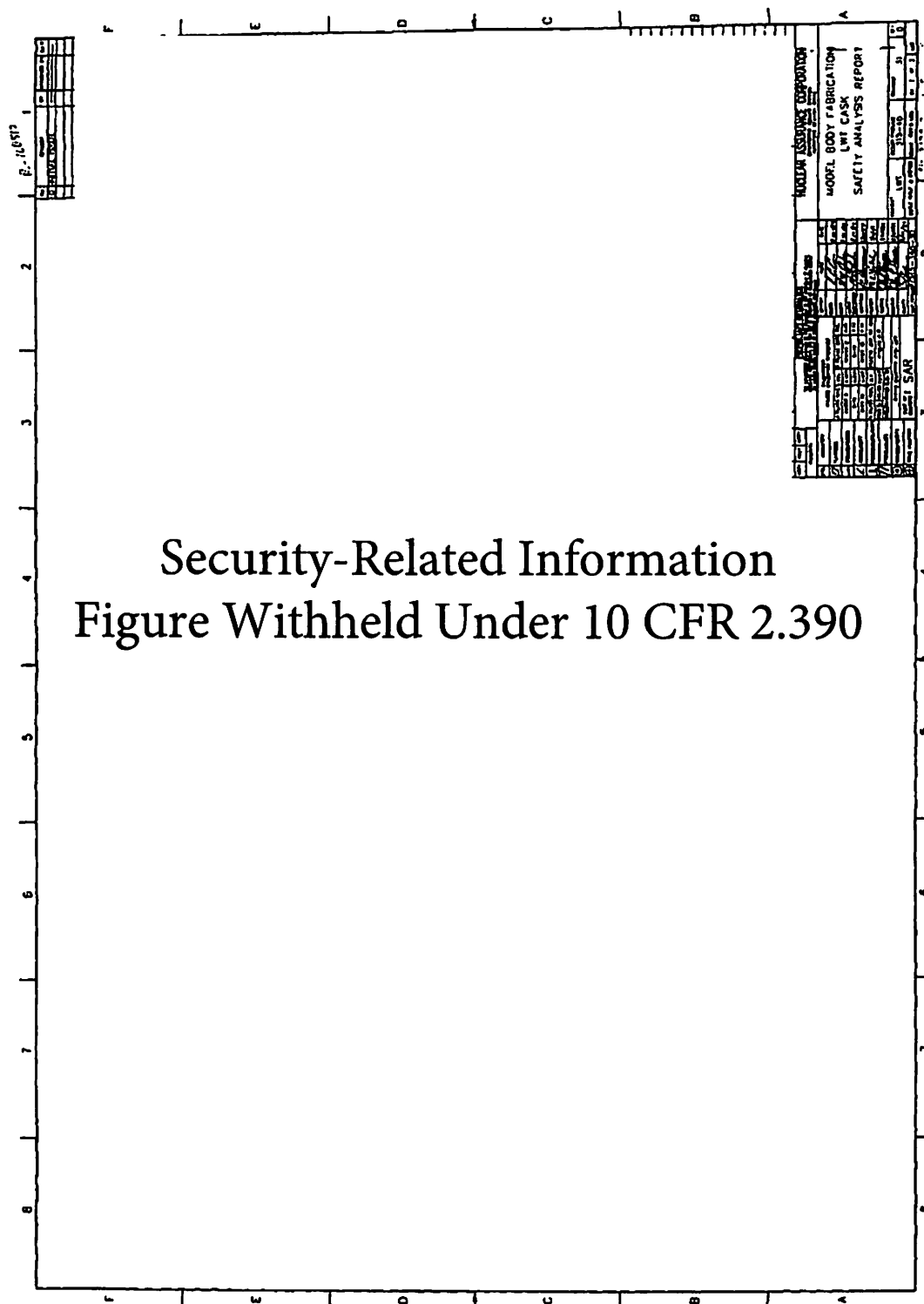


Figure 2.10.8-2 Drawing of Model Body(continued)

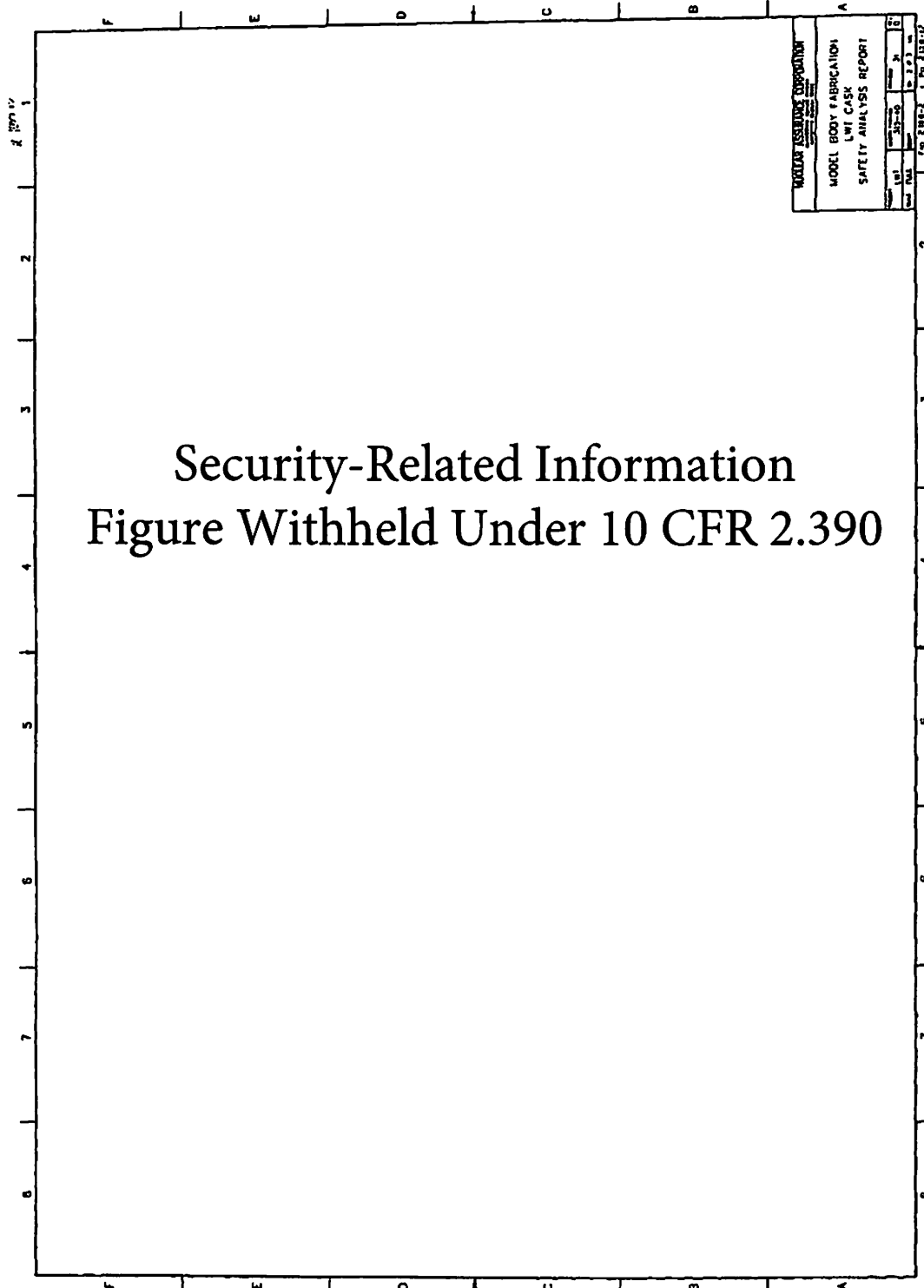


Figure 2.10.8-2 Drawing of Model Body (continued)

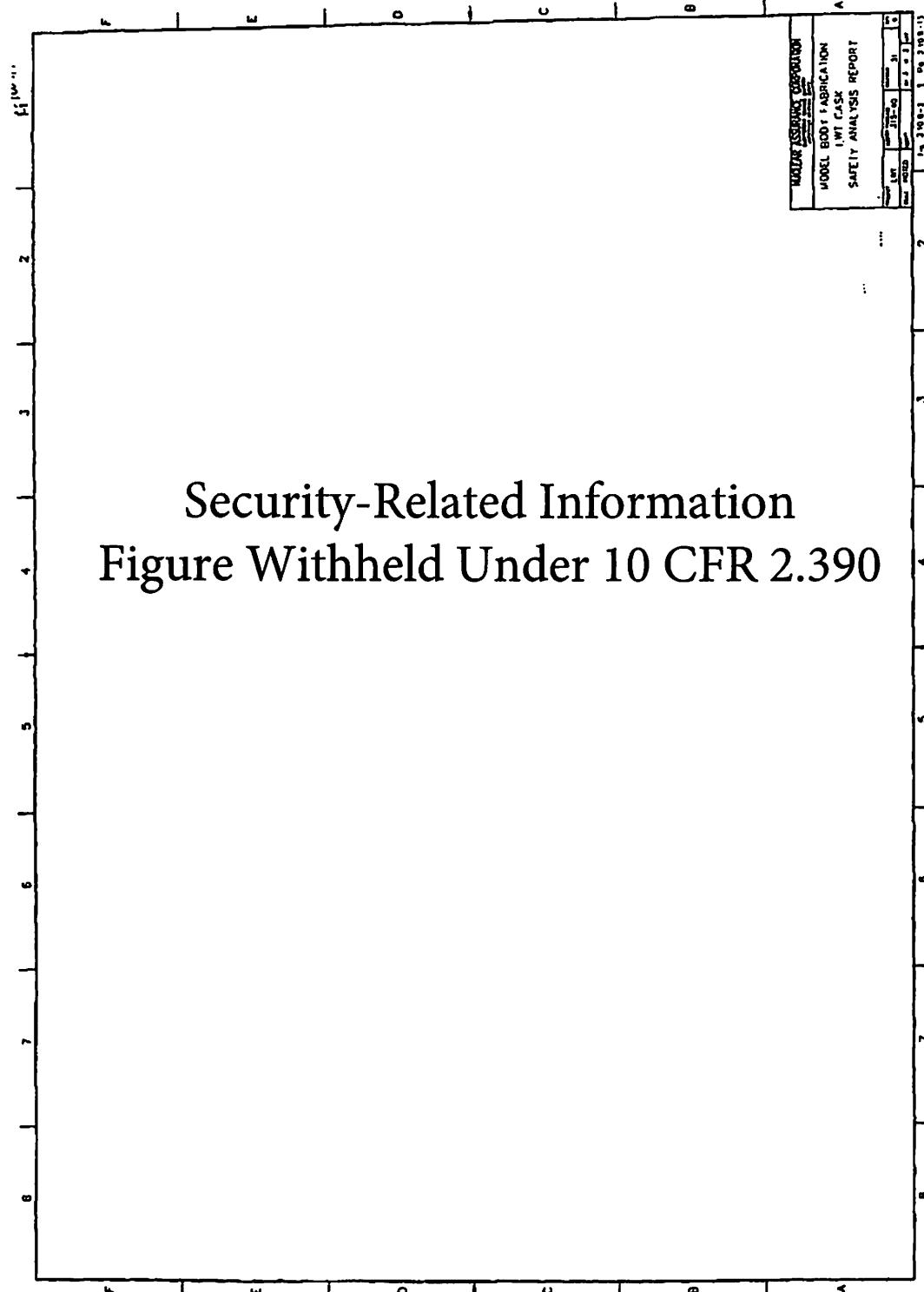
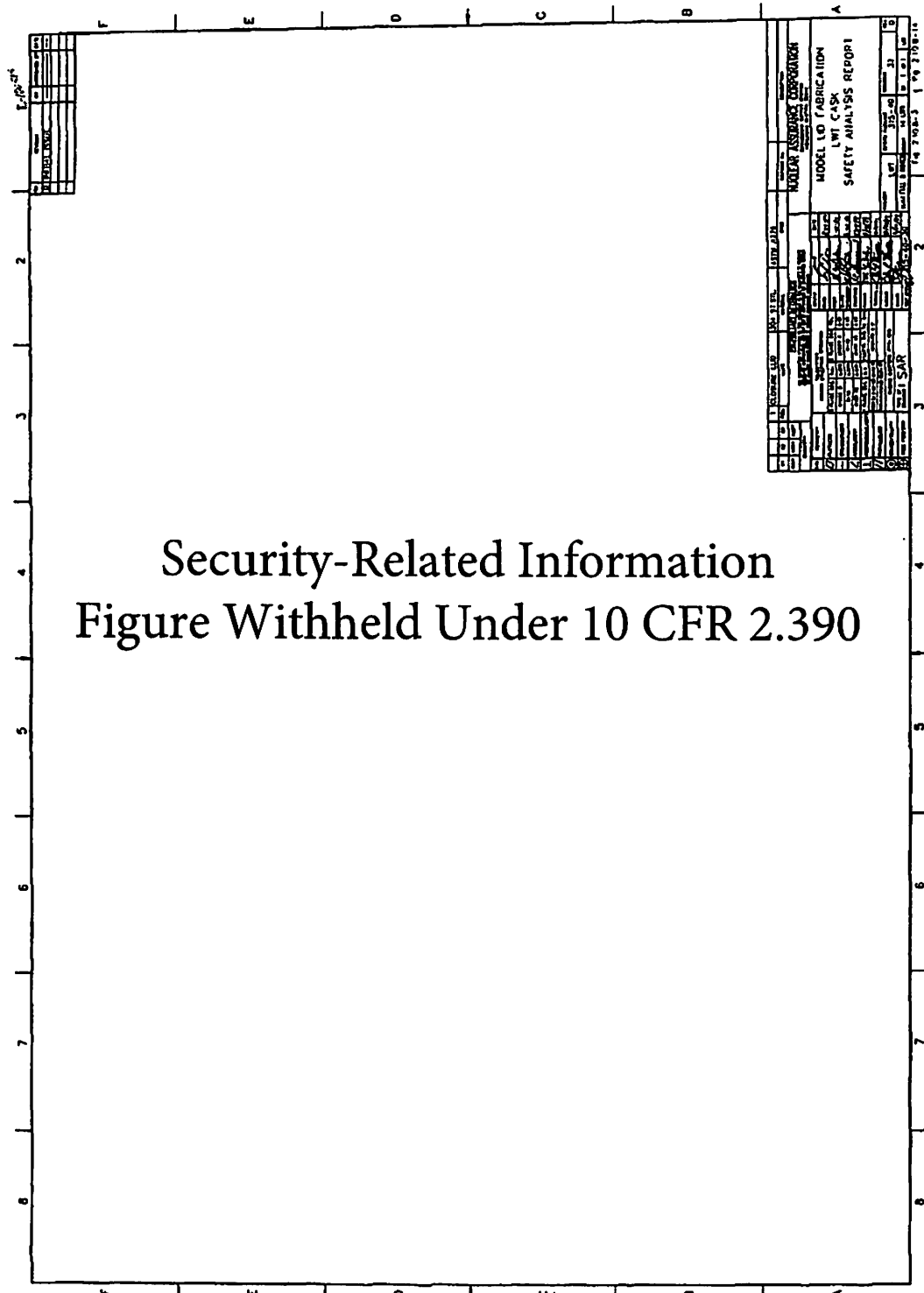


Figure 2.10.8-3 Drawing of Model Lid



Security-Related Information
Figure Withheld Under 10 CFR 2.390

Figure 2.10.8-5 Drawing of Model Lower Impact Limiter

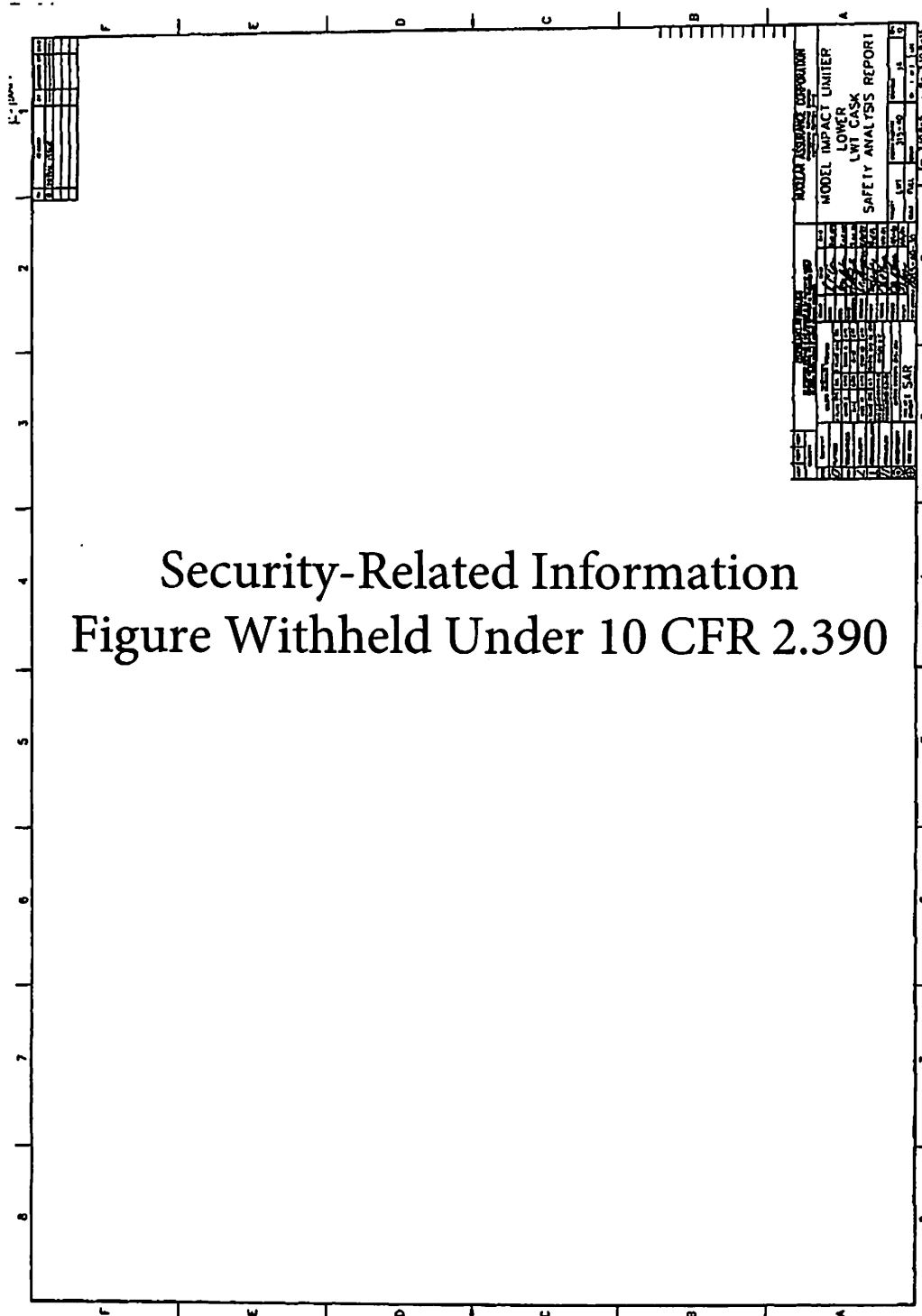


Figure 2.10.8-6 Drawing of Model Simulated Cask Contents

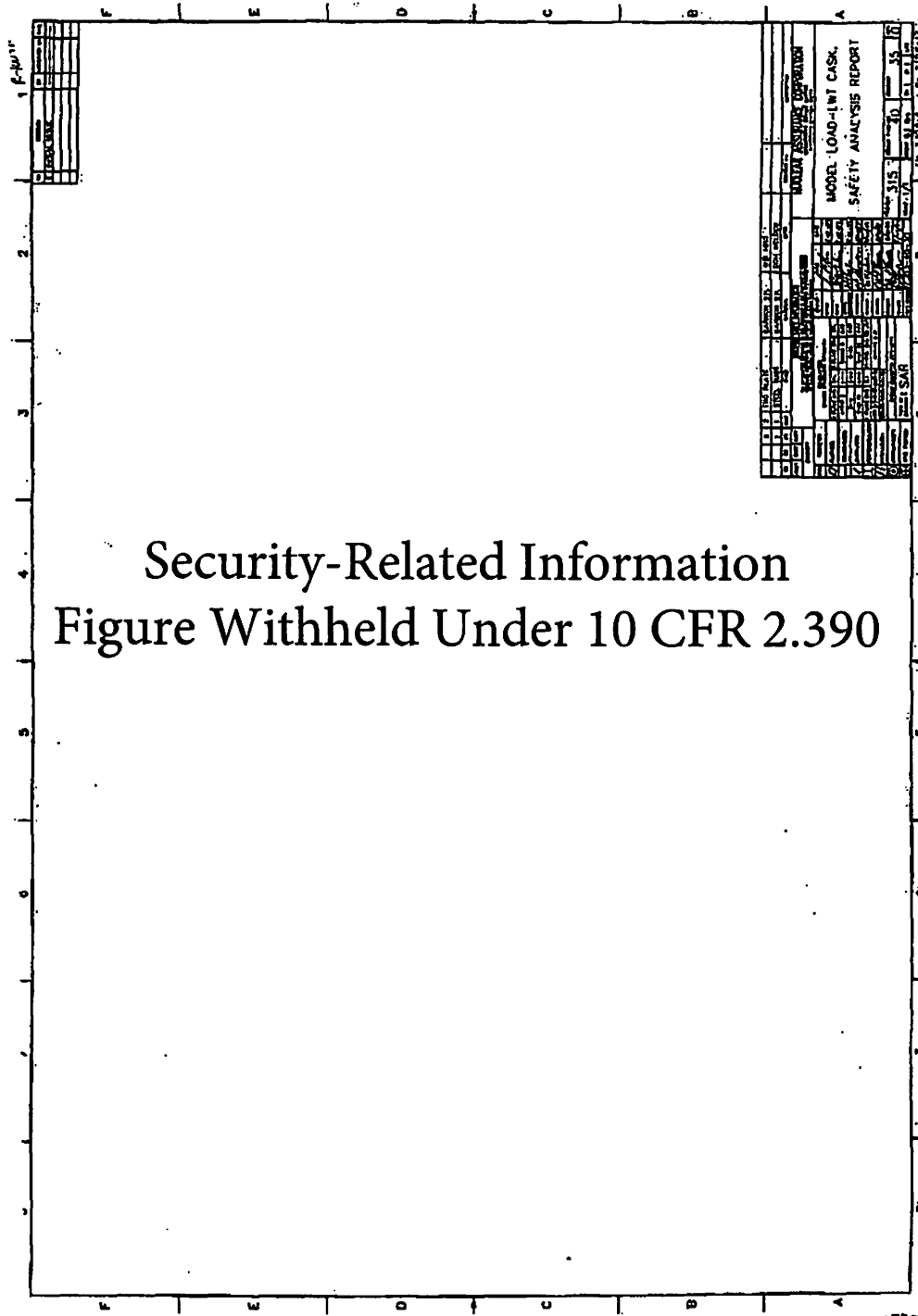


Figure 2.10.8-7 Quarter-Scale Model

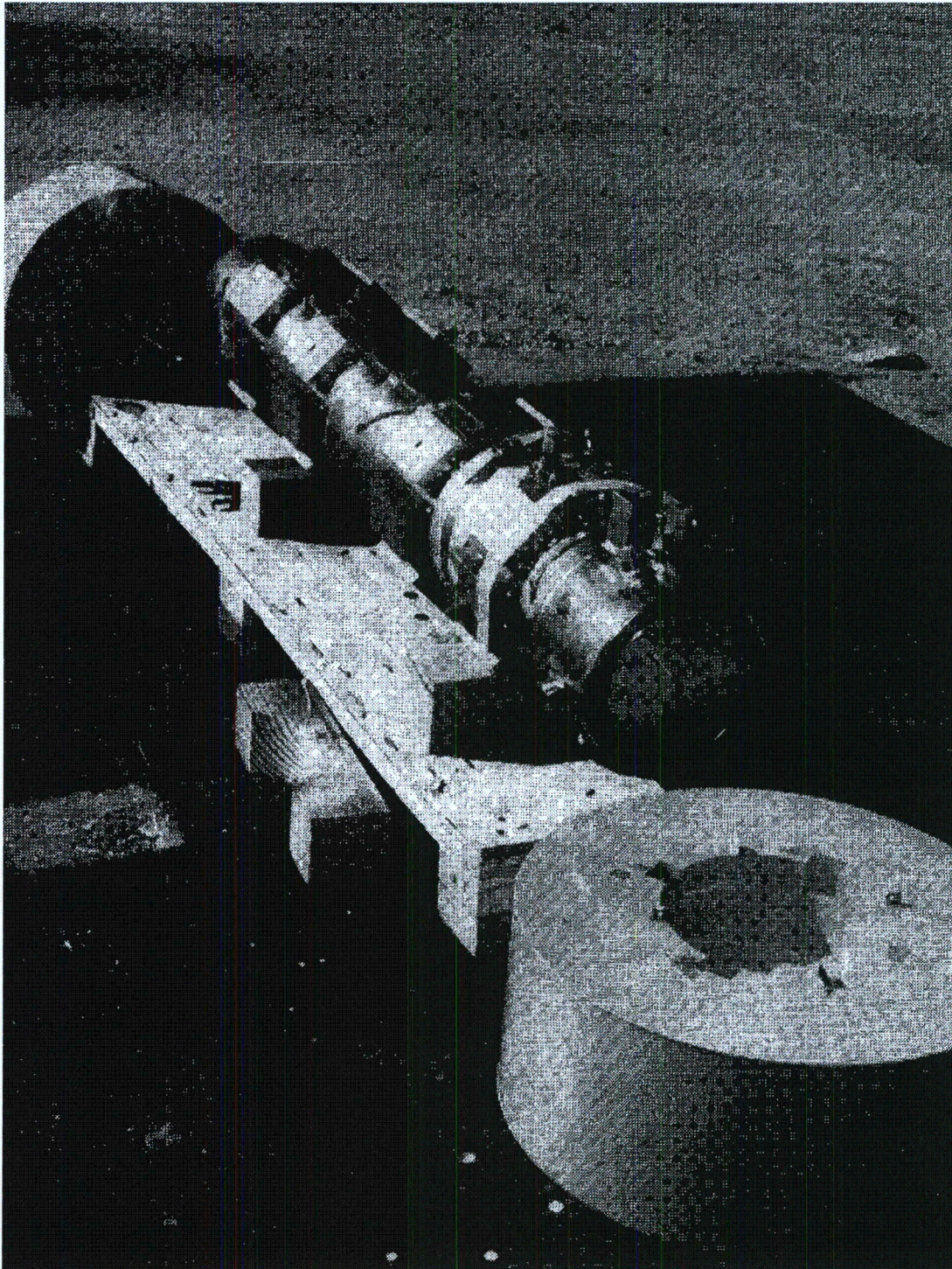


Figure 2.10.8-8 Model Rigged for 30-Foot End Drop

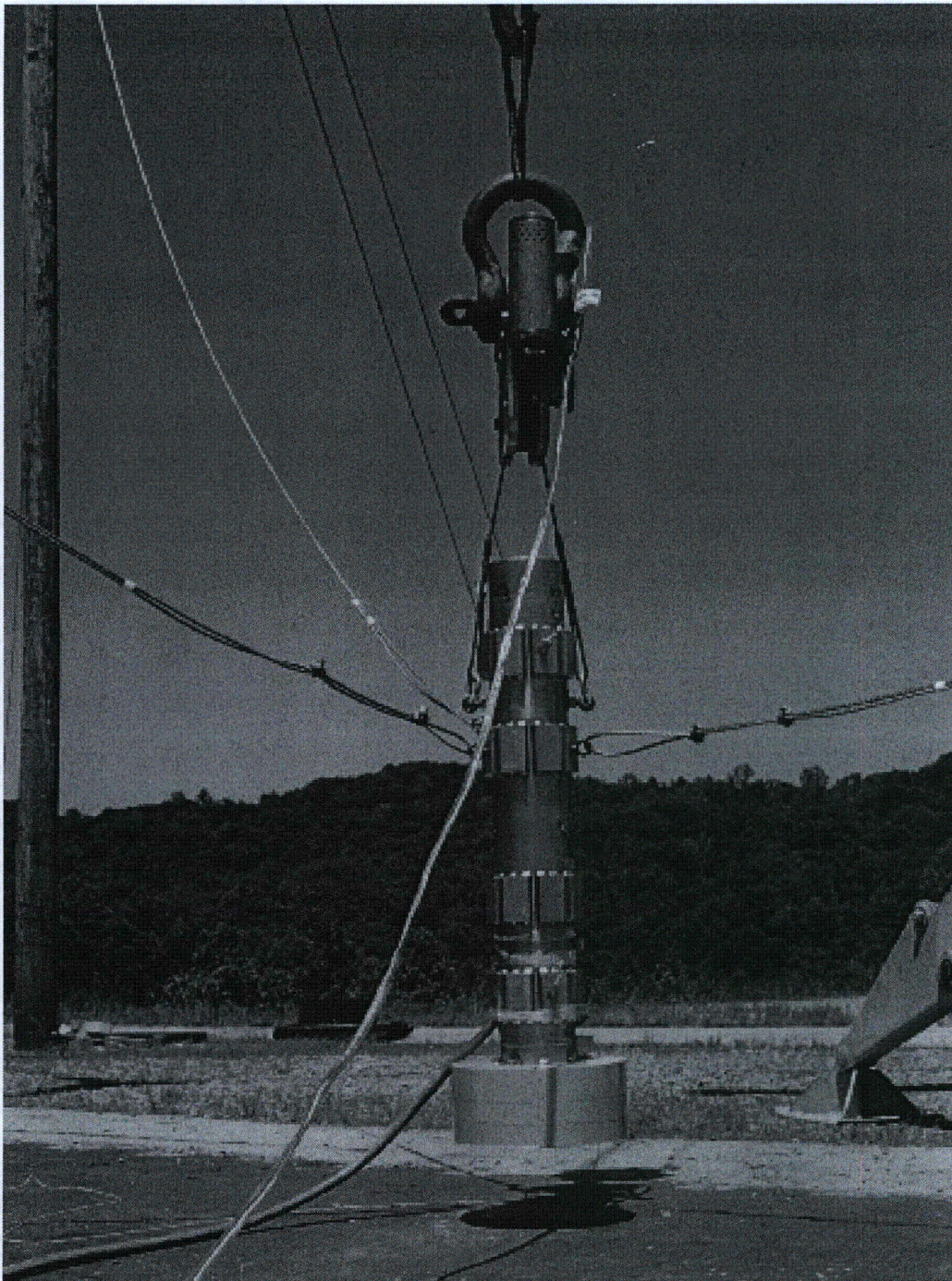


Figure 2.10.8-9 Model Positioned for 30-Foot End Drop



Figure 2.10.8-10 Model Position Following 30-Foot End Drop

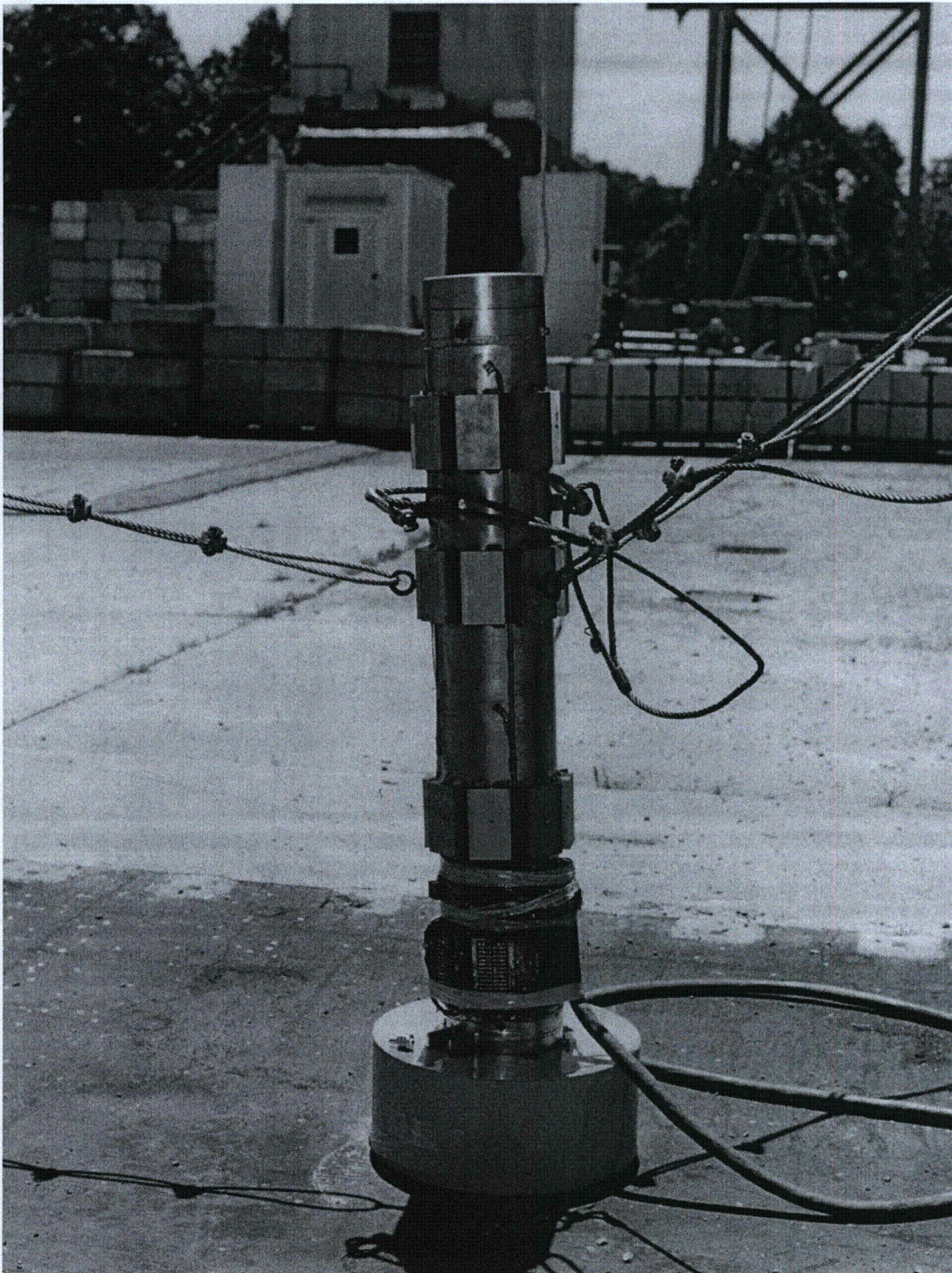


Figure 2.10.8-11 Top End Impact Limiter Following 30-Foot End Drop

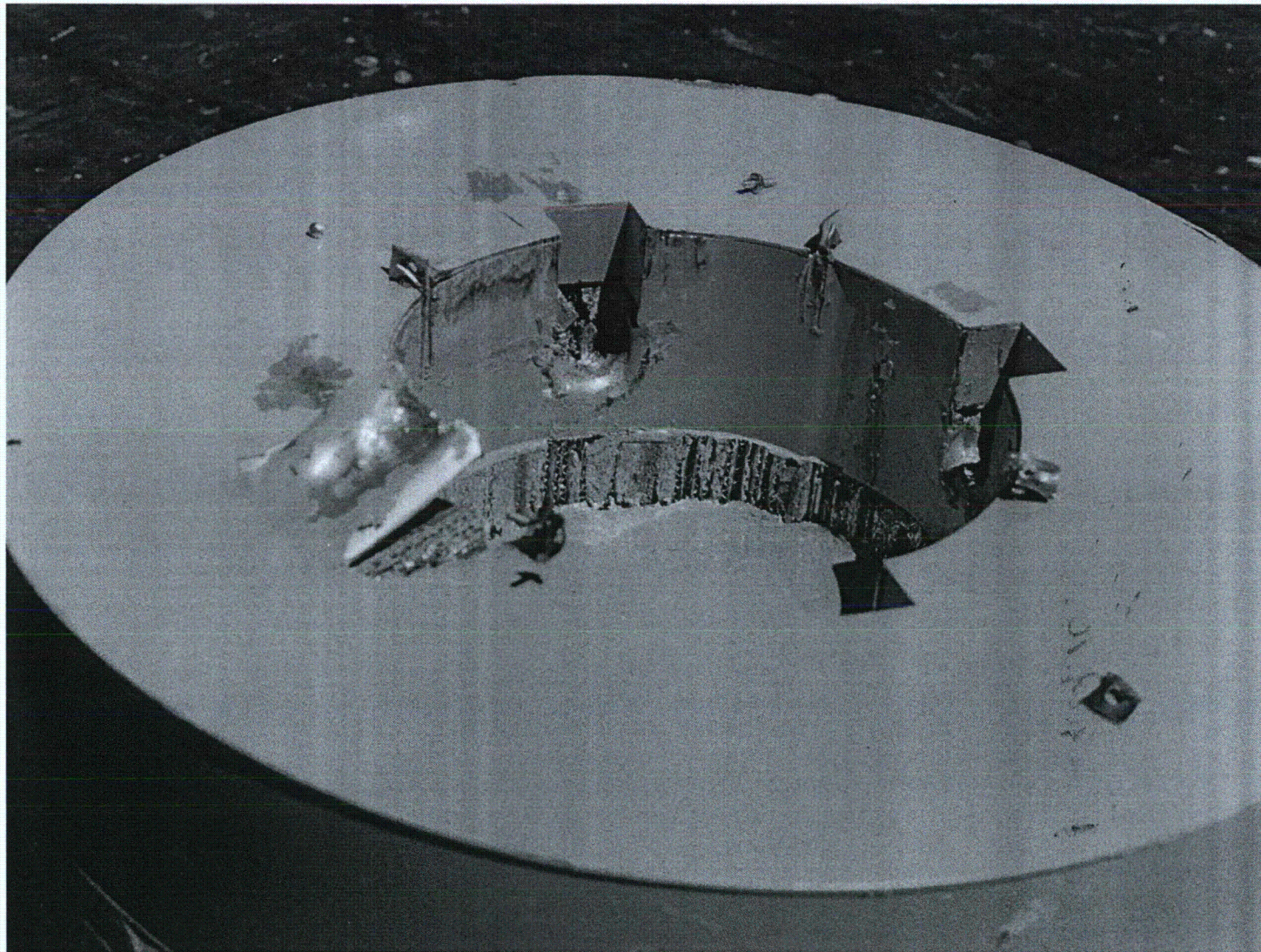


Figure 2.10.8-12 Exterior of Top Impact Limiter Following 30-Foot End Drop



Figure 2.10.8-13 Model Rigged for 30-Foot Corner Drop

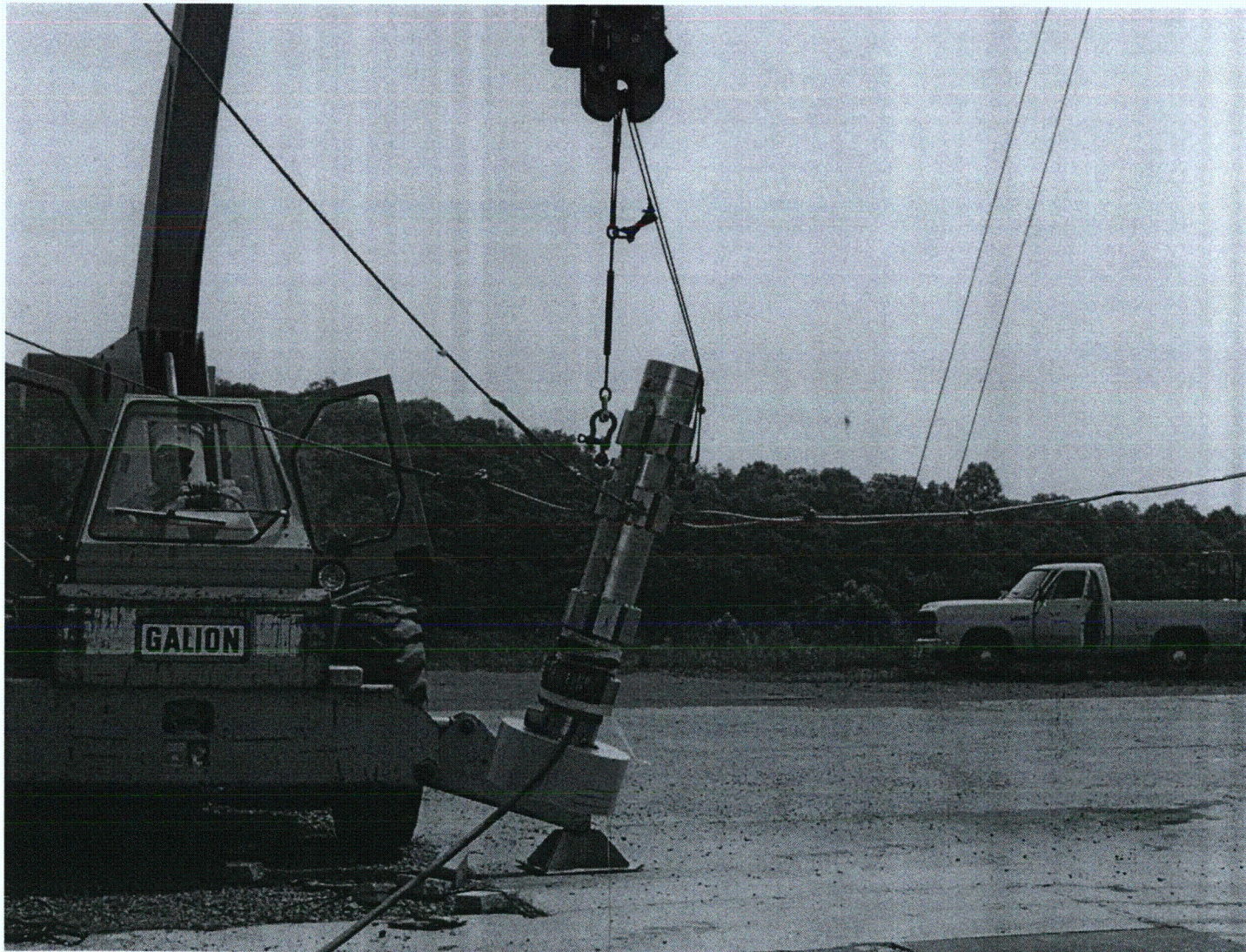


Figure 2.10.8-14 Model Positioned for 30-Foot Corner Drop

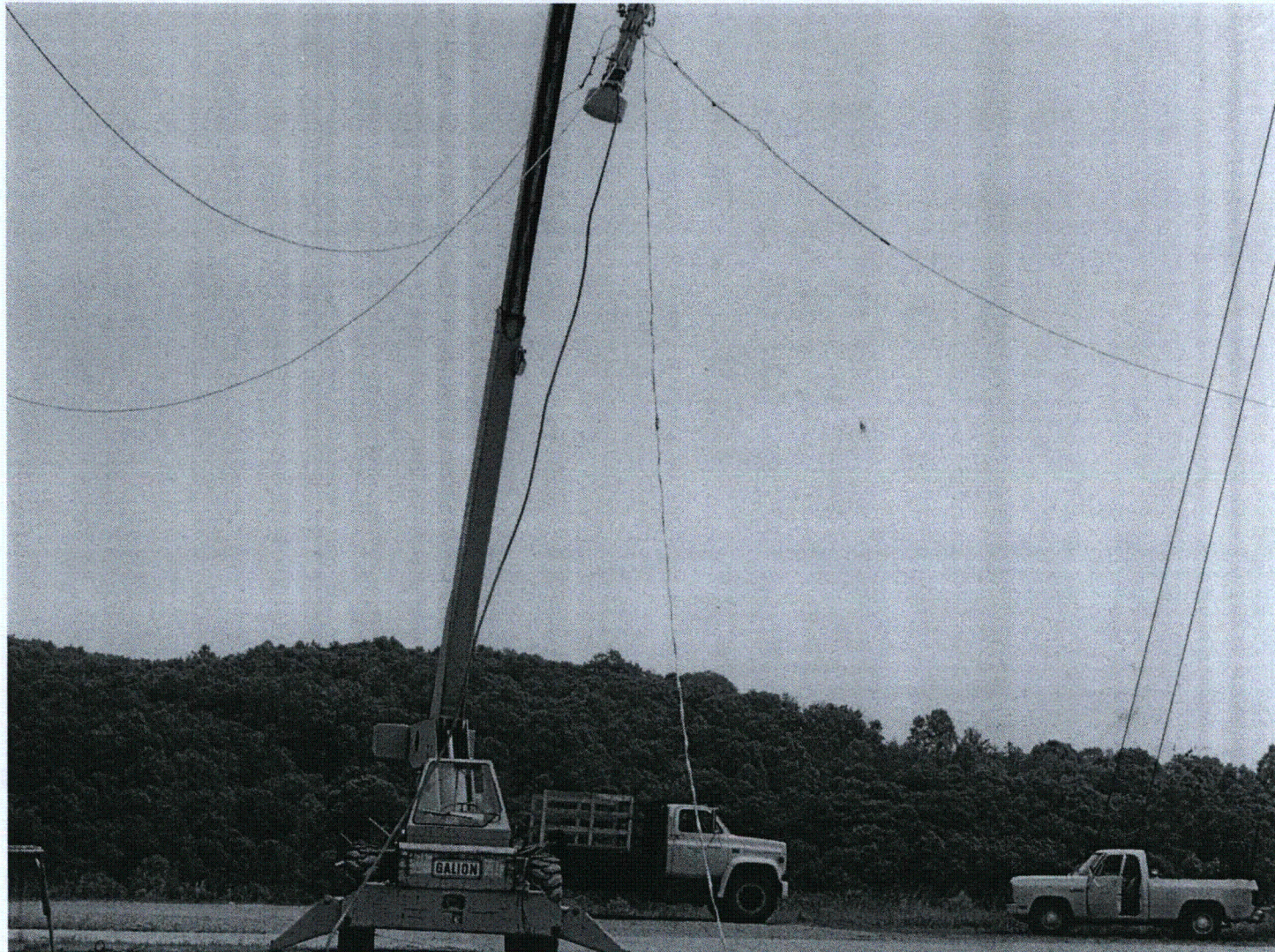


Figure 2.10.8-15 Model Following 30-Foot Corner Drop



Figure 2.10.8-16 Top Impact Limiter Following 30-Foot Corner Drop

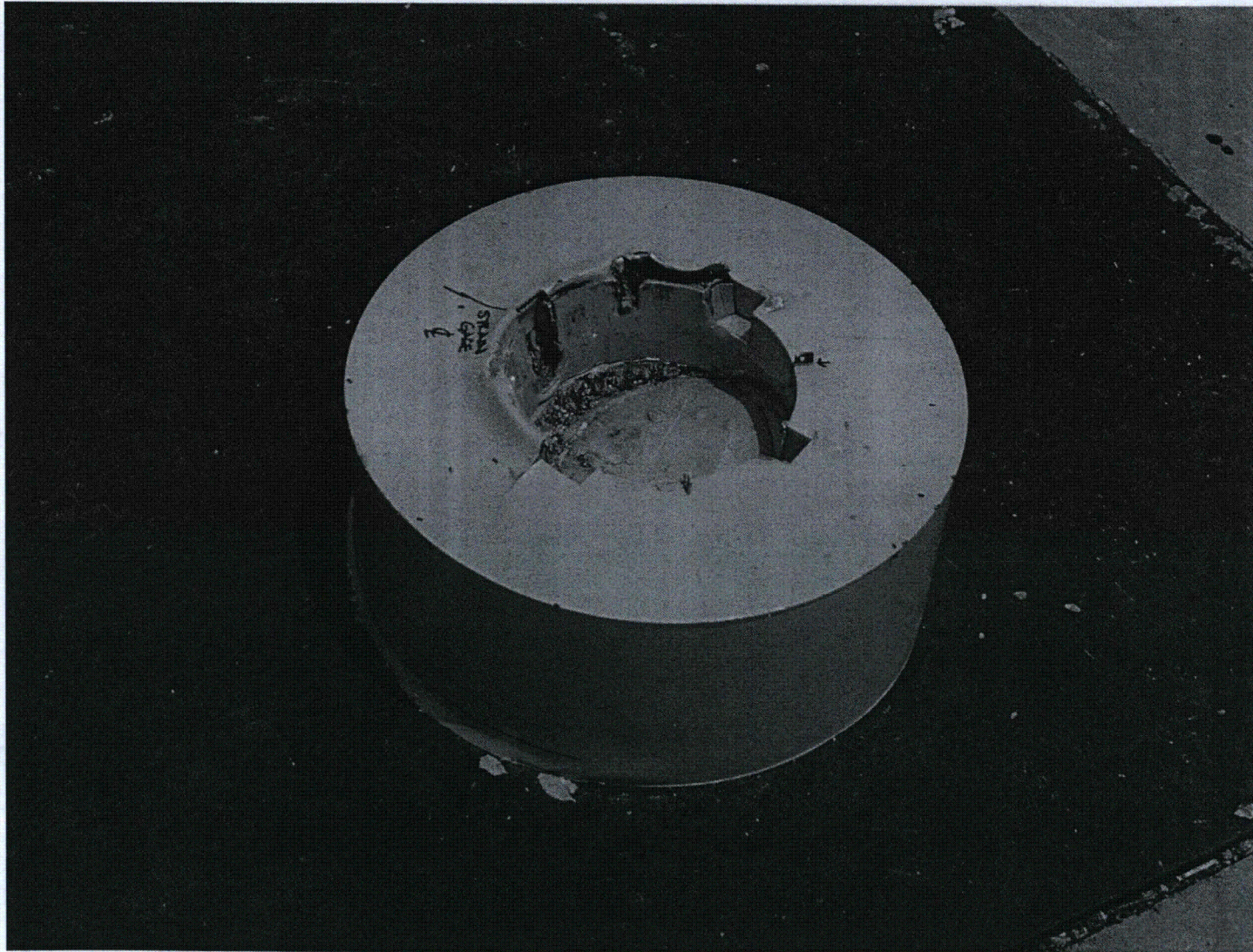


Figure 2.10.8-17 Model Position Following 30-Foot Side Drop – View 1

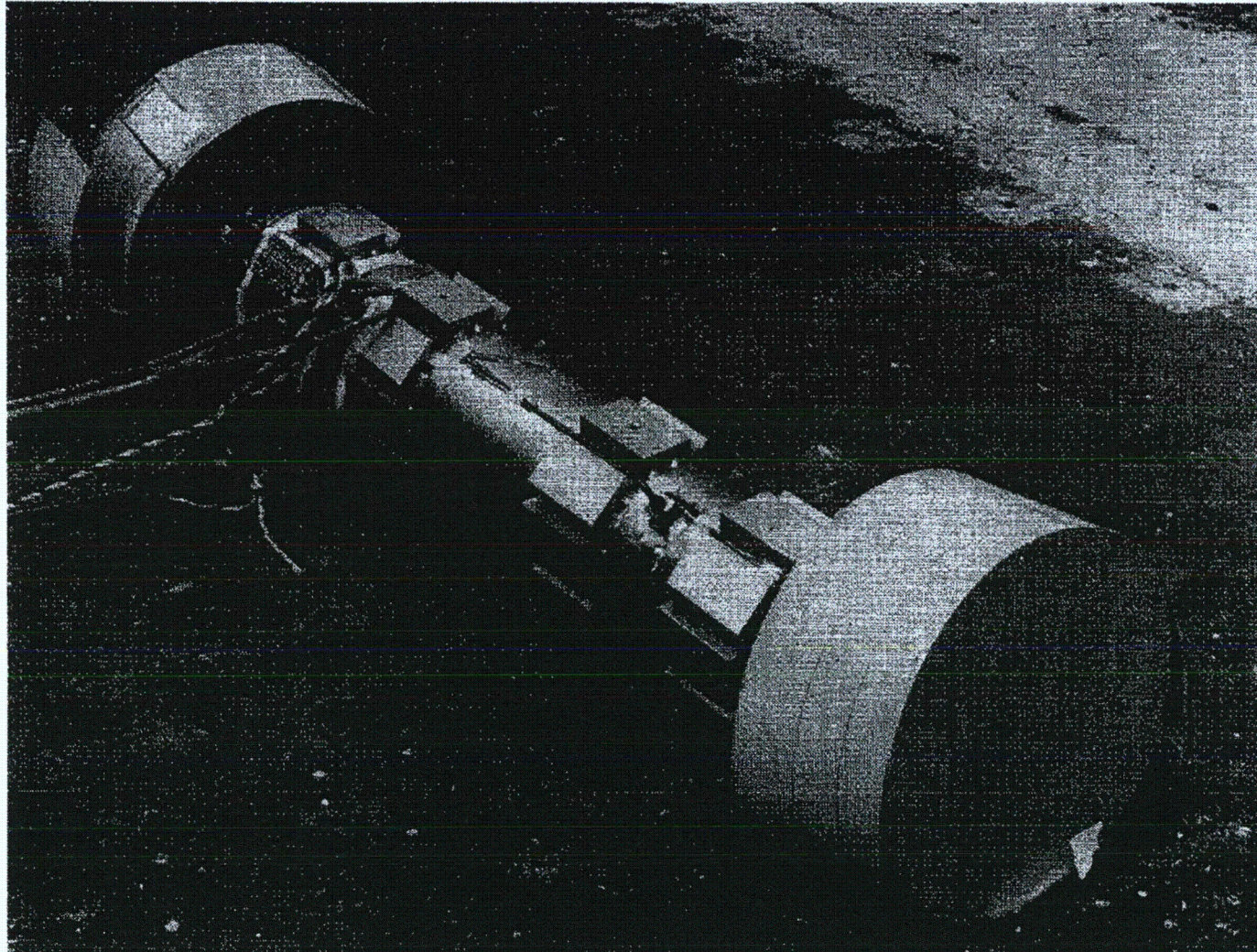


Figure 2.10.8-18 Model Position Following 30-Foot Side Drop – View 2

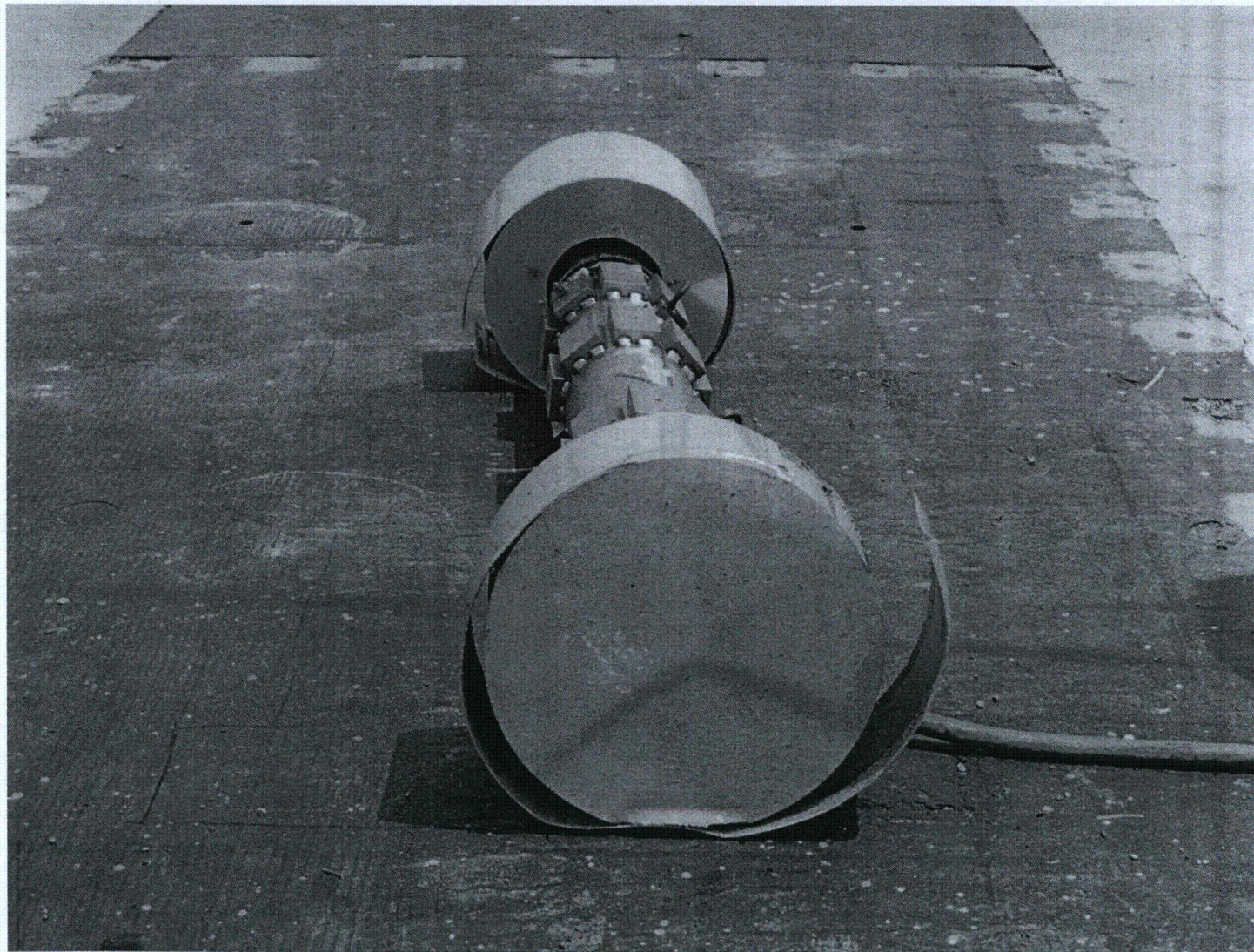


Figure 2.10.8-19 Top Impact Limiter Following 30-Foot Side Drop

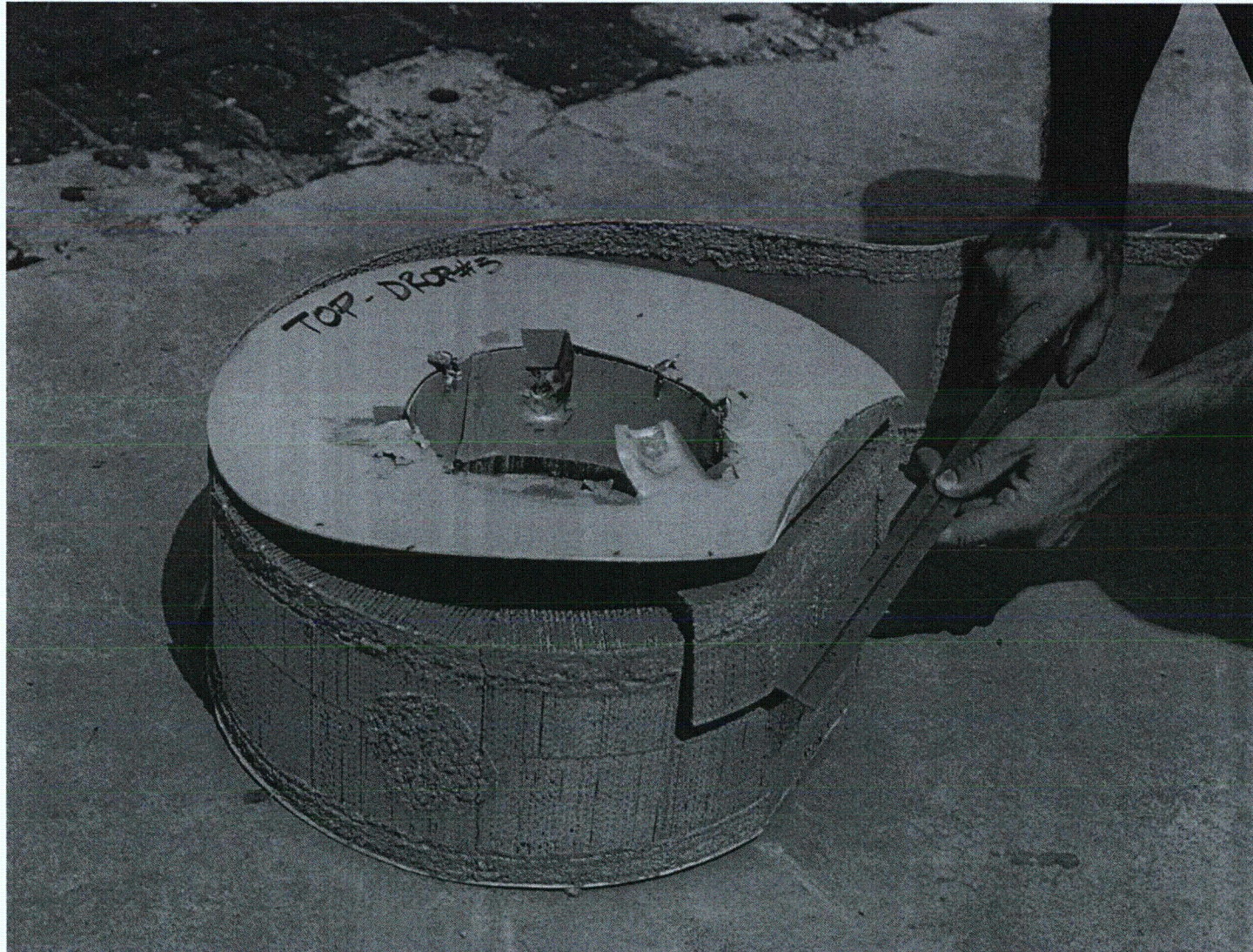


Figure 2.10.8-20 Bottom Impact Limiter Following 30-Foot Side Drop – View 1



Figure 2.10.8-21 Bottom Impact Limiter Following 30-Foot Side Drop – View 2

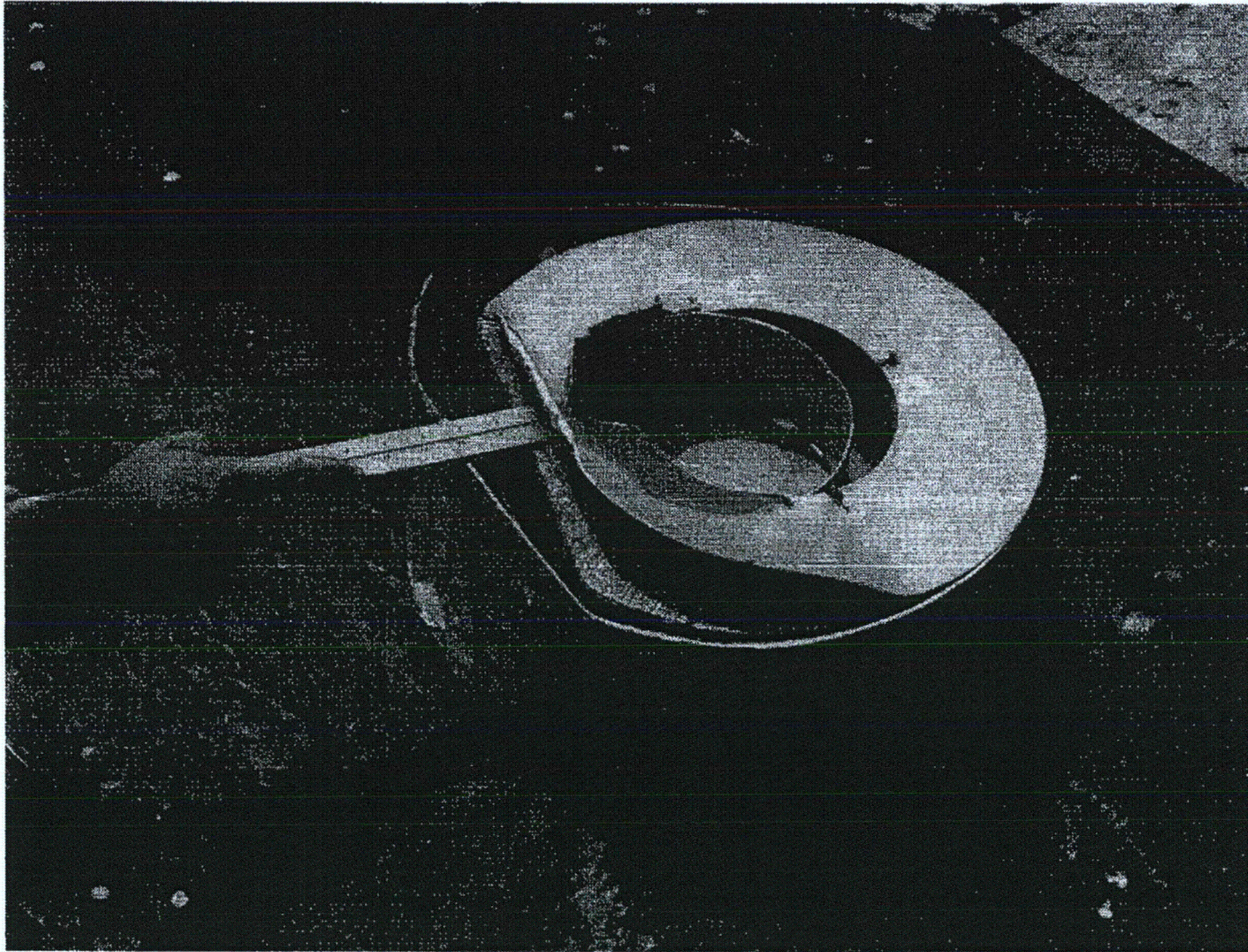


Figure 2.10.8-22 Model Rigged for 30-Foot Oblique Drop

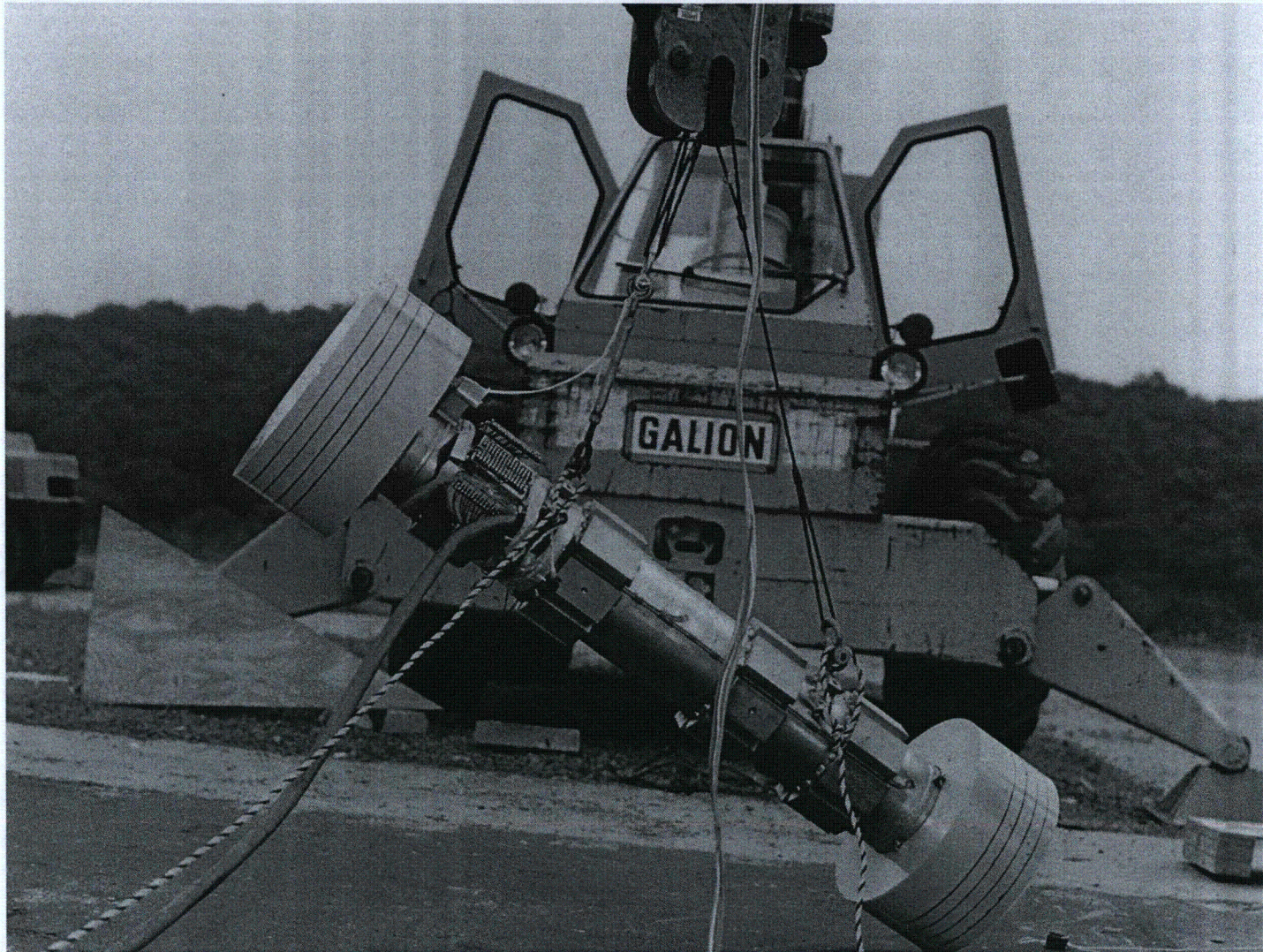


Figure 2.10.8-23 Model Positioned for 30-Foot Oblique Drop

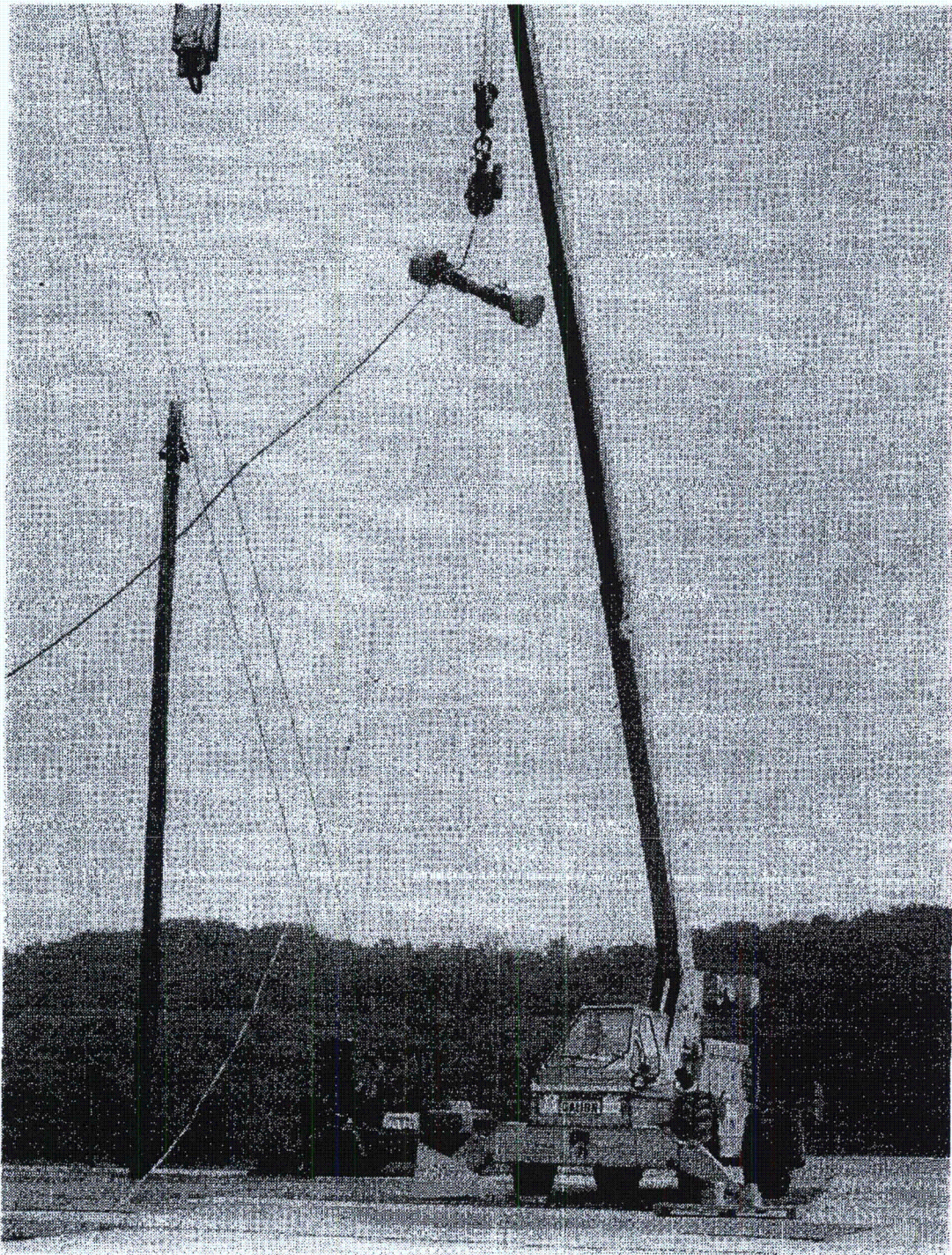


Figure 2.10.8-24 Model Position Following 30-Foot Oblique Drop

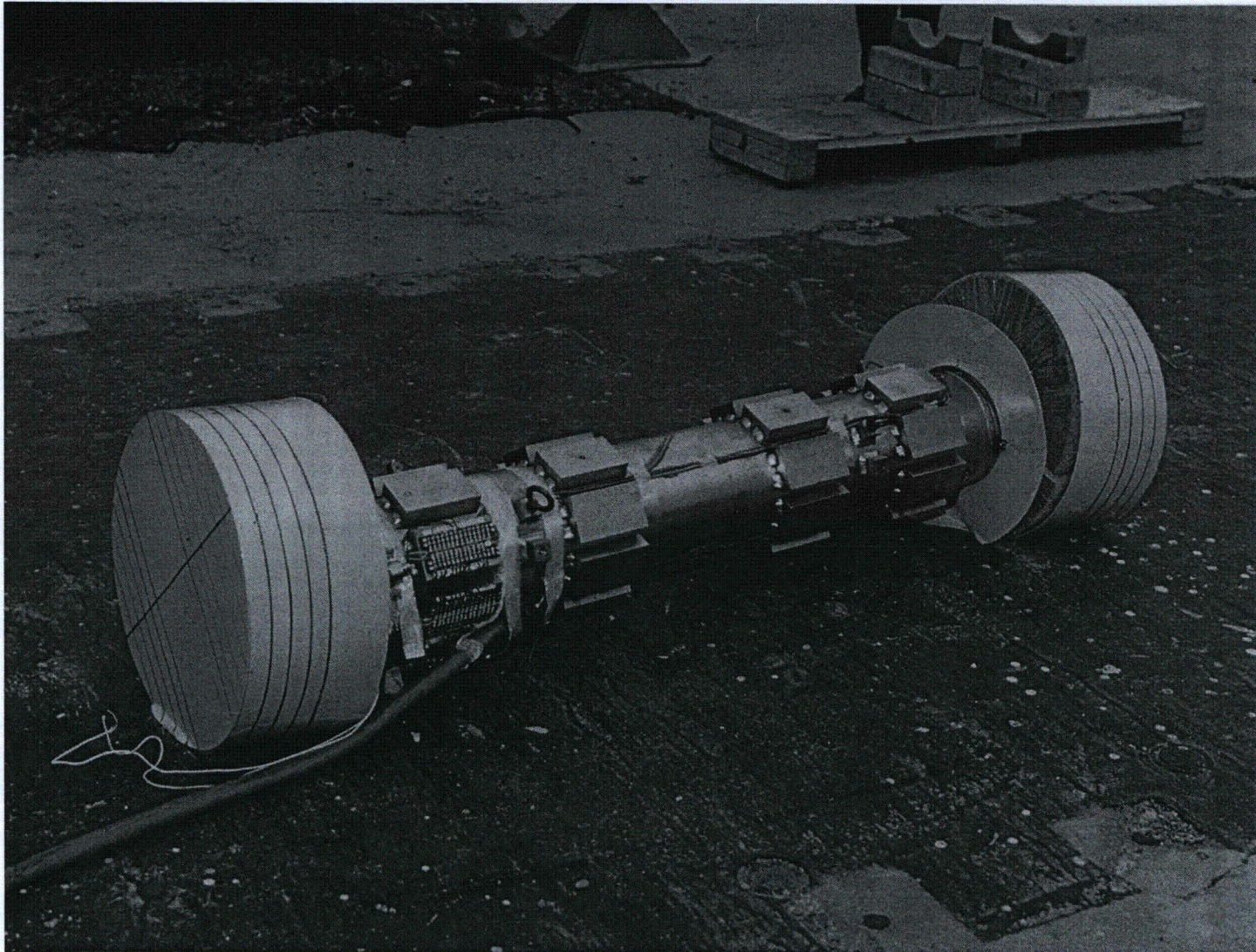


Figure 2.10.8-25 Bottom Impact Limiter Following 30-Foot Oblique Drop



Figure 2.10.8-26 Top Impact Limiter Following 30-Foot Oblique Drop



Figure 2.10.8-27 Model Rigged for Midpoint 40-Inch Pin Drop

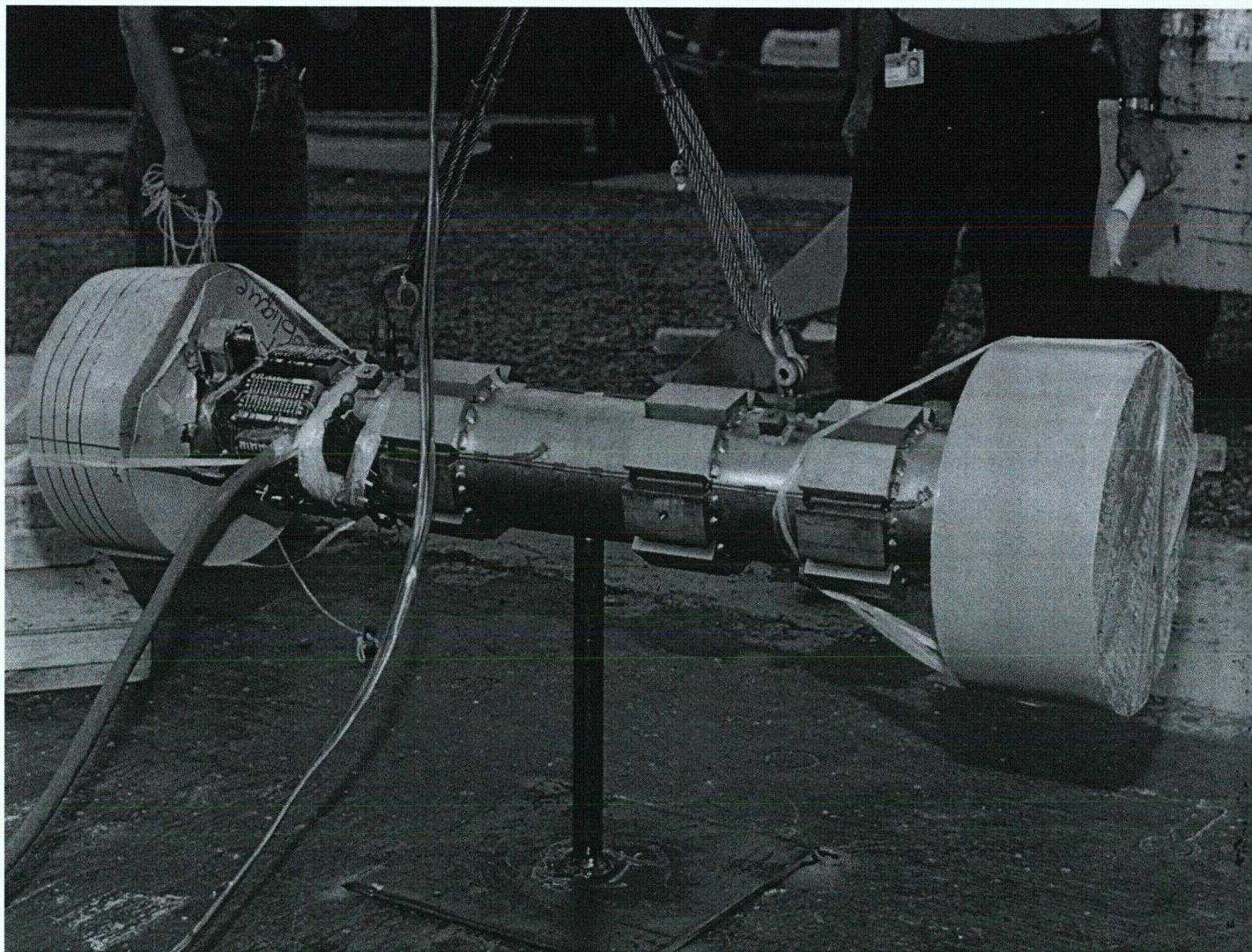


Figure 2.10.8-28 Model Positioned for 40-Inch Pin Drop



Figure 2.10.8-29 Instant Before Midpoint 40-Inch Pin Drop



Figure 2.10.8-30 Model Position Following Midpoint 40-Inch Pin Drop

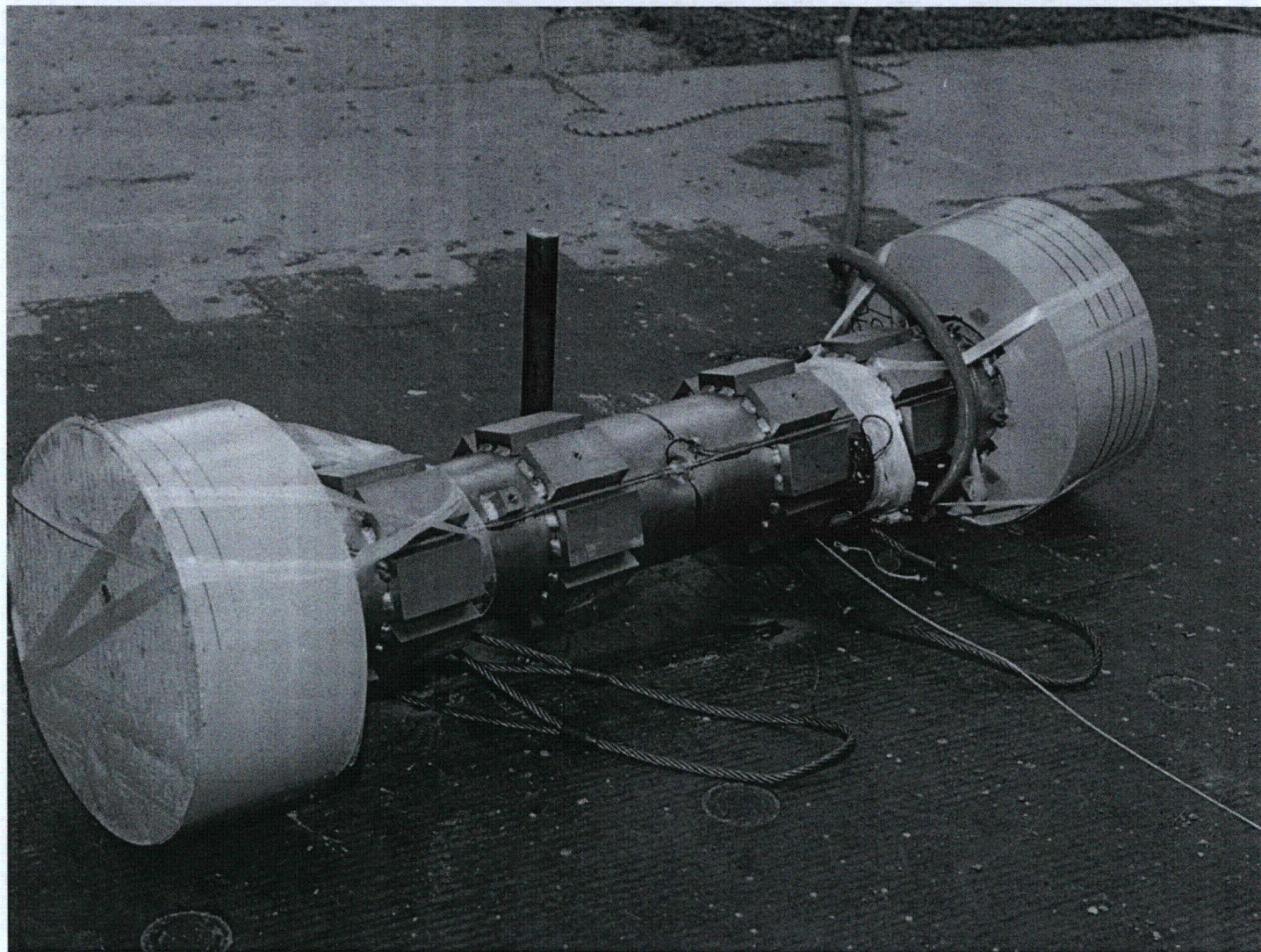


Figure 2.10.8-31 Impact Location – Midpoint 40-Inch Pin Drop

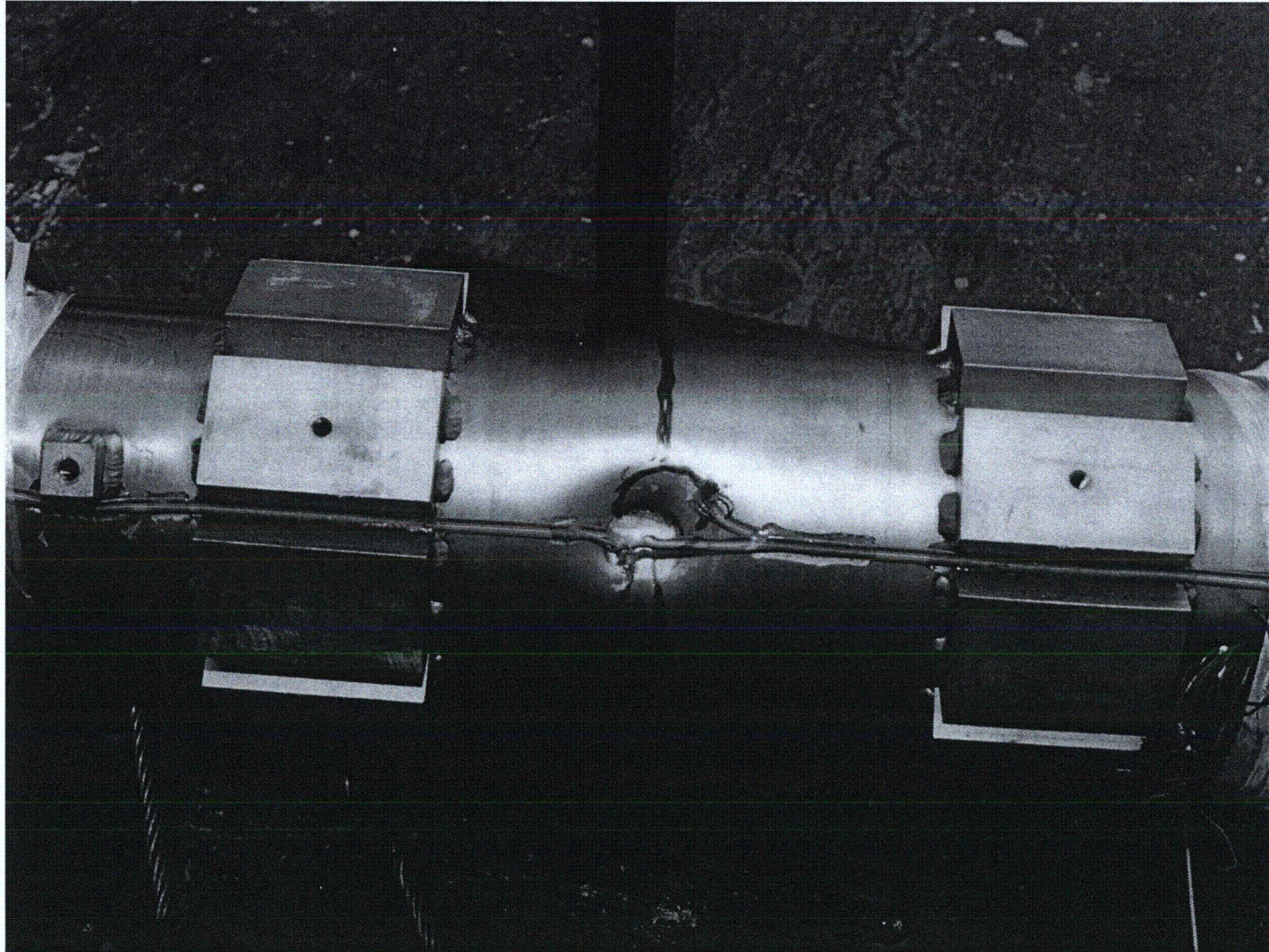


Figure 2.10.8-32 Angular Orientation of Instrumentation

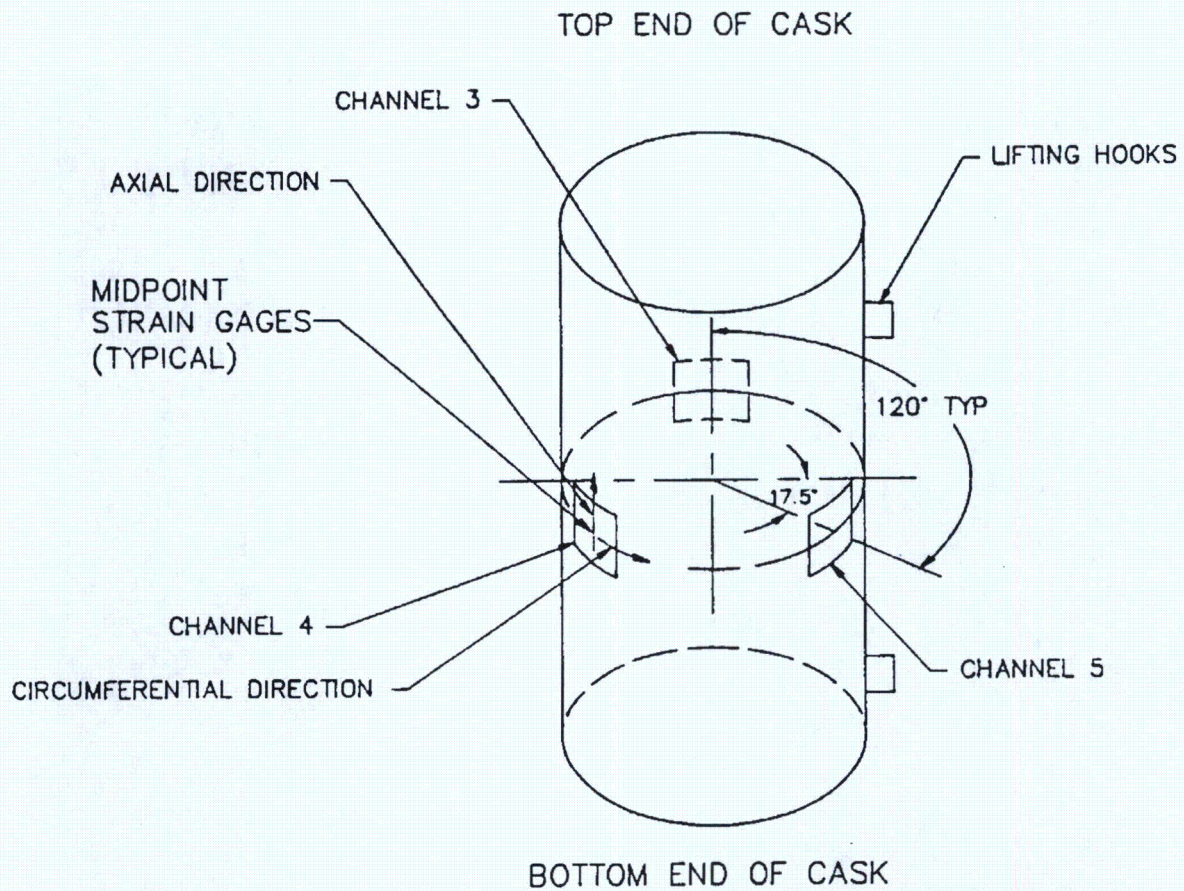


Figure 2.10.8-33 Strain Gauge Time History for Channel 3 – End Drop

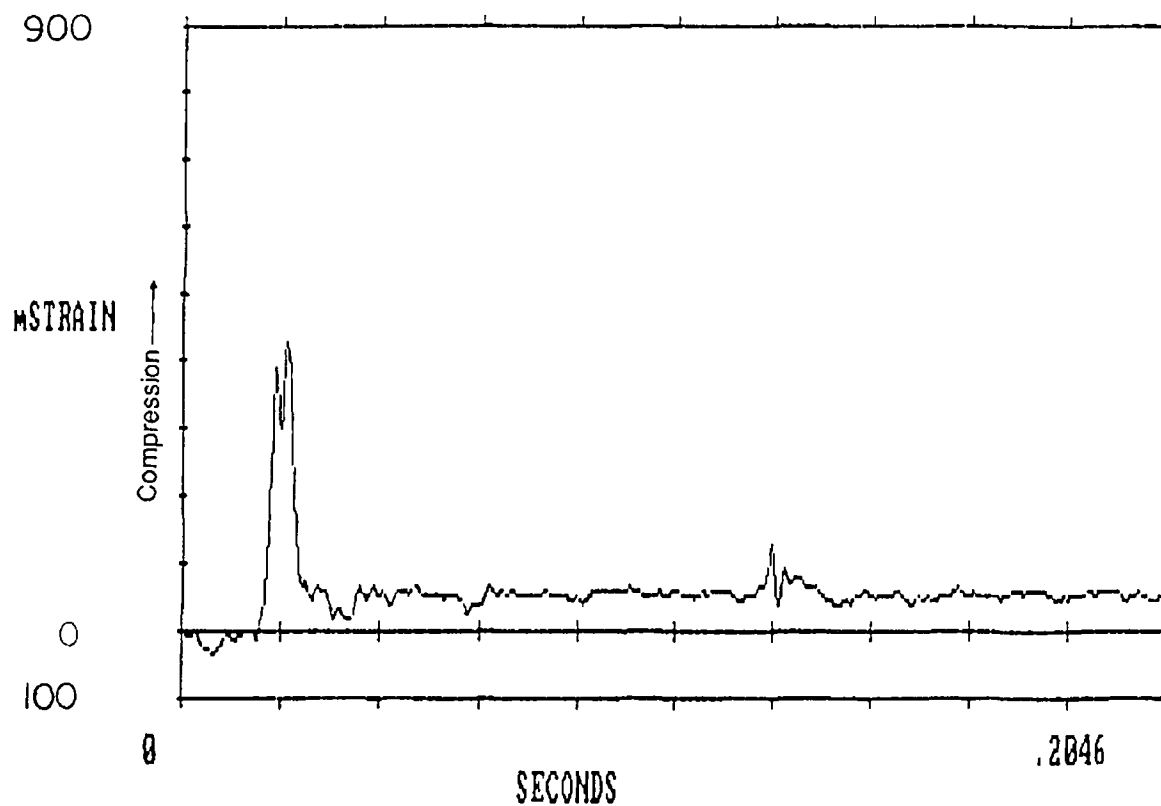


Figure 2.10.8-34 Strain Gauge Time History for Channel 4 – End Drop

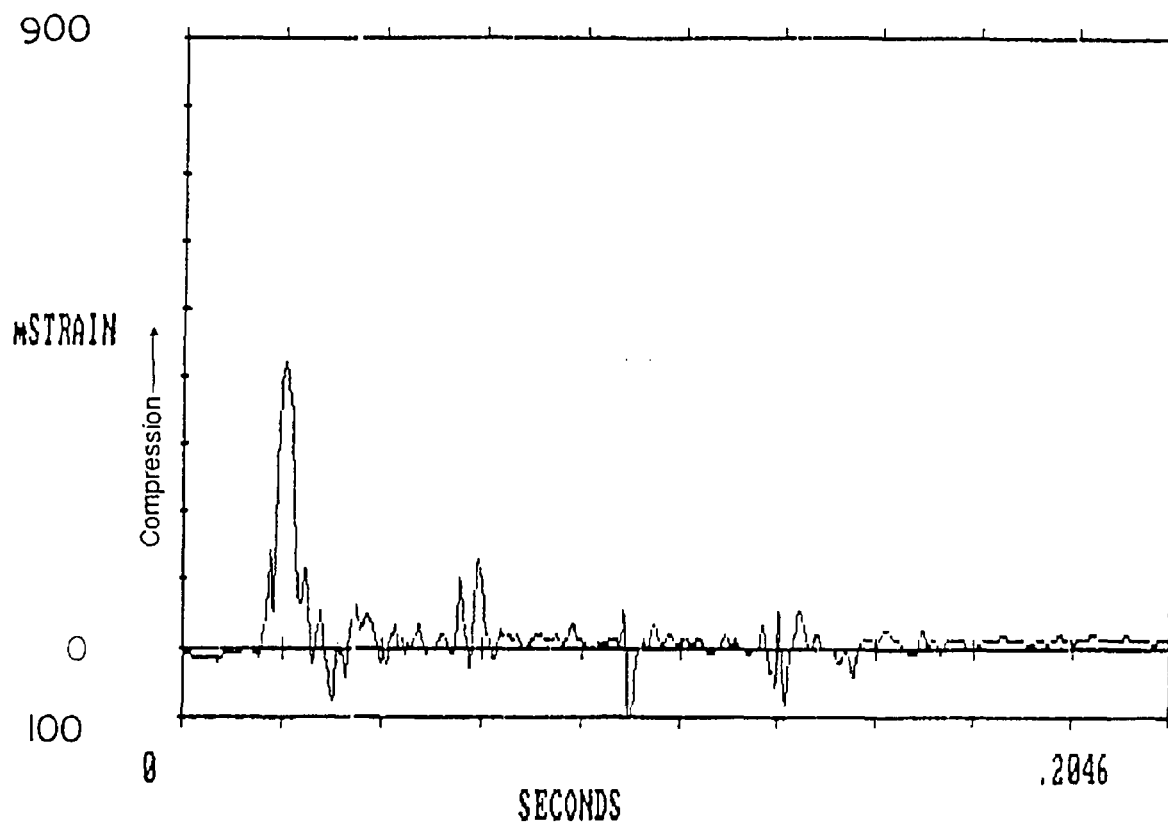


Figure 2.10.8-35 Strain Gauge Time History for Channel 5 – End Drop

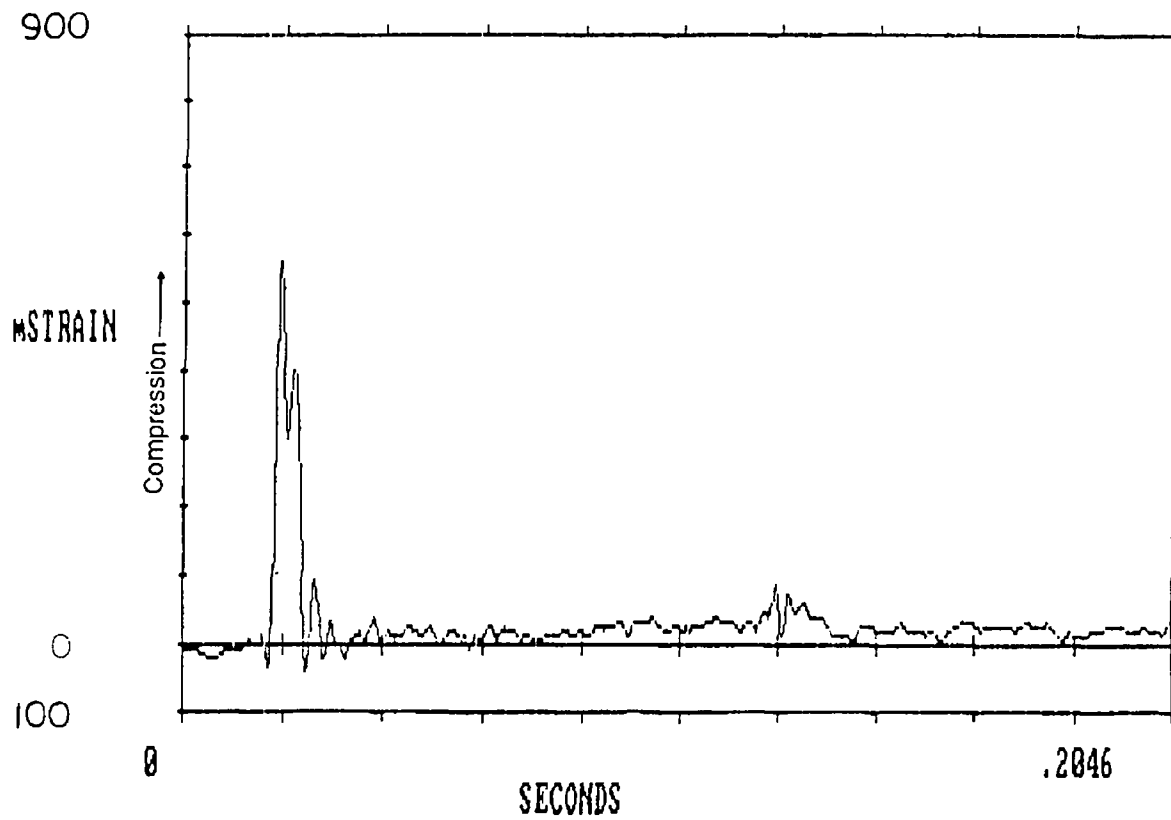


Figure 2.10.8-36 Strain Gauge Time History for Channel 3 – Side Drop

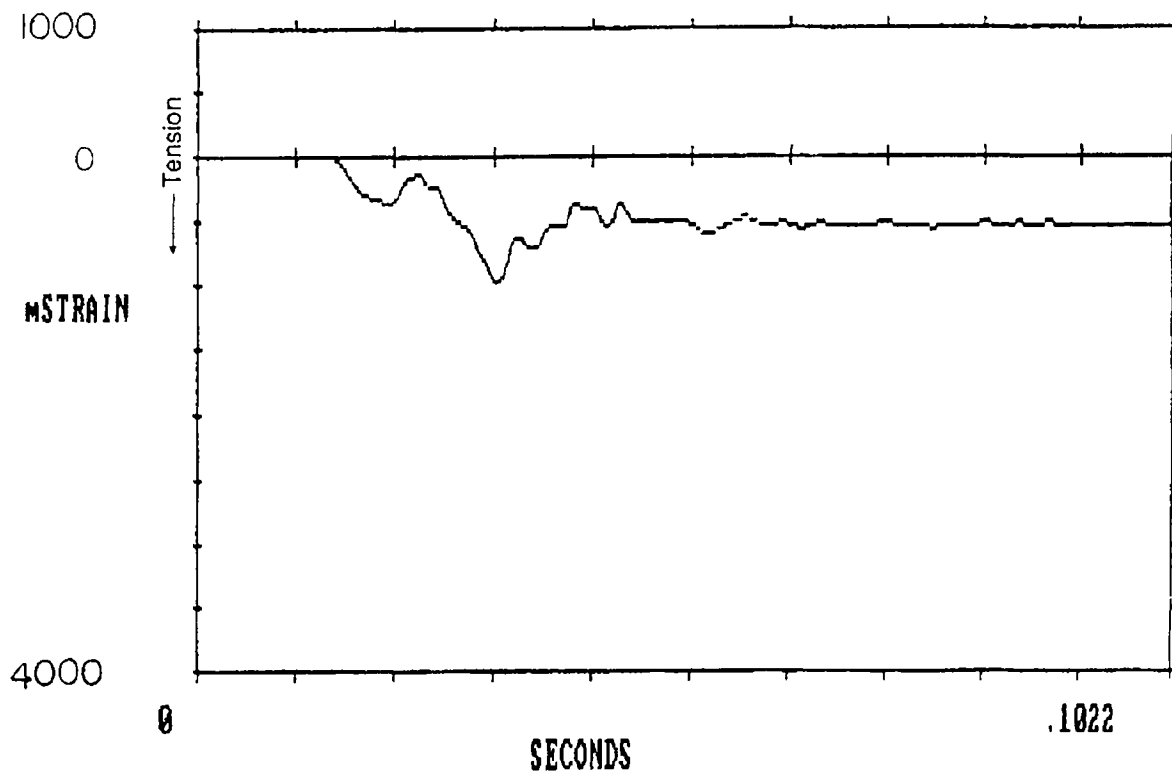


Figure 2.10.8-37 Strain Gauge Time History for Channel 4 – Side Drop

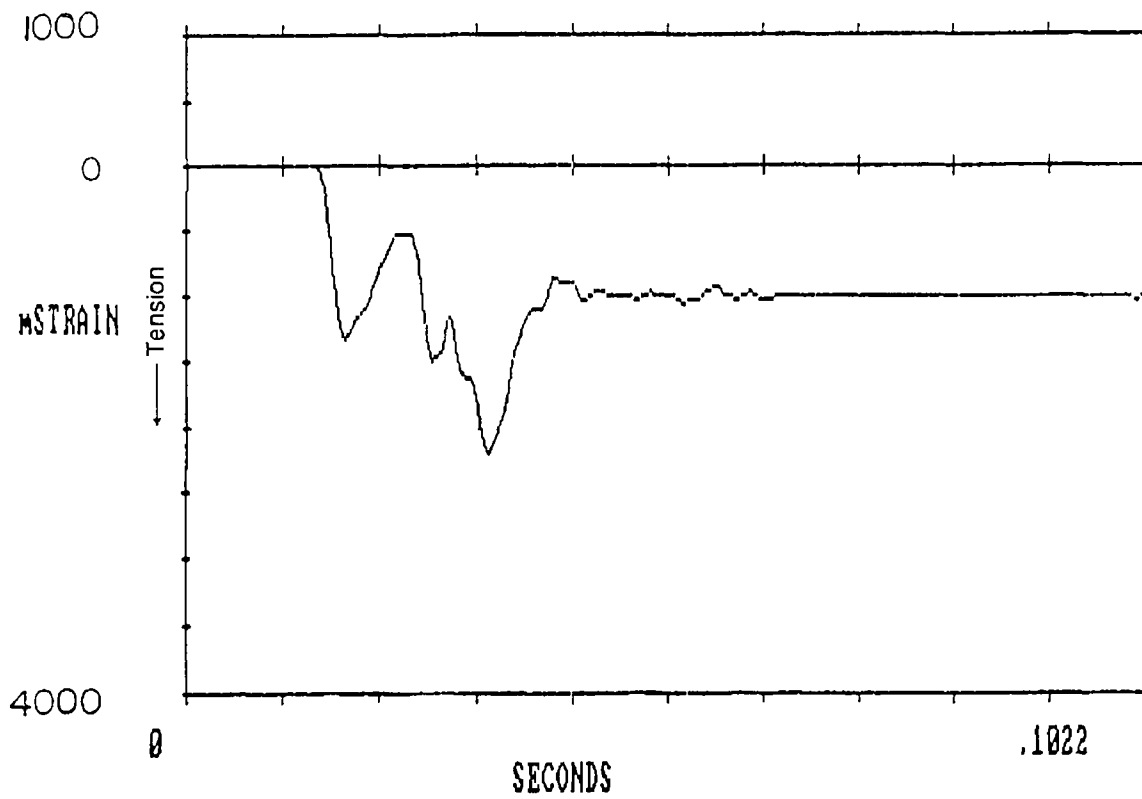


Figure 2.10.8-38 Strain Gauge Time History for Channel 5 – Side Drop

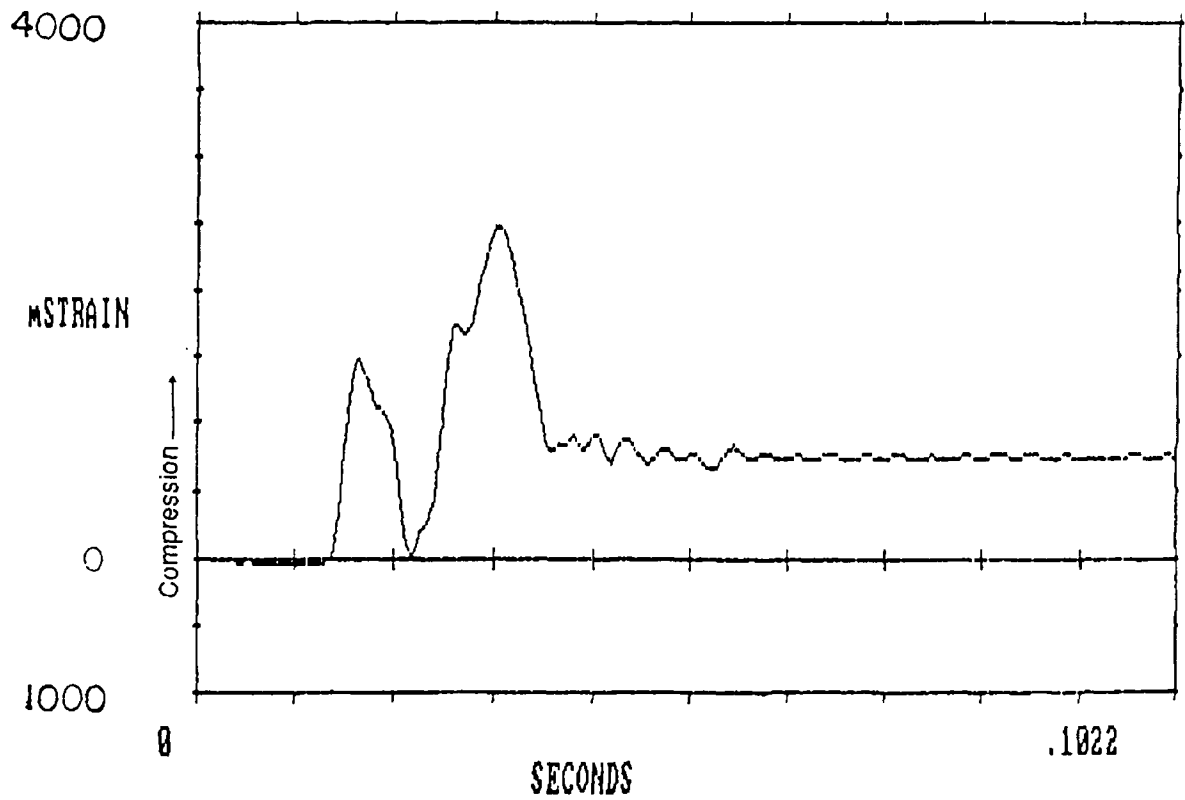
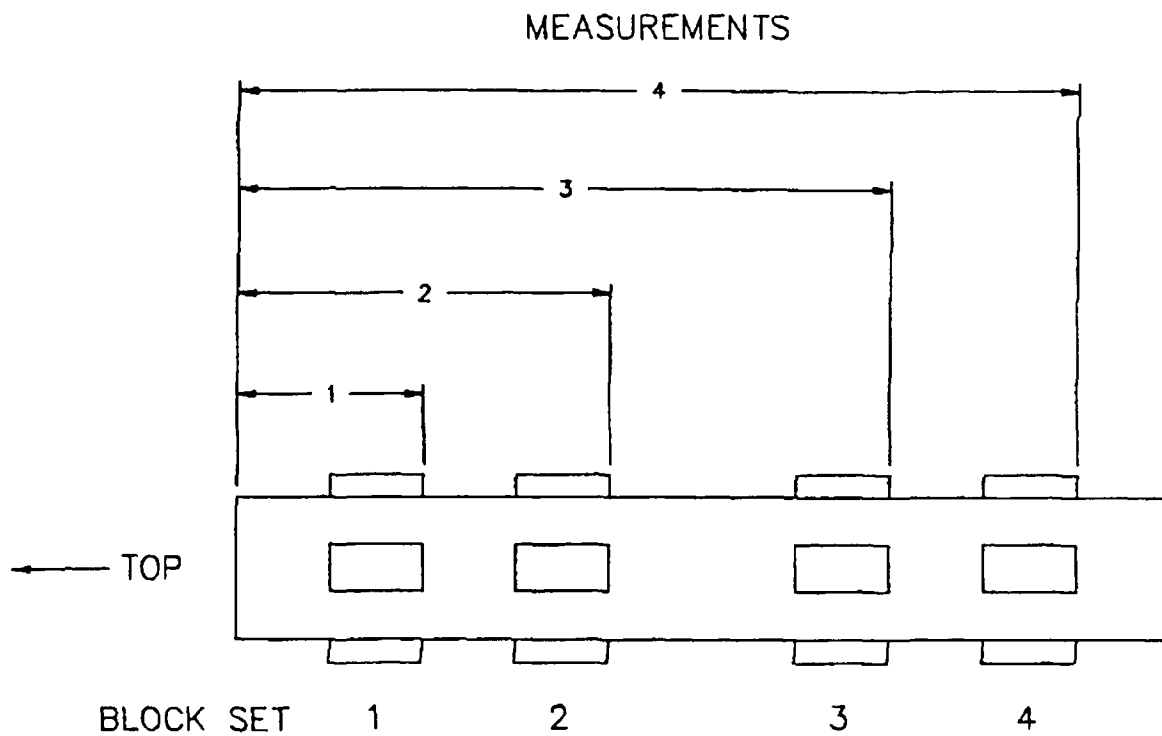


Figure 2.10.8-39 Location of Block Sets¹



¹ This figure identifies the location of the block sets referred to in Tables 2.10.8-4 and 2.10.8-7.

Table 2.10.8-1 Scaling Relations

For 1/4-Scale Model		Law II ^{1,2}
Weight		1.56%
Velocity		100%
Kinetic Energy		1.56%
Momentum		1.56%
Duration		Scaled (25%)
Deformation		25%
Acceleration		400%
Applied Force	$F_m = \ell_m^2 F_p$	$\pi_{Im} = \ell_m^2 \pi_{Ip}$
Mass	$M_m = \ell_m^3 M_p$	
Momentum	$M\theta_m = \ell_m^3 M\theta_p$	

¹ Percentages refer to model as percent of full-scale ($1/64 = 1.56\%$).

² LAW II – Does not account for strain-rate effects or gravity.

Table 2.10.8-1 Scaling Relations (continued)

Energy	$E_m = \ell_m^3 E_p$
Velocity	$V_m = V_p$
Applied Acceleration	$N_{Gm} = \frac{N_{Gp}}{\ell_m}$
Duration	$\tau_m = \ell_m \tau_p$
Deformation	$\delta_m = \ell_m \delta_p$
Natural Frequency	$f_m = \frac{1}{\ell_m} f_p$

Table 2.10.8-2 Metrology Results of Inner Diameter Measurements Before Drop

No.	Location	Vertical (in)	Horizontal (in)
1	1 inch from end	3.3443	3.3436
2	13 inches from end	3.3379	3.3513
3	26 inches from end	3.3358	3.3501
4	38 inches from end	3.3390	3.3480
5	At weld joint	3.3153	3.3246
6	At large bore	5.6591	5.6585
7	At middle bore	5.1550	5.1546

Table 2.10.8-3 Metrology Results of Outer Diameter Measurements Before Drop

No.	Location	Vertical (in)	Horizontal (in)
1	Top 1 inch inside weld	7.1378	7.1448
2	Midpoint	7.1449	7.1474
3	Bottom 1 inch inside weld	7.1562	7.1527

Table 2.10.8-4 Metrology Results of External Length Measurements Before Drop*

No.	Location	0°	90°	180°	270°
1	1st block set	11.219	11.234	11.234	11.234
2	2nd block set	20.203	20.203	20.203	20.234
3	3rd block set	34.047	34.094	34.141	34.094
4	4th block set	43.031	43.078	43.125	43.063

* Length measurements are made from the top (closure) end to the back of the steel blocks, welded to the outside of the cask to simulate the weight of the neutron shield. Four measurements were made at each position down the cask starting with a vertical location and proceeding every 90 degrees around the cask periphery (Figure 2.10.8-39).

Table 2.10.8-5 Metrology Results of Inner Diameter Measurements After Drop

No.	Location	Vertical (in)	Horizontal (in)
1	1 inch from end	3.3445	3.3434
2	13 inches from end	3.3369	3.3524
3	26 inches from end	3.2790	3.3991
4	38 inches from end	3.338	3.3523
5	At weld joint	—	—
6	At large bore	5.6590	5.6585
7	At middle bore	5.1548	5.6585

Table 2.10.8-6 Metrology Results of Outer Diameter Measurements After Drop

No.	Location	Vertical (in)	Horizontal (in)
1	Top 1 inch inside weld	7.1400	7.1450
2	Midpoint	6.6600	7.1680
3	Bottom 1 inch inside weld	7.1500	7.1560

Table 2.10.8-7 Metrology Results of External Length Measurements After Drop

No.	Location	0°	90°	180°	270°
1	1st block set	11.219	11.234	11.375	11.234
2	2nd block set	20.188	20.203	20.203	20.375
3	3rd block set	34.016	34.078	34.156	34.125
4	4th block set	43.000	43.063	43.125	43.094

2.10.9 Bolts – Closure Lid (Stress Evaluations)

Bolt stress analysis results for normal and accident conditions are summarized in four tables. Table 2.6.7-35 and Table 2.6.7-36 summarize bolt stresses for hot and cold normal conditions, respectively. Table 2.7.1-60 and Table 2.7.1-61 summarize bolt stresses under hot and cold accident conditions, respectively.

2.10.9.1 Analysis Approach

The bolt stress analyses for normal and accident conditions consider the impact loads, pressure loads, thermal loads and bolt preloads. Each table is preceded with an explicit listing of relevant geometry, mechanical properties and constant loading data (bolt torque, pressure, etc.) taken directly from Sections 2.1, 2.2, 2.3, and the license drawings in Section 1.4.

Impact loads are expressed in g acceleration loads as summarized in Table 2.6.7-33. The “hot” initial condition bolt temperature for normal and accident impact evaluations is taken at 227°F, as summarized in Table 3.4-2. The “cold” initial condition bolt temperature for normal and accident impact evaluations is -20°F, per regulatory requirements. Allowables and properties for the SA-453, Grade 660 bolts are conservatively taken at 300°F and room temperature (70°F) for hot and cold conditions, respectively. Allowable bolt stress is taken as S_y for normal and accident conditions. For conservatism, external energy absorber reaction forces, which resist separation of the cask lid and body, are completely neglected in all calculations.

An explanatory discussion of bolt stress analytics is found within Section 2.10.9.2. Table 2.10.9-1, which is identical to 2.7.1-60, is fully annotated to “key” to this explanation. An example calculation is included with each note to verify the accuracy of the tabular calculation.

The analysis methodology, allowables and basic assumptions used are consistent with conventional design/analysis codes, such as “AISC Manual of Steel Construction,” 8th Edition, and “ASME Boiler and Pressure Vessel Code,” Section III, Appendix F, Paragraph F-1335, but this analysis is more conservative. Specifically, this analysis includes stresses associated with preloads. Conventional design/analysis codes consider only externally applied loads and ignore preloads because “the ultimate shear strength of a high-strength bolt is independent of the clamping force. Only the slip resistance and fatigue life are improved by high clamping force” (“AISC Manual of Steel Construction,” pages 5-222).

Like the methodology given in the “ASME Boiler and Pressure Vessel Code,” Appendix F, Paragraph F-1335, this analysis uses nominal tensile and shear stresses based on the tabulated stress area of the bolts. It should be noted that the elliptic interaction equations of Paragraph F1335.2 of the “ASME Boiler and Pressure Vessel Code” and the approach used here give nearly

identical results when adjustments in loadings are made to account for the differing treatment of preload tension (This method conservatively includes preloads, whereas, the other ignores preloads).

2.10.9.2 Closure Bolt Analyses – Analytics and Assumptions

All numerical examples pertain to the evaluation of the NAC-LWT cask under hypothetical accident conditions (Table 2.10.9-1). The numbering of equations shown below reflects the annotation of values appearing within Table 2.10.9-1.

$$\begin{aligned} W_A &= \text{weight acting in longitudinal (axial) direction} & (a) \\ &\quad \text{supported by lid bolts, includes payload and lid} \\ &= 4000 + 941 \text{ lb} \\ &= 4941 \text{ lb} \end{aligned}$$

$$\begin{aligned} W_L &= \text{weight acting in lateral direction. This amounts} & (b) \\ &\quad \text{to lid weight only} \\ &= 941 \text{ lb} \end{aligned}$$

$$\begin{aligned} F_t &= \text{bolt thermal load, with example evaluation:} & (c) \\ &= A_b \Delta T [E_l \alpha_l - E_b \alpha_b] \\ &= 1423 \text{ lb} \end{aligned}$$

where:

$$\begin{aligned} A_b &= 6051 \text{ in}^2 && \text{nominal bolt area} \\ \Delta T &= 157^\circ\text{F} && \text{thermal differential.} \end{aligned}$$

For this illustrative case, the thermal differential, ΔT , is the hot service temperature, 227°F , less the temperature at which the cask bolting was torqued, here taken as room temperature, 70°F .

Thus, $\Delta T = 227 - 70 = 157^\circ\text{F}$.

$$\begin{aligned} E_l &= 27.0 \times 10^6 && \text{lid modulus} \\ \alpha_l &= 9.0 \times 10^{-6} && \text{lid expansion coefficient} \\ E_b &= 26.7 \times 10^6 && \text{bolt modulus} \\ \alpha_b &= 8.54 \times 10^{-6} && \text{bolt expansion coefficient} \\ F_i &= \text{bolt preload calculated from torque relation given in Section 2.1.3.2.2} & (d) \end{aligned}$$

$$\begin{aligned} &= 12T/(0.08973d) = (12)(260)/[(0.08973)(1.0)] \\ &= 34,770 \text{ lbs} \end{aligned}$$

where:

$$\begin{aligned} T &= \text{preload torque, ft-lb} \\ d &= \text{nominal bolt diameter, in} \\ F_p &= \text{bolt pressure load} & (e) \\ &= P_p A_p / N_r \\ &= 812 \text{ lbs} \end{aligned}$$

where:

$$\begin{aligned} P_p &= \text{internal pressure, 125 psig} \\ A_p &= \pi d_s^2 / 4 \\ &= 194.8 \text{ in}^2, \text{ pressure area} \\ d_s &= \text{seal diameter} \\ &= 15.75 \text{ inches} \\ N_r &= \text{number of bolts} \\ &= 12 \\ K_b &= \text{bolt stiffness} & (f) \\ &= A_b E_b / L \\ &= 1.903 \times 10^6 \text{ lb/in} \end{aligned}$$

where:

$$\begin{aligned} A_b &= 0.6051 \text{ in}^2 \\ E_b &= 26.7 \times 10^6 \text{ psi} \\ L &= (\text{grip length}) + 1/2 (\text{nominal diameter}) \\ &= 7.99 + 0.50 \\ &= 8.49 \text{ inches} \\ K_m &= \text{lid stiffness} & (g) \\ &= A_L E_\ell / L_g \end{aligned}$$

$$= 2.122 \times 10^7 \text{ lb/in}$$

where:

A_L = an assumed cross-sectional area equal to a thick-walled cylinder with an inner diameter equal to the nominal bolt diameter and an outer diameter equal to three times the nominal bolt diameter (Shigley)

$$= \pi/4 (9d^2 - d^2) = 2\pi d^2$$

$$= 6.28 \text{ in}^2$$

$$E_\ell = 27 \times 10^6 \text{ psi}$$

L_g = grip length

$$= 7.99 \text{ inches}$$

n_g = Impact acceleration based on impact force predictions (Table 2.6.7-33).
The (+) mark in the adjoining column denotes a value determined from linear interpolation. (h)

F_A = end impact bolt force (i)

$$= P_A/N_r = (296,460)/12$$

$$= 24,705 \text{ lbs}$$

where:

$$P_A = n_g W_A \sin \theta = (60.0)(4941)(1)$$

$$= 296,460 \text{ lbs}$$

F_A = oblique impact bolt force

$$= P_A [R_L (R_L + R_B) / I_o] A_b$$

$$= 33,641 \text{ lbs}$$

where:

$$P_A = n_g W_A \sin \theta = (60.13)(4941)(\cos 5^\circ)$$

$$= 295,972 \text{ lbs}$$

A_b = bolt stress area

$$= 0.6051 \text{ in}^2$$

R_L = lid radius

$$= 11.25 \text{ inches}$$

R_B = bolt circle radius

$$= 8.94 \text{ inches}$$

I_o = bolt circle moment of inertia = $\pi R_B^3 t + A_b N_r R_L^2$

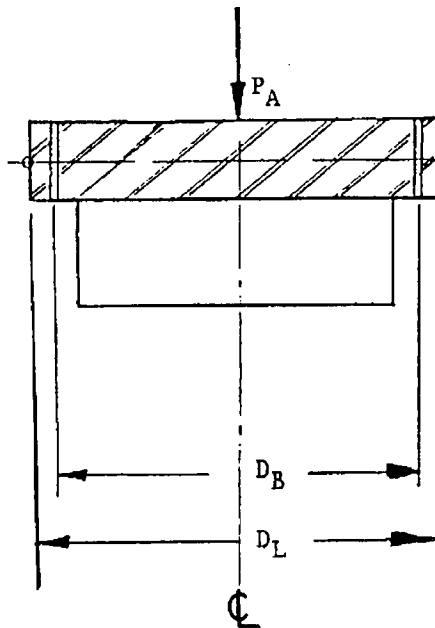
$$= 1209 \text{ in}^4$$

t = equivalent ring thickness

$$= A_b N_r / (2\pi R_B) = (0.6051)(12) / (17.875\pi)$$

$$= 0.1293 \text{ in}$$

The derivation of this relationship for tensile bolt stresses assumes the lid pivots about the outer edge of the lid, point "o". The bolts are approximated as a thin, circular ring with a thickness equivalent to (total bolt area) = (ring area).



Bolt Circle

$$R_B = D_B / 2 \\ = 8.94 \text{ in}$$

Lid

$$R_L = D_L / 2 \\ = 11.25 \text{ in}$$

Equivalent ring thickness is found as:

$$A = \pi D_B t$$

or

$$T = A / (\pi D_B) \\ = 0.1293 \text{ in}$$

where:

$$\begin{aligned} A &= (12 \text{ bolts})(0.6051 \text{ in/bolt}); \text{ Baumeister, pages 8-10} \\ &= 7.26 \text{ in}^2 \end{aligned}$$

The moment of inertia of the bolt ring about point “o” is:

$$\begin{aligned} I_o &= \pi R_B^3 t + AR_L^2 \\ &= 1209 \text{ in}^4 \end{aligned}$$

The applied bending moment about point “o” resulting from the impact force, P_A , is:

$$M_o = P_A R_L$$

Thus, the extreme bolt tension stress is found as:

$$\begin{aligned} f_a &= Mc/I \\ &= [(P_A R_L)(R_L + R_B)]/(\pi R_B^3 t + AR_L^2) \end{aligned}$$

or

$$\begin{aligned} F_A &= f_a A_b \\ &= P_A [R_L (R_L + R_B)/I_o] A_b \end{aligned}$$

In this analysis, which sweeps from vertical (end) impacts through side impacts, the two bolt tension relations, equations (i) and (j), must transition from one to the other at some orientation angle. Both conservatively neglect reaction forces from external energy absorbers. This neglect is extraordinarily conservative for near vertical impacts, but becomes more realistic as the package approaches side impact orientations. Specifically, the center of pressure of the external energy absorber reaction force on the lid moves from the center of the lid towards the impacting corner of the package as the impact orientation moves from near vertical to near horizontal.

For conservatism, this transition from an end relation, equation (i), for bolt force to an oblique relation, equation (j), is assumed to occur reasonably close to vertical; hence, only the 0-degree case uses the uniform force assumption.

$$\begin{aligned} FL &= \text{lateral (shear) bolt load} & (k) \\ &= PL/Nr = 4931/12 \\ &= 411 \text{ lbs} \end{aligned}$$

where:

$$\begin{aligned}
 P_L &= n_g W_L \sin \theta = (60.13)(941) \sin 5^\circ \\
 &= 4931 \text{ lbs} \\
 P &= \text{total applied external bolt load} \\
 &= F_p (\text{pressure}) + F_A (\text{impact}) \\
 &= 812 + 24,705 \\
 &= 25,517 \text{ lbs}
 \end{aligned} \tag{1}$$

$$\begin{aligned}
 F_b &= \text{net bolt tension, considering applied external loads, thermal loads} \\
 &\quad \text{and pretension loads (Shigley)} \\
 &= K_b P / (K_b + K_m) + F_i + F_t \\
 &= 38,292 \text{ lbs (at } 0^\circ); F_m < 0 \\
 &= P; F_m \geq 0
 \end{aligned} \tag{m}$$

where:

$$\begin{aligned}
 P &= \text{external load, equation} \\
 &= 25,517 \text{ lbs}
 \end{aligned} \tag{1}$$

$$\begin{aligned}
 F_t &= \text{thermal load, equation} \\
 &= 1423 \text{ lbs}
 \end{aligned} \tag{c}$$

$$\begin{aligned}
 F_i &= \text{preload, equation} \\
 &= 34,770 \text{ lbs}
 \end{aligned} \tag{d}$$

$$\begin{aligned}
 K_b &= \text{bolt stiffness, equation} \\
 &= 1.903 \times 10^6 \text{ lb/in}
 \end{aligned} \tag{f}$$

$$\begin{aligned}
 K_m &= \text{lid stiffness, equation} \\
 &= 2.112 \times 10^7 \text{ lb/in}
 \end{aligned} \tag{g}$$

$$\begin{aligned}
 F_m &= \text{clamping force} = K_m P / (K_b + K_m) - F_i - F_t \\
 &= -12,785 \text{ lbs}
 \end{aligned}$$

$$\begin{aligned}
 f_b &= \text{bolt tension stress} \\
 &= F_b / A_b = 38,292 / 0.6051
 \end{aligned} \tag{n}$$

$$= 63,282 \text{ psi}$$

$$f_v = \text{bolt nominal shear stress} \quad (o)$$

$$= F_L/A_b$$

$$\text{Principal Stresses } (\sigma_1, \sigma_2) = f_b/2 \pm [(f_b/2)^2 + f_v^2]^{0.5} \quad (p)$$

$$= (59,924)/2 \pm [(59,924/2)^2 + 6752^2]^{0.5} \text{ (at } 90^\circ)$$

$$= 29,962 \pm 30,713$$

$$= -751 \text{ psi and } 60,675 \text{ psi}$$

$$\text{Stress Intensity (at } 90^\circ) \quad (q)$$

$$S_I = \sigma_1 - \sigma_2 = -751 - 60,675$$

$$= 61,427 \text{ psi}$$

$$\text{Margin of Safety (at } 90^\circ) \quad (r)$$

$$MS = S_y/S_I - 1 = 81.9/61.427 - 1$$

$$= +0.33$$

Table 2.10.9-1 NAC-LWT Cask Hot Bolt Analysis Hypothetical Accident Conditions

Nominal Diameter (in):	1.00		Longitudinal Weight (lbs):	4941
Number of Bolts:	12		Lateral Weight (lbs):	941
Service Stress, Sy (ksi):	81.9	} at a 300 degree-F Service Temperature	Service DT (degrees):	157
Bolt Expansion (in/in):	9E-06		[default value =]	230
Bolt Modulus (ksi):	26700			
Lid Expansion (in/in):	9E-06			
Lid Modulus (ksi):	27000		CALCULATED LOADS & STIFFNESS	
Stress Area (in2):	0.6051		Bolt Thermal Load (lbs):	1423
Grip Length (in):	7.99		Bolt Preload (lbs):	34770
Maximum Pressure (psi):	50		Bolt Pressure Load (lbs):	812
Seal Diameter (in):	15.750		Bolt Stiffness (lbs/in):	1.9E+06
Preload Torque (ft-lbs):	260	at RT	Lid Stiffness (lbs/in):	2.1E+07
Nominal Room Temp, RT:	70	deg-F		
Bolt Circle Diameter (in):	17.88			
Lid Diameter (in):	22.50			

Angle wrt Vert. (Deg)	Impact Accel. (g)	<**** LOADS (lbs.) ****>				<**** STRESSES (psi) ****>				Margin of Safety	
		Impact Tension	Shear	Bolt Tension Applied	Net	Direct Tension	Shear	Principal Sig-1	Principal Sig-2		Stress Intens.
0 End	15.80	6506	0	7317	36795	60808	0	0	60808	60808	0.35
5 (+)	14.69	8216	100	9028	36936	61041	166	0	61041	61042	0.34
10 (+)	13.57	7506	185	8318	36877	60944	305	-2	60946	60947	0.34
15.7 Corner	12.30	6650	261	7462	36807	60828	431	-3	60831	60834	0.35
20 (+)	12.99	6858	349	7670	36824	60856	576	-5	60862	60867	0.35
25 (+)	13.80	7025	457	7837	36838	60879	756	-9	60888	60898	0.34
30 (+)	14.61	7106	573	7918	36845	60890	947	-15	60905	60919	0.34
35 (+)	15.42	7093	693	7905	36843	60888	1146	-22	60910	60931	0.34
40 (+)	16.22	6980	818	7792	36834	60873	1352	-30	60903	60933	0.34
45 (+)	17.03	6764	944	7576	36816	60844	1561	-40	60884	60924	0.34
50 (+)	17.84	6440	1072	7252	36790	60800	1771	-52	60851	60903	0.34
55 (+)	18.65	6007	1198	6819	36754	60741	1980	-64	60805	60870	0.35
60 (+)	19.45	5463	1321	6275	36709	60667	2183	-78	60745	60824	0.35
65 (+)	20.26	4809	1440	5621	36656	60578	2380	-93	60671	60765	0.35
70 (+)	21.07	4047	1553	4859	36593	60474	2566	-109	60583	60692	0.35
75 (+)	21.88	3180	1657	3992	36522	60356	2739	-124	60480	60604	0.35
80 (+)	22.68	2212	1752	3024	36442	60225	2895	-139	60364	60503	0.35
85 (+)	23.49	1150	1835	1962	36355	60080	3033	-153	60233	60386	0.36
90 Side	24.30	0	1906	812	36260	59924	3149	-165	60089	60254	0.36

Minimum Margin of Safety: 0.34

2.10.10 Finite Element Stress Results for the 30-Foot Drop Accident Conditions

2.10.10.1 Discussion

The following accident conditions were identified for a detailed finite element stress presentation:

- A 30-foot top end drop (drop orientation = $\phi = 0^\circ$, where ϕ is defined as the impact orientation; that is, the angle between the impact direction and the cask centerline), 130°F ambient temperature, maximum decay heat load.
- A 30-foot top corner drop (drop orientation = $\phi = 15.74^\circ$), 130°F ambient temperature, maximum decay heat load.
- A 30-foot top oblique drop (drop orientation = $\phi = 60^\circ$), 130°F ambient temperature, maximum decay heat load.
- A 30-foot side drop (drop orientation = $\phi = 90^\circ$), 130°F ambient temperature, maximum decay heat load.

The top end ($\phi = 0^\circ$), top corner ($\phi = 15.74^\circ$), top oblique ($\phi = 60^\circ$) and side ($\phi = 90^\circ$) drops envelope all of the drop orientations.

A 1.12-inch outer shell thickness is considered in the finite element analyses for the top end, top corner and top oblique drop conditions. The analyses results are conservative because the current NAC-LWT cask design has a 1.20-inch thick outer shell. The 30-foot side drop analysis considers the 1.20-inch outer shell thickness. The structural stiffness of the neutron shield shell is not considered in the finite element stress analyses.

2.10.10.2 Procedures

The analysis procedures for the above selected events are as follows:

- Perform an ANSYS analysis for each of the individual loadings:
 - a. Thermal Hot (130°F)
 - b. Maximum Internal Pressure (50 psi)
 - c. Bolt Preload (250,000 lbs)¹
 - d. Impact and Inertial Loads/30-Foot Top End Drop (60 g impact load; $\phi = 0^\circ$)
 - e. Impact and Inertial Loads/30-Foot Top Corner Drop (60.4 g impact load; $\phi = 15.74^\circ$)

¹ The total bolt preload has been increased to 418,116 lbs (34,843 lb/bolt) to provide the required compression force for the metal O-ring seal. Since the stresses at the locations evaluated in this analysis are less than 0.3 ksi for the bolt preload condition, this change is negligible.

- | | | |
|----|--|--|
| f. | Impact and Inertial Loads/30-Foot Top Oblique Drop | (44.4 g impact load; $\phi = 60^\circ$) |
| g. | Impact and Inertial Loads/30-Foot Side Drop | (49.7 g impact load; $\phi = 90^\circ$) |

Note that the fabrication stresses are considered negligible as explained in Section 2.6.11. The puncture analysis is performed using classical hand calculations and, therefore, is not discussed here.

- Tabulate the stress results that are calculated for the 123 selected points on the cask for each load condition. Both the stress components and the principal stresses are included. The 123 selected points are located at the 26 selected sections shown in Figure 2.10.10-1. The stress point locations are tabulated in Table 2.10.10-1. The constraint forces for the 30-foot top end drop ($\phi = 0^\circ$), the 30-foot top corner drop ($\phi = 15.74^\circ$), the 30-foot top oblique drop ($\phi = 60^\circ$), and the 30-foot side drop ($\phi = 90^\circ$) conditions are tabulated in Table 2.10.10-2 through Table 2.10.10-5, respectively.

For the thin cylinder sections (those selected in the central region of the inner and outer shells), it is only necessary to show the stresses at the inner surface and the outer surface because a linear stress distribution is present for the stress linearization calculations. For thick sections and for thin sections at structural discontinuities, the stresses are presented for several points through the thickness to adequately define the stress distribution for the stress linearization calculations.

- Provide additional stress tables, which show the combined stresses (that is, the primary and the primary plus secondary stress categories) at the same selected points mentioned in step 2. The primary stress is obtained from the stress results induced by all of the primary loads (that is, internal pressure, bolt preload, impact and inertial loads). The primary plus secondary stress is the result of all of the primary loads plus the thermal load.

As explained in Appendix 2.10.2, the ANSYS STIF12 element (the gap or interface element) is used in the finite element model to accurately represent the fact that no physical bonding exists between the lead and the surrounding stainless steel. The gap (interface) element is nonlinear; that is, the element operates bilinearly and requires an iterative solution process with the stiffness matrix reformulated during each iteration. This implies that the gap element status (being active or not) could change between the load analyses; therefore, it is preferable to calculate the primary stresses using the combined load finite element analysis. The same is true for the primary plus secondary stresses.

- Use the results of the combined stresses obtained in step 3 (the primary stresses) to calculate the primary membrane (P_m) and primary membrane plus primary bending ($P_m + P_b$) stresses, as specified in Regulatory Guide 7.6. The P_m and $P_m + P_b$ stresses will be calculated for 26 selected sections in the cask. The methodology used to calculate the P_m and $P_m + P_b$ stresses at a selected section is explained in detail on pages 5.2.2 through 5.2.12 in the ANSYS Theoretical Manual, Rev. 4.2, "Stress Linearization."

- The P_m and $P_m + P_b$ stresses calculated in step 4 are then compared with the allowable stresses in accordance with the stress requirements specified in Regulatory Guide 7.6.

2.10.10.3 Analysis and Results

A thorough discussion of the NAC-LWT cask finite element model can be found in Section 2.10.2.

Figure 2.10.10-1 presents a sketch of the selected sections in the cask. Each section contains two or more nodal points. The locations for the 123 selected nodal points are given in Table 2.10.10-1.

The stress results, calculated for each individual loading (hot temperature, internal pressure, bolt preload and impact loads) at the 123 nodal points on the cask, are tabulated in Table 2.10.10-6 through Table 2.10.10-14. The combined stresses, classified as the primary, primary plus secondary, P_m and $P_m + P_b$ stress categories, are derived from performing steps 3 and 4 of Section 2.10.10.2 and are tabulated for each drop accident. The stress qualifications of P_m and $P_m + P_b$ are derived from step 5, in accordance with Regulatory Guide 7.6, and are tabulated for each drop accident.

2.10.10.3.1 30-Foot Top End Drop ($\phi = 0^\circ$)

The event scenario is that the cask, equipped with impact limiters, falls through a distance of 30 feet and strikes the unyielding surface on the top end of the package.

The types of loading involved in a top end drop accident include: (1) thermal, (2) internal pressure, (3) closure lid bolt preload, and (4) impact and inertial loads resulting from the end impact. These loadings and the boundary conditions, used in the finite element top end drop analysis, have been discussed in Section 2.7.1.1.2. In addition, the displacement constrained nodes and applied forces used for the 30-foot top end drop are given in Appendix 2.10.2.

The primary, primary plus secondary, P_m , and $P_m + P_b$ stresses induced by the 30-foot top end drop are documented in Table 2.10.10-15 through Table 2.10.10-18. As discussed in Step 3, Section 2.10.10.2, the primary stresses are preferably obtained from the stress results induced by all of the primary loads; that is, internal pressure, bolt preload, impact and inertial loads. The primary stress may also be obtained by algebraically adding the stresses induced by each of the primary loads. A comparison was made of the primary stresses calculated from the combined load method versus the superposition method, which adds the stress results of each separate loading to obtain the primary stresses. The difference is insignificant. The same is true for the primary plus secondary stresses. The stress qualification of P_m and $P_m + P_b$ is presented in Table 2.10.10-19. The P_m and $P_m + P_b$ stress tables, documented in Table 2.10.7-34 and Table 2.10.7-35, are derived based on the primary plus secondary stresses. This provides conservative results

for the P_m and $P_m + P_b$ stresses because the primary plus secondary stresses are larger than the primary stresses.

The hand-calculated method used to evaluate the cask stress for a 30-foot top end drop impact condition is provided in Section 2.10.11.1. The compressive stresses calculated by the finite element method are -3,260 psi and -2,990 psi at the cask midsection in the inner and outer shell, respectively, with an average of -3,125 psi. The hand-calculated stress at the cask midsection is -3,213 psi. The difference is less than three percent.

All margins of safety are positive. Thus, the NAC-LWT cask satisfies the 10 CFR 71 requirements for the end drop accident condition.

2.10.10.3.2 30-Foot Top Corner Drop ($\phi = 15.74^\circ$)

The event scenario is that the cask, equipped with impact limiters, falls through a distance of 30 feet and strikes the unyielding surface on the top corner of the package with the package center of gravity directly above the point of impact.

The types of loading involved in a top corner drop accident include: (1) thermal, (2) internal pressure, (3) closure lid bolt preload, and (4) impact and inertial loads resulting from the corner drop impact. These loadings and the boundary conditions, used in the finite element top corner drop analysis, have been discussed in Section 2.7.1.3.2. In addition, the displacement constrained nodes and applied forces used for the 30-foot top corner drop are given in Appendix 2.10.2.

The primary, primary plus secondary, P_m , and $P_m + P_b$ stresses induced by the 30-foot top corner drop are documented in Table 2.10.10-20 through Table 2.10.10-23. The stress qualification of P_m and $P_m + P_b$ is presented in Table 2.10.10-24. An unrealistic stress is induced by the boundary effect because of the displacement restraints at node 2561. Stresses in the region near the restraint are disregarded. As discussed in Section 2.7.1.3.3, the oblique drop condition induces an eccentric (angular) momentum, which causes a rigid body rotation of the cask and a secondary impact onto the unyielding surface. To provide dynamic equilibrium of the cask body in the oblique drop evaluation, displacement restraints are imposed on the finite element model. These restraints cause localized peak stresses in the immediate vicinity of boundary conditions.

This boundary effect attenuates very rapidly at locations slightly away from the boundary region.

To obtain a more realistic stress distribution in the free end of the cask, the method of superposition described in Section 2.7.1.3.3 is used. By this method, the stresses for the following nodes and sections have been revised for the tables in Section 2.10.10.

Impact End	Section Cuts ¹	Node Number (S) ²
Top	A through J	1 through 698
Bottom	S through Z	1481 through 2561

All margins of safety are positive. Thus, the NAC-LWT cask satisfies the 10 CFR 71 requirements for the corner drop accident condition.

2.10.10.3.3 30-Foot Top Oblique Drop ($\phi = 60^\circ$)

The event scenario is that the cask, equipped with impact limiters, falls with a drop orientation of 60 degrees from vertical through a distance of 30 feet and strikes the unyielding surface on the top corner of the cask.

The types of loading involved in a top oblique drop accident include: (1) thermal, (2) internal pressure, (3) closure lid bolt preload, and (4) impact and inertial loads resulting from the oblique drop impact. These loadings and the boundary conditions, used in the finite element top oblique drop analysis, have been discussed in Section 2.7.1.3.2. In addition, the displacement constrained nodes and applied forces used for the 30-foot top oblique drop are given in Appendix 2.10.2.

The primary, primary plus secondary, P_m , and $P_m + P_b$ stresses induced by the 30-foot top oblique drop are documented in Table 2.10.10-25 through Table 2.10.10-28. The stress qualification of P_m and $P_m + P_b$ is presented in Table 2.10.10-29. The unrealistic stresses induced by the boundary effect at node 2561 should be disregarded as explained in Section 2.10.10.3.2. For this drop evaluation, the stresses in the vicinity of the free end are revised as described in Section 2.7.1.3.3.

All margins of safety are positive. Thus, the NAC-LWT cask satisfies the 10 CFR 71 requirements for the top oblique drop accident condition.

2.10.10.3.4 30-Foot Side Drop ($\phi = 90^\circ$)

The event scenario is that the cask, equipped with impact limiters, falls with a drop orientation of 90 degrees through a distance of 30 feet and strikes the unyielding surface in the horizontal position.

The types of loading involved in a side drop accident include: (1) thermal, (2) internal pressure, (3) closure lid bolt preload, and (4) impact and inertial loads resulting from the side drop impact. These loadings and the boundary conditions, used in the finite element side drop analysis, have been discussed in Section 2.7.1.2. The 30-foot side drop analysis includes a 1.20-inch thick outer shell. Furthermore, the impact g load has been revised to 49.7 g from 52.1 g to reflect the

¹ The section cuts are identified in Figure 2.10.7-1 and their coordinates are listed in Table 2.10.7-1.

² The node numbers versus nodal coordinates are specified in Table 2.10.2-1.

final impact limiter design criteria. Based on improved fabrication techniques, the honeycomb crush strength tolerance has been revised to 3,500 psi, +5, -10 percent; thus, the maximum tolerance crush strength of the honeycomb is 3,675 psi. Since the impact load is directly proportional to the honeycomb crush strength, the maximum side impact g-load is $(3,675/3,850)(52.1) = 49.7$ g. This value has been verified by an RBCUBED program analysis.

The displacement constrained nodes and applied forces used for the 30-foot side drop are given in Appendix 2.10.2.

The finite element stress results are compared with the hand-calculated stress results (Section 2.10.11.2). The finite element method calculates the most critical stress as 68.23 ksi versus 67.24 ksi from the hand-calculated method. The difference is less than 1.5 percent.

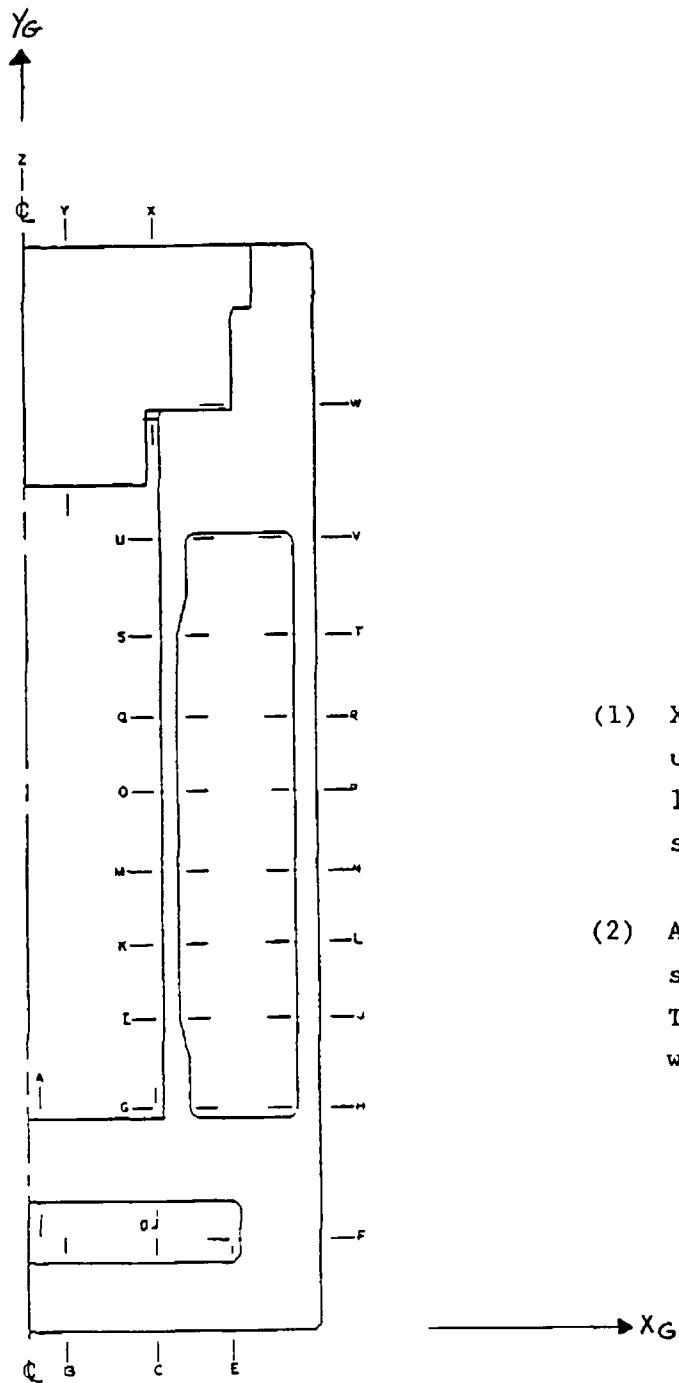
The primary, primary plus secondary, P_m , and $P_m + P_b$ stresses induced by the 30-foot side drop are documented in Table 2.10.10-30 through Table 2.10.10-33. In addition, the P_m and $P_m + P_b$ stresses at circular locations 90° and 180° are provided in Table 2.10.10-34 through Table 2.10.10-37. The stresses at circular location 0° are the most critical; therefore, they are the ones used for the stress qualification. Table 2.10.10-38 presents the stress qualification of P_m and $P_m + P_b$.

All margins of safety are positive. Thus, the NAC-LWT cask satisfies the 10 CFR 71 requirements for the side drop accident condition.

2.10.10.4 Conclusion

Based on the finite element stress analysis results for the four critical 30-foot drop conditions selected, the NAC-LWT cask design satisfies the allowable stress criteria specified in Regulatory Guide 7.6.

Figure 2.10.10-1 Stress Point Locations



- (1) X_G and Y_G are global axes used to measure the location of selected sections.
- (2) A, ...Z are selected section designations. There are 26 sections with 52 stress points.

Table 2.10.10-1 Stress Point Locations

Designation	Node No.	Location	
		x	y
A1	327	0.85	10.50
A2	302	0.85	10.25
A3	277	0.85	10.00
A4	252	0.85	9.50
A5	227	0.85	8.50
A6	202	0.85	7.50
A7	177	0.85	6.50
B1	104	2.55	3.50
B2	79	2.55	2.50
B3	54	2.55	1.50
B4	29	2.55	0.50
B5	4	2.55	0.00
C1	110	6.6875	3.50
C2	85	6.6875	2.50
C3	60	6.6875	1.50
C4	35	6.6875	0.50
C5	10	6.6875	0.00
D1	335	6.6875	10.50
D2	310	6.6875	10.25
D3	285	6.6875	10.00
D4	260	6.6875	9.50
D5	235	6.6875	8.50
D6	210	6.6875	7.50
D7	185	6.6875	6.50
E1	118	10.375	3.50
E2	93	10.375	2.50
E3	68	10.375	1.50
E4	43	10.375	0.50
E5	18	10.375	0.00
F1	143	10.375	4.50
F2	144	11.315	4.50

Table 2.10.10-1 Stress Point Locations (continued)

Designation	Node No.	Location	
		x	y
F3	145	12.001	4.50
F4	146	12.688	4.50
F5	147	13.188	4.50
F6	148	13.561	4.50
F7	149	13.934	4.50
F8	150	14.307	4.50
G1	335	6.6875	10.50
G2	336	6.9375	10.50
G3	337	7.1875	10.50
G4	338	7.4375	10.50
G5	339	7.9375	10.50
G6	340	8.4375	10.50
H1	346	12.688	10.50
H2	347	13.188	10.50
H3	348	13.561	10.50
H4	349	13.934	10.50
H5	350	14.307	10.50
I1	621	6.6875	16.50
I2	624	7.4375	16.50
J1	635	13.188	16.50
J2	638	14.307	16.50
K1	841	6.6875	35.50
K2	844	7.4375	35.50
L1	855	13.188	35.50
L2	858	14.307	35.50
M1	941	6.6875	60.50
M2	944	7.4375	60.50
N1	955	13.188	60.50
N2	958	14.307	60.50
O1	1101	6.6875	100.50
O2	1104	7.4375	100.50

Table 2.10.10-1 Stress Point Locations (continued)

Designation	Node No.	Location	
		x	y
P1	1115	13.188	100.50
P2	1118	14.307	100.50
Q1	1261	6.6875	140.50
Q2	1264	7.4375	140.50
R1	1275	13.188	140.50
R2	1278	14.307	1450.50
S1	1561	6.6875	179.50
S2	1564	7.4375	179.50
T1	1575	13.188	179.50
T2	1578	14.307	179.50
U1	1841	6.6875	185.50
U2	1844	8.4375	185.50
V1	1852	12.688	185.50
V2	1856	14.307	185.50
W1	1969	10.315	191.75
W2	1970	11.315	191.75
W3	1971	12.001	191.75
W4	1972	12.688	191.75
W5	1973	13.188	191.75
W6	1974	13.561	191.75
W7	1975	13.934	191.75
W8	1976	14.307	191.75
X1	2370	6.6875	191.75
X2	2390	6.6875	192.75
X3	2410	6.6875	193.75
X4	2430	6.6875	194.75
X5	2450	6.6875	195.75
X6	2470	6.6875	196.75
X7	2490	6.6875	197.75
X8	2510	6.6875	198.25
X9	2530	6.6875	198.75

Table 2.10.10-1 Stress Point Locations (continued)

Designation	Node No.	Location	
		x	y
X10	2550	6.6875	199.25
X11	2570	6.6875	199.75
Y1	2305	3.40	188.50
Y2	2325	3.40	189.75
Y3	2345	3.40	190.75
Y4	2365	3.40	191.75
Y5	2385	3.40	192.75
Y6	2405	3.40	193.75
Y7	2425	3.40	194.75
Y8	2445	3.40	195.75
Y9	2465	3.40	196.75
Y10	2485	3.40	197.75
Y11	2505	3.40	198.25
Y12	2525	3.40	198.75
Y13	2545	3.40	199.25
Y14	2565	3.40	199.75
Z1	2301	0.00	188.50
Z2	2321	0.00	189.75
Z3	2341	0.00	190.75
Z4	2361	0.00	191.75
Z5	2381	0.00	192.75
Z6	2404	0.00	193.75
Z7	2421	0.00	194.75
Z8	2441	0.00	195.75
Z9	2461	0.00	196.75
Z10	2481	0.00	197.75
Z11	2501	0.00	198.25
Z12	2521	0.00	198.75
Z13	2541	0.00	199.25
Z14	2561	0.00	199.75

Table 2.10.10-2 Constraint Forces for the 30-Foot Top End Drop Condition ($\phi = 0^\circ$)

Node	FX	FY	FZ
1	0.722137		
25		-3487.13	
26	0.509030		
51	0.242975		
76	-0.581758		
101	-0.893385		
126	0.417712-001		
151	-0.425787-001		
176	1.21218		
201	0.902732		
226	-0.669590-001		
251	-0.522695		
276	-0.406303		
301	-0.717323		
326	-0.401629		
2301	-9.15600		
2321	-5.97171		
2341	-0.331048		
2361	2.36181		
2381	2.07107		
2401	-0.284169		
2421	-2.24827		
2441	-2.50453		
2461	-0.548714		
2481	1.73193		
2501	2.51800		
2521	3.71850		
2541	3.87877		
2561	4.73436		
3101	0.789074-001		
3176	-0.780999-001		
TOTAL	-0.280365-011	-3487.13	0.000000

**Table 2.10.10-3 Constraint Forces for the 30-Foot Top Corner Drop Condition
($\phi = 15.74^\circ$)**

Node	FX	FY	FZ
1	-3122.0370	-3760.2436	1159.4410
25	-183131.11		58533.923
2561	50113.502		-44114.872
TOTAL	-136139.64	-3760.2436	15578.492

**Table 2.10.10-4 Constraint Forces for the 30-Foot Top Oblique Drop Condition
($\phi = 60^\circ$)**

Node	FX	FY	FZ
1	-5429.7002	-2619.1410	3662.7469
2561	151886.32		-134475.85
TOTAL	146456.62	-2619.1410	-130813.10

**Table 2.10.10-5 Constraint Forces for the 30-Foot Side Drop Condition
($\phi = 90^\circ$)**

Node	FX	FY	FZ
1	4322.1611	1098.7180	-3316.9233
2561	7223.3599		-6394.6917
TOTAL	11545.521	1098.7180	-9711.6149

Table 2.10.10-6 Stress Components – Thermal; 130°F; 1.12-Inch Outer Shell Thickness

Stress Points		Stresses						
Location	Node	S _x	S _y	S _z	S _{xy}	S ₁	S ₂	S ₃
A1	327	5.32	0.07	5.30	0.24	5.33	5.30	0.06
A2	302	4.45	0.07	4.45	-0.02	4.45	4.45	0.07
A3	277	3.58	0.01	3.57	-0.10	3.58	3.57	0.01
A4	252	1.85	-0.03	1.85	-0.02	1.85	1.85	-0.03
A5	227	-1.57	-0.05	-1.58	-0.02	-0.05	-1.57	-1.58
A6	202	-4.97	-0.08	-4.98	-0.01	-0.08	-4.97	-4.98
A7	177	-8.41	-0.09	-8.36	0.00	-0.09	-8.36	-8.41
B1	104	0.27	0.03	0.25	0.08	0.30	0.25	0.01
B2	79	1.18	0.05	1.19	0.05	1.19	1.18	0.04
B3	54	2.13	0.09	2.15	0.04	2.15	2.13	0.09
B4	29	3.14	0.05	3.13	0.07	3.14	3.13	0.05
B5	4	4.87	-0.03	4.82	-0.41	4.91	4.82	-0.06
C1	110	0.53	-0.79	0.72	0.22	0.72	0.56	-0.83
C2	85	1.27	-0.64	1.54	0.22	1.54	1.29	-0.66
C3	60	2.09	-0.32	5.52	0.24	2.52	2.11	-0.35
C4	35	3.15	-0.10	3.64	0.08	3.64	3.15	-0.10
C5	10	5.05	-0.02	5.47	-0.12	5.47	5.05	-0.03
D1	335	0.10	-8.29	1.64	-0.89	1.64	0.19	-8.38
D2	310	2.81	-4.74	2.74	-0.98	2.93	2.74	-4.86
D3	285	2.62	-3.03	2.62	-0.87	2.75	2.62	-3.16
D4	260	1.45	-2.10	1.46	-0.80	1.63	1.46	-2.27
D5	235	-0.83	-1.81	-1.23	-0.61	-0.54	-1.23	-2.10
D6	210	-3.47	-1.74	-4.13	0.02	-1.74	-3.47	-4.13
D7	185	-6.52	-1.67	-7.26	0.95	-1.49	-6.70	-7.26
E1	118	3.57	-3.22	2.02	3.56	5.10	2.02	-4.75
E2	93	0.78	0.62	2.50	1.53	2.50	2.24	-0.83
E3	68	0.99	0.23	2.89	1.13	2.89	1.80	-0.58
E4	43	1.03	0.05	3.42	0.54	3.42	1.27	-0.19
E5	18	2.13	0.02	4.88	0.16	4.88	2.14	0.01
F1	143	-9.96	-8.38	-1.96	6.23	-1.96	-2.89	-15.45
F2	144	-8.66	5.37	1.53	3.39	6.15	1.53	-9.44

Table 2.10.10-6 Stress Components – Thermal; 130°F; 1.12-Inch Outer Shell Thickness
(continued)

Stress Points		Stresses						
Location	Node	S _x	S _y	S _z	S _{xy}	S ₁	S ₂	S ₃
F3	145	-5.57	3.38	1.40	0.44	3.40	1.40	-5.59
F4	146	-2.45	2.61	1.89	-0.26	2.62	1.89	-2.46
F5	147	-1.21	2.14	2.08	-0.40	2.18	2.08	-1.26
F6	148	-0.61	1.92	2.19	-0.38	2.19	1.98	-0.66
F7	149	-0.27	1.83	2.29	-0.24	2.29	1.86	-0.30
F8	150	-0.12	1.98	2.40	-0.14	2.40	1.99	-0.13
G1	335	0.10	-8.29	1.64	-0.89	1.64	0.19	-8.38
G2	336	0.33	-4.60	2.80	0.11	2.80	0.33	-4.60
G3	337	1.57	-1.77	3.93	0.59	3.93	1.67	-1.87
G4	338	2.62	1.52	5.11	-0.04	5.11	2.62	1.52
G5	339	5.97	6.96	7.44	-2.85	9.36	7.44	3.58
G6	340	7.46	1.89	6.59	-3.30	8.99	6.59	0.36
H1	346	-9.25	-3.91	-2.66	0.10	-2.66	-3.90	-9.26
H2	347	-4.69	3.46	0.77	0.32	3.47	0.77	-4.70
H3	348	-2.27	7.91	2.87	-0.15	7.91	2.87	-2.28
H4	349	-0.79	10.55	4.07	-0.31	10.55	4.07	-0.80
H5	350	-0.23	14.21	5.20	-0.27	14.22	5.20	-0.24
I1	621	0.00	3.12	0.38	0.03	3.12	0.38	0.00
I2	624	0.01	1.94	0.19	0.01	1.94	0.19	0.01
J1	635	0.00	10.71	0.23	0.05	10.71	0.23	0.00
J2	638	0.01	8.43	-0.14	0.05	8.43	0.00	-0.14
K1	841	0.00	2.27	-0.21	-0.01	2.27	0.00	-0.21
K2	844	0.00	2.69	0.19	0.01	2.69	0.19	0.00
L1	855	0.00	9.25	-0.36	0.00	9.25	0.00	-0.36
L2	858	0.00	9.78	0.18	0.00	9.78	0.18	0.00
M1	941	0.00	2.21	-0.27	0.00	2.21	0.00	-0.27
M2	944	0.00	2.75	0.25	0.00	2.75	0.25	0.00
N1	955	0.00	9.13	-0.45	0.00	9.13	0.00	-0.45
N2	958	0.00	9.84	0.23	0.00	9.84	0.23	0.00
O1	1101	0.00	2.22	-0.27	0.00	2.22	0.00	-0.27
O2	1104	0.00	2.75	0.25	0.00	2.75	0.25	0.00

Table 2.10.10-6 Stress Components – Thermal; 130°F; 1.12-Inch Outer Shell Thickness
(continued)

Stress Points		Stresses						
Location	Node	S _x	S _y	S _z	S _{xy}	S ₁	S ₂	S ₃
P1	1115	0.00	9.10	-0.49	0.00	9.10	0.00	-0.49
P2	1118	0.00	9.85	0.24	0.00	9.85	0.24	0.00
Q1	1261	0.00	2.28	-0.18	0.00	2.28	0.00	-0.18
Q2	1264	0.00	2.69	0.22	0.00	2.69	0.22	0.00
R1	1275	0.00	9.15	-0.46	0.00	9.15	0.00	-0.46
R2	1278	-0.01	9.88	0.09	0.00	9.88	0.09	-0.01
S1	1561	0.00	2.12	0.24	0.04	2.12	0.24	0.00
S2	1564	-0.03	2.90	0.56	0.05	2.90	0.56	-0.03
T1	1575	0.00	10.66	0.09	-0.06	10.66	0.09	0.00
T2	1578	0.00	8.45	-0.12	-0.05	8.45	0.00	-0.12
U1	1841	0.02	0.16	-0.54	-0.09	0.21	-0.03	-0.54
U2	1844	0.21	1.24	0.17	-0.07	1.24	0.21	0.17
V1	1852	-5.69	-2.17	-2.44	-1.18	-1.81	-2.44	-6.05
V2	1856	-0.31	12.07	3.55	0.16	12.07	3.55	-0.32
W1	1969	-0.77	-1.85	0.01	-0.81	0.01	-0.34	-2.28
W2	1970	-0.02	-0.76	0.70	-0.68	0.70	0.38	-1.16
W3	1971	-0.11	-0.09	0.96	-0.56	0.96	0.46	-0.65
W4	1972	-0.09	0.54	1.21	-0.48	1.21	0.80	-0.35
W5	1973	-0.07	0.95	1.37	-0.38	1.37	1.07	-0.20
W6	1974	-0.06	1.27	1.52	-0.26	1.52	1.32	-0.11
W7	1975	-0.03	1.55	1.66	-0.13	1.66	1.56	-0.04
W8	1976	0.01	1.81	1.79	-0.07	1.81	1.79	0.01
X1	2370	-1.24	-0.33	-0.33	0.60	-0.03	-0.33	-1.54
X2	2390	-0.33	-0.94	-0.24	0.44	-0.10	-0.24	-1.17
X3	2410	-0.36	-0.54	-0.07	0.06	-0.07	-0.34	-0.56
X4	2430	-0.34	-0.39	0.00	-0.13	0.00	-0.23	-0.50
X5	2450	-0.40	-0.23	0.06	-0.26	0.06	-0.04	-0.60
X6	2470	-0.41	-0.13	0.13	-0.33	0.13	0.08	-0.63
X7	2490	-0.38	-0.06	0.25	-0.34	0.25	0.15	-0.59
X8	2510	-0.34	-0.03	0.34	-0.32	0.34	0.17	-0.54
X9	2530	-0.28	-0.01	0.46	-0.26	0.46	0.15	-0.44

Table 2.10.10-6 Stress Components – Thermal; 130°F; 1.12-Inch Outer Shell Thickness
(continued)

Stress Points		Stresses						
Location	Node	S _x	S _y	S _z	S _{xy}	S ₁	S ₂	S ₃
X10	2550	-0.22	0.00	0.61	-0.17	0.61	0.09	-0.31
X11	2570	0.62	0.00	1.58	-0.05	1.58	0.62	-0.01
Y1	2305	0.57	-0.03	0.49	-0.04	0.57	0.49	-0.03
Y2	2325	0.02	-0.05	-0.01	0.05	0.05	-0.01	-0.08
Y3	2345	-0.28	-0.11	-0.34	0.05	-0.10	-0.29	-0.34
Y4	2365	-0.55	-0.16	-0.61	0.04	-0.16	-0.56	-0.61
Y5	2385	-0.71	-0.21	-0.78	0.05	-0.20	-0.74	-0.78
Y6	2405	-0.80	-0.25	-0.87	0.04	-0.25	-0.80	-0.87
Y7	2425	-0.78	-0.27	-0.87	0.00	-0.27	-0.78	-0.87
Y8	2445	-0.71	-0.25	-0.80	-0.05	-0.25	-0.72	-0.80
Y9	2465	-0.61	-0.19	-0.67	-0.08	-0.17	-0.63	-0.67
Y10	2485	-0.43	-0.11	-0.44	-0.08	-0.09	-0.44	-0.45
Y11	2505	-0.29	-0.05	-0.29	-0.04	-0.04	-0.29	-0.30
Y12	2525	-0.11	-0.02	-0.11	-0.01	-0.02	-0.11	-0.11
Y13	2545	0.13	0.00	0.11	-0.01	0.13	0.11	0.00
Y14	2565	1.25	0.00	1.15	0.07	1.26	1.15	0.00
Z1	2301	0.51	0.01	0.49	0.00	0.51	0.49	0.01
Z2	2321	0.08	0.03	0.08	0.00	0.08	0.08	0.03
Z3	2341	-0.24	0.07	-0.24	0.00	0.07	-0.24	-0.24
Z4	2361	-0.51	0.09	-0.50	0.00	0.09	-0.50	-0.51
Z5	2381	-0.68	0.11	-0.68	0.00	0.11	-0.68	-0.68
Z6	2401	-0.78	0.11	-0.78	0.00	0.11	-0.78	-0.78
Z7	2421	-0.80	0.11	-0.80	0.00	0.11	-0.80	-0.80
Z8	2441	-0.73	0.10	-0.72	0.00	0.10	-0.72	-0.73
Z9	2461	-0.58	0.09	-0.58	0.00	0.09	-0.58	-0.58
Z10	2481	-0.35	0.07	-0.34	0.00	0.07	-0.34	-0.35
Z11	2501	-0.21	0.05	-0.21	0.00	0.05	-0.21	-0.21
Z12	2521	-0.05	0.03	-0.06	0.00	0.03	-0.05	-0.06
Z13	2541	0.11	0.01	0.10	0.00	0.11	0.10	0.01
Z14	2561	1.06	0.01	1.06	0.00	1.06	1.06	0.01

Table 2.10.10-7 Stress Components – Internal Pressure; 50 psi; 1.12-Inch Outer Shell Thickness

Stress Points		Stresses						
Location	Node	S _x	S _y	S _z	S _{xy}	S ₁	S ₂	S ₃
A1	327	-0.11	-0.05	-0.11	0.00	-0.05	-0.11	-0.11
A2	302	-0.09	-0.05	-0.09	0.00	-0.05	-0.09	-0.09
A3	277	-0.07	-0.05	-0.07	0.01	-0.05	-0.07	-0.07
A4	252	-0.04	-0.04	-0.04	0.01	-0.03	-0.04	-0.05
A5	227	0.01	-0.03	0.01	0.01	0.01	0.01	-0.03
A6	202	0.06	-0.01	0.06	0.01	0.06	0.06	-0.01
A7	177	0.12	0.00	0.12	0.00	0.12	0.12	0.00
B1	104	0.01	0.00	0.01	0.00	0.01	0.01	0.00
B2	79	0.01	0.00	0.01	0.00	0.01	0.01	0.00
B3	54	0.00	0.00	0.00	0.00	0.00	0.00	0.00
B4	29	0.00	0.00	0.00	0.00	0.00	0.00	0.00
B5	4	0.00	0.00	0.00	0.00	0.00	0.00	0.00
C1	110	0.01	0.00	0.01	0.00	0.01	0.01	0.00
C2	85	0.01	0.00	0.01	0.00	0.01	0.01	0.00
C3	60	0.00	0.00	0.00	0.00	0.00	0.00	0.00
C4	35	0.00	0.00	0.00	0.00	0.00	0.00	0.00
C5	10	0.00	0.00	0.00	0.00	0.00	0.00	0.00
D1	335	0.24	0.39	0.16	0.11	0.45	0.19	0.16
D2	310	0.05	0.23	0.07	0.08	0.23	0.07	0.02
D3	285	0.02	0.14	0.03	0.06	0.16	0.03	0.00
D4	260	0.00	0.07	0.02	0.04	0.09	0.02	-0.02
D5	235	-0.01	0.03	0.01	0.03	0.04	0.01	-0.02
D6	210	-0.01	0.01	0.02	0.02	0.02	0.02	-0.02
D7	185	-0.02	0.00	0.03	0.01	0.03	0.00	-0.03
E1	118	-0.01	-0.01	0.01	0.00	0.01	0.01	-0.01
E2	93	0.00	0.00	0.00	0.00	0.00	0.00	0.00
E3	68	0.00	0.00	0.00	0.00	0.00	0.00	0.00
E4	43	0.00	0.00	0.00	0.00	0.00	0.00	0.00
E5	18	0.00	0.00	0.00	0.00	0.00	0.00	0.00
F1	143	0.00	-0.02	0.00	0.00	0.00	0.00	-0.02
F2	144	0.00	-0.01	0.00	0.01	0.00	0.00	-0.01

Table 2.10.10-7 Stress Components – Internal Pressure; 50 psi; 1.12-Inch Outer Shell Thickness (continued)

Stress Points		Stresses						
Location	Node	S _x	S _y	S _z	S _{xy}	S ₁	S ₂	S ₃
F3	145	0.00	0.00	0.01	0.01	0.01	0.01	-0.01
F4	146	0.00	0.00	0.01	0.01	0.01	0.01	-0.01
F5	147	0.00	0.01	0.01	0.01	0.01	0.01	0.00
F6	148	0.00	0.01	0.01	0.00	0.01	0.01	0.00
F7	149	0.00	0.01	0.01	0.00	0.01	0.01	0.00
F8	150	0.00	0.01	0.01	0.00	0.01	0.01	0.00
G1	335	0.24	0.39	0.16	0.11	0.45	0.19	0.16
G2	336	0.14	0.19	0.08	0.06	0.23	0.10	0.08
G3	337	0.06	0.12	0.04	0.02	0.12	0.05	0.04
G4	338	0.02	0.04	0.01	0.01	0.05	0.01	0.01
G5	339	-0.04	-0.08	-0.04	0.03	-0.02	-0.04	-0.10
G6	340	-0.06	-0.04	-0.04	0.04	-0.01	-0.04	-0.10
H1	346	0.00	0.01	0.00	0.00	0.01	0.00	0.00
H2	347	0.00	0.02	0.00	0.00	0.02	0.00	0.00
H3	348	0.00	0.02	0.00	0.00	0.02	0.00	0.00
H4	349	0.00	0.01	0.00	0.00	0.01	0.00	0.00
H5	350	0.00	0.01	0.00	0.00	0.01	0.00	0.00
I1	621	-0.05	0.08	0.34	-0.01	0.34	0.08	-0.05
I2	624	-0.02	0.16	0.33	0.00	0.33	0.16	-0.02
J1	635	0.00	0.02	0.00	0.00	0.02	0.00	0.00
J2	638	0.00	0.02	0.00	0.00	0.02	0.00	0.00
K1	841	-0.05	0.10	0.36	0.02	0.36	0.10	-0.05
K2	844	-0.01	0.10	0.32	0.02	0.32	0.10	-0.01
L1	855	0.00	0.02	0.00	0.00	0.02	0.00	0.00
L2	858	0.00	0.02	0.00	0.00	0.02	0.00	0.00
M1	941	-0.05	0.10	0.36	0.00	0.36	0.10	-0.05
M2	944	-0.01	0.11	0.32	0.00	0.32	0.10	-0.01
N1	955	0.00	0.02	0.00	0.00	0.02	0.00	0.00
N2	958	0.00	0.02	0.00	0.00	0.02	0.00	0.00
O1	1101	-0.05	0.10	0.36	0.00	0.36	0.10	-0.05
O2	1104	-0.01	0.10	0.32	0.00	0.32	0.10	-0.01

Table 2.10.10-7 Stress Components – Internal Pressure; 50 psi; 1.12-Inch Outer Shell Thickness (continued)

Stress Points		Stresses						
Location	Node	S _x	S _y	S _z	S _{xy}	S ₁	S ₂	S ₃
P1	1115	0.00	0.02	0.00	0.00	0.02	0.00	0.00
P2	1118	0.00	0.02	0.00	0.00	0.02	0.00	0.00
Q1	1261	-0.05	0.10	0.36	0.00	0.36	0.10	-0.05
Q2	1264	-0.01	0.10	0.32	0.00	0.32	0.10	-0.01
R1	1275	0.00	0.02	0.00	0.00	0.02	0.00	0.00
R2	1278	0.00	0.02	0.00	0.00	0.02	0.00	0.00
S1	1561	-0.05	0.10	0.35	0.00	0.35	0.10	-0.05
S2	1564	-0.02	0.14	0.32	0.00	0.32	0.14	-0.02
T1	1575	0.00	0.03	0.00	0.00	0.03	0.00	0.00
T2	1578	0.00	0.01	0.00	0.00	0.01	0.00	0.00
U1	1841	-0.05	0.14	0.15	-0.01	0.15	0.14	-0.05
U2	1844	-0.06	0.09	0.11	-0.01	0.11	0.09	-0.06
V1	1852	-0.03	-0.01	0.02	0.01	0.02	-0.01	-0.03
V2	1856	0.00	0.05	0.04	0.00	0.05	0.04	0.00
W1	1969	0.01	0.01	0.01	0.00	0.01	0.01	0.01
W2	1970	0.01	0.00	0.01	0.00	0.01	0.01	0.00
W3	1971	0.00	0.00	0.01	0.00	0.01	0.00	0.00
W4	1972	0.00	0.00	0.01	0.00	0.01	0.00	0.00
W5	1973	0.00	0.00	0.01	0.00	0.01	0.00	0.00
W6	1974	0.00	0.00	0.01	0.00	0.01	0.00	0.00
W7	1975	0.00	-0.01	0.01	0.00	0.01	0.00	-0.01
W8	1976	0.00	-0.01	0.00	0.00	0.00	0.00	-0.01
X1	2370	0.06	0.00	0.03	-0.04	0.08	0.03	-0.02
X2	2390	0.00	0.04	0.02	-0.04	0.06	0.02	-0.03
X3	2410	0.00	0.01	0.01	-0.02	0.03	0.01	-0.02
X4	2430	0.00	0.01	0.01	-0.02	0.02	0.01	-0.01
X5	2450	0.00	0.01	0.01	-0.01	0.02	0.01	-0.01
X6	2470	0.00	0.00	0.01	-0.01	0.01	0.01	-0.01
X7	2490	0.00	0.00	0.01	-0.01	0.01	0.01	-0.01
X8	2510	0.00	0.00	0.01	-0.01	0.01	0.01	0.00
X9	2530	0.00	0.00	0.01	0.00	0.01	0.01	0.00

Table 2.10.10-7 Stress Components – Internal Pressure; 50 psi; 1.12-Inch Outer Shell Thickness (continued)

Stress Points		Stresses						
Location	Node	S _x	S _y	S _z	S _{xy}	S ₁	S ₂	S ₃
X10	2550	0.00	0.00	0.01	0.00	0.01	0.00	0.00
X11	2570	0.00	0.00	0.01	0.00	0.01	0.00	0.00
Y1	2305	-0.07	-0.05	-0.07	0.01	-0.05	-0.07	-0.08
Y2	2325	-0.05	-0.05	-0.05	0.00	-0.05	-0.05	-0.06
Y3	2345	-0.04	-0.05	-0.04	0.00	-0.03	-0.04	-0.05
Y4	2365	-0.02	-0.04	-0.02	-0.01	-0.02	-0.02	-0.05
Y5	2385	0.00	-0.04	0.00	-0.01	0.00	0.00	-0.04
Y6	2405	0.00	-0.03	0.00	-0.01	0.01	0.00	-0.04
Y7	2425	0.01	-0.03	0.01	-0.01	0.01	0.01	-0.03
Y8	2445	0.01	-0.02	0.01	-0.01	0.01	0.01	-0.02
Y9	2465	0.01	-0.01	0.01	-0.01	0.01	0.01	-0.02
Y10	2485	0.01	-0.01	0.01	-0.01	0.01	0.01	-0.01
Y11	2505	0.01	0.00	0.01	-0.01	0.01	0.01	-0.01
Y12	2525	0.01	0.00	0.02	-0.01	0.02	0.01	0.00
Y13	2545	0.01	0.00	0.02	0.00	0.02	0.01	0.00
Y14	2565	0.02	0.00	0.02	0.00	0.02	0.02	0.00
Z1	2301	-0.08	-0.05	-0.08	0.00	-0.05	-0.08	-0.08
Z2	2321	-0.05	-0.05	-0.05	0.00	-0.05	-0.05	-0.05
Z3	2341	-0.04	-0.05	-0.04	0.00	-0.04	-0.04	-0.05
Z4	2361	-0.02	-0.05	-0.02	0.00	-0.02	-0.02	-0.05
Z5	2381	-0.01	-0.04	-0.01	0.00	-0.01	-0.01	-0.04
Z6	2401	0.00	-0.04	0.00	0.00	0.00	0.00	-0.04
Z7	2421	0.01	-0.03	0.00	0.00	0.01	0.00	-0.03
Z8	2441	0.01	-0.02	0.01	0.00	0.01	0.01	-0.02
Z9	2461	0.01	-0.02	0.01	0.00	0.01	0.01	-0.02
Z10	2481	0.01	-0.01	0.01	0.00	0.01	0.01	-0.01
Z11	2501	0.02	-0.01	0.02	0.00	0.02	0.02	-0.01
Z12	2521	0.02	0.00	0.02	0.00	0.02	0.02	0.00
Z13	2541	0.02	0.00	0.02	0.00	0.02	0.02	0.00
Z14	2561	0.03	0.00	0.03	0.00	0.03	0.03	0.00

Table 2.10.10-8 Stress Components – Bolt Preload; 1.12-Inch Outer Shell Thickness

Stress Points		Stresses						
Location	Node	S _x	S _y	S _z	S _{xy}	S ₁	S ₂	S ₃
A1	327	0.00	0.00	0.00	0.00	0.00	0.00	0.00
A2	302	0.00	0.00	0.00	0.00	0.00	0.00	0.00
A3	277	0.00	0.00	0.00	0.00	0.00	0.00	0.00
A4	252	0.00	0.00	0.00	0.00	0.00	0.00	0.00
A5	227	0.00	0.00	0.00	0.00	0.00	0.00	0.00
A6	202	0.00	0.00	0.00	0.00	0.00	0.00	0.00
A7	177	0.00	0.00	0.00	0.00	0.00	0.00	0.00
B1	104	0.00	0.00	0.00	0.00	0.00	0.00	0.00
B2	79	0.00	0.00	0.00	0.00	0.00	0.00	0.00
B3	54	0.00	0.00	0.00	0.00	0.00	0.00	0.00
B4	29	0.00	0.00	0.00	0.00	0.00	0.00	0.00
B5	4	0.00	0.00	0.00	0.00	0.00	0.00	0.00
C1	110	0.00	0.00	0.00	0.00	0.00	0.00	0.00
C2	85	0.00	0.00	0.00	0.00	0.00	0.00	0.00
C3	60	0.00	0.00	0.00	0.00	0.00	0.00	0.00
C4	35	0.00	0.00	0.00	0.00	0.00	0.00	0.00
C5	10	0.00	0.00	0.00	0.00	0.00	0.00	0.00
D1	335	0.00	0.00	0.00	0.00	0.00	0.00	0.00
D2	310	0.00	0.00	0.00	0.00	0.00	0.00	0.00
D3	285	0.00	0.00	0.00	0.00	0.00	0.00	0.00
D4	260	0.00	0.00	0.00	0.00	0.00	0.00	0.00
D5	235	0.00	0.00	0.00	0.00	0.00	0.00	0.00
D6	210	0.00	0.00	0.00	0.00	0.00	0.00	0.00
D7	185	0.00	0.00	0.00	0.00	0.00	0.00	0.00
E1	118	0.00	0.00	0.00	0.00	0.00	0.00	0.00
E2	93	0.00	0.00	0.00	0.00	0.00	0.00	0.00
E3	68	0.00	0.00	0.00	0.00	0.00	0.00	0.00
E4	43	0.00	0.00	0.00	0.00	0.00	0.00	0.00
E5	18	0.00	0.00	0.00	0.00	0.00	0.00	0.00
F1	143	0.00	0.00	0.00	0.00	0.00	0.00	0.00
F2	144	0.00	0.00	0.00	0.00	0.00	0.00	0.00

**Table 2.10.10-8 Stress Components – Bolt Preload; 1.12-Inch Outer Shell Thickness
(continued)**

Stress Points		Stresses						
Location	Node	S _x	S _y	S _z	S _{xy}	S ₁	S ₂	S ₃
F3	145	0.00	0.00	0.00	0.00	0.00	0.00	0.00
F4	146	0.00	0.00	0.00	0.00	0.00	0.00	0.00
F5	147	0.00	0.00	0.00	0.00	0.00	0.00	0.00
F6	148	0.00	0.00	0.00	0.00	0.00	0.00	0.00
F7	149	0.00	0.00	0.00	0.00	0.00	0.00	0.00
F8	150	0.00	0.00	0.00	0.00	0.00	0.00	0.00
G1	335	0.00	0.00	0.00	0.00	0.00	0.00	0.00
G2	336	0.00	0.00	0.00	0.00	0.00	0.00	0.00
G3	337	0.00	0.00	0.00	0.00	0.00	0.00	0.00
G4	338	0.00	0.00	0.00	0.00	0.00	0.00	0.00
G5	339	0.00	0.01	0.00	0.00	0.01	0.00	0.00
G6	340	0.01	0.00	0.00	0.00	0.01	0.00	0.00
H1	346	0.00	0.00	0.00	0.00	0.00	0.00	0.00
H2	347	0.00	0.00	0.00	0.00	0.00	0.00	0.00
H3	348	0.00	0.00	0.00	0.00	0.00	0.00	0.00
H4	349	0.00	0.00	0.00	0.00	0.00	0.00	0.00
H5	350	0.00	0.00	0.00	0.00	0.00	0.00	0.00
I1	621	0.00	0.01	0.00	0.00	0.01	0.00	0.00
I2	624	0.00	0.01	0.00	0.00	0.01	0.00	0.00
J1	635	0.00	0.00	0.00	0.00	0.00	0.00	0.00
J2	638	0.00	0.00	0.00	0.00	0.00	0.00	0.00
K1	841	0.00	0.01	0.00	0.00	0.01	0.00	0.00
K2	844	0.00	0.01	0.00	0.00	0.01	0.00	0.00
L1	855	0.00	0.00	0.00	0.00	0.00	0.00	0.00
L2	858	0.00	0.00	0.00	0.00	0.00	0.00	0.00
M1	941	0.00	0.01	0.00	0.00	0.01	0.00	0.00
M2	944	0.00	0.01	0.00	0.00	0.01	0.00	0.00
N1	955	0.00	0.00	0.00	0.00	0.00	0.00	0.00
N2	958	0.00	0.00	0.00	0.00	0.00	0.00	0.00
O1	1101	0.00	0.01	0.00	0.00	0.01	0.00	0.00
O2	1104	0.00	0.01	0.00	0.00	0.01	0.00	0.00

**Table 2.10.10-8 Stress Components – Bolt Preload; 1.12-Inch Outer Shell Thickness
(continued)**

Stress Points		Stresses						
Location	Node	S _x	S _y	S _z	S _{xy}	S ₁	S ₂	S ₃
P1	1115	0.00	0.00	0.00	0.00	0.01	0.00	0.00
P2	1118	0.00	0.00	0.00	0.00	0.01	0.00	0.00
Q1	1261	0.00	0.01	0.00	0.00	0.01	0.00	0.00
Q2	1264	0.00	0.01	0.00	0.00	0.01	0.00	0.00
R1	1275	0.00	0.00	0.00	0.00	0.01	0.00	0.00
R2	1278	0.00	0.00	0.00	0.00	0.01	0.00	0.00
S1	1561	0.00	0.04	0.00	0.00	0.04	0.00	0.00
S2	1564	0.00	-0.02	-0.01	0.00	0.00	-0.01	-0.02
T1	1575	0.00	0.00	-0.01	0.00	0.00	0.00	-0.01
T2	1578	0.00	0.00	-0.01	0.00	0.00	0.00	-0.01
U1	1841	-0.01	-0.30	0.07	0.01	0.07	-0.01	-0.30
U2	1844	-0.07	-0.10	0.09	0.12	0.09	0.03	-0.20
V1	1852	0.10	0.02	0.05	0.01	0.10	0.05	0.02
V2	1856	0.00	-0.05	0.01	0.01	0.01	0.01	-0.05
W1	1969	-0.06	-0.20	0.05	0.18	0.06	0.05	-0.32
W2	1970	-0.01	-0.14	0.07	0.02	0.07	0.00	-0.15
W3	1971	0.00	-0.08	0.08	-0.05	0.08	0.02	-0.10
W4	1972	0.00	-0.03	0.09	-0.05	0.09	0.04	-0.07
W5	1973	0.00	0.01	0.10	-0.05	0.10	0.05	-0.04
W6	1974	0.00	0.04	0.10	-0.04	0.10	0.06	-0.03
W7	1975	0.00	0.07	0.10	-0.02	0.10	0.07	-0.01
W8	1976	0.00	0.09	0.11	-0.01	0.11	0.09	0.00
X1	2370	-0.06	0.00	-0.02	0.13	0.11	-0.02	-0.17
X2	2390	-0.05	-0.21	-0.09	0.10	0.00	-0.09	-0.26
X3	2410	0.06	-0.22	-0.04	-0.01	0.06	-0.04	-0.22
X4	2430	0.03	-0.09	-0.01	-0.06	0.05	-0.01	-0.12
X5	2450	0.01	-0.05	0.00	-0.06	0.05	0.00	-0.08
X6	2470	0.00	-0.01	0.01	-0.04	0.04	0.01	-0.04
X7	2490	0.01	0.00	0.02	-0.02	0.03	0.02	-0.02
X8	2510	0.01	0.00	0.03	-0.02	0.03	0.03	-0.01
X9	2530	0.02	0.00	0.03	-0.01	0.03	0.02	-0.01

**Table 2.10.10-8 Stress Components – Bolt Preload; 1.12-Inch Outer Shell Thickness
(continued)**

Stress Points		Stresses						
Location	Node	S _x	S _y	S _z	S _{xy}	S ₁	S ₂	S ₃
X10	2550	0.02	0.00	0.04	-0.01	0.04	0.02	0.00
X11	2570	0.02	0.00	0.04	0.00	0.04	0.02	0.00
Y1	2305	0.02	0.00	0.02	0.00	0.02	0.02	0.00
Y2	2325	0.01	0.00	0.01	0.00	0.01	0.01	0.00
Y3	2345	0.00	-0.01	0.00	0.00	0.00	0.00	-0.01
Y4	2365	-0.01	-0.01	-0.01	0.00	-0.01	-0.01	-0.01
Y5	2385	-0.02	-0.01	-0.02	0.00	-0.01	-0.02	-0.02
Y6	2405	-0.02	-0.01	-0.02	0.00	-0.01	-0.02	-0.02
Y7	2425	-0.01	-0.01	-0.01	0.00	-0.01	-0.01	-0.02
Y8	2445	-0.01	-0.02	0.00	0.00	0.01	0.00	-0.02
Y9	2465	0.02	-0.01	0.01	0.00	0.02	0.01	-0.01
Y10	2485	0.03	-0.01	0.02	0.00	0.03	0.02	-0.01
Y11	2505	0.03	0.00	0.03	-0.01	0.03	0.03	-0.01
Y12	2525	0.04	0.00	0.04	0.00	0.04	0.04	0.00
Y13	2545	0.05	0.00	0.05	0.00	0.05	0.05	0.00
Y14	2565	0.06	0.00	0.06	0.00	0.06	0.06	0.00
Z1	2301	0.02	0.00	0.02	0.00	0.02	0.02	0.00
Z2	2321	0.01	0.00	0.01	0.00	0.01	0.01	0.00
Z3	2341	0.00	0.00	0.00	0.00	0.00	0.00	0.00
Z4	2361	-0.01	0.00	-0.01	0.00	0.01	-0.01	-0.01
Z5	2381	-0.01	0.01	-0.01	0.00	0.01	-0.01	-0.01
Z6	2401	-0.01	0.01	-0.01	0.00	0.01	-0.01	-0.01
Z7	2421	-0.01	0.00	-0.01	0.00	0.00	-0.01	-0.01
Z8	2441	0.00	0.00	0.00	0.00	0.00	0.00	0.00
Z9	2461	0.01	0.00	0.01	0.00	0.01	0.01	0.00
Z10	2481	0.03	0.00	0.03	0.00	0.03	0.03	0.00
Z11	2501	0.03	0.00	0.03	0.00	0.03	0.03	0.00
Z12	2521	0.04	0.00	0.04	0.00	0.04	0.04	0.00
Z13	2541	0.05	0.00	0.05	0.00	0.05	0.05	0.00
Z14	2561	0.06	0.00	0.06	0.00	0.06	0.06	0.00

Table 2.10.10-9 Stress Components – Impact and Inertial Loads; 30-Foot Top End Drop;
 $\phi = 0^\circ$; 1.12-Inch Outer Shell Thickness

Stress Points		Stresses						
Location	Node	S _x	S _y	S _z	S _{xy}	S ₁	S ₂	S ₃
A1	327	0.75	0.01	0.76	0.03	0.76	0.75	0.01
A2	302	0.66	0.01	0.67	-0.01	0.67	0.66	0.01
A3	277	0.58	0.01	0.59	-0.03	0.59	0.58	0.00
A4	252	0.42	-0.01	0.43	-0.02	0.43	0.42	-0.02
A5	227	0.14	-0.04	0.14	-0.03	0.14	0.14	-0.05
A6	202	-0.15	-0.07	-0.15	-0.02	-0.06	-0.15	-0.15
A7	177	-0.48	-0.08	-0.49	-0.01	-0.08	-0.48	-0.49
B1	104	0.31	0.01	0.33	0.00	0.33	0.31	0.01
B2	79	0.04	0.01	0.05	-0.04	0.07	0.05	-0.02
B3	54	-0.21	-0.01	-0.22	-0.05	0.00	-0.21	-0.23
B4	29	-0.47	-0.01	-0.48	-0.04	0.00	-0.47	-0.48
B5	4	-0.61	0.00	-0.63	0.04	0.01	-0.61	-0.63
C1	110	0.02	0.00	0.17	-0.04	0.17	0.06	-0.03
C2	85	-0.09	0.00	-0.02	-0.08	0.05	-0.02	-0.14
C3	60	-0.17	0.00	-0.19	-0.10	0.05	-0.19	-0.22
C4	35	-0.25	0.00	-0.36	-0.06	0.01	-0.27	-0.36
C5	10	-0.31	0.00	-0.46	-0.01	0.00	-0.31	-0.46
D1	335	-0.32	-1.10	-0.01	-0.22	-0.01	-0.25	-1.18
D2	310	0.11	-0.70	0.17	-0.22	0.19	0.15	-0.77
D3	285	0.17	-0.50	0.21	-0.20	0.23	0.21	-0.56
D4	260	0.22	-0.35	0.20	-0.17	0.27	0.20	-0.40
D5	235	0.18	-0.23	0.10	-0.13	0.22	0.10	-0.27
D6	210	0.11	-0.15	-0.02	-0.08	0.13	-0.02	-0.17
D7	185	0.07	-0.12	-0.16	-0.04	0.07	-0.13	-0.16
E1	118	-0.45	-0.42	-0.22	-0.17	-0.22	-0.25	-0.62
E2	93	-0.12	-0.26	-0.15	-0.11	-0.06	-0.15	-0.32
E3	68	-0.06	-0.11	-0.17	-0.06	-0.02	-0.14	-0.18
E4	43	0.00	-0.04	-0.21	-0.02	0.01	-0.05	-0.21
E5	18	0.06	-0.01	-0.23	0.00	0.06	-0.01	-0.23
F1	143	0.03	-0.32	-0.08	-0.16	0.09	-0.08	-0.38
F2	144	-0.03	-0.11	-0.04	-0.19	0.13	-0.04	-0.27

Table 2.10.10-9 Stress Components – Impact and Inertial Loads; 30-Foot Top End Drop;
 $\phi = 0^\circ$; 1.12-Inch Outer Shell Thickness (continued)

Stress Points		Stresses						
Location	Node	S _X	S _Y	S _Z	S _{XY}	S ₁	S ₂	S ₃
F3	145	-0.07	-0.10	-0.05	-0.21	0.12	-0.05	-0.29
F4	146	-0.04	-0.09	-0.04	-0.17	0.11	-0.04	-0.24
F5	147	-0.02	-0.09	-0.03	-0.14	0.09	-0.03	-0.20
F6	148	-0.01	-0.08	-0.03	-0.10	0.06	-0.03	-0.15
F7	149	-0.01	-0.07	-0.02	-0.05	0.03	-0.02	-0.10
F8	150	0.00	-0.05	-0.01	-0.03	0.02	-0.01	-0.07
G1	335	-0.32	-1.10	-0.01	-0.22	-0.01	-0.25	-1.18
G2	336	-0.23	-0.76	0.10	-0.11	0.10	-0.19	-0.79
G3	337	-0.10	-0.62	0.16	-0.03	0.16	-0.09	-0.62
G4	338	-0.02	-0.53	0.19	0.02	0.19	-0.02	-0.53
G5	339	0.05	-0.27	0.27	0.05	0.27	0.05	-0.27
G6	340	0.15	-0.06	0.34	0.03	0.34	0.16	-0.07
H1	346	0.10	-0.21	0.23	-0.14	0.23	0.15	-0.26
H2	347	0.00	-0.74	0.05	-0.13	0.06	0.03	-0.77
H3	348	0.03	-0.96	0.00	0.00	0.03	0.00	-0.96
H4	349	0.01	-0.84	0.03	0.05	0.03	0.01	-0.84
H5	350	-0.01	-0.78	0.04	0.04	0.04	0.00	-0.78
I1	621	0.00	-1.17	-0.15	0.03	0.00	-0.15	-1.17
I2	624	0.02	-1.64	-0.25	0.03	0.02	-0.25	-1.64
J1	635	0.00	-1.12	0.05	0.00	0.05	0.00	-1.12
J2	638	0.00	-1.16	0.03	0.00	0.03	0.00	-1.16
K1	841	0.00	-1.84	0.00	0.00	0.00	0.00	-1.84
K2	844	0.00	-1.83	0.00	0.00	0.00	0.00	-1.83
L1	855	0.00	-1.57	0.00	0.00	0.00	0.00	-1.57
L2	858	0.00	-1.57	0.00	0.00	0.00	0.00	-1.57
M1	941	0.00	-2.37	0.00	0.00	0.00	0.00	-2.37
M2	944	0.00	-2.37	0.00	0.00	0.00	0.00	-2.37
N1	955	0.00	-2.11	0.00	0.00	0.00	0.00	-2.11
N2	958	0.00	-2.11	0.00	0.00	0.00	0.00	-2.11
O1	1101	0.00	-3.26	0.00	0.00	0.00	0.00	-3.26
O2	1104	0.00	-3.26	0.00	0.00	0.00	0.00	-3.26

**Table 2.10.10-9 Stress Components – Impact and Inertial Loads; 30-Foot Top End Drop;
 $\phi = 0^\circ$; 1.12-Inch Outer Shell Thickness (continued)**

Stress Points		Stresses						
Location	Node	S _x	S _y	S _z	S _{xy}	S ₁	S ₂	S ₃
P1	1115	0.00	-2.99	0.00	0.00	0.00	0.00	-2.99
P2	1118	0.00	-2.99	0.00	0.00	0.00	0.00	-2.99
Q1	1261	0.00	-4.14	0.00	0.00	0.00	0.00	-4.14
Q2	1264	0.00	-4.14	0.00	0.00	0.00	0.00	-4.14
R1	1275	0.00	-3.88	0.00	0.00	0.00	0.00	-3.88
R2	1278	0.00	-3.88	0.00	0.00	0.00	0.00	-3.88
S1	1561	0.00	-3.75	-0.59	-0.13	0.01	-0.59	-3.76
S2	1564	0.09	-6.30	-1.16	-0.16	0.10	-1.16	-6.31
T1	1575	0.00	-4.40	0.24	-0.01	0.24	0.00	-4.40
T2	1578	0.00	-5.07	0.04	0.00	0.04	0.00	-5.07
U1	1841	0.02	-6.64	2.17	-0.17	2.17	0.03	-6.65
U2	1844	0.83	-3.38	2.99	-0.17	2.99	0.86	-3.40
V1	1852	-1.06	-5.38	0.68	-0.19	0.68	-1.03	-5.40
V2	1856	0.01	-3.42	1.29	-0.04	1.29	0.01	-3.42
W1	1969	1.83	-1.34	0.29	1.37	2.34	0.29	-1.85
W2	1970	1.22	-3.04	-0.21	0.55	1.29	-0.21	-3.11
W3	1971	0.68	-3.78	-0.46	-0.06	0.69	-0.46	-3.79
W4	1972	0.38	-4.48	-0.66	-0.19	0.39	-0.66	-4.50
W5	1973	0.23	-4.98	-0.78	-0.22	0.24	-0.78	-4.99
W6	1974	0.13	-5.36	-0.88	-0.19	0.14	-0.88	-5.37
W7	1975	0.06	-5.77	-0.97	-0.11	0.07	-0.97	-5.77
W8	1976	0.02	-6.21	-1.07	-0.06	0.02	-1.07	-6.21
X1	2370	4.51	1.44	3.44	2.33	5.77	3.44	0.18
X2	2390	0.34	-2.34	0.68	2.04	1.44	0.68	-3.44
X3	2410	0.11	-4.34	-0.20	1.09	0.36	-0.20	-4.59
X4	2430	-0.65	-4.17	-0.57	1.03	-0.37	-0.57	-4.45
X5	2450	-0.68	-4.58	-0.75	1.01	-0.43	-0.75	-4.83
X6	2470	-0.57	-4.60	-0.67	1.01	-0.33	-0.67	-4.84
X7	2490	-0.14	-4.73	-0.46	0.93	0.04	-0.46	-4.91
X8	2510	0.11	-4.75	-0.33	0.82	0.25	-0.33	-4.88
X9	2530	0.43	-4.81	-0.22	0.63	0.51	-0.22	-4.89

Table 2.10.10-9 Stress Components – Impact and Inertial Loads; 30-Foot Top End Drop;
 $\phi = 0^\circ$; 1.12-Inch Outer Shell Thickness (continued)

Stress Points		Stresses						
Location	Node	S _x	S _y	S _z	S _{xy}	S ₁	S ₂	S ₃
X10	2550	0.78	-4.83	-0.11	0.36	0.81	-0.11	-4.86
X11	2570	1.18	-4.84	-0.04	0.20	1.19	-0.04	-4.85
Y1	2305	0.81	-1.90	1.22	0.12	1.22	0.82	-1.91
Y2	2325	0.95	-2.05	1.07	0.51	1.07	1.03	-2.14
Y3	2345	1.15	-2.40	1.08	0.59	1.26	1.08	-2.51
Y4	2365	1.16	-2.72	1.00	0.46	1.21	1.00	-2.77
Y5	2385	0.80	-2.93	0.71	0.31	0.83	0.71	-2.96
Y6	2405	0.26	-3.08	0.32	0.29	0.32	0.29	-3.11
Y7	2425	-0.17	-3.28	-0.05	0.41	-0.05	-0.12	-3.34
Y8	2445	-0.41	-3.58	-0.30	0.55	-0.29	-0.32	-3.68
Y9	2465	-0.50	-3.95	-0.46	0.63	-0.38	-0.46	-4.07
Y10	2485	-0.51	-4.30	-0.57	0.59	-0.42	-0.57	-4.39
Y11	2505	-0.55	-4.53	-0.68	0.53	-0.48	-0.68	-4.60
Y12	2525	-0.60	-4.68	-0.79	0.40	-0.56	-0.79	-4.72
Y13	2545	-0.70	-4.78	-0.96	0.23	-0.68	-0.96	-4.80
Y14	2565	-0.86	-4.82	-1.19	0.04	-0.86	-1.19	-4.82
Z1	2301	1.78	-1.88	1.78	0.00	1.78	1.78	-1.88
Z2	2321	1.26	-2.02	1.26	0.00	1.26	1.26	-2.02
Z3	2341	1.05	-2.32	1.05	0.00	1.05	1.05	-2.32
Z4	2361	0.87	-2.63	0.87	0.00	0.87	0.87	-2.63
Z5	2381	0.63	-2.91	0.63	0.00	0.63	0.63	-2.91
Z6	2401	0.34	-3.18	0.34	0.00	0.34	0.34	-3.18
Z7	2421	0.04	-3.44	0.04	0.00	0.04	0.04	-3.44
Z8	2441	-0.22	-3.74	-0.22	0.00	-0.22	-0.22	-3.74
Z9	2461	-0.45	-4.06	-0.45	0.00	-0.45	-0.45	-4.06
Z10	2481	-0.67	-4.35	-0.67	0.00	-0.67	-0.67	-4.35
Z11	2501	-0.84	-4.53	-0.84	0.00	-0.84	-0.84	-4.53
Z12	2521	-1.03	-4.66	-1.03	0.00	-1.03	-1.03	-4.66
Z13	2541	-1.28	-4.76	-1.28	0.00	-1.28	-1.28	-4.76
Z14	2561	-1.59	-4.80	-1.59	0.00	-1.59	-1.59	-4.80

Table 2.10.10-10 Stress Components – Impact and Inertial Loads; 30-Foot Top Corner Drop; $\phi = 15.74^\circ$; 1.12-Inch Outer Shell Thickness

Stress Points		Stresses						
Location	Node	S _x	S _y	S _z	S _{xy}	S ₁	S ₂	S ₃
A1	327	-0.28	0.01	1.55	0.08	1.55	0.03	-0.29
A2	302	-0.53	-0.00	1.36	0.15	1.36	0.04	-0.57
A3	277	-0.70	0.03	1.23	0.34	1.23	0.16	-0.84
A4	252	-1.06	-0.02	0.96	0.46	0.96	0.16	-1.23
A5	227	-1.77	-0.74	0.64	0.30	0.64	-0.66	-1.86
A6	202	-0.03	-1.21	2.68	-1.23	2.68	0.75	-1.99
A7	177	-13.24	-0.82	-3.97	-0.56	-0.79	-3.97	-13.27
B1	104	-3.25	-1.05	-0.84	-0.56	-0.84	-0.91	-3.38
B2	79	-2.44	-0.82	-0.29	-0.26	-0.29	-0.78	-2.48
B3	54	-2.17	-0.44	-0.01	-0.40	-0.01	-0.35	-2.26
B4	29	-1.89	-0.11	0.29	-0.28	-0.29	-0.06	-1.94
B5	4	-1.52	-0.02	-0.48	-0.06	0.48	0.02	-1.52
C1	110	-3.71	-0.27	-1.54	-0.26	-0.25	-1.54	-3.73
C2	85	-3.17	-0.22	-1.10	0.12	-0.22	-1.10	-3.18
C3	60	-2.65	-0.12	-0.73	0.14	-0.11	-0.73	-2.66
C4	35	-2.13	-0.03	-0.32	0.14	-0.02	-0.32	-2.14
C5	10	-1.85	-0.00	-0.08	0.15	0.01	-0.08	-1.86
D1	335	-1.22	-0.13	0.21	-0.30	0.21	-0.05	-1.30
D2	310	-1.40	-0.24	0.02	-0.27	0.02	-0.18	-1.46
D3	285	-1.63	-0.28	-0.13	-0.32	-0.13	-0.21	-1.70
D4	260	-2.03	-0.34	-0.39	-0.41	-0.24	-0.39	-2.13
D5	235	-2.82	-0.41	-0.90	-0.35	-0.36	-0.90	-2.87
D6	210	-3.63	-0.44	-1.46	-0.25	-0.42	-1.46	-3.65
D7	185	-4.41	-0.44	-2.13	0.25	-0.42	-2.13	-4.42
E1	118	-3.12	0.84	-2.09	-0.60	0.93	-2.09	-3.21
E2	93	-3.18	0.28	-2.10	-0.17	0.29	-2.10	-3.19
E3	68	-3.07	0.11	-1.98	0.03	0.11	-1.98	-3.07
E4	43	-3.04	0.03	-1.82	0.09	0.03	-1.82	-3.05
E5	18	-3.12	0.01	-1.74	0.14	0.02	-1.74	-3.13
F1	143	-0.61	3.17	-1.06	-0.82	3.34	-0.78	-1.06
F2	144	-0.72	0.80	-2.33	-0.69	1.07	-0.99	-2.33

Table 2.10.10-10 Stress Components – Impact and Inertial Loads; 30-Foot Top Corner Drop; $\phi = 15.74^\circ$; 1.12-Inch Outer Shell Thickness (continued)

Stress Points		Stresses						
Location	Node	S _x	S _y	S _z	S _{xy}	S ₁	S ₂	S ₃
F3	145	-1.06	0.15	-2.95	-0.52	0.35	-1.25	-2.95
F4	146	-1.78	-0.28	-3.58	-0.33	-0.21	-1.85	-3.58
F5	147	-2.25	-0.63	-4.07	-0.24	-0.59	-2.29	-4.07
F6	148	-2.54	-0.95	-4.49	-0.17	-0.93	-2.56	-4.49
F7	149	-2.75	-1.35	-4.92	-0.09	-1.35	-2.75	-4.92
F8	150	-2.85	-1.89	-5.39	-0.04	-1.89	-2.85	-5.39
G1	335	-1.22	-0.13	0.21	-0.30	0.21	-0.05	-1.30
G2	336	-1.01	-0.31	0.01	-0.28	0.01	-0.21	-1.11
G3	337	-1.07	-0.62	-0.25	-0.17	-0.25	-0.56	-1.13
G4	338	-1.37	-0.98	-0.55	0.08	-0.55	-0.96	-1.38
G5	339	-2.17	-1.48	-1.03	0.68	-1.03	-1.06	-2.58
G6	340	-2.96	-0.74	-0.97	0.77	-0.49	-0.97	-3.21
H1	346	-1.61	1.41	-2.58	1.04	1.73	-1.93	-2.58
H2	347	-1.42	4.42	-2.33	0.58	4.48	-1.48	-2.33
H3	348	-2.35	3.00	-3.46	-0.80	3.12	-2.47	-3.46
H4	349	-2.55	-0.63	-4.93	-0.93	-0.25	-2.93	-4.93
H5	350	-2.77	-4.41	-6.40	-0.62	-2.56	-4.61	-6.40
I1	621	-0.06	0.13	0.44	-0.03	0.44	0.13	-0.06
I2	624	-0.01	0.43	0.42	0.04	0.43	0.42	-0.01
J1	635	-0.09	-2.23	0.99	-0.13	2.24	0.99	-0.09
J2	638	-0.01	5.36	0.77	0.05	5.36	0.77	-0.01
K1	841	-0.03	6.09	0.16	-0.01	6.09	0.16	-0.03
K2	844	0.00	6.92	0.41	0.01	6.92	0.41	0.00
L1	855	-0.05	11.83	0.61	-0.04	11.83	0.61	-0.05
L2	858	0.02	12.80	0.69	0.01	12.81	0.69	0.02
M1	941	-0.03	6.32	0.16	0.00	6.32	0.16	-0.03
M2	944	-0.01	7.20	0.41	0.00	7.20	0.41	-0.01
N1	955	-0.05	13.70	0.75	-0.01	13.70	0.75	-0.05
N2	958	0.00	14.87	0.80	0.01	14.87	0.80	0.00
O1	1101	-0.04	2.72	-0.09	0.01	2.72	-0.04	-0.09
O2	1104	-0.03	3.22	0.15	-0.01	3.22	0.15	-0.03

Table 2.10.10-10 Stress Components – Impact and Inertial Loads; 30-Foot Top Corner Drop; $\phi = 15.74^\circ$; 1.12-Inch Outer Shell Thickness (continued)

Stress Points		Stresses						
Location	Node	S _x	S _y	S _z	S _{xy}	S ₁	S ₂	S ₃
P1	1115	-0.07	10.77	1.09	0.03	10.78	1.09	-0.07
P2	1118	0.00	11.75	0.86	-0.03	11.75	0.86	0.00
Q1	1261	-0.03	-3.27	0.21	0.02	0.21	-0.03	-3.27
Q2	1264	-0.01	-3.30	0.35	-0.03	0.35	-0.01	-3.30
R1	1275	-0.04	-0.13	1.33	0.06	1.33	-0.01	-0.16
R2	1278	0.00	-0.34	0.24	-0.07	0.24	0.01	-0.36
S1	1561	-0.04	-11.67	0.24	-0.40	0.24	-0.02	-11.68
S2	1564	0.34	-23.09	-4.92	-0.60	0.36	-4.92	-23.11
T1	1575	-0.14	-17.88	2.76	0.15	2.76	-0.14	-17.88
T2	1578	0.02	-19.72	1.70	-0.06	1.70	0.02	-19.72
U1	1841	0.28	-19.99	8.13	-0.19	8.13	0.29	-19.99
U2	1844	3.40	-11.67	9.78	-0.69	9.78	3.43	-11.70
V1	1852	6.10	-10.08	7.23	0.13	7.23	6.10	-10.08
V2	1856	0.59	-23.74	0.54	-0.42	0.60	0.54	-23.75
W1	1969	-19.40	-16.45	-8.37	3.91	-8.37	-13.75	-22.11
W2	1970	-14.06	-8.78	-5.45	1.32	-5.45	-8.47	-14.37
W3	1971	-7.44	-9.92	-4.43	-0.56	-4.43	-7.32	-10.04
W4	1972	-5.36	-10.65	-4.36	-0.73	-4.36	-5.26	-10.75
W5	1973	-4.37	-11.07	-4.37	-0.72	-4.29	-4.37	-11.15
W6	1974	-3.83	-11.20	-4.36	-0.60	-3.78	-4.36	-11.25
W7	1975	-3.57	-11.11	-4.37	-0.36	-3.55	-4.37	-11.13
W8	1976	-3.50	-10.64	-4.31	-0.25	-3.50	-4.31	-10.65
X1	2370	-6.70	-8.14	-1.89	1.84	-1.89	-5.44	-9.39
X2	2390	-5.84	-11.37	-2.73	3.06	-2.73	-4.48	-12.73
X3	2410	-5.21	-12.98	-2.78	3.61	-2.78	-3.79	-14.40
X4	2430	-4.12	-14.33	-2.51	3.72	-2.51	-2.90	-15.55
X5	2450	-3.36	-14.88	-2.09	3.64	-2.09	-2.30	-15.94
X6	2470	-2.49	-15.02	-1.63	3.50	-1.57	-1.63	-15.93
X7	2490	-1.31	-14.92	-1.25	3.23	-0.59	-1.25	-15.65
X8	2510	-0.55	-14.80	-1.14	2.79	-0.03	-1.14	-15.33
X9	2530	0.33	-14.69	-1.14	2.16	0.64	-1.14	-15.00

Table 2.10.10-10 Stress Components – Impact and Inertial Loads; 30-Foot Top Corner Drop; $\phi = 15.74^\circ$; 1.12-Inch Outer Shell Thickness (continued)

Stress Points		Stresses						
Location	Node	S _x	S _y	S _z	S _{xy}	S ₁	S ₂	S ₃
X10	2550	1.43	-14.62	-1.27	1.24	1.52	-1.27	-14.72
X11	2570	2.78	-14.60	-1.55	0.73	2.81	-1.55	-14.63
Y1	2305	-0.37	-5.19	1.81	-0.20	1.81	-0.36	-5.20
Y2	2325	-0.64	-5.37	1.53	-0.42	1.53	-0.60	-5.40
Y3	2345	-1.22	-5.61	1.09	-0.49	1.09	-1.16	-5.66
Y4	2365	-2.12	-5.93	0.53	-0.32	0.53	-2.09	-5.96
Y5	2385	-2.85	-6.52	-0.04	0.17	-0.04	-2.84	-6.53
Y6	2405	-3.08	-7.53	-0.47	0.91	-0.47	-2.91	-7.71
Y7	2425	-2.89	-9.01	-0.69	1.79	-0.69	-2.41	-9.50
Y8	2445	-2.65	-10.83	-0.74	2.81	-0.74	-1.78	-11.70
Y9	2465	-3.02	-12.59	-0.74	3.94	-0.74	-1.61	-14.00
Y10	2485	-5.09	-13.75	-1.13	4.77	-1.13	-2.98	-15.86
Y11	2505	-7.13	-14.32	-1.93	4.59	-1.93	-4.89	-16.55
Y12	2525	-8.44	-14.62	-2.95	3.70	-2.95	-6.71	-16.35
Y13	2545	-9.98	-14.55	-4.58	2.23	-4.58	-9.07	-15.46
Y14	2565	-11.04	-14.54	-7.14	0.91	-7.14	-10.82	-14.77
Z1	2301	-0.59	-2.18	2.56	0.14	2.56	-0.58	-2.19
Z2	2321	-1.21	-1.70	2.32	-0.01	2.32	-1.21	-1.70
Z3	2341	-1.56	-1.85	1.74	-0.12	1.74	-1.51	-1.89
Z4	2361	-1.90	-2.04	1.27	-0.33	1.27	-1.63	-2.31
Z5	2381	-2.08	-2.27	0.85	-0.46	0.85	-1.70	-2.65
Z6	2401	-2.04	-2.54	0.46	-0.53	0.46	-1.71	-2.88
Z7	2421	-1.78	-2.88	0.11	-0.56	0.11	-1.54	-3.11
Z8	2441	-1.32	-3.26	-0.20	-0.56	-0.20	-1.17	-3.41
Z9	2461	-0.71	-3.64	-0.50	-0.06	-0.50	-0.71	-3.64
Z10	2481	0.02	-4.03	-0.78	2.71	1.37	-0.78	-5.38
Z11	2501	0.37	-4.21	-1.08	10.55	8.88	-1.08	-12.72
Z12	2521	0.73	-4.37	-1.44	34.89	33.17	-1.44	-36.80
Z13	2541	0.88	-4.93	-2.15	164.65	162.65	-2.15	-166.70
Z14	2561	1.59	-6.27	-4.64	215.93	213.63	-4.64	-218.31

**Table 2.10.10-11 Impact and Inertial Loads; 30-Foot Top Oblique Drop; $\phi = 60^\circ$;
1.12-Inch Outer Shell Thickness**

Stress Points		Stresses						
Location	Node	S _x	S _y	S _z	S _{xy}	S ₁	S ₂	S ₃
A1	327	-2.08	-0.00	2.19	0.12	2.19	0.00	-2.09
A2	302	-2.50	-0.03	1.92	0.37	1.92	0.03	-2.55
A3	277	-2.76	0.04	1.75	0.86	1.75	0.28	-3.00
A4	252	-3.29	-0.02	1.42	1.12	1.42	0.33	-3.64
A5	227	-4.44	-1.67	1.23	0.76	1.23	-1.47	-4.63
A6	202	0.22	-2.72	6.57	-2.85	6.57	1.96	-4.45
A7	177	-30.18	-1.77	-8.38	-1.30	-1.71	-8.38	-30.24
B1	104	-8.22	-2.48	-2.60	-1.31	-2.19	-2.60	-8.51
B2	79	-5.81	-1.94	-0.78	-0.53	-0.78	-1.87	-5.89
B3	54	-4.70	-1.01	0.40	-0.84	0.40	-0.83	-4.89
B4	29	-3.55	-0.23	1.60	-0.59	1.60	-0.13	-3.65
B5	4	-2.40	0.05	2.32	0.06	2.32	0.05	-2.40
C1	110	-8.76	-0.64	-3.94	-0.54	-0.60	-3.94	-8.79
C2	85	-7.28	-0.53	-2.53	0.44	-0.50	-2.53	-7.31
C3	60	-5.90	-0.28	-1.34	0.51	-0.23	-1.34	-5.95
C4	35	-4.52	-0.06	-0.07	0.44	-0.02	-0.07	-4.56
C5	10	-3.76	-0.01	0.70	0.37	0.70	0.03	-3.79
D1	335	-2.25	1.79	0.52	-0.29	1.81	0.52	-2.27
D2	310	-3.50	0.77	-0.27	-0.22	0.76	-0.27	-3.51
D3	285	-4.15	0.30	-0.71	-0.37	0.33	-0.71	-4.18
D4	260	-5.19	-0.13	-1.31	-0.64	-0.05	-1.31	-5.27
D5	235	-6.96	-0.53	-2.31	-0.58	-0.48	-2.31	-7.02
D6	210	-8.72	-0.74	-3.39	-0.44	-0.71	-3.39	-8.75
D7	185	-10.48	-0.80	-4.69	0.67	-0.75	-4.69	-10.53
E1	118	-6.47	2.78	-4.49	-1.08	2.91	-4.49	-6.60
E2	93	-7.24	1.15	-4.64	-0.20	1.16	-4.64	-7.24
E3	68	-7.11	0.47	-4.33	0.18	0.48	-4.33	-7.11
E4	43	-7.15	0.15	-3.87	0.26	0.16	-3.87	-7.15
E5	18	-7.44	0.05	-3.65	0.32	0.06	-3.65	-7.45
F1	143	-1.49	8.06	-2.34	-1.62	8.33	-1.76	-2.34
F2	144	-1.63	2.10	-5.40	-1.26	2.49	-2.02	-5.40

Table 2.10.10-11 Impact and Inertial Loads; 30-Foot Top Oblique Drop; $\phi = 60^\circ$; 1.12-Inch Outer Shell Thickness (continued)

Stress Points		Stresses						
Location	Node	S _x	S _y	S _z	S _{xy}	S ₁	S ₂	S ₃
F3	145	-2.35	0.54	-6.82	-0.83	0.77	-2.57	-6.82
F4	146	-4.11	-0.48	-8.33	-0.45	-0.43	-4.16	-8.33
F5	147	-5.25	-1.30	-9.51	-0.30	-1.28	-5.27	-9.51
F6	148	-5.95	-2.08	-10.49	-0.22	-2.06	-5.96	-10.49
F7	149	-6.43	-3.05	-11.52	-0.12	-3.04	-6.43	-11.52
F8	150	-6.70	-4.35	-12.64	-0.04	-4.35	-6.70	-12.64
G1	335	-2.25	1.79	0.52	-0.29	1.81	0.52	-2.27
G2	336	-1.94	0.72	-0.16	-0.44	0.79	-0.16	-2.01
G3	337	-2.33	-0.28	-0.89	-0.35	-0.22	-0.89	-2.39
G4	338	-3.17	-1.29	-1.66	0.15	-1.28	-1.66	-3.18
G5	339	-5.18	-2.97	-2.92	1.50	-2.21	-2.92	-5.94
G6	340	-7.24	-1.62	-2.94	1.76	-1.11	-2.94	-7.75
H1	346	-3.96	3.72	-6.50	2.70	4.57	-4.82	-6.50
H2	347	-3.33	11.79	-5.57	1.61	11.96	-3.50	-5.57
H3	348	-5.58	8.88	-8.13	-1.88	9.12	-5.83	-8.13
H4	349	-6.00	0.12	-11.64	-2.28	0.88	-6.76	-11.64
H5	350	-6.49	-8.86	-15.10	-1.53	-5.74	-9.61	-15.10
I1	621	-0.14	2.53	-1.32	-0.12	2.53	1.32	-0.14
I2	624	-0.06	4.13	1.47	0.04	4.13	1.47	-0.06
J1	635	-0.20	7.38	2.23	-0.29	7.39	2.23	-0.21
J2	638	-0.02	14.80	1.74	0.11	14.80	1.74	-0.02
K1	841	-0.12	15.76	-0.17	-0.07	15.76	-0.12	-0.17
K2	844	-0.03	18.29	1.41	0.07	18.30	1.41	-0.03
L1	855	-0.12	31.01	1.46	-0.14	31.01	1.46	-0.12
L2	858	0.04	34.02	1.59	0.08	34.02	1.59	0.04
M1	941	-0.12	21.41	-0.22	-0.01	21.41	-0.12	-0.22
M2	944	-0.05	24.48	1.44	0.01	24.48	1.44	-0.05
N1	955	-0.13	42.12	1.74	-0.07	42.12	1.74	-0.13
N2	958	0.01	46.04	1.89	0.06	46.04	1.89	0.01
O1	1101	-0.13	21.18	-0.78	0.00	21.18	-0.13	-0.78
O2	1104	-0.11	24.10	0.83	-0.01	24.10	0.83	-0.11

Table 2.10.10-11 Impact and Inertial Loads; 30-Foot Top Oblique Drop; $\phi = 60^\circ$; 1.12-Inch Outer Shell Thickness (continued)

Stress Points		Stresses						
Location	Node	S _x	S _y	S _z	S _{xy}	S ₁	S ₂	S ₃
P1	1115	-0.17	45.92	1.85	0.03	45.92	1.85	-0.17
P2	1118	0.01	50.50	2.64	-0.03	50.50	2.64	0.01
Q1	1261	-0.12	15.22	-0.19	0.04	15.22	-0.12	-0.19
Q2	1264	-0.05	17.63	1.38	-0.05	17.63	1.38	-0.05
R1	1275	-0.14	31.45	0.52	0.11	31.45	0.52	-0.14
R2	1278	0.02	35.18	2.79	-0.11	35.18	2.79	0.02
S1	1561	-0.11	-3.35	1.59	-0.18	1.59	-0.10	-3.36
S2	1564	0.17	-9.66	-2.11	-0.41	0.19	-2.11	-9.68
T1	1575	-0.30	3.08	2.37	0.21	3.09	2.37	-0.31
T2	1578	0.01	7.19	4.65	-0.11	7.19	4.65	0.01
U1	1841	0.30	-16.34	10.62	-0.13	10.62	0.30	-16.34
U2	1844	3.93	-7.62	11.06	-0.84	11.06	3.99	-7.68
V1	1852	9.88	1.29	5.59	-2.99	10.82	5.59	0.35
V2	1856	0.78	-7.74	-2.34	0.06	0.78	-2.34	-7.74
W1	1969	-66.69	-41.51	-24.01	-0.65	-24.01	-41.49	-66.71
W2	1970	-48.82	-4.73	-12.06	-3.65	-4.43	-12.06	-49.12
W3	1971	-27.03	-1.84	-8.96	-5.41	-0.73	-8.96	-28.14
W4	1972	-19.48	2.31	-9.40	-4.62	3.25	-9.40	-20.42
W5	1973	-15.85	5.40	-10.14	-3.65	6.01	-10.14	-16.46
W6	1974	-13.87	8.22	-10.72	-2.66	8.53	-10.72	-14.19
W7	1975	-12.85	11.77	-11.35	-1.48	11.86	-11.35	-12.94
W8	1976	-12.54	16.63	-11.84	-0.65	16.64	-11.84	-12.56
X1	2370	-34.36	-16.88	-7.62	1.24	-7.62	-16.79	-34.45
X2	2390	-16.19	-14.00	-1.50	4.84	-1.50	-10.13	-20.06
X3	2410	-12.71	-11.84	0.08	7.40	0.08	-4.86	-19.68
X4	2430	-8.05	-13.16	1.09	7.27	1.09	-2.90	-18.31
X5	2450	-6.21	-12.61	1.72	6.36	1.72	-2.30	-16.53
X6	2470	-5.21	-11.98	1.94	5.21	1.94	-2.38	-14.81
X7	2490	-4.60	-11.11	1.71	4.19	1.71	-2.55	-13.17
X8	2510	-4.03	-10.62	1.43	3.25	1.43	-2.69	-11.95
X9	2530	-3.30	-10.25	0.91	2.35	0.91	-2.58	-10.98

Table 2.10.10-11 Impact and Inertial Loads; 30-Foot Top Oblique Drop; $\phi = 60^\circ$; 1.12-Inch Outer Shell Thickness (continued)

Stress Points		Stresses						
Location	Node	S _x	S _y	S _z	S _{xy}	S ₁	S ₂	S ₃
X10	2550	-2.22	-10.08	0.08	1.28	0.08	-2.02	-10.28
X11	2570	-0.71	-10.03	-1.13	0.85	-0.63	-1.13	-10.11
Y1	2305	-0.46	-3.26	2.57	-0.40	2.57	-0.40	-3.32
Y2	2325	-2.95	-3.23	2.89	-0.90	2.89	-2.18	-4.00
Y3	2345	-5.69	-3.25	2.66	-0.90	2.66	-2.96	-5.98
Y4	2365	-8.34	-3.57	2.37	0.16	2.37	-3.56	-8.35
Y5	2385	-9.41	-4.50	2.28	2.00	2.28	-3.79	-10.13
Y6	2405	-8.79	-6.18	2.42	4.01	2.42	-3.27	-11.70
Y7	2425	-7.68	-8.46	2.68	5.92	2.68	-2.14	-14.01
Y8	2445	-7.43	-10.82	3.07	8.05	3.07	-0.89	-17.36
Y9	2465	-9.60	-12.26	3.66	10.53	3.66	-0.31	-21.55
Y10	2485	-16.60	-12.11	3.71	12.23	3.71	-1.92	-26.79
Y11	2505	-22.30	-11.70	2.69	11.42	2.69	-4.42	-29.59
Y12	2525	-25.19	-11.20	1.52	8.79	1.52	-6.96	-29.43
Y13	2545	-27.90	-10.20	-0.77	5.06	-0.77	-8.85	-29.24
Y14	2565	-28.38	-9.99	-5.27	2.37	-5.27	-9.69	-28.68
Z1	2301	-2.89	-0.88	2.35	-0.10	2.35	-0.88	-2.90
Z2	2321	-3.57	-0.45	2.73	-0.22	2.73	-0.44	-3.59
Z3	2341	-4.26	-0.43	2.69	-0.18	2.69	-0.42	-4.27
Z4	2361	-4.90	-0.43	2.68	-0.02	2.68	-0.43	-4.90
Z5	2381	-5.16	-0.47	2.62	0.27	2.62	-0.45	-5.18
Z6	2401	-4.97	-0.58	2.45	0.60	2.45	-0.49	-5.06
Z7	2421	-4.39	-0.75	2.18	0.94	2.18	-0.52	-4.62
Z8	2441	-3.54	-0.96	1.86	1.42	1.86	-0.33	-4.17
Z9	2461	-2.54	-1.17	1.51	3.69	1.90	1.51	-5.61
Z10	2481	-1.50	-1.38	1.18	12.69	11.25	1.18	-14.14
Z11	2501	-1.00	-1.49	0.99	36.68	35.44	0.99	-37.93
Z12	2521	-0.51	-1.56	0.76	110.29	109.25	0.76	-111.32
Z13	2541	-0.23	-1.98	0.30	500.97	499.87	0.30	-502.08
Z14	2561	0.45	-3.06	-1.58	655.17	653.86	-1.58	-656.48

**Table 2.10.10-12 Stress Components – Impact and Inertial Loads; 30-Foot Side Drop;
 $\phi = 90^\circ$; 1.20-Inch Outer Shell Thickness; Circumferential Location = 0°**

Stress Points		Stresses						
Location	Node	S _x	S _y	S _z	S _{xy}	S ₁	S ₂	S ₃
A1	327	-3.04	-0.01	2.46	0.14	2.46	0.00	-3.04
A2	302	-3.54	-0.04	2.16	0.48	2.16	0.02	-3.60
A3	277	-3.84	0.05	1.98	1.12	1.98	0.35	-4.14
A4	252	-4.45	-0.02	1.63	1.45	1.63	0.41	-4.88
A5	227	-5.79	-2.13	1.52	1.00	1.52	-1.87	-6.05
A6	202	0.36	-3.47	8.55	-3.67	8.55	2.59	-5.69
A7	177	-38.71	-2.24	-10.58	-1.67	-2.17	-10.58	-38.78
B1	104	-10.76	-3.20	-3.51	-1.69	-2.84	-3.51	-11.12
B2	79	-7.52	-2.51	-1.03	-0.67	-1.03	-2.42	-7.61
B3	54	-5.97	-1.30	0.62	-1.06	0.62	-1.07	-6.20
B4	29	-4.36	-0.29	2.29	-0.74	2.29	-0.16	-4.50
B5	4	-2.81	0.06	3.30	0.06	3.30	0.07	-2.81
C1	110	-11.31	-0.82	-5.16	0.68	-0.78	-5.16	-11.35
C2	85	-9.35	-0.68	-3.26	0.60	-0.64	-3.26	-9.39
C3	60	-7.53	-0.36	-1.64	0.71	-0.29	-1.64	-7.60
C4	35	-5.71	-0.08	0.08	0.59	0.08	-0.02	-5.77
C5	10	-4.70	-0.01	1.12	0.48	1.12	0.04	-4.75
D1	335	-2.75	2.83	0.68	-0.27	2.85	0.68	-2.77
D2	310	-4.57	1.33	-0.43	-0.18	1.34	-0.43	-4.57
D3	285	-5.44	0.62	-1.01	-0.38	0.64	-1.01	-5.46
D4	260	-6.80	0.00	-1.78	-0.75	0.09	-1.78	-6.88
D5	235	-9.07	-0.58	-3.03	-0.69	-0.52	-3.03	-9.13
D6	210	-11.31	-0.88	-4.37	-0.53	-0.86	-4.37	-11.34
D7	185	-13.56	-0.97	-5.98	0.89	-0.91	-5.98	-13.63
E1	118	-8.14	3.79	-5.69	-1.31	3.94	-5.69	-8.29
E2	93	-9.28	1.61	-5.92	-0.20	1.61	-5.92	-9.28
E3	68	-9.14	0.66	-5.50	0.26	0.67	-5.50	-9.15
E4	43	-9.22	0.21	-4.89	0.34	0.22	-4.89	-9.23
E5	18	-9.63	0.07	-4.60	0.41	0.09	-4.60	-9.64
F1	143	-1.94	10.55	-2.98	-2.02	10.87	-2.26	-2.98
F2	144	-2.09	2.76	-6.95	-1.54	3.20	-2.53	-6.95

**Table 2.10.10-12 Stress Components – Impact and Inertial Loads; 30-Foot Side Drop;
 $\phi = 90^\circ$; 1.20-Inch Outer Shell Thickness; Circumferential Location = 0°
(continued)**

Stress Points		Stresses						
Location	Node	S _x	S _y	S _z	S _{xy}	S ₁	S ₂	S ₃
F3	145	-3.00	0.75	-8.78	-0.97	0.99	-3.24	-8.78
F4	146	-5.28	-0.58	-10.73	-0.50	-0.53	-5.33	-10.73
F5	147	-6.76	-1.64	-12.26	-0.32	-1.62	-6.78	-12.26
F6	148	-7.67	-2.64	-13.52	-0.23	-2.63	-7.68	-13.52
F7	149	-8.29	-3.90	-14.85	-0.13	-3.90	-8.30	-14.85
F8	150	-8.64	-5.59	-16.31	-0.04	-5.59	-8.64	-16.31
G1	335	-2.75	2.83	0.68	-0.27	2.85	0.68	-2.77
G2	336	-2.39	1.29	-0.25	-0.52	1.36	-0.25	-2.46
G3	337	-2.96	-0.07	-1.22	-0.44	-0.01	-1.22	-3.03
G4	338	-4.08	-1.41	-2.23	0.18	-1.40	-2.23	-4.09
G5	339	-6.71	-3.70	-3.90	1.91	-2.78	-3.90	-7.63
G6	340	-9.42	-2.06	-3.95	2.26	-1.42	-3.95	-10.05
H1	346	-5.16	4.90	-8.50	3.55	6.03	-6.29	-8.50
H2	347	-4.30	15.57	-7.21	2.14	15.80	-4.53	-7.21
H3	348	-7.22	11.92	-10.49	-2.43	12.22	-7.52	-10.49
H4	349	-7.75	0.56	-15.03	-2.97	1.51	-8.70	-15.03
H5	350	-8.37	-11.06	-19.50	-1.99	-7.32	-12.12	-19.50
I1	621	-0.18	3.82	1.77	-0.17	3.83	1.77	-0.18
I2	624	-0.09	6.11	2.02	0.04	6.11	2.02	-0.09
J1	635	-0.26	10.06	2.86	-0.38	10.07	2.86	-0.27
J2	638	-0.03	19.65	2.23	0.14	19.65	2.23	-0.03
K1	841	-0.19	16.70	-0.42	-0.10	16.70	-0.19	-0.42
K2	844	-0.06	19.71	1.97	0.10	19.71	1.97	-0.06
L1	855	-0.14	33.28	2.54	-0.22	33.29	2.54	-0.14
L2	858	0.04	36.59	1.36	0.14	36.60	1.36	0.04
M1	941	-0.18	25.27	-0.76	0.01	25.27	-0.18	-0.76
M2	944	-0.10	29.01	1.80	0.06	29.01	1.80	-0.10
N1	955	-0.16	50.99	2.49	-0.12	50.99	2.49	-0.16
N2	958	0.02	55.99	2.11	0.11	55.99	2.11	0.02
O1	1101	-0.19	29.22	-1.08	0.00	29.22	-0.19	-1.08
O2	1104	-0.14	33.31	1.44	0.01	33.31	1.44	-0.14

**Table 2.10.10-12 Stress Components – Impact and Inertial Loads; 30-Foot Side Drop;
 $\phi = 90^\circ$; 1.20-Inch Outer Shell Thickness; Circumferential Location = 0°
(continued)**

Stress Points		Stresses						
Location	Node	S _x	S _y	S _z	S _{xy}	S ₁	S ₂	S ₃
P1	1115	-0.21	61.81	2.28	0.01	61.81	2.28	-0.21
P2	1118	0.02	68.23	3.05	-0.01	68.23	3.05	0.02
Q1	1261	-0.18	26.83	-0.54	0.03	26.83	-0.18	-0.54
Q2	1264	-0.07	30.77	2.02	-0.04	30.77	2.02	-0.07
R1	1275	-0.19	50.03	0.64	0.12	50.03	0.64	-0.19
R2	1278	0.03	55.92	3.40	-0.12	55.92	3.40	0.03
S1	1561	-0.17	6.33	1.32	0.19	6.34	1.32	-0.17
S2	1564	-0.13	9.95	2.91	0.03	9.95	2.91	-0.13
T1	1575	-0.24	20.03	0.94	0.26	20.03	0.94	-0.25
T2	1578	0.01	28.31	4.66	-0.11	28.31	4.66	0.01
U1	1841	-0.09	-0.34	2.86	0.01	2.86	-0.09	-0.34
U2	1844	0.52	0.75	1.96	-0.38	1.96	1.03	0.24
V1	1852	10.10	10.65	-0.06	-7.17	17.55	3.20	-0.06
V2	1856	0.69	5.00	-6.41	0.52	5.06	0.63	-6.41
W1	1969	-42.89	-26.04	-16.32	-3.90	-16.32	-25.18	-43.75
W2	1970	-32.16	0.28	-8.46	-4.48	0.89	-8.46	-32.77
W3	1971	-18.52	3.25	-6.83	-4.78	4.25	-6.83	-19.52
W4	1972	-13.78	6.93	-7.57	-3.93	7.66	-7.57	-14.50
W5	1973	-11.51	9.51	-8.43	-3.02	9.93	-8.43	-11.94
W6	1974	-10.24	11.82	-9.20	-2.15	12.03	-9.20	-10.45
W7	1975	-9.59	14.59	-10.02	-1.17	14.64	-9.65	-10.02
W8	1976	-9.43	18.26	-10.75	-0.43	18.27	-9.44	-10.75
X1	2370	-20.82	-8.25	-5.44	-0.92	-5.44	-8.19	-20.89
X2	2390	-8.75	-3.95	-0.74	0.91	-0.74	-3.78	-8.91
X3	2410	-6.38	-1.85	0.14	2.51	0.14	-0.74	-7.49
X4	2430	-3.31	-2.19	0.55	2.27	0.55	-0.41	-5.09
X5	2450	-1.90	-1.64	0.72	1.63	0.72	-0.13	-3.41
X6	2470	-1.04	-1.20	0.75	0.97	0.75	-0.15	-2.09
X7	2490	-0.58	-0.65	0.76	0.51	0.76	-0.10	-1.13
X8	2510	-0.32	-0.41	0.81	0.29	0.81	-0.07	-0.66

**Table 2.10.10-12 Stress Components – Impact and Inertial Loads; 30-Foot Side Drop;
 $\phi = 90^\circ$; 1.20-Inch Outer Shell Thickness; Circumferential Location = 0°
(continued)**

Stress Points		Stresses						
Location	Node	S _x	S _y	S _z	S _{xy}	S ₁	S ₂	S ₃
X9	2530	-0.05	-0.19	0.88	0.16	0.88	0.05	-0.29
X10	2550	0.30	-0.06	0.98	0.05	0.98	0.30	-0.07
X11	2570	0.76	-0.01	1.15	0.06	1.15	0.76	-0.02
Y1	2305	-0.12	0.28	0.92	-0.23	0.92	0.38	-0.22
Y2	2325	-1.93	0.19	0.78	-0.67	0.78	0.38	-2.12
Y3	2345	-3.60	0.26	0.80	-0.77	0.80	0.41	-3.75
Y4	2365	-5.05	0.33	0.86	-0.29	0.86	0.35	-5.06
Y5	2385	-5.42	0.26	1.02	0.49	1.02	0.30	-5.46
Y6	2405	-4.76	0.02	1.21	1.13	1.21	0.28	-5.02
Y7	2425	-3.76	-0.26	1.32	1.42	1.32	0.25	-4.27
Y8	2445	-2.87	-0.44	1.33	1.46	1.33	0.24	-3.55
Y9	2465	-2.24	-0.45	1.33	1.38	1.33	0.30	-2.99
Y10	2485	-1.96	-0.30	1.35	1.21	1.35	0.34	-2.59
Y11	2505	-1.96	-0.25	1.35	1.07	1.35	0.27	-2.47
Y12	2525	-1.82	-0.13	1.40	0.78	1.40	0.18	-2.13
Y13	2545	-1.66	-0.01	1.47	0.43	1.47	0.09	-1.76
Y14	2565	-1.36	0.03	1.56	0.19	1.56	0.05	-1.39
Z1	2301	-1.64	0.12	0.74	-0.01	0.74	0.12	-1.64
Z2	2321	-2.03	0.13	0.98	-0.04	0.98	0.13	-2.03
Z3	2341	-2.54	0.20	1.19	-0.04	1.19	0.20	-2.54
Z4	2361	-2.97	0.27	1.39	0.01	1.39	0.27	-2.97
Z5	2381	-3.18	0.31	1.52	0.07	1.52	0.31	-3.19
Z6	2401	-3.12	0.31	1.57	0.15	1.57	0.31	-3.12
Z7	2421	-2.82	0.27	1.56	0.21	1.56	0.28	-2.83
Z8	2441	-2.39	0.21	1.49	0.25	1.49	0.23	-2.42
Z9	2461	-1.93	0.14	1.42	0.36	1.42	0.21	-1.99
Z10	2481	-1.50	0.10	1.36	0.77	1.36	0.41	-1.81
Z11	2501	-1.32	0.05	1.39	1.88	1.39	1.36	-2.63
Z12	2521	-1.16	0.05	1.43	5.35	4.83	1.43	-5.94
Z13	2541	-1.05	0.04	1.49	23.86	23.35	1.49	-24.37
Z14	2561	-1.03	0.03	1.57	31.16	30.66	1.57	-31.66

Table 2.10.10-13 Stress Components – Thermal; 130°F; 1.20-Inch Outer Shell Thickness

Stress Points		Stresses						
Location	Node	S _x	S _y	S _z	S _{xy}	S ₁	S ₂	S ₃
A1	327	5.20	0.07	5.19	0.23	5.21	5.19	0.06
A2	302	4.34	0.07	4.34	-0.02	4.34	4.34	0.07
A3	277	3.48	0.01	3.48	-0.10	3.48	3.48	0.01
A4	252	1.77	-0.04	1.77	-0.02	1.77	1.77	-0.04
A5	227	-1.61	-0.06	-1.61	-0.03	-0.06	-1.61	-1.61
A6	202	-4.97	-0.10	-4.98	-0.01	-0.10	-4.97	-4.98
A7	177	-8.36	-0.11	-8.32	0.00	-0.11	-8.32	-8.36
B1	104	0.17	0.03	0.14	0.07	0.20	0.14	0.00
B2	79	1.14	0.05	1.15	0.06	1.15	1.14	0.04
B3	54	2.17	0.10	2.19	0.04	2.19	2.17	0.10
B4	29	3.26	0.05	3.24	0.07	3.26	3.24	0.05
B5	4	5.03	-0.03	4.97	-0.42	5.06	4.97	-0.06
C1	110	0.36	-0.85	0.58	0.23	0.58	0.40	-0.89
C2	85	1.26	-0.69	1.50	0.24	1.50	1.29	-0.72
C3	60	2.13	-0.36	2.55	0.27	2.55	2.16	-0.39
C4	35	3.23	-0.11	3.75	0.10	3.75	3.24	-0.11
C5	10	5.17	-0.02	5.61	-0.11	5.61	5.17	-0.03
D1	335	-0.14	-8.26	1.45	-0.93	1.45	-0.03	-8.37
D2	310	2.59	-4.75	2.56	-1.01	2.72	2.56	-4.89
D3	285	2.42	-3.05	2.46	-0.90	2.57	2.46	-3.19
D4	260	1.31	-2.12	1.35	-0.84	1.51	1.35	-2.32
D5	235	-0.85	-1.84	-1.25	-0.66	-0.52	-1.25	-2.17
D6	210	-3.33	-1.79	-4.06	-0.02	-1.79	-3.33	-4.06
D7	185	-6.26	-1.74	-7.10	0.91	-1.56	-6.44	-7.10
E1	118	3.74	-2.61	2.21	3.55	5.33	2.21	-4.20
E2	93	0.78	0.82	2.56	1.59	2.56	2.39	-0.79
E3	68	0.98	0.29	2.93	1.17	2.93	1.85	-0.58
E4	43	0.97	0.06	3.46	0.55	3.46	1.23	-0.20
E5	18	2.03	0.02	4.91	0.16	4.91	2.04	0.01
F1	143	-9.75	-8.25	-1.88	6.09	-1.88	-2.87	-15.13
F2	144	-8.47	5.17	1.53	3.40	5.97	1.53	-9.27

Table 2.10.10-13 Stress Components – Thermal; 130°F; 1.20-Inch Outer Shell Thickness
(continued)

Stress Points		Stresses						
Location	Node	S _x	S _y	S _z	S _{xy}	S ₁	S ₂	S ₃
F3	145	-5.46	3.27	1.42	0.59	3.31	1.42	-5.50
F4	146	-2.43	2.55	1.90	-0.12	2.56	1.90	-2.43
F5	147	-1.22	2.11	2.09	-0.28	2.14	2.09	-1.24
F6	148	-0.61	1.87	2.19	-0.29	2.19	1.91	-0.65
F7	149	-0.27	1.76	2.27	-0.19	2.27	1.78	-0.29
F8	150	-0.11	1.87	2.37	-0.12	2.37	1.88	-0.12
G1	335	-0.14	-8.26	1.45	-0.93	1.45	-0.03	-8.37
G2	336	0.15	-4.60	2.62	0.06	2.62	0.15	-4.60
G3	337	1.39	-1.85	3.73	0.55	3.73	1.48	-1.94
G4	338	2.41	1.34	4.88	-0.02	4.88	2.41	1.34
G5	339	5.62	6.62	7.12	-2.70	8.87	7.12	3.37
G6	340	7.01	1.74	6.29	-3.12	8.46	6.29	0.29
H1	346	-9.21	-3.92	-2.76	0.17	-2.76	-3.92	-9.21
H2	347	-4.67	3.43	0.67	0.34	3.44	0.67	-4.68
H3	348	-2.25	7.59	2.68	-0.20	7.59	2.68	-2.26
H4	349	-0.76	10.01	3.82	-0.34	10.02	3.82	-0.77
H5	350	-0.23	13.48	4.89	-0.29	13.48	4.89	-0.23
I1	621	0.00	2.73	0.33	0.03	2.73	0.33	0.00
I2	624	0.01	1.51	0.14	0.01	1.51	0.14	0.01
J1	635	0.00	10.28	0.27	0.05	10.28	0.27	0.00
J2	638	0.01	8.00	-0.11	0.05	8.00	0.01	-0.11
K1	841	0.00	1.87	-0.21	-0.01	1.87	0.00	-0.21
K2	844	0.00	2.29	0.19	0.01	2.29	0.19	0.00
L1	855	0.00	8.82	-0.36	0.00	8.82	0.00	-0.36
L2	858	0.00	9.35	0.18	0.00	9.35	0.18	0.00
M1	941	0.00	1.81	-0.27	0.00	1.81	0.00	-0.27
M2	944	0.00	2.34	0.25	0.00	2.34	0.25	0.00
N1	955	0.00	8.70	-0.45	0.00	8.70	0.00	-0.45
N2	958	0.00	9.41	0.23	0.00	9.41	0.23	0.00
O1	1101	0.00	1.81	-0.27	0.00	1.81	0.00	-0.27
O2	1104	0.00	2.34	0.25	0.00	2.34	0.25	0.00

**Table 2.10.10-13 Stress Components – Thermal; 130°F; 1.20-Inch Outer Shell Thickness
(continued)**

Stress Points		Stresses						
Location	Node	S _x	S _y	S _z	S _{xy}	S ₁	S ₂	S ₃
P1	1115	0.00	8.67	-0.49	0.00	8.67	0.00	-0.49
P2	1118	0.00	9.42	0.24	0.00	9.42	0.24	0.00
Q1	1261	0.00	1.87	-0.18	0.00	1.87	0.00	-0.18
Q2	1264	0.00	2.28	0.22	0.00	2.28	0.22	0.00
R1	1275	0.00	8.71	-0.47	0.00	8.71	0.00	-0.47
R2	1278	-0.01	9.46	0.09	0.00	9.46	0.09	-0.01
S1	1561	0.00	1.74	0.20	0.03	1.74	0.20	0.00
S2	1564	-0.03	2.46	0.51	0.05	2.46	0.51	-0.03
T1	1575	0.00	10.28	0.14	-0.06	10.28	0.14	0.00
T2	1578	0.00	7.98	-0.10	-0.05	7.98	0.00	-0.10
U1	1841	0.02	0.16	-0.68	-0.08	0.20	-0.02	-0.68
U2	1844	0.16	1.04	-0.02	-0.08	1.04	0.15	-0.02
V1	1852	-5.61	-2.18	-2.49	-1.23	-1.79	-2.49	-6.00
V2	1856	-0.29	11.50	3.33	0.18	11.50	3.33	-0.29
W1	1969	-0.74	-1.93	0.01	-0.86	0.01	-0.29	-2.38
W2	1970	0.00	-0.82	0.71	-0.72	0.71	0.42	-1.24
W3	1971	-0.10	-0.13	0.97	-0.59	0.97	0.47	-0.71
W4	1972	-0.08	0.52	1.22	-0.52	1.22	0.82	-0.39
W5	1973	-0.07	0.95	1.39	-0.42	1.39	1.10	-0.22
W6	1974	-0.06	1.30	1.54	-0.29	1.54	1.36	-0.12
W7	1975	-0.03	1.61	1.68	-0.15	1.68	1.62	-0.05
W8	1976	0.01	1.88	1.81	-0.07	1.88	1.81	0.01
X1	2370	-1.24	-0.34	-0.33	0.62	-0.03	-0.33	-1.56
X2	2390	-0.31	-0.98	-0.24	0.45	-0.08	-0.24	-1.21
X3	2410	-0.34	-0.56	-0.07	0.06	-0.07	-0.33	-0.58
X4	2430	-0.33	-0.41	0.01	-0.14	0.01	-0.22	-0.51
X5	2450	-0.39	-0.24	0.07	-0.27	0.07	-0.04	-0.60
X6	2470	-0.40	-0.14	0.14	-0.33	0.14	0.09	-0.63
X7	2490	-0.38	-0.06	0.26	-0.34	0.26	0.16	-0.60
X8	2510	-0.33	-0.03	0.35	-0.32	0.35	0.17	-0.54

Table 2.10.10-13 Stress Components – Thermal; 130°F; 1.20-Inch Outer Shell Thickness
(continued)

Stress Points		Stresses						
Location	Node	S _x	S _y	S _z	S _{xy}	S ₁	S ₂	S ₃
X9	2530	-0.28	-0.01	0.47	-0.27	0.47	0.15	-0.44
X10	2550	-0.22	0.00	0.62	-0.17	0.62	0.09	-0.31
X11	2570	0.62	0.00	1.59	-0.05	1.59	0.63	-0.01
Y1	2305	0.57	-0.03	0.50	-0.04	0.57	0.50	-0.03
Y2	2325	0.03	-0.05	-0.01	0.05	0.05	-0.01	-0.08
Y3	2345	-0.28	-0.11	-0.33	0.05	-0.10	-0.29	-0.33
Y4	2365	-0.55	-0.17	-0.60	0.05	-0.16	-0.55	-0.60
Y5	2385	-0.73	-0.21	-0.78	0.05	-0.21	-0.73	-0.78
Y6	2405	-0.79	-0.25	-0.87	0.04	-0.25	-0.79	-0.87
Y7	2425	-0.77	-0.28	-0.87	0.00	-0.28	-0.77	-0.87
Y8	2445	-0.71	-0.26	-0.79	-0.05	-0.25	-0.71	-0.79
Y9	2465	-0.60	-0.19	-0.66	-0.08	-0.18	-0.62	-0.66
Y10	2485	-0.42	-0.11	-0.44	-0.09	-0.09	-0.44	-0.44
Y11	2505	-0.28	-0.05	-0.28	-0.04	-0.04	-0.28	-0.29
Y12	2525	-0.10	-0.02	-0.10	-0.01	-0.02	-0.10	-0.10
Y13	2545	0.14	0.00	0.12	-0.01	0.14	0.12	0.00
Y14	2565	1.26	0.00	1.16	0.07	1.27	1.16	0.00
Z1	2301	0.51	0.01	0.50	0.00	0.51	0.50	0.01
Z2	2321	0.09	0.03	0.09	0.00	0.09	0.09	0.03
Z3	2341	-0.23	0.07	-0.23	0.00	0.07	-0.23	-0.23
Z4	2361	-0.50	0.09	-0.50	0.00	0.09	-0.50	-0.50
Z5	2381	-0.68	0.10	-0.68	0.00	0.10	-0.68	-0.68
Z6	2401	-0.78	0.10	-0.78	0.00	0.10	-0.78	-0.78
Z7	2421	-0.79	0.10	-0.79	0.00	0.10	-0.79	-0.79
Z8	2441	-0.72	0.10	-0.72	0.00	0.10	-0.72	-0.72
Z9	2461	-0.57	-0.09	-0.57	0.00	0.09	-0.57	-0.57
Z10	2481	-0.34	0.07	-0.33	0.00	0.07	-0.33	-0.34
Z11	2501	-0.20	0.05	-0.20	0.00	0.05	-0.20	-0.20
Z12	2521	-0.04	0.03	-0.05	0.00	0.03	-0.04	-0.05
Z13	2541	0.11	0.01	0.10	0.00	0.11	0.10	0.01
Z14	2561	1.07	0.01	1.07	0.00	1.07	1.07	0.01

Table 2.10.10-14 Stress Components – 50 psi Internal Pressure and Bolt Preload; 1.20-Inch Outer Shell Thickness

Stress Points		Stresses						
Location	Node	S _x	S _y	S _z	S _{xy}	S ₁	S ₂	S ₃
A1	327	-0.10	-0.05	-0.11	0.00	-0.05	-0.10	-0.11
A2	302	-0.09	-0.05	-0.09	0.00	-0.05	-0.09	-0.09
A3	277	-0.07	-0.05	-0.07	0.01	-0.05	-0.07	-0.07
A4	252	-0.04	-0.04	-0.04	0.01	-0.03	-0.04	-0.05
A5	227	0.01	-0.03	0.01	0.01	0.01	0.01	-0.03
A6	202	0.06	-0.01	0.06	0.01	0.06	0.06	-0.01
A7	177	0.12	0.00	0.12	0.00	0.12	0.12	0.00
B1	104	0.01	0.00	0.01	0.00	0.01	0.01	0.00
B2	79	0.00	0.00	0.00	0.00	0.00	0.00	0.00
B3	54	0.00	0.00	0.00	0.00	0.00	0.00	0.00
B4	29	0.00	0.00	0.00	0.00	0.00	0.00	0.00
B5	4	0.00	0.00	0.00	0.00	0.00	0.00	0.00
C1	110	0.01	0.00	0.01	0.00	0.01	0.01	0.00
C2	85	0.00	0.00	0.00	0.00	0.00	0.00	0.00
C3	60	0.00	0.00	0.00	0.00	0.00	0.00	0.00
C4	35	0.00	0.00	0.00	0.00	0.00	0.00	0.00
C5	10	0.00	0.00	0.00	0.00	0.00	0.00	0.00
D1	335	0.25	0.39	0.17	0.11	0.45	0.19	0.17
D2	310	0.06	0.23	0.07	0.08	0.27	0.07	0.02
D3	285	0.02	0.14	0.04	0.06	0.16	0.04	0.00
D4	260	0.00	0.07	0.02	0.04	0.09	0.02	-0.02
D5	235	-0.01	0.03	0.01	0.03	0.04	0.01	-0.02
D6	210	-0.01	0.01	0.02	0.02	0.02	0.02	-0.02
D7	185	-0.03	0.00	0.03	0.01	0.03	0.00	-0.03
E1	118	0.01	0.00	0.01	0.00	0.01	0.01	0.00
E2	93	0.00	0.00	0.00	0.00	0.00	0.00	0.00
E3	68	0.00	0.00	0.00	0.00	0.00	0.00	0.00
E4	43	0.00	0.00	0.00	0.00	0.00	0.00	0.00
E5	18	0.00	0.00	0.00	0.00	0.00	0.00	0.00
F1	143	0.00	-0.01	0.00	0.00	0.00	0.00	-0.01
F2	144	0.00	-0.01	0.00	0.00	0.00	0.00	-0.01

Table 2.10.10-14 Stress Components – 50 psi Internal Pressure and Bolt Preload; 1.20-Inch Outer Shell Thickness (continued)

Stress Points		Stresses						
Location	Node	S _x	S _y	S _z	S _{xy}	S ₁	S ₂	S ₃
F3	145	0.00	0.00	0.01	0.01	0.01	0.00	-0.01
F4	146	0.00	0.00	0.01	0.01	0.01	0.01	0.00
F5	147	0.00	0.00	0.01	0.00	0.01	0.01	0.00
F6	148	0.00	0.01	0.01	0.00	0.01	0.01	0.00
F7	149	0.00	0.01	0.01	0.00	0.01	0.01	0.00
F8	150	0.00	0.01	0.01	0.00	0.01	0.01	0.00
G1	335	0.25	0.39	0.17	0.11	0.45	0.19	0.17
G2	336	0.14	0.20	0.09	0.06	0.23	0.11	0.09
G3	337	0.06	0.12	0.04	0.02	0.13	0.06	0.04
G4	338	0.02	0.05	0.01	0.01	0.05	0.02	0.01
G5	339	-0.03	-0.07	-0.03	0.03	-0.01	-0.03	-0.09
G6	340	-0.06	-0.04	-0.03	0.04	-0.01	-0.03	-0.09
H1	346	0.00	0.00	0.00	0.00	0.01	0.00	0.00
H2	347	0.00	0.01	0.00	0.00	0.01	0.00	0.00
H3	348	0.00	0.01	0.00	0.00	0.01	0.00	0.00
H4	349	0.00	0.01	0.00	0.00	0.01	0.00	0.00
H5	350	0.00	0.01	0.00	0.00	0.01	0.00	0.00
I1	621	-0.05	0.10	0.35	-0.01	0.35	0.10	-0.05
I2	624	-0.02	0.18	0.33	0.00	0.33	0.18	-0.02
J1	635	0.00	0.01	0.00	0.00	0.01	0.00	0.00
J2	638	0.00	0.01	0.00	0.00	0.01	0.00	0.00
K1	841	-0.05	0.11	0.36	0.02	0.36	0.11	-0.05
K2	844	-0.01	0.10	0.32	0.03	0.32	0.11	-0.01
L1	855	0.00	0.01	0.00	0.00	0.01	0.00	0.00
L2	858	0.00	0.01	0.00	0.00	0.01	0.00	0.00
M1	941	-0.05	0.11	0.36	0.00	0.36	0.11	-0.05
M2	944	-0.01	0.11	0.32	0.00	0.32	0.11	-0.01
N1	955	0.00	0.01	0.00	0.00	0.01	0.00	0.00
N2	958	0.00	0.01	0.00	0.00	0.01	0.00	0.00
O1	1101	-0.05	0.11	0.36	0.00	0.36	0.11	-0.05
O2	1104	-0.01	0.11	0.32	0.00	0.32	0.11	-0.01

Table 2.10.10-14 Stress Components – 50 psi Internal Pressure and Bolt Preload; 1.20-Inch Outer Shell Thickness (continued)

Stress Points		Stresses						
Location	Node	S _x	S _y	S _z	S _{xy}	S ₁	S ₂	S ₃
P1	1115	0.00	0.01	0.00	0.00	0.01	0.00	0.00
P2	1118	0.00	0.01	0.00	0.00	0.01	0.00	0.00
Q1	1261	-0.05	0.11	0.36	0.00	0.36	0.11	-0.05
Q2	1264	-0.01	0.11	0.32	0.00	0.32	0.11	-0.01
R1	1275	0.00	0.01	0.00	0.00	0.01	0.00	0.00
R2	1278	0.00	0.01	0.00	0.00	0.01	0.00	0.00
S1	1561	-0.05	0.11	0.35	0.00	0.35	0.11	-0.05
S2	1564	-0.01	0.14	0.32	0.00	0.32	0.14	-0.01
T1	1575	0.00	0.03	0.00	0.00	0.03	0.00	0.00
T2	1578	0.00	0.00	-0.01	0.00	0.00	0.00	-0.01
U1	1841	-0.06	-0.17	0.22	0.01	0.22	-0.06	-0.17
U2	1844	-0.13	-0.01	0.21	0.10	0.21	0.05	-0.19
V1	1852	0.07	0.01	0.07	0.01	0.07	0.07	0.01
V2	1856	0.00	0.00	0.05	0.01	0.05	0.01	0.00
W1	1969	-0.05	-0.19	0.07	0.18	0.07	0.07	-0.31
W2	1970	0.00	-0.14	0.08	0.02	0.08	0.00	-0.14
W3	1971	0.01	-0.08	0.09	-0.05	0.09	0.03	-0.10
W4	1972	0.00	-0.03	0.10	-0.05	0.10	0.04	-0.07
W5	1973	0.00	0.01	0.10	-0.05	0.10	0.05	-0.05
W6	1974	0.00	0.03	0.11	-0.04	0.11	0.06	-0.03
W7	1975	0.00	0.06	0.11	-0.02	0.11	0.07	-0.01
W8	1976	0.00	0.08	0.11	-0.01	0.11	0.08	0.00
X1	2370	0.01	-0.04	-0.01	0.09	0.08	-0.01	-0.10
X2	2390	-0.05	-0.20	-0.08	0.05	-0.03	-0.08	-0.21
X3	2410	0.06	-0.20	-0.03	-0.04	0.07	-0.03	-0.21
X4	2430	0.03	-0.09	0.00	-0.08	0.07	0.00	-0.12
X5	2450	0.01	-0.04	0.01	-0.07	0.06	0.01	-0.09
X6	2470	0.00	-0.01	0.02	-0.05	0.05	0.02	-0.05
X7	2490	0.01	0.00	0.03	-0.03	0.04	0.03	-0.03
X8	2510	0.02	0.00	0.04	-0.02	0.04	0.03	-0.02

Table 2.10.10-14 Stress Components – 50 psi Internal Pressure and Bolt Preload; 1.20-Inch Outer Shell Thickness (continued)

Stress Points		Stresses						
Location	Node	S _x	S _y	S _z	S _{xy}	S ₁	S ₂	S ₃
X9	2530	0.02	0.00	0.04	-0.02	0.04	0.03	-0.01
X10	2550	0.02	0.00	0.05	-0.01	0.05	0.03	0.00
X11	2570	0.03	0.00	0.05	0.00	0.05	0.03	0.00
Y1	2305	-0.05	-0.05	-0.05	0.01	-0.04	-0.05	-0.06
Y2	2325	-0.04	-0.05	-0.04	0.00	-0.04	-0.04	-0.05
Y3	2345	-0.03	-0.05	-0.04	0.00	-0.03	-0.04	-0.05
Y4	2365	-0.03	-0.05	-0.03	-0.01	-0.03	-0.03	-0.05
Y5	2385	-0.03	-0.05	-0.03	-0.01	-0.02	-0.03	-0.05
Y6	2405	-0.02	-0.05	-0.02	-0.01	-0.01	-0.02	-0.05
Y7	2425	0.00	-0.04	-0.01	-0.01	0.00	-0.01	-0.04
Y8	2445	0.01	-0.03	0.01	-0.01	0.02	0.01	-0.04
Y9	2465	0.03	-0.02	0.02	-0.02	0.03	0.02	-0.03
Y10	2485	0.04	-0.01	0.04	-0.01	0.04	0.04	-0.02
Y11	2505	0.04	-0.01	0.05	-0.01	0.05	0.05	-0.01
Y12	2525	0.05	0.00	0.06	-0.01	0.06	0.05	-0.01
Y13	2545	0.06	0.00	0.07	-0.01	0.07	0.06	0.00
Y14	2565	0.07	0.00	0.08	0.00	0.08	0.07	0.00
Z1	2301	-0.05	-0.05	-0.05	0.00	-0.05	-0.05	-0.05
Z2	2321	-0.04	-0.05	-0.04	0.00	-0.04	-0.04	-0.05
Z3	2341	-0.04	-0.04	-0.04	0.00	-0.04	-0.04	-0.04
Z4	2361	-0.03	-0.04	-0.03	0.00	-0.03	-0.03	-0.04
Z5	2381	-0.03	-0.04	-0.03	0.00	-0.03	-0.03	-0.04
Z6	2401	-0.02	-0.03	-0.02	0.00	-0.02	-0.02	-0.03
Z7	2421	0.00	-0.03	0.00	0.00	0.00	0.00	-0.03
Z8	2441	0.01	-0.02	0.01	0.00	0.01	0.01	-0.02
Z9	2461	0.02	-0.01	0.02	0.00	0.02	0.02	-0.01
Z10	2481	0.04	-0.01	0.04	0.00	0.04	0.04	-0.01
Z11	2501	0.05	0.00	0.05	0.00	0.05	0.05	0.00
Z12	2521	0.06	0.00	0.06	0.00	0.06	0.06	0.00
Z13	2541	0.08	0.00	0.08	0.00	0.08	0.08	0.00
Z14	2561	0.09	0.00	0.09	0.00	0.09	0.09	0.00

**Table 2.10.10-15 Primary Stresses; 30-Foot Top End Drop; $\phi = 0^\circ$;
1.12-Inch Outer Shell Thickness**

Stress Points		Stresses						
Location	Node	S _x	S _y	S _z	S _{xy}	S ₁	S ₂	S ₃
A1	327	0.64	-0.04	0.65	0.03	0.65	0.64	-0.04
A2	302	0.57	-0.04	0.58	-0.01	0.58	0.57	-0.04
A3	277	0.50	-0.04	0.51	-0.02	0.51	0.50	-0.04
A4	252	0.38	-0.05	0.38	-0.02	0.38	0.38	-0.05
A5	227	0.14	-0.07	0.14	-0.02	0.14	0.14	-0.07
A6	202	-0.09	-0.08	-0.10	-0.02	-0.07	-0.10	-0.10
A7	177	-0.36	-0.09	-0.37	-0.01	-0.09	-0.36	-0.37
B1	104	0.32	0.01	0.34	0.00	0.34	0.32	0.01
B2	79	0.04	0.01	0.05	-0.04	0.07	0.05	-0.02
B3	54	-0.21	-0.01	-0.21	-0.05	0.00	-0.21	-0.22
B4	29	-0.46	-0.01	-0.48	-0.04	-0.01	-0.47	-0.48
B5	4	-0.61	0.00	-0.63	0.04	0.00	-0.61	-0.63
C1	110	0.03	0.00	0.18	-0.04	0.18	0.06	-0.03
C2	85	-0.08	0.00	-0.02	-0.08	0.05	-0.02	-0.13
C3	60	-0.17	0.00	-0.19	-0.10	0.05	-0.19	-0.22
C4	35	-0.25	0.00	-0.36	-0.06	0.01	-0.26	-0.36
C5	10	-0.31	0.00	-0.46	-0.01	0.00	-0.31	-0.46
D1	335	-0.08	-0.71	0.15	-0.12	0.15	-0.06	-0.73
D2	310	0.16	-0.47	0.24	-0.14	0.24	0.19	-0.50
D3	285	0.19	-0.36	0.24	-0.15	0.24	0.23	-0.40
D4	260	0.21	-0.28	0.21	-0.13	0.25	0.21	-0.31
D5	235	0.17	-0.20	0.12	-0.11	0.20	0.12	-0.23
D6	210	0.10	-0.14	0.01	-0.07	0.12	0.01	-0.16
D7	185	0.05	-0.12	-0.13	-0.03	0.05	-0.12	-0.13
E1	118	-0.44	-0.43	-0.22	-0.17	-0.22	-0.27	-0.60
E2	93	-0.12	-0.26	-0.15	-0.11	-0.06	-0.15	-0.32
E3	68	-0.06	-0.11	-0.16	-0.06	-0.02	-0.15	-0.16
E4	43	0.00	-0.04	-0.21	-0.02	0.01	-0.05	-0.21
E5	18	0.06	-0.01	-0.23	0.00	0.06	-0.01	-0.23
F1	143	0.03	-0.33	-0.08	-0.16	0.09	-0.08	-0.39
F2	144	-0.03	-0.12	-0.03	-0.18	0.11	-0.03	-0.26

Table 2.10.10-15 Primary Stresses; 30-Foot Top End Drop; $\phi = 0^\circ$;
1.12-Inch Outer Shell Thickness (continued)

Stress Points		Stresses						
Location	Node	S _x	S _y	S _z	S _{xy}	S ₁	S ₂	S ₃
F3	145	-0.07	-0.10	-0.04	-0.20	0.11	-0.04	-0.28
F4	146	-0.04	-0.09	-0.03	-0.17	0.10	-0.03	-0.23
F5	147	-0.02	-0.08	-0.02	-0.13	0.08	-0.02	-0.19
F6	148	-0.01	-0.07	-0.02	-0.09	0.06	-0.02	-0.14
F7	149	-0.01	-0.06	-0.01	-0.05	0.03	-0.01	-0.09
F8	150	0.00	-0.04	0.00	-0.03	0.01	0.00	-0.05
G1	335	-0.08	-0.71	0.15	-0.12	0.15	-0.06	-0.73
G2	336	-0.09	-0.56	0.18	-0.05	0.18	-0.08	-0.57
G3	337	-0.03	-0.51	0.20	-0.01	0.20	-0.03	-0.51
G4	338	0.00	-0.50	0.20	0.03	0.20	0.00	-0.50
G5	339	0.01	-0.36	0.22	0.08	0.22	0.02	-0.37
G6	340	0.08	-0.10	0.29	0.08	0.29	0.11	-0.13
H1	346	0.10	-0.21	0.23	-0.13	0.23	0.15	-0.26
H2	347	0.00	-0.72	0.05	-0.13	0.05	0.02	-0.74
H3	348	0.03	-0.93	0.00	0.00	0.03	0.00	-0.93
H4	349	0.01	-0.82	0.03	0.05	0.03	0.01	-0.83
H5	350	0.00	-0.77	0.04	0.04	0.04	0.00	-0.77
I1	621	-0.05	-1.12	0.32	0.02	0.32	-0.05	-1.12
I2	624	0.02	-1.40	0.22	0.03	0.22	0.02	-1.40
J1	635	0.00	-1.09	0.05	0.00	0.05	0.00	-1.09
J2	638	0.00	-1.13	0.03	0.00	0.03	0.00	-1.13
K1	841	-0.05	-1.68	0.47	0.03	0.47	-0.05	-1.68
K2	844	0.00	-1.69	0.42	0.02	0.42	0.00	-1.69
L1	855	0.00	-1.55	0.00	0.00	0.00	0.00	-1.55
L2	858	0.00	-1.55	0.00	0.00	0.00	0.00	-1.55
M1	941	-0.05	-2.22	0.47	0.00	0.47	-0.05	-2.22
M2	944	0.00	-2.22	0.42	0.00	0.42	0.00	-2.22
N1	955	0.00	-2.09	0.00	0.00	0.00	0.00	-2.09
N2	958	0.00	-2.09	0.00	0.00	0.00	0.00	-2.09
O1	1101	-0.05	-3.11	0.47	0.00	0.47	-0.05	-3.11
O2	1104	0.00	-3.11	0.42	0.00	0.42	0.00	-3.11

**Table 2.10.10-15 Primary Stresses; 30-Foot Top End Drop; $\phi = 0^\circ$;
1.12-Inch Outer Shell Thickness (continued)**

Stress Points		Stresses						
Location	Node	S _x	S _y	S _z	S _{xy}	S ₁	S ₂	S ₃
P1	1115	0.00	-2.97	0.00	0.00	0.00	0.00	-2.97
P2	1118	0.00	-2.97	0.00	0.00	0.00	0.00	-2.97
Q1	1261	-0.05	-3.99	0.47	0.00	0.47	-0.05	-3.99
Q2	1264	0.00	-3.99	0.42	0.00	0.42	0.00	-3.99
R1	1275	0.00	-3.85	0.00	0.00	0.00	0.00	-3.85
R2	1278	0.00	-3.86	0.00	0.00	0.00	0.00	-3.86
S1	1561	-0.05	-3.64	-0.12	-0.13	-0.04	-0.12	-3.64
S2	1564	0.09	-6.12	-0.72	-0.16	0.09	-0.72	-6.12
T1	1575	0.00	-4.36	0.24	-0.01	0.24	0.00	-4.36
T2	1578	0.00	-5.06	0.04	-0.01	0.04	0.00	-5.06
U1	1841	-0.05	-6.77	2.41	-0.16	2.41	-0.04	-6.78
U2	1844	0.71	-3.39	3.21	-0.07	3.21	0.71	-3.39
V1	1852	-1.00	-5.38	0.75	-0.18	0.75	-0.99	-5.38
V2	1856	0.02	-3.40	1.35	-0.03	1.35	0.02	-3.40
W1	1969	1.88	-1.46	0.39	1.51	2.46	0.39	-2.04
W2	1970	1.30	-3.17	-0.12	0.55	1.36	-0.12	-3.24
W3	1971	0.71	-3.85	-0.36	-0.11	0.71	-0.36	-3.85
W4	1972	0.39	-4.51	-0.56	-0.25	0.40	-0.56	-4.52
W5	1973	0.23	-4.97	-0.69	-0.27	0.24	-0.69	-4.99
W6	1974	0.13	-5.33	-0.78	-0.23	0.14	-0.78	-5.34
W7	1975	0.06	-5.71	-0.87	-0.13	0.07	-0.87	-5.72
W8	1976	0.02	-6.14	-0.97	-0.07	0.02	-0.97	-6.14
X1	2370	4.33	1.35	3.33	2.45	5.71	3.33	-0.02
X2	2390	0.30	-2.59	0.57	2.12	1.42	0.57	-3.71
X3	2410	0.19	-4.58	-0.24	1.04	0.41	-0.24	-4.80
X4	2430	-0.61	-4.28	-0.57	0.94	-0.38	-0.57	-4.50
X5	2450	-0.67	-4.63	-0.74	0.93	-0.47	-0.74	-4.83
X6	2470	-0.57	-4.61	-0.64	0.95	-0.35	-0.64	-4.82
X7	2490	-0.12	-4.73	-0.43	0.89	0.04	-0.43	-4.90
X8	2510	0.14	-4.75	-0.29	0.79	0.26	-0.29	-4.87
X9	2530	0.46	-4.81	-0.17	0.61	0.53	-0.17	-4.88

Table 2.10.10-15 Primary Stresses; 30-Foot Top End Drop; $\phi = 0^\circ$;
1.12-Inch Outer Shell Thickness (continued)

Stress Points		Stresses						
Location	Node	S _x	S _y	S _z	S _{xy}	S ₁	S ₂	S ₃
X10	2550	0.81	-4.83	-0.05	0.35	0.84	-0.05	-4.85
X11	2570	1.22	-4.84	0.02	0.20	1.22	0.02	-4.85
Y1	2305	0.76	-1.95	1.17	0.12	1.17	0.77	-1.95
Y2	2325	0.90	-2.10	1.01	0.50	1.01	0.98	-2.19
Y3	2345	1.10	-2.45	1.03	0.58	1.19	1.03	-2.54
Y4	2365	1.10	-2.76	0.94	0.46	1.15	0.94	-2.82
Y5	2385	0.75	-2.97	0.66	0.31	0.77	0.66	-3.00
Y6	2405	0.23	-3.13	0.28	0.29	0.28	0.25	-3.15
Y7	2425	-0.18	-3.32	-0.06	0.40	-0.06	-0.13	-3.38
Y8	2445	-0.40	-3.62	-0.30	0.54	-0.30	-0.31	-3.70
Y9	2465	-0.47	-3.98	-0.43	0.61	-0.37	-0.43	-4.08
Y10	2485	-0.47	-4.32	-0.53	0.57	-0.39	-0.53	-4.40
Y11	2505	-0.50	-4.54	-0.62	0.51	-0.44	-0.62	-4.60
Y12	2525	-0.54	-4.68	-0.72	0.39	-0.50	-0.72	-4.72
Y13	2545	-0.62	-4.78	-0.87	0.22	-0.61	-0.87	-4.80
Y14	2565	-0.77	-4.82	-1.09	0.04	-0.77	-1.09	-4.82
Z1	2301	1.72	-1.93	1.72	0.00	1.72	1.72	-1.93
Z2	2321	1.21	-2.07	1.21	0.00	1.21	1.21	-2.07
Z3	2341	1.00	-2.36	1.00	0.00	1.00	1.00	-2.36
Z4	2361	0.82	-2.66	0.82	0.00	0.82	0.82	-2.66
Z5	2381	0.59	-2.94	0.59	0.00	0.59	0.59	-2.94
Z6	2401	0.31	-3.20	0.31	0.00	0.31	0.31	-3.20
Z7	2421	0.03	-3.46	0.03	0.00	0.03	0.03	-3.46
Z8	2441	-0.22	-3.75	-0.22	0.00	-0.22	-0.22	-3.75
Z9	2461	-0.42	-4.07	-0.42	0.00	-0.42	-0.42	-4.07
Z10	2481	-0.62	-4.35	-0.62	0.00	-0.62	-0.62	-4.35
Z11	2501	-0.78	-4.54	-0.78	0.00	-0.78	-0.78	-4.54
Z12	2521	-0.96	-4.66	-0.96	0.00	-0.96	-0.96	-4.66
Z13	2541	-1.19	-4.76	-1.19	0.00	-1.19	-1.19	-4.76
Z14	2561	-1.49	-4.80	-1.49	0.00	-1.49	-1.49	-4.80

**Table 2.10.10-16 Primary Plus Secondary Stresses; 30-Foot Top End Drop; $\phi = 0^\circ$;
1.12-Inch Outer Shell Thickness**

Stress Points		Stresses						
Location	Node	S _x	S _y	S _z	S _{xy}	S ₁	S ₂	S ₃
A1	327	2.83	-0.01	2.82	0.13	2.84	2.82	-0.01
A2	302	2.43	-0.01	2.43	-0.01	2.43	2.43	-0.01
A3	277	2.04	-0.03	2.04	-0.06	2.04	2.04	-0.03
A4	252	1.26	-0.04	1.27	-0.01	1.27	1.26	-0.04
A5	227	-0.24	-0.06	-0.24	-0.03	-0.05	-0.24	-0.25
A6	202	-1.68	-0.09	-1.68	-0.03	-0.09	-1.68	-1.68
A7	177	-3.11	-0.10	-3.12	0.00	-0.10	-3.11	-3.12
B1	104	-4.55	-0.21	-4.57	-0.25	-0.20	-4.56	-4.57
B2	79	-1.30	-0.14	-1.30	0.16	-0.12	-1.30	-1.32
B3	54	2.04	0.03	2.06	0.16	2.06	2.05	0.02
B4	29	5.50	0.04	5.49	0.18	5.51	5.49	0.04
B5	4	8.51	-0.05	8.41	-0.71	8.57	8.41	-0.11
C1	110	-2.98	-1.71	-3.67	0.33	-1.63	-3.07	-3.67
C2	85	-0.30	-1.44	-0.61	0.94	0.23	-0.61	-1.97
C3	60	1.84	-0.83	2.30	1.20	2.31	2.30	-1.29
C4	35	4.12	-0.27	5.36	0.67	5.36	4.22	-0.37
C5	10	6.86	-0.07	8.31	0.08	8.31	6.86	-0.07
D1	335	-1.76	-6.70	-0.25	-1.20	-0.25	-1.48	-6.98
D2	310	0.59	-4.20	0.79	-1.20	0.87	0.79	-4.49
D3	285	0.75	-2.97	0.96	-1.11	1.05	0.96	-3.28
D4	260	0.61	-2.27	0.69	-1.01	0.93	0.69	-2.59
D5	235	0.03	-2.00	-0.16	-0.85	0.34	-0.16	-2.31
D6	210	-0.71	-1.98	-1.10	-0.50	-0.54	-1.10	-2.15
D7	185	-1.58	-2.00	-2.14	-0.11	-1.55	-2.03	-2.14
E1	118	8.44	9.55	5.26	4.18	13.22	5.26	4.77
E2	93	0.81	5.31	3.04	2.95	6.77	3.04	-0.65
E3	68	0.07	1.54	2.88	1.97	2.90	2.88	-1.30
E4	43	-1.46	0.42	3.42	0.94	3.42	0.81	-1.85
E5	18	-1.68	0.15	4.84	0.35	4.84	0.22	-1.75
F1	143	-7.67	6.79	1.34	2.96	7.37	1.34	-8.26
F2	144	-4.89	5.03	1.29	2.40	5.58	1.29	-5.44

**Table 2.10.10-16 Primary Plus Secondary Stresses; 30-Foot Top End Drop; $\phi = 0^\circ$;
1.12-Inch Outer Shell Thickness (continued)**

Stress Points		Stresses						
Location	Node	S _x	S _y	S _z	S _{xy}	S ₁	S ₂	S ₃
F3	145	-1.64	2.90	1.49	1.57	3.40	1.49	-2.13
F4	146	-0.56	1.59	1.48	0.95	1.95	1.48	-0.92
F5	147	-0.23	0.80	1.42	0.65	1.42	1.11	-0.55
F6	148	-0.11	0.25	1.36	0.44	1.36	0.54	-0.40
F7	149	-0.04	-0.29	1.30	0.23	1.30	0.10	-0.43
F8	150	0.00	-0.83	1.23	0.12	1.23	0.02	-0.85
G1	335	-1.76	-6.70	-0.25	-1.20	-0.25	-1.48	-6.98
G2	336	-1.24	-4.36	0.63	-0.45	0.63	-1.17	-4.43
G3	337	-0.40	-3.09	1.26	0.05	1.26	-0.40	-3.09
G4	338	-0.04	-1.87	1.72	0.13	1.72	-0.03	-1.88
G5	339	0.56	0.61	2.52	-0.54	2.52	1.12	0.04
G6	340	0.66	-0.58	2.19	-0.86	2.19	1.09	-1.02
H1	346	-4.63	-1.72	-0.36	-1.06	-0.36	-1.38	-4.97
H2	347	-2.72	-1.01	0.62	-0.74	0.62	-0.73	-2.99
H3	348	-1.24	1.65	2.03	-0.03	2.03	1.66	-1.24
H4	349	-0.52	4.14	3.03	0.07	4.14	3.03	-0.52
H5	350	-0.18	6.96	3.92	0.05	6.96	3.92	-0.18
I1	621	-0.06	-3.85	-0.07	0.10	-0.05	-0.07	-3.85
I2	624	0.08	-5.60	-0.33	0.12	0.08	-0.33	-5.60
J1	635	-0.01	3.34	0.36	0.03	3.34	0.36	-0.01
J2	638	0.01	1.52	0.09	0.02	1.52	0.09	0.01
K1	841	-0.05	-5.34	0.26	0.02	0.26	-0.05	-5.34
K2	844	0.00	-4.93	0.61	0.03	0.61	0.00	-4.93
L1	855	0.00	1.67	-0.37	0.00	1.67	0.00	-0.37
L2	858	0.00	2.21	0.18	0.00	2.21	0.18	0.00
M1	941	-0.05	-5.94	0.20	0.00	0.20	-0.05	-5.94
M2	944	0.00	-5.41	0.67	0.00	0.67	0.00	-5.41
N1	955	0.00	1.03	-0.45	0.00	1.03	0.00	-0.45
N2	958	0.00	1.73	0.23	0.00	1.73	0.23	0.00
O1	1101	-0.05	-6.82	0.21	0.00	0.21	-0.05	-6.82
O2	1104	0.00	-6.29	0.68	0.00	0.68	0.00	-6.29

**Table 2.10.10-16 Primary Plus Secondary Stresses; 30-Foot Top End Drop; $\phi = 0^\circ$;
1.12-Inch Outer Shell Thickness (continued)**

Stress Points		Stresses						
Location	Node	S _x	S _y	S _z	S _{xy}	S ₁	S ₂	S ₃
P1	1115	0.00	0.11	-0.49	0.00	0.11	0.00	-0.49
P2	1118	0.00	0.86	0.24	0.00	0.86	0.24	0.00
Q1	1261	-0.05	-7.65	0.29	0.00	0.29	-0.05	-7.65
Q2	1264	0.00	-7.24	0.64	0.00	0.64	0.00	-7.24
R1	1275	0.00	-0.73	-0.46	0.00	0.00	-0.46	-0.73
R2	1278	-0.01	0.00	0.09	0.00	0.09	0.00	-0.01
S1	1561	-0.06	-7.10	-0.52	-0.16	-0.05	-0.52	-7.11
S2	1564	0.12	-9.61	-0.92	-0.20	0.13	-0.92	-9.61
T1	1575	-0.01	-0.04	0.42	-0.03	0.42	0.02	-0.06
T2	1578	0.01	-2.33	0.16	-0.03	0.16	0.01	-2.33
U1	1841	-0.11	-6.70	0.01	-0.10	0.01	-0.11	-6.70
U2	1844	-0.07	-5.11	0.73	-0.20	0.73	-0.06	-5.12
V1	1852	-3.44	-6.09	-0.58	-0.03	-0.58	-3.44	-6.09
V2	1856	-0.13	2.31	3.33	-0.04	3.33	2.31	-0.13
W1	1969	1.02	-3.29	0.10	0.75	1.15	0.10	-3.41
W2	1970	0.69	-3.78	0.17	0.02	0.69	0.17	-3.78
W3	1971	0.34	-3.90	0.24	-0.48	0.39	0.24	-3.95
W4	1972	0.16	-4.04	0.31	-0.54	0.31	0.23	-4.11
W5	1973	0.08	-4.14	0.36	-0.49	0.36	0.13	-4.19
W6	1974	0.03	-4.19	0.43	-0.37	0.43	0.07	-4.22
W7	1975	0.01	-4.27	0.50	-0.21	0.50	0.02	-4.28
W8	1976	0.02	-4.39	0.55	-0.11	0.55	0.02	-4.40
X1	2370	3.53	1.78	3.46	3.07	5.84	3.46	-0.53
X2	2390	-0.35	-3.06	0.36	2.67	1.29	0.36	-4.70
X3	2410	-0.15	-5.23	-0.35	1.21	0.12	-0.35	-5.50
X4	2430	-0.98	-4.64	-0.58	0.88	-0.58	-0.79	-4.84
X5	2450	-1.05	-4.91	-0.69	0.70	-0.69	-0.93	-5.03
X6	2470	-0.97	-4.74	-0.52	0.65	-0.52	-0.86	-4.85
X7	2490	-0.49	-4.81	-0.18	0.57	-0.18	-0.42	-4.88
X8	2510	-0.20	-4.77	0.05	0.47	0.05	-0.15	-4.82
X9	2530	0.18	-4.83	0.28	0.35	0.28	0.20	-4.86

**Table 2.10.10-16 Primary Plus Secondary Stresses; 30-Foot Top End Drop; $\phi = 0^\circ$;
1.12-Inch Outer Shell Thickness (continued)**

Stress Points		Stresses						
Location	Node	S _x	S _y	S _z	S _{xy}	S ₁	S ₂	S ₃
X10	2550	0.59	-4.83	0.54	0.19	0.60	0.54	-4.84
X11	2570	1.84	-4.84	1.60	0.15	1.84	1.60	-4.85
Y1	2305	1.30	-1.98	1.65	0.10	1.65	1.30	-1.98
Y2	2325	0.94	-2.16	1.03	0.57	1.04	1.03	-2.26
Y3	2345	0.88	-2.57	0.75	0.64	1.00	0.75	-2.69
Y4	2365	0.64	-2.94	0.41	0.49	0.70	0.41	-3.01
Y5	2385	0.09	-3.18	-0.05	0.33	0.12	-0.05	-3.21
Y6	2405	-0.54	-3.36	-0.55	0.31	-0.51	-0.55	-3.39
Y7	2425	-0.96	-3.56	-0.92	0.39	-0.90	-0.92	-3.62
Y8	2445	-1.12	-3.84	-1.09	0.49	-1.03	-1.09	-3.93
Y9	2465	-1.09	-4.15	-1.10	0.55	-1.00	-1.10	-4.24
Y10	2485	-0.91	-4.41	-0.98	0.50	-0.84	-0.98	-4.48
Y11	2505	-0.80	-4.58	-0.92	0.49	-0.74	-0.92	-4.64
Y12	2525	-0.66	-4.70	-0.85	0.39	-0.62	-0.85	-4.73
Y13	2545	-0.51	-4.78	-0.79	0.22	-0.49	-0.79	-4.80
Y14	2565	0.46	-4.82	0.03	0.11	0.46	0.03	-4.82
Z1	2301	2.24	-1.92	2.24	0.00	2.24	2.24	-1.92
Z2	2321	1.32	-2.04	1.32	0.00	1.32	1.32	-2.04
Z3	2341	0.80	-2.31	0.80	0.00	0.80	0.80	-2.31
Z4	2361	0.36	-2.59	0.36	0.00	0.36	0.36	-2.59
Z5	2381	-0.04	-2.85	-0.04	0.00	-0.04	-0.04	-2.85
Z6	2401	-0.43	-3.10	-0.43	0.00	-0.43	-0.43	-3.10
Z7	2421	-0.75	-3.36	-0.75	0.00	-0.75	-0.75	-3.36
Z8	2441	-0.93	-3.65	-0.93	0.00	-0.93	-0.93	-3.65
Z9	2461	-1.00	-3.98	-1.00	0.00	-1.00	-1.00	-3.98
Z10	2481	-0.98	-4.28	-0.98	0.00	-0.98	-0.98	-4.28
Z11	2501	-1.01	-4.49	-1.01	0.00	-1.01	-1.01	-4.49
Z12	2521	-1.04	-4.63	-1.04	0.00	-1.04	-1.04	-4.63
Z13	2541	-1.12	-4.74	-1.12	0.00	-1.12	-1.12	-4.74
Z14	2561	-0.46	-4.79	-0.46	0.00	-0.46	-0.46	-4.79

**Table 2.10.10-17 Primary Membrane (P_m) Stresses; 30-Foot Top End Drop; $\phi = 0^\circ$;
1.12-Inch Outer Shell Thickness**

Section	Node to Node	Stresses* (ksi)							
		S_x	S_y	S_z	S_{xy}	S_1	S_2	S_3	S_I
A	327 – 177	0.14	-0.07	0.14	-0.01	0.14	0.14	-0.07	0.21
B	104 – 4	-0.14	0.00	-0.14	-0.03	0.01	-0.14	-0.15	0.16
C	110 – 10	-0.14	0.00	-0.14	-0.07	0.03	-0.14	-0.17	0.21
D	335 – 185	0.14	-0.24	0.10	-0.10	0.16	0.10	-0.26	0.42
E	118 – 18	-0.11	-0.18	-0.18	-0.08	-0.06	-0.18	-0.22	0.17
F	143 – 150	-0.03	-0.11	-0.03	-0.14	0.08	-0.03	-0.22	0.30
G	335 – 340	-0.01	-0.42	0.21	0.02	0.21	-0.01	-0.42	0.63
H	346 – 350	0.02	-0.72	0.06	-0.04	0.06	0.03	-0.73	0.79
I	621 – 624	-0.02	-1.25	0.27	0.03	0.27	-0.02	-1.25	1.52
J	635 – 638	0.00	-1.11	0.04	0.00	0.04	0.00	-1.11	1.15
K	841 – 844	-0.02	-1.69	0.44	0.02	0.44	-0.02	-1.69	2.13
L	855 – 858	0.00	-1.55	0.00	0.00	0.00	0.00	-1.55	1.55
M	941 – 944	-0.02	-2.22	0.45	0.00	0.45	-0.02	-2.22	2.67
N	955 – 958	0.00	-2.09	0.00	0.00	0.00	0.00	-2.09	2.09
O	1101 – 1104	-0.02	-3.11	0.45	0.00	0.45	-0.02	-3.11	3.55
P	1115 – 1118	0.00	-2.97	0.00	0.00	0.00	0.00	-2.97	2.97
Q	1261 – 1264	-0.02	-3.99	0.45	0.00	0.45	-0.02	-3.99	4.44
R	1275 – 1278	0.00	-3.85	0.00	0.00	0.00	0.00	-3.85	3.85
S	1561 – 1564	0.01	-4.85	-0.41	-0.18	0.02	-0.41	-4.85	4.88
T	1575 – 1578	0.00	-4.72	0.14	-0.01	0.14	0.00	-4.72	4.85
U	1841 – 1846	0.79	-3.15	3.22	0.85	3.22	0.97	-3.32	6.54
V	1852 – 1856	-0.37	-4.23	1.11	0.05	0.00	-0.37	-4.23	5.34
W	1969 – 1976	0.73	-4.16	-0.40	0.14	0.74	-0.40	-4.17	4.90
X	2370 – 2570	0.16	-4.04	-0.13	1.06	0.41	-0.13	-4.29	4.71
Y	2305 – 2565	0.20	-3.31	0.20	0.43	0.25	0.20	-3.36	3.61
Z	2301 – 2561	0.20	-3.33	0.20	0.00	0.20	0.00	-3.33	3.52

* Stresses are taken at 0 degrees (under the load) at each section.

Table 2.10.10-18 Primary Membrane Plus Primary Bending ($P_m + P_b$) Stresses; 30-Foot Top End Drop; $\phi = 0^\circ$; 1.12-Inch Outer Shell Thickness

Section	Node to Node	Stresses* (ksi)							
		S_x	S_y	S_z	S_{xy}	S_1	S_2	S_3	S_I
A	327 – 177	0.63	-0.04	0.63	-0.01	0.63	0.63	-0.04	0.67
B	104 – 4	-0.60	-0.01	-0.62	-0.03	-0.01	-0.60	-0.62	0.61
C	110 – 10	-0.30	0.00	-0.45	-0.06	0.01	-0.31	-0.45	0.46
D	335 – 185	0.19	-0.43	0.29	-0.16	0.29	0.23	-0.46	0.75
E	118 – 18	-0.31	-0.39	-0.16	-0.16	-0.16	-0.19	-0.51	0.35
F	143 – 150	0.03	-0.22	-0.06	-0.14	0.09	-0.06	-0.28	0.38
G	335 – 340	-0.08	-0.68	0.16	0.02	0.16	-0.08	-0.68	0.83
H	346 – 350	0.00	-0.97	-0.02	-0.04	0.00	-0.02	-0.97	0.96
I	621 – 624	0.02	-1.39	0.22	0.03	0.22	0.02	-1.39	1.61
J	635 – 638	0.00	-1.13	0.03	0.00	0.03	0.00	-1.13	1.16
K	841 – 844	-0.05	-1.68	0.47	0.02	0.47	-0.05	-1.68	2.15
L	855 – 858	0.00	-1.55	0.00	0.00	0.00	0.00	-1.55	-1.55
M	941 – 944	-0.05	-2.22	0.47	0.00	0.47	-0.05	-2.22	2.69
N	955 – 958	0.00	-2.09	0.00	0.00	0.00	0.00	-2.09	2.09
O	1101 – 1104	-0.05	-3.11	0.47	0.00	0.47	-0.05	-3.11	3.58
P	1115 – 1118	0.00	-2.97	0.00	0.00	0.00	0.00	-2.97	2.97
Q	1261 – 1264	-0.05	-3.99	0.47	0.00	0.47	-0.05	-3.99	4.46
R	1275 – 1278	0.00	-3.85	0.00	0.00	0.00	0.00	-3.85	3.85
S	1561 – 1564	0.09	-6.05	-0.70	-0.18	0.09	-0.70	-6.06	6.15
T	1575 – 1578	0.00	-5.06	0.04	-0.01	0.04	0.00	-5.06	5.09
U	1841 – 1846	-0.05	-5.53	2.76	0.85	2.76	0.08	-5.66	8.42
V	1852 – 1856	-1.00	-4.81	0.90	0.05	0.90	-1.00	-4.81	5.71
W	1969 – 1976	0.02	-6.20	-1.04	0.14	0.03	-1.04	-6.20	6.23
X	2370 – 2570	-0.23	-5.65	-0.77	0.34	-0.21	-0.77	-5.67	5.46
Y	2305 – 2565	-0.87	-4.81	-1.00	0.44	-0.82	-1.00	-4.86	4.04
Z	2301 – 2561	-1.22	-4.89	-1.22	0.00	-1.22	-1.22	-4.89	3.67

* Stresses are taken at 0 degrees (under the load) at each section.

Table 2.10.10-19 Primary Membrane (P_m) and Primary Membrane Plus Primary Bending ($P_m + P_b$) Stress Qualification; 30-Foot Top End Drop; $\phi = 0^\circ$; 1.12-Inch Outer Shell Thickness

Section	Node to Node	Max. Temp. (°F)	P _m Stresses (ksi)			P _m + P _b Stresses (ksi)		
			Allow. * 0.7 S _u	Calc.	MS	Allow. * 1.0 S _u	Calc.	MS
A	327 – 177	222	48.93	0.21	+Large	69.90	0.67	+Large
B	104 – 4	215	49.18	0.16	+Large	70.25	0.61	+Large
C	110 – 10	212	49.28	0.21	+Large	70.40	0.46	+Large
D	335 – 185	221	48.96	0.42	+Large	69.95	0.75	+Large
E	118 – 18	208	49.42	0.17	+Large	70.60	0.35	+Large
F	143 – 150	209	49.38	0.30	+Large	70.55	0.38	+Large
G	335 – 340	221	48.96	0.63	+Large	69.95	0.83	+Large
H	346 – 350	212	49.28	0.79	+Large	70.40	0.96	+Large
I	621 – 624	222	48.93	1.52	+Large	69.90	1.61	+Large
J	635 – 638	199	49.73	1.15	+Large	71.04	1.16	+Large
K	841 – 844	232	68.49	2.13	+Large	97.84	2.15	+Large
L	855 – 858	204	69.50	1.55	+Large	99.29	1.55	+Large
M	941 – 944	247	67.94	2.67	+Large	97.06	2.69	+Large
N	955 – 958	211	69.25	2.09	+Large	98.93	2.09	+Large
O	1101 – 1104	255	67.65	3.55	+Large	96.64	3.58	+Large
P	1115 – 1118	216	69.07	2.97	+Large	98.67	2.97	+Large
Q	1261 – 1264	251	67.80	4.44	+Large	96.85	4.46	+Large
R	1275 – 1278	216	69.07	3.85	+Large	98.67	3.85	+Large
S	1561 – 1564	217	49.10	4.88	+Large	70.15	6.15	+Large
T	1575 – 1578	197	49.78	4.85	+Large	71.12	5.09	+Large
U	1841 – 1846	212	49.28	6.54	+Large	70.40	8.42	+Large
V	1852 – 1856	205	49.52	5.34	+Large	70.75	5.71	+Large
W	1969 – 1976	198	49.76	4.90	+Large	71.08	6.23	+Large
X	2370 – 2570	201	49.66	4.71	+Large	70.95	5.46	+Large
Y	2305 – 2565	205	49.52	3.61	+Large	70.75	4.04	+Large
Z	2301 – 2561	204	49.56	3.52	+Large	70.80	3.67	+Large

* Allowable stresses for sections “K” through “R” are taken from Type XM-19 stainless steel; all others are from Type 304 stainless steel.

Table 2.10.10-20 Primary Stresses; 30-Foot Top Corner Drop; $\phi = 15.74^\circ$;
1.12-Inch Outer Shell Thickness

Stress Points		Stresses						
Location	Node	S _x	S _y	S _z	S _{xy}	S ₁	S ₂	S ₃
A1	327	-0.42	-0.06	1.41	0.07	1.41	-0.04	-0.43
A2	302	-0.64	-0.07	1.25	0.15	1.25	-0.03	-0.68
A3	277	-0.81	-0.04	1.13	0.35	1.13	0.10	-0.94
A4	252	-1.11	-0.07	0.89	0.46	0.89	0.10	-1.29
A5	227	-1.77	-0.78	0.64	0.31	0.64	-0.69	-1.86
A6	202	0.05	-1.23	2.74	-1.23	2.74	0.80	-1.97
A7	177	-13.08	-0.83	-3.81	-0.56	-0.80	-3.81	-13.11
B1	104	-3.24	-1.05	-0.83	-0.56	-0.83	-0.91	-3.37
B2	79	-2.44	-0.82	-0.29	-0.26	-0.29	-0.78	-2.48
B3	54	-2.17	-0.44	0.00	-0.40	0.00	-0.35	-2.26
B4	29	-1.89	-0.11	0.29	-0.28	0.29	-0.06	-1.93
B5	4	-1.52	0.02	0.48	0.06	0.48	0.02	-1.52
C1	110	-3.70	-0.27	-1.52	-0.26	-0.25	-1.52	-3.72
C2	85	-3.16	-0.22	-1.10	0.12	-0.22	-1.10	-3.17
C3	60	-2.65	-0.12	-0.73	0.14	-0.11	-0.73	-2.66
C4	35	-2.13	-0.03	-0.32	0.14	-0.02	-0.32	-2.14
C5	10	-1.85	-0.00	-0.08	0.15	0.01	-0.08	-1.86
D1	335	-0.90	0.38	0.43	-0.17	0.43	0.40	-0.93
D2	310	-1.33	0.06	0.12	-0.17	0.12	0.08	-1.35
D3	285	-1.60	-0.10	-0.09	-0.25	-0.06	-0.09	-1.65
D4	260	-2.04	-0.25	-0.38	-0.36	-0.17	-0.38	-2.11
D5	235	-2.83	-0.38	-0.88	-0.32	-0.33	-0.88	-2.87
D6	210	-3.64	-0.43	-1.43	-0.24	-0.41	-1.43	-3.66
D7	185	-4.44	-0.44	-2.09	0.27	-0.42	-2.09	-4.45
E1	118	-3.11	0.83	-2.09	-0.60	0.92	-2.09	-3.20
E2	93	-3.18	0.28	-2.10	-0.17	0.29	-2.10	-3.19
E3	68	-3.07	0.11	-1.97	0.03	0.11	-1.97	-3.07
E4	43	-3.04	0.03	-1.82	0.09	0.03	-1.82	-3.05
E5	18	-3.12	0.01	-1.74	0.14	0.02	-1.74	-3.13
F1	143	-0.61	3.16	-1.06	-0.82	3.33	-0.78	-1.06
F2	144	-0.72	0.79	-2.32	-0.68	1.05	-0.98	-2.32

Table 2.10.10-20 Primary Stresses; 30-Foot Top Corner Drop; $\phi = 15.74^\circ$;
1.12-Inch Outer Shell Thickness (continued)

Stress Points		Stresses						
Location	Node	S _x	S _y	S _z	S _{xy}	S ₁	S ₂	S ₃
F3	145	-1.06	0.15	-2.94	-0.51	0.34	-1.25	-2.94
F4	146	-1.78	-0.28	-3.57	-0.33	-0.21	-1.85	-3.57
F5	147	-2.25	-0.62	-4.06	-0.23	-0.58	-2.28	-4.06
F6	148	-2.54	-0.94	-4.48	-0.16	-0.92	-2.56	-4.48
F7	149	-2.75	-1.34	-4.91	-0.09	-1.34	-2.75	-4.91
F8	150	-2.85	-1.88	-5.38	-0.04	-1.88	-2.85	-5.38
G1	335	-0.90	0.38	0.43	-0.17	0.43	0.40	-0.93
G2	336	-0.83	-0.05	0.12	-0.20	0.12	-0.01	-0.88
G3	337	-0.99	-0.48	-0.20	-0.15	-0.20	-0.44	-1.02
G4	338	-1.34	-0.93	-0.54	0.09	-0.54	-0.91	-1.36
G5	339	-2.21	-1.59	-1.09	0.71	-1.09	-1.12	-2.68
G6	340	-3.05	-0.79	-1.04	0.84	-0.51	-1.04	-3.32
H1	346	-1.61	1.42	-2.58	1.05	1.74	-1.93	-2.58
H2	347	-1.42	4.44	-2.33	0.58	4.50	-1.48	-2.33
H3	348	-2.35	3.03	-3.46	-0.80	3.15	-2.47	-3.46
H4	349	-2.55	-0.61	-4.93	-0.93	-0.23	-2.92	-4.93
H5	350	-2.76	-4.40	-6.40	-0.62	-2.55	-4.60	-6.40
I1	621	-0.12	0.21	1.01	-0.04	1.01	0.21	-0.13
I2	624	-0.02	0.72	0.99	0.04	0.99	0.72	-0.02
J1	635	-0.09	2.27	0.99	-0.13	2.27	0.99	-0.09
J2	638	-0.01	5.39	0.77	0.05	5.39	0.77	-0.01
K1	841	-0.08	6.20	0.52	0.00	6.20	0.52	-0.08
K2	844	-0.01	7.03	0.73	0.03	7.03	0.73	-0.01
L1	855	-0.05	11.85	0.61	-0.04	11.85	0.61	-0.05
L2	858	0.02	12.82	0.69	0.01	12.82	0.69	0.02
M1	941	-0.08	6.43	0.52	0.00	6.43	0.52	-0.08
M2	944	-0.02	7.31	0.74	0.00	7.31	0.74	-0.02
N1	955	-0.05	13.71	0.75	-0.01	13.71	0.75	-0.05
N2	958	0.00	14.88	0.80	0.01	14.88	0.80	0.00
O1	1101	-0.09	2.83	0.28	0.01	2.83	0.28	-0.09
O2	1104	-0.04	3.33	0.48	-0.01	3.33	0.48	-0.04

**Table 2.10.10-20 Primary Stresses; 30-Foot Top Corner Drop; $\phi = 15.74^\circ$;
1.12-Inch Outer Shell Thickness (continued)**

Stress Points		Stresses						
Location	Node	S _x	S _y	S _z	S _{xy}	S ₁	S ₂	S ₃
P1	1115	-0.07	10.79	1.09	0.03	10.79	1.09	-0.07
P2	1118	0.00	11.76	0.86	-0.03	11.76	0.86	0.00
Q1	1261	-0.08	-3.16	0.58	0.02	0.58	-0.08	-3.16
Q2	1264	-0.02	-3.19	0.67	-0.03	0.67	-0.02	-3.19
R1	1275	-0.04	-0.11	1.33	0.06	1.33	0.00	-0.15
R2	1278	0.00	-0.33	0.24	-0.07	0.24	0.01	-0.34
S1	1561	-0.09	-11.56	0.60	-0.40	0.60	-0.07	-11.57
S2	1564	0.33	-22.95	-4.59	-0.60	0.34	-4.59	-22.97
T1	1575	-0.14	-17.85	2.76	0.15	2.76	-0.14	-17.85
T2	1578	0.02	-19.72	1.69	-0.06	1.69	0.02	-19.72
U1	1841	0.23	-20.15	8.35	-0.18	8.35	0.23	-20.15
U2	1844	3.27	-11.67	9.99	-0.59	9.99	3.29	-11.69
V1	1852	6.17	-10.07	7.30	0.15	7.30	6.17	-10.07
V2	1856	0.60	-23.74	0.58	-0.41	0.60	0.58	-23.75
W1	1969	-19.47	-16.62	-8.31	4.08	-8.31	-13.72	-22.37
W2	1970	-14.06	-8.92	-5.38	1.34	-5.38	-8.59	-14.39
W3	1971	-7.43	-10.00	-4.34	-0.60	-4.34	-7.29	-10.13
W4	1972	-5.37	-10.68	-4.26	-0.78	-4.26	-5.25	-10.79
W5	1973	-4.37	-11.06	-4.27	-0.77	-4.27	-4.28	-11.15
W6	1974	-3.83	-11.17	-4.26	-0.63	-3.78	-4.26	-11.22
W7	1975	-3.57	-11.06	-4.26	-0.38	-3.55	-4.26	-11.08
W8	1976	-3.50	-10.56	-4.20	-0.26	-3.49	-4.20	-10.57
X1	2370	-6.70	-8.27	-1.94	1.91	-1.94	-5.42	-9.55
X2	2390	-5.86	-11.62	-2.81	3.08	-2.81	-4.52	-12.96
X3	2410	-5.16	-13.15	-2.80	3.56	-2.80	-3.81	-14.51
X4	2430	-4.08	-14.42	-2.50	3.65	-2.50	-2.93	-15.58
X5	2450	-3.35	-14.91	-2.08	3.57	-2.08	-2.34	-15.93
X6	2470	-2.48	-15.03	-1.61	3.45	-1.59	-1.61	-15.92
X7	2490	-1.30	-14.93	-1.22	3.20	-0.59	-1.22	-15.64
X8	2510	-0.54	-14.80	-1.11	2.76	-0.02	-1.11	-15.32
X9	2530	0.35	-14.70	-1.10	2.14	0.65	-1.10	-15.00

**Table 2.10.10-20 Primary Stresses; 30-Foot Top Corner Drop; $\phi = 15.74^\circ$;
1.12-Inch Outer Shell Thickness (continued)**

Stress Points		Stresses						
Location	Node	S _x	S _y	S _z	S _{xy}	S ₁	S ₂	S ₃
X10	2550	1.45	-14.62	-1.22	1.23	1.54	-1.22	-14.71
X11	2570	2.80	-14.60	-1.49	0.73	2.83	-1.49	-14.63
Y1	2305	-0.42	-5.24	1.76	-0.19	1.76	-0.41	-5.25
Y2	2325	-0.68	-5.42	1.49	-0.43	1.49	-0.64	-5.46
Y3	2345	-1.25	-5.66	1.05	-0.50	1.05	-1.20	-5.72
Y4	2365	-2.15	-5.98	0.49	-0.32	0.49	-2.12	-6.01
Y5	2385	-2.88	-6.57	-0.07	0.16	-0.07	-2.87	-6.58
Y6	2405	-3.10	-7.58	-0.49	0.90	-0.49	-2.93	-7.75
Y7	2425	-2.89	-9.05	-0.70	1.78	-0.70	-2.42	-9.53
Y8	2445	-2.63	-10.87	-0.74	2.79	-0.74	-1.78	-11.73
Y9	2465	-3.00	-12.61	-0.72	3.93	-0.72	-1.60	-14.01
Y10	2485	-5.06	-13.76	-1.09	4.76	-1.09	-2.96	-15.86
Y11	2505	-7.08	-14.33	-1.89	4.58	-1.89	-4.87	-16.55
Y12	2525	-8.39	-14.62	-2.89	3.69	-2.89	-6.68	-16.33
Y13	2545	-9.92	-14.55	-4.51	2.23	-4.51	-9.02	-15.45
Y14	2565	-10.96	-14.54	-7.06	0.92	-7.06	-10.74	-14.76
Z1	2301	-0.64	-2.23	2.51	0.14	2.51	-0.63	-2.24
Z2	2321	-1.26	-1.75	2.27	-0.01	2.27	-1.26	-1.75
Z3	2341	-1.60	-1.89	1.70	-0.12	1.70	-1.55	-1.94
Z4	2361	-1.94	-2.08	1.24	-0.33	1.24	-1.67	-2.35
Z5	2381	-2.11	-2.30	0.82	-0.46	0.82	-1.73	-2.68
Z6	2401	-2.06	-2.57	0.44	-0.53	0.44	-1.73	-2.90
Z7	2421	-1.78	-2.90	0.10	-0.56	0.10	-1.55	-3.14
Z8	2441	-1.31	-3.28	-0.19	-0.56	-0.19	-1.17	-3.43
Z9	2461	-0.68	-3.66	-0.48	-0.06	-0.48	-0.68	-3.66
Z10	2481	0.06	-4.04	-0.74	2.70	1.40	-0.74	-5.38
Z11	2501	0.42	-4.21	-1.03	10.55	8.90	-1.03	-12.70
Z12	2521	0.79	-4.37	-1.38	34.89	33.20	-1.38	-36.77
Z13	2541	0.96	-4.93	-2.08	164.70	162.74	-2.08	-166.71
Z14	2561	1.68	-6.27	-4.55	215.90	213.64	-4.55	-218.23

Table 2.10.10-21 Primary Plus Secondary Stresses; 30-Foot Top Corner Drop;
 $\phi = 15.74^\circ$; 1.12-Inch Outer Shell Thickness

Stress Points		Stresses						
Location	Node	S _x	S _y	S _z	S _{xy}	S ₁	S ₂	S ₃
A1	327	3.42	-0.01	5.22	0.24	5.22	3.44	-0.02
A2	302	2.59	-0.02	4.48	0.14	4.48	2.60	-0.02
A3	277	1.84	-0.02	3.76	0.28	3.76	1.88	-0.06
A4	252	0.32	-0.07	2.34	0.46	2.34	0.63	-0.38
A5	227	-2.67	-0.79	-0.26	0.30	-0.26	-0.74	-2.72
A6	202	-3.13	-1.27	-0.44	-1.24	-0.44	-0.65	-3.75
A7	177	-18.51	-0.87	-9.22	-0.55	-0.86	-9.22	-18.53
B1	104	-7.90	-1.25	-5.54	-0.77	-1.16	-5.54	-7.99
B2	79	-3.37	-0.95	-1.22	-0.05	-0.95	-1.22	-3.37
B3	54	0.72	-0.37	2.93	-0.18	2.93	0.75	-0.40
B4	29	4.97	-0.04	7.15	-0.05	7.15	4.97	-0.04
B5	4	8.98	-0.04	10.88	-0.81	10.88	9.06	-0.11
C1	110	-6.50	-2.21	-5.07	0.17	-2.21	-5.07	-6.51
C2	85	-2.96	-1.85	-1.17	1.19	-1.09	-1.17	-3.72
C3	60	0.00	-1.04	2.53	1.49	2.53	1.06	-2.09
C4	35	3.18	-0.32	6.46	0.88	6.43	3.39	-0.53
C5	10	6.81	-0.08	10.28	0.20	10.28	6.82	-0.08
D1	335	-2.58	-8.16	0.52	-1.53	0.52	-2.19	-8.55
D2	310	-0.06	-5.12	1.49	-1.53	1.49	0.36	-5.55
D3	285	-0.26	-3.64	1.42	-1.48	1.42	0.29	-4.19
D4	260	-1.22	-2.88	0.53	-1.49	0.53	-0.34	-3.76
D5	235	-3.25	-2.73	-1.56	-1.26	-1.56	-1.70	-4.27
D6	210	-5.53	-2.80	-3.84	-0.66	-2.65	-3.84	-5.68
D7	185	-8.08	-2.83	-6.38	0.49	-2.79	-6.38	-8.13
E1	118	6.73	9.65	3.96	4.79	13.20	3.96	3.18
E2	93	-2.02	5.95	1.84	3.32	7.15	1.84	-3.22
E3	68	-2.62	1.81	1.95	2.38	2.85	1.95	-3.66
E4	43	-4.14	0.50	2.85	1.21	2.85	0.79	-4.43
E5	18	-4.14	0.18	4.80	0.53	4.80	0.24	-4.20
F1	143	-11.30	7.34	-0.30	4.21	8.25	-0.30	-12.21
F2	144	-8.23	7.49	-0.54	2.95	8.03	-0.54	-8.76

**Table 2.10.10-21 Primary Plus Secondary Stresses: 30-Foot Top Corner Drop;
 $\phi = 15.74^\circ$; 1.12-Inch Outer Shell Thickness (continued)**

Stress Points		Stresses						
Location	Node	S _x	S _y	S _z	S _{xy}	S ₁	S ₂	S ₃
F3	145	-4.38	4.14	-0.98	1.40	4.36	-0.98	-4.61
F4	146	-3.09	2.20	-1.48	0.72	2.29	-1.48	-3.18
F5	147	-2.86	0.93	-1.98	0.43	0.98	-1.98	-2.91
F6	148	-2.84	-0.01	-2.42	0.26	0.01	-2.42	-2.87
F7	149	-2.86	-0.98	-2.89	0.12	-0.98	-2.87	-2.89
F8	150	-2.89	-2.03	-3.40	0.07	-2.02	-2.89	-3.40
G1	335	-2.58	-8.16	0.52	-1.53	0.52	-2.19	-8.55
G2	336	-1.89	-5.26	1.42	-0.57	1.42	-1.80	-5.35
G3	337	-0.89	-3.59	2.06	0.09	2.06	-0.88	-3.59
G4	338	-0.58	-1.82	2.55	0.18	2.55	-0.56	-1.85
G5	339	0.17	1.53	3.49	-0.78	3.49	1.89	-0.18
G6	340	-0.17	-0.68	2.89	-1.10	2.89	0.71	-1.56
H1	346	-9.23	-1.35	-4.06	0.20	-1.34	-4.06	-9.24
H2	347	-5.60	5.29	-1.56	0.10	5.29	-1.56	-5.60
H3	348	-4.33	8.04	-0.61	-0.90	8.11	-0.61	-4.39
H4	349	-3.31	7.51	-0.76	-1.02	7.60	-0.76	-3.40
H5	350	-3.01	7.55	-1.02	-0.70	7.60	-1.02	-3.06
I1	621	-0.13	-1.54	0.74	0.05	0.74	-0.13	-1.54
I2	624	0.04	-2.86	0.50	0.14	0.50	0.05	-2.86
J1	635	-0.10	9.96	1.38	-0.08	9.96	1.38	-0.10
J2	638	0.00	10.60	0.79	0.08	10.60	0.79	0.00
K1	841	-0.08	8.51	0.42	0.00	8.51	0.42	-0.08
K2	844	0.00	9.75	1.02	0.04	9.75	1.02	0.00
L1	855	-0.05	21.09	0.25	-0.04	21.09	0.25	-0.05
L2	858	0.02	22.60	0.87	0.01	22.60	0.87	0.02
M1	941	-0.08	8.68	0.36	0.00	8.68	0.36	-0.08
M2	944	-0.01	10.09	1.08	-0.01	10.09	1.08	-0.01
N1	955	-0.06	22.85	0.30	-0.01	22.85	0.30	-0.06
N2	958	0.00	24.72	1.03	0.01	24.72	1.03	0.00
O1	1101	-0.09	5.08	0.12	0.01	5.08	0.12	-0.09
O2	1104	-0.03	6.11	0.83	-0.01	6.11	0.83	-0.03

Table 2.10.10-21 Primary Plus Secondary Stresses; 30-Foot Top Corner Drop;
 $\phi = 15.74^\circ$; 1.12-Inch Outer Shell Thickness (continued)

Stress Points		Stresses						
Location	Node	S _x	S _y	S _z	S _{xy}	S ₁	S ₂	S ₃
P1	1115	-0.07	19.90	0.61	0.03	19.90	0.61	-0.07
P2	1118	0.00	21.62	1.10	-0.03	21.62	1.10	0.00
Q1	1261	-0.08	-0.85	0.50	0.02	0.50	-0.08	-0.85
Q2	1264	-0.01	-0.47	0.99	-0.04	0.99	0.00	-0.47
R1	1275	-0.04	9.04	0.87	0.06	9.04	0.87	-0.04
R2	1278	-0.02	9.55	0.34	-0.07	9.56	0.34	-0.02
S1	1561	-0.09	-9.44	0.96	-0.36	0.96	-0.07	-9.46
S2	1564	0.31	-20.02	-3.92	-0.54	0.32	-3.92	-20.03
T1	1575	-0.14	-7.19	2.84	0.09	2.84	-0.14	-7.19
T2	1578	0.03	-11.27	1.57	-0.12	1.57	0.03	-11.27
U1	1841	0.24	-19.96	7.82	-0.27	7.82	0.25	-19.96
U2	1844	3.47	-10.45	10.15	-0.66	10.15	3.50	-10.48
V1	1852	0.48	-12.25	4.85	-1.04	4.85	0.56	-12.33
V2	1856	0.28	-11.67	4.13	-0.25	4.13	0.29	-11.68
W1	1969	-20.24	-18.47	-8.30	3.27	-8.30	-15.97	-22.74
W2	1970	-14.08	-9.68	-4.67	0.66	-4.67	-9.58	-14.18
W3	1971	-7.53	-10.09	-3.38	-1.16	-3.38	-7.09	-10.54
W4	1972	-5.45	-10.14	-3.05	-1.26	-3.05	-5.13	-10.46
W5	1973	-4.44	-10.11	-2.89	-1.15	-2.89	-4.22	-10.33
W6	1974	-3.89	-9.90	-2.74	-0.89	-2.74	-3.76	-10.03
W7	1975	-3.60	-9.50	-2.60	-0.52	-2.60	-3.56	-9.55
W8	1976	-3.49	-8.75	-2.42	-0.33	-2.42	-3.47	-8.77
X1	2370	-7.94	-8.60	-2.27	2.51	-2.27	-5.74	-10.80
X2	2390	-6.18	-12.56	-3.05	3.52	-3.05	-4.62	-14.12
X3	2410	-5.53	-13.69	-2.88	3.62	-2.88	-4.15	-15.07
X4	2430	-4.43	-14.82	-2.50	3.51	-2.50	-3.35	-15.90
X5	2450	-3.75	-15.15	-2.02	3.31	-2.02	-2.86	-16.04
X6	2470	-2.89	-15.16	-1.48	3.13	-1.48	-2.14	-15.91
X7	2490	-1.68	-14.99	-0.97	2.86	-0.97	-1.09	-15.58
X8	2510	-0.87	-14.83	-0.77	2.45	-0.46	-0.77	-15.25
X9	2530	0.07	-14.71	-0.64	1.88	0.30	-0.64	-14.95

**Table 2.10.10-21 Primary Plus Secondary Stresses; 30-Foot Top Corner Drop;
 $\phi = 15.74^\circ$; 1.12-Inch Outer Shell Thickness (continued)**

Stress Points		Stresses						
Location	Node	S _x	S _y	S _z	S _{xy}	S ₁	S ₂	S ₃
X10	2550	1.23	-14.63	-0.61	1.06	1.30	-0.61	-14.70
X11	2570	3.42	-14.60	0.09	0.68	3.45	0.09	-14.63
Y1	2305	0.15	-5.27	2.25	-0.22	2.25	0.16	-5.28
Y2	2325	-0.66	-5.47	1.48	-0.37	1.48	-0.63	-5.50
Y3	2345	-1.53	-5.77	0.72	-0.45	0.72	-1.49	-5.82
Y4	2365	-2.70	-6.15	-0.11	-0.28	-0.11	-2.68	-6.17
Y5	2385	-3.61	-6.78	-0.86	0.21	-0.86	-3.60	-6.79
Y6	2405	-3.90	-7.83	-1.36	0.94	-1.36	-3.69	-8.04
Y7	2425	-3.67	-9.32	-1.57	1.78	-1.57	-3.16	-9.84
Y8	2445	-3.35	-11.12	-1.54	2.75	-1.54	-2.48	-11.99
Y9	2465	-3.61	-12.80	-1.39	3.85	-1.39	-2.21	-14.20
Y10	2485	-5.49	-13.87	-1.53	4.67	-1.53	-3.40	-15.96
Y11	2505	-7.38	-14.38	-2.17	4.54	-2.17	-5.14	-16.61
Y12	2525	-8.50	-14.64	-2.99	3.68	-2.99	-6.78	-16.36
Y13	2545	-9.79	-14.55	-4.41	2.22	-4.41	-8.91	-15.43
Y14	2565	-9.71	-14.54	-5.90	0.98	-5.90	-9.52	-14.73
Z1	2301	-0.13	-2.21	3.00	0.14	3.00	-0.12	-2.22
Z2	2321	-1.17	-1.71	2.35	-0.01	2.35	-1.17	-1.71
Z3	2341	-1.84	-1.83	1.47	-0.12	1.47	-1.71	-1.95
Z4	2361	-2.44	-1.99	0.73	-0.33	0.73	-1.82	-2.62
Z5	2381	-2.79	-2.20	0.14	-0.46	0.14	-1.95	-3.04
Z6	2401	-2.84	-2.47	-0.34	-0.53	-0.34	-2.10	-3.21
Z7	2421	-2.58	-2.80	-0.69	-0.56	-0.69	-2.12	-3.26
Z8	2441	-2.04	-3.18	-0.92	-0.56	-0.92	-1.81	-3.41
Z9	2461	-1.26	-3.57	-1.05	-0.06	-1.05	-1.26	-3.57
Z10	2481	-0.29	-3.97	-1.08	2.70	1.14	-1.08	-5.40
Z11	2501	0.21	-4.16	-1.23	10.55	8.80	-1.23	-12.75
Z12	2521	0.74	-4.34	-1.43	34.89	33.18	-1.43	-36.78
Z13	2541	1.06	-4.92	-1.98	164.70	162.80	-1.98	-166.66
Z14	2561	2.74	-6.25	-3.49	215.90	214.19	-3.49	-217.70

**Table 2.10.10-22 Primary Membrane (Pm) Stresses; 30-Foot Top Corner Drop;
 $\phi = 15.74^\circ$; 1.12-Inch Outer Shell Thickness**

Section	Node to Node	Stresses* (ksi)							
		S _x	S _y	S _z	S _{xy}	S ₁	S ₂	S ₃	SI
A	177 – 327	-2.41	-0.63	0.76	-0.16	0.76	-0.62	-2.42	3.18
B	4 – 104	-2.29	-0.53	-0.10	-0.32	-0.10	-0.47	-2.34	2.25
C	10 – 110	-2.77	-0.14	-0.81	0.08	-0.14	-0.81	-2.77	2.64
D	185 – 335	-2.81	-0.30	-0.89	-0.22	-0.28	-0.89	-2.83	2.56
E	18 – 118	-3.11	0.23	-1.97	-0.10	0.24	-1.97	-3.11	3.35
F	143 – 150	-1.59	0.02	-3.28	-0.40	0.11	-1.68	-3.28	3.39
G	335 – 340	-1.68	-0.85	-0.56	0.30	-0.56	-0.75	-1.78	1.22
H	346 – 350	-2.09	1.37	-3.72	-0.20	1.39	-2.10	-3.72	5.11
I	621 – 624	-0.07	0.46	0.99	0.01	0.99	0.46	-0.07	1.07
J	635 – 638	-0.05	3.86	0.87	-0.04	3.86	0.87	-0.05	3.90
K	841 – 844	-0.04	6.62	0.63	0.02	6.62	0.63	-0.04	6.67
L	855 – 858	-0.01	12.34	0.65	-0.01	12.34	0.65	-0.01	12.36
M	941 – 944	-0.05	6.88	0.63	0.00	6.88	0.63	-0.05	6.93
N	955 – 958	-0.02	14.31	0.77	0.00	14.31	0.77	-0.02	14.33
O	1101 – 1104	-0.06	3.09	0.38	0.00	3.09	0.38	-0.06	3.15
P	1115 – 1118	-0.03	11.28	0.97	0.00	11.28	0.97	-0.03	11.31
Q	1261 – 1264	-0.05	-3.17	0.63	-0.01	0.63	-0.05	-3.17	3.80
R	1275 – 1278	-0.02	-0.22	0.77	-0.01	0.77	-0.02	-0.22	0.99
S	1561 – 1564	0.12	-17.16	-2.01	-0.63	0.14	-2.01	-17.18	17.32
T	1575 – 1578	-0.05	-18.80	2.21	0.06	2.21	-0.05	-18.80	21.01
U	1841 – 1846	4.10	-9.86	10.67	0.76	10.67	4.14	-9.90	20.57
V	1822 – 1856	2.83	-17.30	3.49	0.29	3.49	2.84	-17.31	20.79
W	1969 – 1976	-8.82	-11.00	-5.01	0.27	-5.01	-8.78	-11.03	6.02
X	2370 – 2570	-2.99	-13.78	-1.98	2.99	-1.98	-2.22	-14.56	12.58
Y	2305 – 2565	-3.39	-9.19	-0.50	1.53	-0.50	-3.02	-9.57	9.07
Z	2301 – 2561	-1.04	-2.97	0.34	14.17	12.20	0.34	-16.21	28.42

* Stresses are taken at 0 degrees (under the load) at each section.

Table 2.10.10-23 Primary Membrane Plus Primary Bending ($P_m + P_b$) Stresses; 30-Foot Top Corner Drop; $\phi = 15.74^\circ$; 1.12-Inch Outer Shell Thickness

Section	Node to Node	Stresses* (ksi)							
		S_x	S_y	S_z	S_{xy}	S_1	S_2	S_3	SI
A	177 – 327	-4.96	-1.25	0.80	-1.00	0.80	-1.00	-5.21	6.01
B	4 – 104	-3.88	-1.12	-1.63	-0.46	-1.05	-1.63	-3.96	2.91
C	10 – 110	-4.00	-0.29	-2.11	-0.05	-0.29	-2.11	-4.00	3.71
D	185 – 335	-4.37	-0.93	-1.67	-0.16	-0.92	-1.67	-4.38	3.46
E	18 – 118	-3.16	0.60	-2.16	-0.43	0.65	-2.16	-3.21	3.86
F	143 – 150	-0.61	2.16	-1.24	-0.40	2.21	-0.67	-1.24	3.46
G	335 – 340	-3.20	-2.08	-1.48	0.30	-1.48	-2.00	-3.28	1.80
H	346 – 350	-1.70	4.56	-1.74	-0.20	4.56	-1.71	-1.74	6.30
I	621 – 624	-0.02	0.71	0.98	0.01	0.98	0.71	-0.02	1.00
J	635 – 638	-0.01	5.39	0.76	-0.04	5.39	0.76	-0.01	5.40
K	841 – 844	-0.01	7.03	0.73	0.02	7.03	0.73	-0.01	7.04
L	855 – 858	0.02	12.82	0.69	-0.01	12.82	0.69	0.02	12.80
M	941 – 944	-0.01	7.31	0.74	0.00	7.31	0.74	-0.01	7.32
N	955 – 958	0.00	14.88	0.80	0.00	14.88	0.80	0.00	14.88
O	1101 – 1104	-0.04	3.33	0.48	0.00	3.33	0.48	-0.04	3.37
P	1115 – 1118	0.00	11.76	0.86	0.00	11.76	0.86	0.00	11.76
Q	1261 – 1264	-0.02	-3.19	0.68	-0.01	0.68	-0.02	-3.19	3.86
R	1275 – 1278	-0.04	-0.11	1.31	-0.01	1.31	-0.04	-0.11	1.43
S	1561 – 1564	0.33	-22.71	-4.58	-0.63	0.35	-4.58	-22.72	-23.07
T	1575 – 1578	0.02	-19.71	1.68	0.06	1.68	0.02	-19.71	21.39
U	1841 – 1846	0.23	-18.32	8.31	0.76	8.31	0.26	-18.35	26.66
V	1822 – 1856	0.59	-24.92	-0.15	0.29	0.60	-0.15	-24.93	25.53
W	1969 – 1976	-19.47	-11.87	-6.68	0.27	-6.68	-11.86	-19.48	12.80
X	2370 – 2570	1.23	-16.09	-1.01	2.42	1.56	-1.01	-16.42	17.98
Y	2305 – 2565	-7.29	-15.03	-3.15	4.26	-3.15	-5.40	-16.91	13.77
Z	2301 – 2561	0.12	-4.66	-2.02	53.49	51.27	-2.02	-55.81	107.10

* Stresses are taken at 0 degrees (under the load) at each section.

Table 2.10.10-24 Primary Membrane (P_m) and Primary Membrane Plus Primary Bending ($P_m + P_b$) Stresses; 30-Foot Top Corner Drop; $\phi = 15.74^\circ$; 1.12-Inch Outer Shell Thickness

Section	Node to Node	Max. Temp. (°F)	P _m Stresses (ksi)			P _m + P _b Stresses (ksi)		
			Allow. * 0.7 S _u	Calc.	MS	Allow. * 1.0 S _u	Calc.	MS
A	327 – 177	222	48.93	3.18	+Large	69.90	6.01	+Large
B	104 – 4	215	49.18	2.25	+Large	70.25	2.91	+Large
C	110 – 10	212	49.28	2.64	+Large	70.40	3.71	+Large
D	335 – 185	221	48.96	2.56	+Large	69.95	3.46	+Large
E	118 – 18	208	49.42	3.35	+Large	70.60	3.86	+Large
F	143 – 150	209	49.38	3.39	+Large	70.55	3.46	+Large
G	335 – 340	221	48.96	1.22	+Large	69.95	1.80	+Large
H	346 – 350	212	49.28	5.11	+Large	70.40	6.30	+Large
I	621 – 624	222	48.93	1.07	+Large	69.90	1.00	+Large
J	635 – 638	199	49.73	3.90	+Large	71.04	5.40	+Large
K	841 – 844	232	68.49	6.67	+Large	97.84	7.04	+Large
L	855 – 858	204	69.50	12.36	+Large	99.29	12.80	+Large
M	941 – 944	247	67.94	6.93	+Large	97.06	7.32	+Large
N	955 – 958	211	69.25	14.33	+3.83	98.93	14.88	+Large
O	1101 – 1104	255	67.65	3.15	+Large	96.64	3.37	+Large
P	1115 – 1118	216	69.07	11.31	+Large	98.67	11.76	+Large
Q	1261 – 1264	251	67.80	3.80	+Large	96.85	3.86	+Large
R	1275 – 1278	216	69.07	0.99	+Large	98.67	1.43	+Large
S	1561 – 1564	217	49.10	17.32	+1.83	70.15	23.07	+2.04
T	1575 – 1578	197	49.78	21.01	+1.37	71.12	21.39	+2.32
U	1841 – 1846	212	49.28	20.57	+1.40	70.40	26.66	+1.64
V	1852 – 1856	205	49.52	20.79	+1.38	70.75	25.53	+1.77
W	1969 – 1976	198	49.76	6.02	+Large	71.08	12.80	+Large
X	2370 – 2570	201	49.66	12.58	+2.95	70.95	17.98	+2.95
Y	2305 – 2565	205	49.52	9.07	+Large	70.75	13.77	+Large
Z	2301 – 2561	204	49.56	28.42	+0.74	70.80	107.10**	**

* Allowable stresses for sections “K” through “R” are taken from Type XM-19 stainless steel; all others are from Type 304 stainless steel.

** This stress is induced by the boundary effect from the displacement restraints at node 2561 and, therefore, is disregarded.

Table 2.10.10-25 Primary Stresses; 30-Foot Top Oblique Drop; $\phi = 60^\circ$; 1.12-Inch Outer Shell Thickness

Stress Points		Stresses						
Location	Node	S _x	S _y	S _z	S _{xy}	S ₁	S ₂	S ₃
A1	327	-2.20	-0.06	2.06	0.11	2.06	-0.06	-2.20
A2	302	-2.59	-0.08	1.82	0.38	1.82	-0.03	-2.65
A3	277	-2.85	-0.01	1.67	0.87	1.67	0.24	-3.09
A4	252	-3.34	-0.06	1.37	1.12	1.37	0.28	-3.68
A5	227	-4.43	-1.70	1.24	0.78	1.24	-1.49	-4.63
A6	202	0.29	-2.73	6.63	-2.85	6.63	2.01	-4.44
A7	177	-30.04	-1.78	-8.24	-1.29	-1.72	-8.24	-30.10
B1	104	-8.21	-2.48	-2.59	-1.31	-2.19	-2.59	-8.50
B2	79	-5.81	-1.94	-0.78	-0.53	-0.78	-1.87	-5.89
B3	54	-4.70	-1.01	0.41	-0.84	0.41	-0.83	-4.89
B4	29	-3.55	-0.23	1.60	-0.59	1.60	-0.13	-3.65
B5	4	-2.40	0.05	2.32	0.06	2.32	0.05	-2.40
C1	110	-8.75	-0.64	-3.92	-0.53	-0.60	-3.92	-8.78
C2	85	-7.28	-0.53	-2.53	0.44	-0.50	-2.53	-7.30
C3	60	-5.90	-0.28	-1.34	0.51	-0.23	-1.34	-5.95
C4	35	-4.52	-0.06	-0.07	0.44	-0.02	-0.07	-4.56
C5	10	-3.76	-0.01	0.70	0.37	0.70	0.03	-3.79
D1	335	-1.97	2.24	0.71	-0.18	2.25	0.71	-1.97
D2	310	-3.44	1.04	-0.18	-0.13	1.05	-0.18	-3.44
D3	285	-4.13	0.45	-0.66	-0.30	0.47	-0.66	-4.15
D4	260	-5.19	-0.04	-1.29	-0.61	0.03	-1.29	-5.26
D5	235	-6.97	-0.50	-2.29	-0.55	-0.45	-2.29	-7.02
D6	210	-8.74	-0.73	-3.37	-0.43	-0.71	-3.37	-8.77
D7	185	-10.51	-0.80	-4.66	0.69	-0.75	-4.66	-10.56
E1	118	-6.47	2.78	-4.48	-1.08	2.90	-4.48	-6.60
E2	93	-7.24	1.15	-4.64	-0.20	1.16	-4.64	-7.24
E3	68	-7.11	0.47	-4.32	0.18	0.48	-4.32	-7.11
E4	43	-7.15	0.14	-3.87	0.26	0.15	-3.87	-7.15
E5	18	-7.44	0.05	-3.65	0.32	0.06	-3.65	-7.45
F1	143	-1.49	8.05	-2.34	-1.62	8.32	-1.76	-2.34
F2	144	-1.63	2.09	-5.40	-1.25	2.47	-2.01	-5.40

Table 2.10.10-25 Primary Stresses; 30-Foot Top Oblique Drop; $\phi = 60^\circ$; 1.12-Inch Outer Shell Thickness (continued)

Stress Points		Stresses						
Location	Node	S _x	S _y	S _z	S _{xy}	S ₁	S ₂	S ₃
F3	145	-2.35	0.54	-6.82	-0.83	0.76	-2.57	-6.82
F4	146	-4.11	-0.48	-8.33	-0.44	-0.43	-4.16	-8.33
F5	147	-5.25	-1.29	-9.50	-0.30	-1.27	-5.27	-9.50
F6	148	-5.95	-2.06	-10.49	-0.20	-2.05	-5.96	-10.49
F7	149	-6.43	-3.04	-11.51	-0.12	-3.03	-6.43	-11.51
F8	150	-6.70	-4.34	-12.63	-0.04	-4.34	-6.70	-12.63
G1	335	-1.97	2.24	0.71	-0.18	2.25	0.71	-1.97
G2	336	-1.78	0.94	-0.07	-0.38	0.99	-0.07	-1.83
G3	337	-2.26	-0.15	-0.84	-0.32	-0.10	-0.84	-2.31
G4	338	-3.15	-1.24	-1.65	0.16	-1.23	-1.65	-3.16
G5	339	-5.22	-3.05	-2.97	1.53	-2.27	-2.97	-6.01
G6	340	-7.31	-1.66	-2.98	1.81	-1.13	-2.98	-7.84
H1	346	-3.96	3.73	-6.50	2.70	4.58	-4.82	-6.50
H2	347	-3.33	11.81	-5.57	1.61	11.98	-3.50	-5.57
H3	348	-5.58	8.90	-8.13	-1.88	9.14	-5.83	-8.13
H4	349	-6.00	0.14	-11.64	-2.28	0.89	-6.76	-11.64
H5	350	-6.49	-8.86	-15.10	-1.53	-5.74	-9.60	-15.10
I1	621	-0.20	2.62	1.76	-0.13	2.63	1.76	-0.20
I2	624	-0.08	4.36	1.90	0.04	4.36	1.90	-0.08
J1	635	-0.20	7.40	2.23	-0.29	7.41	2.23	-0.21
J2	638	-0.02	14.82	1.74	0.11	14.82	1.74	-0.02
K1	841	-0.17	15.88	0.19	-0.05	15.88	0.19	-0.17
K2	844	-0.04	18.40	1.73	0.09	18.40	1.73	-0.04
L1	855	-0.12	31.03	1.46	-0.14	31.03	1.46	-0.12
L2	858	0.04	34.03	1.59	0.08	34.03	1.59	0.04
M1	941	-0.17	21.52	0.15	-0.01	21.52	0.15	-0.17
M2	944	-0.06	24.59	1.76	0.01	24.59	1.76	-0.06
N1	955	-0.13	42.13	1.74	-0.07	42.13	1.74	-0.13
N2	958	0.01	46.06	1.89	0.06	46.06	1.89	0.01
O1	1101	-0.18	21.29	-0.41	0.00	21.29	-0.18	-0.41
O2	1104	-0.12	24.21	1.16	-0.01	24.21	1.16	-0.12

Table 2.10.10-25 Primary Stresses; 30-Foot Top Oblique Drop; $\phi = 60^\circ$; 1.12-Inch Outer Shell Thickness (continued)

Stress Points		Stresses						
Location	Node	S _x	S _y	S _z	S _{xy}	S ₁	S ₂	S ₃
P1	1115	-0.17	45.94	1.85	0.03	45.94	1.85	-0.17
P2	1118	0.01	50.51	2.64	-0.03	50.51	2.64	0.01
Q1	1261	-0.17	15.33	0.18	0.04	15.33	0.18	-0.17
Q2	1264	-0.06	17.74	1.70	-0.05	17.74	1.70	-0.06
R1	1275	-0.14	31.46	0.52	0.11	31.46	0.52	-0.14
R2	1278	0.02	35.19	2.79	-0.11	35.19	2.79	0.02
S1	1561	-0.16	-3.23	1.96	-0.18	1.96	-0.15	-3.25
S2	1564	0.16	-9.52	-1.78	-0.41	0.17	-1.78	-9.54
T1	1575	-0.30	3.10	2.37	0.21	3.12	2.37	-0.31
T2	1578	0.01	7.20	4.64	-0.12	7.20	4.64	0.01
U1	1841	0.24	-16.50	10.84	-0.13	10.84	0.24	-16.50
U2	1844	3.80	-7.62	11.27	-0.74	11.27	3.85	-7.67
V1	1852	9.95	1.30	5.66	-2.98	10.88	5.66	0.37
V2	1856	0.78	-7.73	-2.30	0.06	0.78	-2.30	-7.73
W1	1969	-66.76	-41.68	-23.95	-0.48	-23.95	-41.67	-66.77
W2	1970	-48.81	-4.87	-11.98	-3.63	-4.57	-11.98	-49.11
W3	1971	-27.02	-1.92	-8.87	-5.46	-0.78	-8.87	-28.15
W4	1972	-19.49	2.28	-9.31	-4.67	3.24	-9.31	-20.45
W5	1973	-15.85	5.41	-10.04	-3.70	6.03	-10.04	-16.48
W6	1974	-13.88	8.25	-10.62	-2.69	8.57	-10.62	-14.20
W7	1975	-12.85	11.83	-11.25	-1.50	11.92	-11.25	-12.94
W8	1976	-12.54	16.71	-11.73	-0.67	16.73	-11.73	-12.56
X1	2370	-34.36	-17.01	-7.66	1.31	-7.66	-16.91	-34.46
X2	2390	-16.21	-14.25	-1.58	4.86	-1.58	-10.27	-20.19
X3	2410	-12.66	-12.01	0.06	7.35	0.06	-4.98	-19.69
X4	2430	-8.01	-13.25	1.10	7.19	1.10	-2.98	-18.29
X5	2450	-6.21	-12.65	1.73	6.28	1.73	-2.37	-16.49
X6	2470	-5.20	-11.99	1.96	5.16	1.96	-2.42	-14.77
X7	2490	-4.59	-11.11	1.74	4.16	1.74	-2.56	-13.14
X8	2510	-4.01	-10.62	1.46	3.23	1.46	-2.70	-11.93
X9	2530	-3.28	-10.25	0.95	2.34	0.95	-2.57	-10.96

Table 2.10.10-25 Primary Stresses; 30-Foot Top Oblique Drop; $\phi = 60^\circ$; 1.12-Inch Outer Shell Thickness (continued)

Stress Points		Stresses						
Location	Node	S _x	S _y	S _z	S _{xy}	S ₁	S ₂	S ₃
X10	2550	-2.20	-10.08	0.13	1.27	0.13	-2.00	-10.28
X11	2570	-0.68	-10.03	-1.07	0.85	-0.61	-1.07	-10.11
Y1	2305	-0.50	-3.31	2.52	-0.39	2.52	-0.45	-3.37
Y2	2325	-2.99	-3.28	2.85	-0.90	2.85	-2.22	-4.05
Y3	2345	-5.73	-3.30	2.62	-0.90	2.62	-3.00	-6.02
Y4	2365	-8.38	-3.62	2.34	0.15	2.34	-3.61	-8.38
Y5	2385	-9.44	-4.55	2.25	2.00	2.25	-3.84	-10.15
Y6	2405	-8.81	-6.23	2.40	4.00	2.40	-3.31	-11.73
Y7	2425	-7.68	-8.50	2.67	5.91	2.67	-2.17	-14.02
Y8	2445	-7.41	-10.86	3.08	8.04	3.08	-0.91	-17.36
Y9	2465	-9.57	-12.29	3.68	10.52	3.68	-0.32	-21.54
Y10	2485	-16.57	-12.12	3.75	12.22	3.75	-1.92	-26.77
Y11	2505	-22.26	-11.71	2.74	11.40	2.74	-4.42	-29.55
Y12	2525	-25.13	-11.21	1.58	8.78	1.58	-6.96	-29.38
Y13	2545	-27.83	-10.20	-0.70	5.06	-0.70	-8.85	-29.18
Y14	2565	-28.31	-9.99	-5.19	2.37	-5.19	-9.69	-28.61
Z1	2301	-2.94	-0.93	2.30	-0.10	2.30	-0.92	-2.95
Z2	2321	-3.62	-0.50	2.68	-0.22	2.68	-0.48	-3.63
Z3	2341	-4.30	-0.47	2.65	-0.18	2.65	-0.46	-4.31
Z4	2361	-4.93	-0.47	2.65	-0.02	2.65	-0.47	-4.93
Z5	2381	-5.19	-0.50	2.59	0.27	2.59	-0.49	-5.21
Z6	2401	-4.99	-0.61	2.43	0.60	2.43	-0.53	-5.07
Z7	2421	-4.39	-0.77	2.17	0.94	2.17	-0.54	-4.62
Z8	2441	-3.53	-0.98	1.86	1.42	1.86	-0.34	-4.17
Z9	2461	-2.52	-1.18	1.53	3.69	1.90	1.53	-5.60
Z10	2481	-1.46	-1.39	1.23	12.69	11.26	1.23	-14.12
Z11	2501	-0.95	-1.49	1.04	36.69	35.47	1.04	-37.91
Z12	2521	-0.45	-1.56	0.83	110.30	109.30	0.83	-111.31
Z13	2541	-0.15	-1.98	0.37	501.00	499.93	0.37	-502.07
Z14	2561	0.54	-3.06	-1.49	655.20	653.94	-1.49	-656.46

**Table 2.10.10-26 Primary Plus Secondary Stresses; 30-Foot Top Oblique Drop;
 $\phi = 60^\circ$; 1.12-Inch Outer Shell Thickness**

Stress Points		Stresses						
Location	Node	S _x	S _y	S _z	S _{xy}	S ₁	S ₂	S ₃
A1	327	2.64	0.00	6.89	0.33	6.89	2.68	-0.04
A2	302	1.46	-0.02	5.87	0.35	5.87	1.54	-0.10
A3	277	0.42	0.00	4.93	0.78	4.93	1.02	-0.59
A4	252	-1.64	-0.09	3.07	1.10	3.07	0.48	-2.22
A5	227	-5.82	-1.74	-0.16	0.76	-0.16	-1.61	-5.95
A6	202	-4.15	-2.81	2.18	-2.86	2.18	-0.54	-6.42
A7	177	-37.54	-1.86	-15.71	-1.29	-1.81	-15.71	-37.58
B1	104	-9.88	-2.53	-4.29	-1.34	-2.30	-4.29	-10.12
B2	79	-5.43	-1.96	-0.38	-0.41	-0.38	-1.91	-5.47
B3	54	-2.19	-0.92	2.95	-0.73	2.95	-0.59	-2.52
B4	29	1.17	-0.17	6.32	-0.45	6.32	1.31	-0.31
B5	4	4.86	0.01	9.51	-0.54	9.51	4.92	-0.05
C1	110	-9.58	-1.93	-4.90	-0.23	-1.93	-4.90	-9.59
C2	85	-6.38	-1.59	-1.59	1.00	-1.39	-1.59	-6.58
C3	60	-3.50	-0.86	1.56	1.20	1.56	-0.39	-3.97
C4	35	-0.39	-0.25	4.95	0.78	4.95	0.47	-1.10
C5	10	2.90	-0.05	8.29	0.32	8.29	2.94	-0.08
D1	335	-2.70	-6.38	1.69	-1.30	1.69	-2.29	-6.80
D2	310	-1.28	-4.02	2.00	-1.30	2.00	-0.76	-4.54
D3	285	-2.05	-2.87	1.50	-1.36	1.50	-1.04	-3.88
D4	260	-4.03	-2.42	-0.06	-1.58	-0.06	-1.45	-5.00
D5	235	-7.68	-2.59	-3.37	-1.34	-2.26	-3.37	-8.01
D6	210	-11.62	-2.80	-6.92	-0.60	-2.76	-6.92	-11.66
D7	185	-15.97	-2.84	-10.91	1.36	-2.70	-10.91	-16.11
E1	118	-0.29	4.45	-0.74	3.28	6.13	-0.74	-1.97
E2	93	-6.29	3.85	-1.48	2.17	4.29	-1.48	-6.73
E3	68	-6.30	1.31	-0.92	1.84	1.73	-0.92	-6.72
E4	43	-6.93	0.36	0.16	1.05	0.51	0.16	-7.08
E5	18	-6.51	0.13	2.03	0.57	2.03	0.17	-6.56
F1	143	-11.90	4.29	-3.27	4.25	5.33	-3.27	-12.95
F2	144	-9.99	8.00	-3.72	2.34	8.30	-3.72	-10.29

**Table 2.10.10-26 Primary Plus Secondary Stresses; 30-Foot Top Oblique Drop;
 $\phi = 60^\circ$; 1.12-Inch Outer Shell Thickness (continued)**

Stress Points		Stresses						
Location	Node	S _x	S _y	S _z	S _{xy}	S ₁	S ₂	S ₃
F3	145	-7.16	4.19	-5.14	0.29	4.20	-5.14	-7.17
F4	146	-6.18	2.12	-6.30	-0.12	2.12	-6.18	-6.30
F5	147	-6.27	0.67	-7.35	-0.22	0.68	-6.28	-7.35
F6	148	-6.47	-0.50	-8.28	-0.24	-0.49	-6.48	-8.28
F7	149	-6.65	-1.76	-9.26	-0.16	-1.75	-6.65	-9.26
F8	150	-6.78	-3.18	-10.34	-0.07	-3.18	-6.78	-10.34
G1	335	-2.70	-6.38	1.69	-1.30	1.69	-2.29	-6.80
G2	336	-2.08	-4.03	2.13	-0.48	2.13	-1.97	-4.14
G3	337	-1.32	-2.54	2.44	0.13	2.44	-1.31	-2.55
G4	338	-1.29	-0.71	2.70	0.17	2.70	-0.66	-1.34
G5	339	-0.66	2.43	3.40	-0.80	3.40	2.63	-0.85
G6	340	-1.66	-0.49	2.60	-0.95	2.60	0.04	-2.20
H1	346	-12.85	0.12	-8.85	2.49	0.58	-8.85	-13.31
H2	347	-7.96	14.36	-4.84	1.64	14.48	-4.84	-8.08
H3	348	-7.80	15.74	-5.31	-2.05	15.92	-5.31	-7.98
H4	349	-6.78	9.73	-7.57	-2.53	10.11	-7.16	-7.57
H5	350	-6.73	4.45	-9.87	-1.75	4.72	-7.00	-9.87
I1	621	-0.20	3.73	1.87	-0.08	3.73	1.87	-0.20
I2	624	-0.05	3.97	1.81	0.09	3.98	1.81	-0.05
J1	635	-0.21	17.01	2.55	-0.24	17.02	2.55	-0.21
J2	638	-0.01	22.00	1.68	0.15	22.00	1.68	-0.01
K1	841	-0.17	18.19	0.09	-0.05	18.19	0.09	-0.17
K2	844	-0.03	21.13	2.02	0.10	21.13	2.02	-0.03
L1	855	-0.12	40.27	1.10	-0.14	40.27	1.10	-0.12
L2	858	0.05	43.81	1.77	0.08	43.81	1.77	0.05
M1	941	-0.17	23.77	-0.02	-0.02	23.77	-0.02	-0.17
M2	944	-0.05	27.37	2.11	0.01	27.37	2.11	-0.05
N1	955	-0.13	51.27	1.29	-0.06	51.27	1.29	-0.13
N2	958	0.01	55.90	2.12	0.06	55.90	2.12	0.01
O1	1101	-0.18	23.55	-0.57	0.00	23.55	-0.18	-0.57
O2	1104	-0.11	26.99	1.51	-0.01	26.99	1.51	-0.11

**Table 2.10.10-26 Primary Plus Secondary Stresses; 30-Foot Top Oblique Drop;
 $\phi = 60^\circ$; 1.12-Inch Outer Shell Thickness (continued)**

Stress Points		Stresses						
Location	Node	S _x	S _y	S _z	S _{xy}	S ₁	S ₂	S ₃
P1	1115	-0.17	55.04	1.36	0.03	55.04	1.36	-0.17
P2	1118	0.01	60.36	2.88	-0.03	60.36	2.88	0.01
Q1	1261	-0.17	17.64	0.10	0.03	17.64	0.10	-0.17
Q2	1264	-0.05	20.46	2.02	-0.06	20.46	2.02	-0.05
R1	1275	-0.14	40.61	0.06	0.11	40.61	0.06	-0.14
R2	1278	0.01	45.07	2.88	-0.11	45.07	2.88	0.01
S1	1561	-0.16	-1.12	2.31	-0.14	2.31	-0.14	-1.14
S2	1564	0.14	-6.58	-1.11	-0.36	0.15	-1.11	-6.60
T1	1575	-0.30	13.77	2.45	0.15	13.77	2.45	-0.30
T2	1578	0.02	15.65	4.52	-0.17	15.65	4.52	0.02
U1	1841	0.26	-16.32	10.30	-0.22	10.30	0.26	-16.32
U2	1844	4.00	-6.40	11.44	-0.71	11.44	4.07	-6.46
V1	1852	4.26	-0.87	3.22	-4.16	6.58	3.22	-3.20
V2	1856	0.46	4.34	1.25	0.22	4.35	1.25	0.45
W1	1969	-67.53	-43.53	-23.94	-1.29	-23.94	-43.46	-67.60
W2	1970	-48.84	-5.63	-11.28	-4.31	-5.20	-11.28	-49.27
W3	1971	-27.13	-2.01	-7.91	-6.01	-0.64	-7.91	-28.49
W4	1972	-19.57	2.81	-8.10	-5.16	3.95	-8.10	-20.70
W5	1973	-15.93	6.35	-8.66	-4.08	7.08	-8.66	-16.65
W6	1974	-13.94	9.52	-9.09	-2.95	9.88	-9.09	-14.31
W7	1975	-12.89	13.38	-9.59	-1.63	13.48	-9.59	-12.99
W8	1976	-12.53	18.52	-9.94	-0.73	18.54	-9.94	-12.55
X1	2370	-35.61	-17.34	-7.99	1.91	-7.99	-17.14	-35.81
X2	2390	-16.54	-15.19	-1.82	5.30	-1.82	-10.52	-21.21
X3	2410	-13.03	-12.55	-0.02	7.41	-0.02	-5.37	-20.21
X4	2430	-8.36	-13.64	1.09	7.06	1.09	-3.46	-18.54
X5	2450	-6.61	-12.88	1.79	6.02	1.79	-2.95	-16.54
X6	2470	-5.61	-12.12	2.09	4.84	2.09	-3.04	-14.70
X7	2490	-4.97	-11.18	1.99	3.82	1.99	-3.15	-13.00
X8	2510	-4.35	-10.65	1.81	2.91	1.81	-3.21	-11.79
X9	2530	-3.57	-10.27	1.40	2.07	1.40	-2.98	-10.86

Table 2.10.10-26 Primary Plus Secondary Stresses; 30-Foot Top Oblique Drop;
 $\phi = 60^\circ$; 1.12-Inch Outer Shell Thickness (continued)

Stress Points		Stresses						
Location	Node	S _x	S _y	S _z	S _{xy}	S ₁	S ₂	S ₃
X10	2550	-2.42	-10.09	0.74	1.10	0.74	-2.27	-10.24
X11	2570	-0.06	-10.03	0.51	0.80	0.51	0.00	-10.09
Y1	2305	0.06	-3.34	3.01	-0.43	3.01	0.12	-3.40
Y2	2325	-2.97	-3.33	2.84	-0.85	2.84	-2.28	-4.02
Y3	2345	-6.01	-3.41	2.29	-0.85	2.29	-3.16	-6.26
Y4	2365	-8.93	-3.78	1.73	0.20	1.73	-3.77	-8.94
Y5	2385	-10.17	-4.76	1.46	2.04	1.46	-4.07	-10.86
Y6	2405	-9.61	-6.48	1.53	4.04	1.53	-3.71	-12.38
Y7	2425	-8.47	-8.77	1.79	5.91	1.79	-2.71	-14.53
Y8	2445	-8.13	-11.11	2.28	7.99	2.28	-1.49	-17.75
Y9	2465	-10.18	-12.47	3.01	10.44	3.01	-0.82	-21.83
Y10	2485	-17.00	-12.23	3.30	12.13	3.30	-2.25	-26.98
Y11	2505	-22.55	-11.76	2.45	11.37	2.45	-4.57	-29.74
Y12	2525	-25.24	-11.22	1.47	8.77	1.47	-7.00	-29.46
Y13	2545	-27.70	-10.20	-0.60	5.05	-0.60	-8.85	-29.05
Y14	2565	-27.05	-9.99	-4.04	2.44	-4.04	-9.65	-27.39
Z1	2301	-2.44	-0.91	2.79	-0.10	2.79	-0.91	-2.44
Z2	2321	-3.53	-0.47	2.76	-0.22	2.76	-0.45	-3.55
Z3	2341	-4.54	-0.40	2.41	-0.18	2.41	-0.40	-4.55
Z4	2361	-5.44	-0.38	2.14	-0.02	2.14	-0.38	-5.44
Z5	2381	-5.87	-0.40	1.91	0.27	1.91	-0.39	-5.89
Z6	2401	-5.78	-0.50	1.65	0.60	1.65	-0.43	-5.84
Z7	2421	-5.19	-0.67	1.38	0.94	1.38	-0.48	-5.38
Z8	2441	-4.25	-0.88	1.14	1.42	1.14	-0.36	-4.78
Z9	2461	-3.10	-1.09	0.96	3.69	1.73	0.96	-5.92
Z10	2481	-1.81	-1.32	0.89	12.69	11.13	0.89	-14.26
Z11	2501	-1.16	-1.44	0.84	36.69	35.39	0.84	-37.99
Z12	2521	-0.50	-1.53	0.77	110.30	109.28	0.77	-111.32
Z13	2541	-0.05	-1.97	0.47	501.00	499.99	0.47	-502.01
Z14	2561	1.60	-3.05	-0.43	655.20	654.48	-0.43	-655.93

**Table 2.10.10-27 Primary Membrane (P_m) Stresses; 30-Foot Top Oblique Drop;
 $\phi = 60^\circ$; 1.12-Inch Outer Shell Thickness**

Section	Node to Node	Stresses* (ksi)							
		S_x	S_y	S_z	S_{xy}	S_1	S_2	S_3	S_I
A	177 – 327	-5.92	-1.35	1.52	-0.36	1.52	-1.32	-5.94	7.47
B	4 – 104	-5.10	-1.24	0.03	-0.70	0.03	-1.12	-5.23	5.26
C	10 – 110	-6.24	-0.33	-1.63	0.32	-0.32	-1.63	-6.26	5.94
D	185 – 335	-6.88	-0.24	-2.29	-0.32	-0.22	-2.29	-6.89	6.67
E	18 – 118	-7.09	0.89	-4.29	-0.08	0.90	-4.29	-7.09	7.98
F	143 – 150	-3.67	0.25	-7.65	-0.67	0.36	-3.78	-7.65	8.01
G	335 – 340	-3.93	-1.19	-1.70	0.67	-1.04	-1.70	-4.08	3.04
H	346 – 350	-4.95	4.60	-8.86	-0.40	4.62	-4.97	-8.86	13.48
I	621 – 624	-0.13	3.47	1.82	-0.04	3.47	1.82	-0.13	3.61
J	635 – 638	-0.11	11.18	1.97	-0.09	11.18	1.97	-0.11	11.29
K	841 – 844	-0.12	17.17	0.99	0.02	17.17	0.99	-0.012	17.28
L	855 – 858	-0.04	32.55	1.53	-0.03	32.55	1.53	-0.04	32.59
M	941 – 944	-0.13	23.09	0.98	0.00	23.09	0.98	-0.13	23.21
N	955 – 958	-0.06	44.12	1.82	0.00	44.12	1.82	-0.06	44.18
O	1101 – 1104	-0.16	22.78	0.40	0.00	22.78	0.40	-0.16	22.95
P	1115 – 1118	-0.08	48.26	2.25	0.00	48.26	2.25	-0.08	48.34
Q	1261 – 1264	-0.12	16.56	0.97	-0.01	16.56	0.97	-0.12	16.68
R	1275 – 1278	-0.07	33.36	1.68	0.00	33.36	1.68	-0.07	33.43
S	1561 – 1564	0.01	-6.35	0.06	-0.39	0.06	0.04	-6.38	6.43
T	1575 – 1578	-0.15	5.18	3.53	0.03	5.18	3.53	-0.15	5.33
U	1841 – 1846	4.88	-3.27	11.92	0.21	11.92	4.89	-6.28	18.20
V	1852 – 1856	4.46	-0.13	1.97	-1.03	4.68	1.97	-0.34	5.02
W	1969 – 1976	-31.03	-1.79	-12.13	-3.28	-1.43	-12.13	-31.40	29.97
X	2370 – 2570	-9.19	-12.12	0.30	4.82	0.30	-5.62	-15.69	15.99
Y	2305 – 2565	-10.47	-7.40	2.41	4.52	2.41	-4.17	-13.71	16.11
Z	2301 – 2561	-3.33	-0.93	1.95	45.03	42.91	1.95	-47.18	90.09

* Stresses are taken at 0 degrees (under the load) at each section.

Table 2.10.10-28 Primary Membrane Plus Primary Bending ($P_m + P_b$) Stresses; 30-Foot Top Oblique Drop; $\phi = 60^\circ$; 1.12-Inch Outer Shell Thickness

Section	Node to Node	Stresses* (ksi)							
		S_x	S_y	S_z	S_{xy}	S_1	S_2	S_3	SI
A	177 – 327	-12.85	-2.87	0.67	-2.34	0.67	-2.35	-13.37	14.04
B	4 – 104	-7.97	-2.62	-2.64	-1.03	-2.43	-2.64	-8.16	5.74
C	10 – 110	-8.82	-0.69	-4.10	-0.01	-0.69	-4.10	-8.82	8.13
D	185 – 335	-10.62	-1.35	-4.47	-0.07	-1.35	-4.47	-10.63	9.27
E	18 – 118	-6.83	2.15	-4.77	-0.71	2.21	-4.77	-6.88	9.09
F	143 – 150	-1.49	5.48	-2.80	-0.67	5.55	-1.56	-2.80	8.35
G	335 – 340	-7.37	-3.58	-3.78	0.67	-3.47	-3.78	-7.48	4.01
H	346 – 350	-4.00	12.55	-4.04	-0.40	12.56	-4.01	-4.04	16.60
I	621 – 624	-0.08	4.31	1.89	-0.04	4.31	1.89	-0.08	4.39
J	635 – 638	-0.02	14.82	1.72	-0.09	14.82	1.72	-0.02	14.84
K	841 – 844	-0.04	18.41	1.75	0.02	18.41	1.75	-0.04	18.45
L	855 – 858	0.04	34.03	1.59	-0.03	34.03	1.59	0.04	33.98
M	941 – 944	-0.06	24.59	1.79	0.00	24.59	1.79	-0.06	24.65
N	955 – 958	0.01	46.06	1.89	0.00	46.06	1.89	0.01	46.05
O	1101 – 1104	-0.12	24.21	1.18	0.00	24.21	1.18	-0.12	24.34
P	1115 – 1118	0.01	50.51	2.64	0.00	50.51	2.64	0.01	50.50
Q	1261 – 1264	-0.06	17.74	1.72	-0.01	17.74	1.72	-0.06	17.80
R	1275 – 1278	0.02	35.19	2.81	0.00	35.19	2.81	0.02	35.17
S	1561 – 1564	0.16	-9.42	-1.80	-0.39	0.17	-1.80	-9.44	9.61
T	1575 – 1578	0.01	7.20	4.66	0.03	7.20	4.66	0.01	7.19
U	1841 – 1846	0.24	-14.53	10.39	0.21	10.39	0.24	-14.54	24.92
V	1852 – 1856	0.78	-5.40	-2.35	-1.03	0.94	-2.35	-5.57	6.51
W	1969 – 1976	-66.76	-24.50	-16.52	-3.28	-16.52	-24.25	-67.01	50.49
X	2370 – 2570	-20.23	-14.00	-1.74	6.55	-1.74	-9.86	-24.37	22.63
Y	2305 – 2565	-21.21	-13.13	1.72	11.16	1.72	-5.31	-29.04	30.75
Z	2301 – 2561	-1.37	-1.67	0.72	166.60	165.08	0.72	-168.12	333.20

* Stresses are taken at 0 degrees (under the load) at each section.

Table 2.10.10-29 Primary Membrane (P_m) and Primary Membrane Plus Primary Bending ($P_m + P_b$) Stresses; 30-Foot Top Oblique Drop; $\phi = 60^\circ$; 1.12-Inch Outer Shell Thickness

Section	Node to Node	Max. Temp. (°F)	P_m Stresses (ksi)			$P_m + P_b$ Stresses (ksi)		
			Allow. ¹ 0.7 S_u	Calc.	MS	Allow. ¹ 1.0 S_u	Calc.	MS
A	327 – 177	222	48.93	7.47	+Large	69.90	14.04	+3.97
B	104 – 4	215	49.18	5.26	+Large	70.25	5.74	+Large
C	110 – 10	212	49.28	5.94	+Large	70.40	8.13	+Large
D	335 – 185	221	48.96	6.67	+Large	69.95	9.27	+Large
E	118 – 18	208	49.42	7.98	+Large	70.60	9.09	+Large
F	143 – 150	209	49.38	8.01	+Large	70.55	8.35	+Large
G	335 – 340	221	48.96	3.04	+Large	69.95	4.01	+Large
H	346 – 350	212	49.28	13.48	+2.66	70.40	16.60	+3.24
I	621 – 624	222	48.93	3.61	+Large	69.90	4.39	+Large
J	635 – 638	199	49.73	11.29	+3.40	71.04	14.84	+3.79
K	841 – 844	232	68.49	17.28	+2.96	97.84	18.45	+Large
L	855 – 858	204	69.50	32.59	+1.13	99.29	33.98	+1.92
M	941 – 944	247	67.94	23.21	+1.93	97.06	24.65	+2.94
N	955 – 958	211	69.25	44.18	+0.57	98.93	46.05	+1.15
O	1101 – 1104	255	67.65	22.95	+1.95	96.64	24.34	+2.97
P	1115 – 1118	216	69.07	48.34	+0.43	98.67	50.50	+0.95
Q	1261 – 1264	251	67.80	16.68	+3.06	96.85	17.80	+Large
R	1275 – 1278	216	69.07	33.43	+1.07	98.67	35.17	+1.81
S	1561 – 1564	217	49.10	6.43	+Large	70.15	9.61	+Large
T	1575 – 1578	197	49.78	5.33	+Large	71.12	7.19	+Large
U	1841 – 1846	212	49.28	18.20	+1.71	70.40	24.92	+1.83
V	1852 – 1856	205	49.52	5.02	+Large	70.75	6.51	+Large
W	1969 – 1976	198	49.76	29.97	+0.66	71.08	50.49	+0.41
X	2370 – 2570	201	49.66	15.99	+2.11	70.95	22.63	+2.14
Y	2305 – 2565	205	49.52	16.11	+2.07	70.75	30.75	+1.30
Z	2301 – 2561	204	49.56	90.09 ²	²	70.80	333.202	²

¹ Allowable stresses for sections “K” through “R” are taken from Type XM-19 stainless steel; all others are from Type 304 stainless steel.

² This stress is induced by the boundary effect from the displacement restraints at node 2561 and, therefore, is disregarded.

Table 2.10.10-30 Primary Stresses; 30-Foot Side Drop; $\phi = 90^\circ$; 1.20-Inch Outer Shell Thickness; Circumferential Location = 0°

Stress Points		Stresses (ksi)						
Location	Node	S _x	S _y	S _z	S _{xy}	S ₁	S ₂	S ₃
A1	327	-3.14	-0.06	2.35	0.13	2.35	-0.05	-3.15
A2	302	-3.62	-0.09	2.07	0.49	2.07	-0.03	-3.69
A3	277	-3.91	0.01	1.91	1.13	1.91	0.31	-4.21
A4	252	-4.49	-0.06	1.58	1.45	1.58	0.37	-4.92
A5	227	-5.78	-2.16	1.53	1.01	1.53	-1.89	-6.05
A6	202	0.42	-3.48	8.60	-3.67	8.60	2.62	-5.68
A7	177	-38.59	-2.25	-10.46	-1.66	-2.17	-10.46	-38.67
B1	104	-10.75	-3.20	-3.50	-1.69	-2.84	-3.50	-11.11
B2	79	-7.52	-2.51	-1.03	-0.67	-1.03	-2.42	-7.61
B3	54	-5.97	-1.30	0.63	-1.06	0.63	-1.07	-6.20
B4	29	-4.36	-0.29	2.29	-0.74	2.29	-0.16	-4.49
B5	4	-2.81	0.06	3.30	0.06	3.30	0.07	-2.81
C1	110	-11.30	-0.82	-5.15	-0.67	-0.78	-5.15	-11.34
C2	85	-9.35	-0.68	-3.26	0.60	-0.64	-3.26	-9.39
C3	60	-7.53	-0.36	-1.64	0.71	-0.29	-1.64	-7.60
C4	35	-5.71	-0.08	0.08	0.59	0.08	-0.02	-5.77
C5	10	-4.70	-0.01	1.12	0.48	1.12	0.04	-4.75
D1	335	-2.50	3.23	0.85	-0.17	3.23	0.85	-2.51
D2	310	-4.51	1.57	-0.35	-0.10	1.57	-0.35	-4.51
D3	285	-5.42	0.75	-0.97	-0.32	0.77	-0.97	-5.43
D4	260	-6.80	0.08	-1.76	-0.72	0.15	-1.76	-6.87
D5	235	-9.08	-0.55	-3.01	-0.66	-0.50	-3.01	-9.13
D6	210	-11.33	-0.88	-4.35	-0.52	-0.85	-4.35	-11.35
D7	185	-13.59	-0.97	-5.95	0.90	-0.90	-5.95	-13.65
E1	118	-8.14	3.79	-5.68	-1.31	3.93	-5.68	-8.28
E2	93	-9.28	1.61	-5.92	-0.20	1.61	-5.92	-9.28
E3	68	-9.14	0.66	-5.50	0.26	0.66	-5.50	-9.15
E4	43	-9.22	0.20	-4.89	0.34	0.22	-4.89	-9.23
E5	18	-9.63	0.07	-4.60	0.41	0.09	-4.60	-9.64
F1	143	-1.94	10.54	-2.98	-2.02	10.86	-2.26	-2.98
F2	144	-2.09	2.75	-6.95	-1.53	3.19	-2.53	-6.95

Table 2.10.10-30 Primary Stresses; 30-Foot Side Drop; $\phi = 90^\circ$; 1.20-Inch Outer Shell Thickness; Circumferential Location = 0° (continued)

Stress Points		Stresses (ksi)						
Location	Node	S _x	S _y	S _z	S _{xy}	S ₁	S ₂	S ₃
F3	145	-3.00	0.75	-8.78	-0.97	0.98	-3.23	-8.78
F4	146	-5.28	-0.58	-10.73	-0.49	-0.53	-5.33	-10.73
F5	147	-6.76	-1.63	-12.25	-0.32	-1.61	-6.78	-12.25
F6	148	-7.67	-2.63	-13.52	-0.22	-2.62	-7.68	-13.52
F7	149	-8.29	-3.89	-14.85	-0.13	-3.89	-8.30	-14.85
F8	150	-8.64	-5.58	-16.30	-0.04	-5.58	-8.64	-16.30
G1	335	-2.50	3.23	0.85	-0.17	3.23	0.85	-2.51
G2	336	-2.25	1.48	-0.17	-0.46	1.54	-0.17	-2.30
G3	337	-2.90	0.05	-1.18	-0.41	0.11	-1.18	-2.95
G4	338	-4.06	-1.36	-2.22	0.19	-1.35	-2.22	-4.07
G5	339	-6.74	-3.77	-3.94	1.93	-2.82	-3.94	-7.69
G6	340	-9.47	-2.10	-3.99	2.30	-1.44	-3.99	-10.13
H1	346	-5.16	4.91	-8.50	3.55	6.03	-6.29	-8.50
H2	347	-4.30	15.58	-7.21	2.14	15.81	-4.52	-7.21
H3	348	-7.22	11.93	-10.49	-2.43	12.24	-7.52	-10.49
H4	349	-7.75	0.57	-15.03	-2.97	1.52	-8.70	-15.03
H5	350	-8.37	-11.06	-19.50	-1.99	-7.31	-12.11	-19.50
I1	621	-0.23	3.92	2.12	-0.18	3.93	2.12	-0.24
I2	624	-0.11	6.29	2.35	0.04	6.29	2.35	-0.11
J1	635	-0.26	10.07	2.86	-0.38	10.09	2.86	-0.27
J2	638	-0.03	19.66	2.23	0.14	19.66	2.23	-0.03
K1	841	-0.23	16.81	-0.06	-0.08	16.81	-0.06	-0.24
K2	844	-0.07	19.81	2.28	0.11	19.81	2.28	-0.07
L1	855	-0.14	33.30	2.54	-0.22	33.30	2.54	-0.14
L2	858	0.04	36.61	1.36	0.14	36.61	1.36	0.04
M1	941	-0.23	25.38	-0.40	0.01	25.38	-0.23	-0.40
M2	944	-0.11	29.12	2.12	0.06	29.12	2.12	-0.11
N1	955	-0.16	51.01	2.49	-0.12	51.01	2.49	-0.16
N2	958	0.02	56.00	2.11	0.11	56.00	2.11	0.02
O1	1101	-0.24	29.33	-0.72	0.00	29.33	-0.24	-0.72
O2	1104	-0.15	33.42	1.76	0.01	33.42	1.76	-0.15

Table 2.10.10-30 Primary Stresses; 30-Foot Side Drop; $\phi = 90^\circ$; 1.20-Inch Outer Shell Thickness; Circumferential Location = 0° continued)

Stress Points		Stresses (ksi)						
Location	Node	S _x	S _y	S _z	S _{xy}	S ₁	S ₂	S ₃
P1	1115	-0.21	61.83	2.28	0.01	61.83	2.28	-0.21
P2	1118	0.02	68.25	3.05	-0.01	68.25	3.05	0.02
Q1	1261	-0.23	26.93	-0.18	0.03	26.93	-0.18	-0.23
Q2	1264	-0.08	30.88	2.34	-0.04	30.88	2.34	-0.08
R1	1275	-0.19	50.04	0.64	0.12	50.04	0.64	-0.19
R2	1278	0.03	55.93	3.40	-0.12	55.93	3.40	0.03
S1	1561	-0.22	6.45	1.68	0.19	6.45	1.68	-0.22
S2	15.64	-0.15	10.08	3.23	0.03	10.08	3.23	-0.15
T1	1575	-0.24	20.06	0.94	0.25	20.06	0.94	-0.25
T2	1578	0.01	28.31	4.65	-0.11	28.31	4.65	0.01
U1	1841	-0.15	-0.51	3.08	0.02	3.08	-0.15	-0.51
U2	1844	0.39	0.74	2.17	-0.27	2.17	0.89	0.24
V1	1852	10.17	10.66	0.01	-7.15	17.57	3.26	0.01
V2	1856	0.69	5.00	-6.36	0.52	5.06	0.63	-6.36
W1	1969	-42.95	-26.22	-16.25	-3.73	-16.25	-25.43	-43.74
W2	1970	-32.16	0.14	-8.38	-4.46	0.75	-8.38	-32.76
W3	1971	-18.51	3.17	-6.74	-4.82	4.19	-6.74	-19.54
W4	1972	-13.78	6.90	-7.47	-3.98	7.64	-7.47	-14.52
W5	1973	-11.52	9.51	-8.33	-3.07	9.95	-8.33	-11.96
W6	1974	-10.25	11.85	-9.09	-2.18	12.07	-9.09	-10.46
W7	1975	-9.60	14.64	-9.91	-1.19	14.70	-9.65	-9.91
W8	1976	-9.43	18.35	-10.64	-0.44	18.35	-9.44	-10.64
X1	2370	-20.80	-8.29	-5.45	-0.83	-5.45	-8.24	-20.86
X2	2390	-8.80	-4.14	-0.82	0.96	-0.82	-3.95	-8.99
X3	2410	-6.31	-2.06	0.11	2.47	0.11	-0.93	-7.44
X4	2430	-3.28	-2.28	0.55	2.20	0.55	-0.53	-5.04
X5	2450	-1.90	-1.68	0.73	1.56	0.73	-0.22	-3.35
X6	2470	-1.04	-1.21	0.77	0.92	0.77	-0.20	-2.05
X7	2490	-0.57	-0.66	0.79	0.48	0.79	-0.13	-1.09
X8	25.10	-0.30	-0.41	0.84	0.27	0.84	-0.08	-0.63

Table 2.10.10-30 Primary Stresses; 30-Foot Side Drop; $\phi = 90^\circ$; 1.20-Inch Outer Shell Thickness; Circumferential Location = 0° (continued)

Stress Points		Stresses (ksi)						
Location	Node	S _x	S _y	S _z	S _{xy}	S ₁	S ₂	S ₃
X9	2530	-0.03	-0.19	0.92	0.14	0.92	0.05	-0.27
X10	2550	0.32	-0.06	1.03	0.05	1.03	0.33	-0.07
X11	2570	0.78	-0.01	1.20	0.06	1.20	0.79	-0.02
Y1	2305	-0.17	0.22	0.87	-0.22	0.87	0.32	-0.26
Y2	2325	-1.97	0.14	0.73	-0.67	0.73	0.33	-2.16
Y3	2345	-3.64	0.20	0.77	-0.78	0.77	0.35	-3.79
Y4	2365	-5.08	0.28	0.82	-0.30	0.82	0.30	-5.09
Y5	2385	-5.44	0.21	0.99	0.49	0.99	0.25	-5.48
Y6	2405	-4.78	-0.02	1.19	1.13	1.19	0.23	-5.03
Y7	2425	-3.77	-0.30	1.31	1.41	1.31	0.21	-4.27
Y8	2445	-2.86	-0.47	1.34	1.44	1.34	0.21	-3.54
Y9	2465	-2.22	-0.47	1.35	1.37	1.35	0.27	-2.97
Y10	2485	-1.92	-0.31	1.39	1.20	1.39	0.33	-2.56
Y11	2505	-1.92	-0.25	1.39	1.06	1.39	0.26	-2.43
Y12	2525	-1.77	-0.14	1.45	0.77	1.45	0.17	-2.08
Y13	2545	-1.59	-0.02	1.54	0.42	1.54	0.09	-1.70
Y14	2565	-1.29	0.03	1.64	0.19	1.64	0.05	-1.32
Z1	2301	-1.69	0.08	0.69	-0.01	0.69	0.08	-1.69
Z2	2321	-2.07	0.08	0.94	-0.04	0.94	0.08	-2.07
Z3	2341	-2.58	0.16	1.15	-0.04	1.15	0.16	-2.58
Z4	2361	-3.01	0.23	1.36	0.01	1.36	0.23	-3.01
Z5	2381	-3.21	0.27	1.50	0.07	1.50	0.27	-3.21
Z6	2401	-3.13	0.28	1.56	0.15	1.56	0.28	-3.14
Z7	2421	-2.83	0.24	1.55	0.21	1.55	0.26	-2.84
Z8	2441	-2.38	0.19	1.50	0.25	1.50	0.21	-2.41
Z9	2461	-1.90	0.13	1.45	0.36	1.45	0.19	-1.97
Z10	2481	-1.46	0.09	1.40	0.77	1.40	0.40	-1.77
Z11	2501	-1.26	0.05	1.44	1.88	1.44	1.38	-2.60
Z12	2521	-1.09	0.05	1.49	5.35	4.85	1.49	-5.90
Z13	25541	-0.98	0.04	1.56	23.86	23.39	1.56	-24.33
Z14	2561	-0.94	0.03	1.65	31.16	30.70	1.65	-31.61

Table 2.10.10-31 Primary Plus Secondary Stresses; 30-Foot Side Drop; $\phi = 90^\circ$; 1.20-Inch Outer Shell Thickness; Circumferential Location = 0°

Stress Points		Stresses (ksi)						
Location	Node	S _x	S _y	S _z	S _{xy}	S ₁	S ₂	S ₃
A1	327	2.06	0.01	7.54	0.36	7.54	2.12	-0.05
A2	302	0.72	-0.02	6.42	0.46	6.42	0.94	-0.25
A3	277	-0.43	0.02	5.39	1.03	5.39	0.84	-1.26
A4	252	-2.72	-0.10	3.35	1.43	3.35	0.53	-3.35
A5	227	-7.39	-2.22	-0.09	0.99	-0.09	-2.04	-7.57
A6	202	-4.55	-3.58	3.62	-3.68	3.62	-0.36	-7.77
A7	177	-46.95	-2.35	-18.78	-1.66	-2.29	-18.78	-47.01
B1	104	-10.58	-3.17	-3.36	-1.61	-2.83	-3.36	-10.92
B2	79	-6.38	-2.46	0.13	-0.61	0.13	-2.37	-6.47
B3	54	-3.80	-1.20	2.82	-1.02	2.82	-0.85	-4.15
B4	29	-1.11	-0.24	5.53	-0.67	5.53	0.12	-1.47
B5	4	2.21	0.04	8.26	-0.36	8.26	2.27	-0.02
C1	110	-10.94	-1.68	-4.57	-0.45	-1.66	-4.57	-10.96
C2	85	-8.09	-1.37	-1.76	0.84	-1.26	-1.76	-8.19
C3	60	-5.40	-0.71	0.91	0.98	0.91	-0.52	-5.60
C4	35	-2.47	-0.19	3.83	0.69	3.83	0.00	-2.67
C5	10	0.47	-0.03	6.73	0.37	6.73	0.66	-0.23
D1	335	-2.64	-5.04	2.30	-1.10	2.30	-2.21	-5.46
D2	310	-1.93	-3.18	2.20	-1.11	2.20	-1.28	-3.83
D3	285	-3.00	-2.29	1.48	-1.22	1.48	-1.37	-3.91
D4	260	-5.49	-2.04	-0.41	-1.56	-0.41	-1.44	-6.09
D5	235	-9.93	-2.39	-4.27	-1.32	-2.16	-4.27	-10.16
D6	210	-14.66	-2.67	-8.41	-0.53	-2.64	-8.41	-14.68
D7	185	-19.85	-2.71	-13.05	1.81	-2.52	-13.05	-20.04
E1	118	-4.40	1.18	-3.47	2.24	1.97	-3.47	-5.19
E2	93	-8.50	2.43	-3.36	1.39	2.60	-3.36	-8.67
E3	68	-8.16	0.95	-2.56	1.43	1.17	-2.56	-8.38
E4	43	-8.25	0.27	-1.43	0.90	0.36	-1.43	-8.34
E5	18	-7.60	0.09	0.31	0.57	0.31	0.13	-7.64
F1	143	-11.69	2.29	-4.86	4.07	3.39	-4.86	-12.78
F2	144	-10.56	7.92	-5.42	1.87	8.10	-5.42	-10.75

Table 2.10.10-31 Primary Plus Secondary Stresses; 30-Foot Side Drop; $\phi = 90^\circ$; 1.20-Inch Outer Shell Thickness; Circumferential Location = 0° (continued)

Stress Points		Stresses (ksi)						
Location	Node	S _x	S _y	S _z	S _{xy}	S ₁	S ₂	S ₃
F3	145	-8.46	4.02	-7.35	-0.38	4.03	-7.35	-8.47
F4	146	-7.71	1.98	-8.83	-0.61	2.01	-7.75	-8.83
F5	147	-7.98	0.48	-10.16	-0.60	0.52	-8.02	-10.16
F6	148	-8.29	-0.76	-11.33	-0.52	-0.72	-8.32	-11.33
F7	149	-8.56	-2.13	-12.57	-0.32	-2.12	-8.58	-12.57
F8	150	-8.75	-3.71	-13.93	-0.15	-3.71	-8.76	-13.93
G1	335	-2.64	-5.04	2.30	-1.10	2.30	-2.21	-5.46
G2	336	-2.09	-3.12	2.45	-0.40	2.45	-1.96	-3.26
G3	337	-1.51	-1.80	2.55	0.14	2.55	-1.45	-1.86
G4	338	-1.65	-0.02	2.66	0.16	2.66	-0.01	-1.67
G5	339	-1.12	2.85	3.18	-0.77	3.18	3.00	-1.26
G6	340	-2.46	-0.36	2.31	-0.82	2.31	-0.08	-2.74
H1	346	-14.37	0.98	-11.25	3.72	1.84	-11.25	-15.22
H2	347	-8.97	19.01	-6.54	2.47	19.23	-6.54	-9.18
H3	348	-9.47	19.52	-7.82	-2.63	19.76	-7.82	-9.71
H4	349	-8.50	10.58	-11.21	-3.30	11.14	-9.06	-11.21
H5	350	-8.60	2.42	-14.61	-2.28	2.87	-9.05	-14.61
I1	621	-0.23	6.65	2.45	-0.15	6.65	2.45	-0.23
I2	624	-0.10	7.80	2.49	0.06	7.80	2.49	-0.10
J1	635	-0.26	20.36	3.12	-0.33	20.36	3.12	-0.26
J2	638	-0.02	27.66	2.12	0.18	27.66	2.12	-0.02
K1	841	-0.23	18.68	-0.27	-0.09	18.68	-0.24	-0.27
K2	844	-0.07	22.10	2.48	0.12	22.10	2.48	-0.07
L1	855	-0.14	42.12	2.18	-0.21	42.12	2.18	-0.14
L2	858	0.04	45.96	1.54	0.14	45.96	1.54	0.04
M1	941	-0.23	27.19	-0.67	0.01	27.19	-0.23	-0.67
M2	944	-0.11	31.46	2.37	0.06	31.46	2.37	-0.11
N1	955	-0.16	59.71	2.04	-0.12	59.71	2.04	-0.16
N2	9.58	0.02	64.41	2.34	0.11	65.41	2.34	0.02
O1	1101	-0.24	31.14	-0.98	0.00	31.14	-0.24	-0.98
O2	1104	-0.15	35.76	2.01	0.01	35.76	2.01	-0.15

Table 2.10.10-31 Primary Plus Secondary Stresses; 30-Foot Side Drop; $\phi = 90^\circ$; 1.20-Inch Outer Shell Thickness; Circumferential Location = 0° (continued)

Stress Points		Stresses (ksi)						
Location	Node	S _x	S _y	S _z	S _{xy}	S ₁	S ₂	S ₃
P1	1115	-0.22	70.50	1.79	0.01	70.50	1.79	-0.22
P2	1118	0.02	77.67	3.29	-0.01	77.67	3.29	0.02
Q1	1261	-0.23	28.81	-0.36	0.02	28.81	-0.23	-0.36
Q2	1264	-0.08	33.16	2.56	-0.04	33.16	2.56	-0.08
R1	1275	-0.18	58.75	0.17	0.12	58.75	0.17	-0.18
R2	1278	0.01	65.39	3.49	-0.11	65.39	3.49	0.01
S1	1561	-0.22	8.19	1.88	0.23	8.20	1.88	-0.22
S2	1564	-0.17	12.54	3.74	0.08	12.54	3.74	-0.17
T1	1575	-0.24	30.33	1.07	0.19	30.33	1.07	-0.25
T2	1578	0.01	36.29	4.55	-0.16	36.29	4.55	0.01
U1	1841	-0.13	-0.35	2.40	-0.07	2.40	-0.11	-0.37
U2	1844	0.55	1.78	2.15	-0.36	2.15	1.87	0.45
V1	1852	4.57	8.47	-2.48	-8.39	15.13	-2.09	-2.48
V2	1856	0.41	16.50	-3.03	0.70	16.53	0.38	-3.03
W1	1969	-43.69	-28.15	-16.24	-4.59	-16.24	-26.90	-44.95
W2	1970	-32.16	-0.68	-7.68	-5.18	0.15	-7.68	-32.99
W3	1971	-18.61	3.03	-5.77	-5.41	4.31	-5.77	-19.89
W4	1972	-13.86	7.42	-6.25	-4.51	8.33	-6.25	-14.78
W5	1973	-11.59	10.46	-6.94	-3.49	11.00	-6.94	-12.13
W6	1974	-10.31	13.15	-7.55	-2.47	13.41	-7.55	-10.57
W7	1975	-9.63	16.25	-8.23	-1.33	16.32	-8.23	-9.70
W8	1976	-9.42	20.23	-8.83	-0.51	20.24	-8.83	-9.43
X1	2370	-22.05	-8.63	-5.78	-0.21	-5.78	-8.63	-22.05
X2	2390	-9.10	-5.13	-1.06	1.41	-1.06	-4.68	-9.55
X3	2410	-6.66	-2.62	0.05	2.53	0.05	-1.40	-7.87
X4	2430	-3.61	-2.69	0.56	2.06	0.56	-1.04	-5.26
X5	2450	-2.29	-1.91	0.80	1.29	0.80	-0.80	-3.41
X6	2470	-1.44	-1.34	0.91	0.59	0.91	-0.81	-1.98
X7	2490	-0.94	-0.72	1.05	0.14	1.05	-0.65	-1.01
X8	2510	-0.63	-0.44	1.19	-0.05	1.19	-0.43	-0.65

Table 2.10.10-31 Primary Plus Secondary Stresses; 30-Foot Side Drop; $\phi = 90^\circ$; 1.20-Inch Outer Shell Thickness; Circumferential Location = 0° (continued)

Stress Points		Stresses (ksi)						
Location	Node	S _x	S _y	S _z	S _{xy}	S ₁	S ₂	S ₃
X9	2530	-0.31	-0.20	1.38	-0.13	1.38	-0.12	-0.40
X10	2550	0.10	-0.07	1.64	-0.12	1.64	0.17	-0.13
X11	2570	1.40	-0.02	2.79	0.01	2.79	1.40	-0.02
Y1	2305	0.40	0.20	1.37	-0.25	1.37	0.57	0.03
Y2	2325	-1.94	0.08	0.73	-0.62	0.73	0.26	-2.11
Y3	2345	-3.92	0.09	0.43	-0.73	0.43	0.22	-4.04
Y4	2365	-5.62	0.12	0.22	-0.25	0.22	0.13	-5.64
Y5	2385	-6.17	0.00	0.21	0.54	0.21	0.04	-6.21
Y6	2405	-5.57	-0.28	0.33	1.16	0.33	-0.03	-5.82
Y7	2425	-4.54	-0.57	0.44	1.41	0.44	-0.12	-4.99
Y8	2445	-3.56	-0.73	0.55	1.40	0.55	-0.16	-4.13
Y9	2465	-2.82	-0.66	0.69	1.29	0.69	-0.07	-3.42
Y10	2485	-2.34	-0.42	0.96	1.11	0.96	0.09	-2.85
Y11	2505	-2.20	-0.31	1.12	1.02	1.12	0.14	-2.64
Y12	2525	-1.87	-0.15	1.36	0.76	1.36	0.14	-2.16
Y13	2545	-1.45	-0.02	1.65	0.41	1.65	0.09	-1.56
Y14	2565	-0.03	0.03	2.81	0.26	2.81	0.26	-0.26
Z1	2301	-1.18	0.09	1.19	-0.01	1.19	0.09	-1.18
Z2	2321	-1.98	0.11	1.02	-0.04	1.02	0.11	-1.98
Z3	2341	-2.81	0.22	0.92	-0.04	0.92	0.22	-2.81
Z4	2361	-3.51	0.32	0.86	0.01	0.86	0.32	-3.51
Z5	2381	-3.89	0.37	0.82	0.07	0.82	0.37	-3.89
Z6	2401	-3.91	0.38	0.78	0.15	0.78	0.38	-3.91
Z7	2421	-3.62	0.35	0.76	0.21	0.76	0.36	-3.63
Z8	2441	-3.10	0.29	0.78	0.25	0.78	0.31	-3.12
Z9	2461	-2.47	0.22	0.88	0.36	0.88	0.27	-2.52
Z10	2481	-1.80	0.16	1.07	0.77	1.07	0.42	-2.06
Z11	2501	-1.46	0.09	1.25	1.88	1.35	1.25	-2.72
Z12	2521	-1.14	0.07	1.45	5.35	4.85	1.45	-5.91
Z13	2541	-0.86	0.05	1.67	23.86	23.45	1.67	-24.27
Z14	2561	0.13	0.05	2.73	31.16	31.25	2.73	-31.07

Table 2.10.10-32 Primary Membrane (P_m) Stresses; 30-Foot Side Drop; $\phi = 90^\circ$; 1.20-Inch Outer Shell Thickness; Circumferential Location = 0°

Section	Node to Node	Stresses* (ksi)							
		S_x	S_y	S_z	S_{xy}	S_1	S_2	S_3	SI
A	177 – 327	-7.70	-1.71	1.90	-0.46	1.90	-1.67	-7.73	9.64
B	4 – 104	-6.52	-1.60	0.11	-0.89	0.11	-1.45	-6.68	6.79
C	10 – 110	-7.99	-0.43	-2.04	0.44	-0.41	-2.04	-8.02	7.61
D	185 – 335	-8.94	-0.19	-3.00	-0.36	-0.18	-3.00	-8.96	8.78
E	18 – 118	-9.09	1.24	-5.45	-0.07	1.24	-5.45	-9.09	10.32
F	143 – 150	-4.72	0.37	-9.86	-0.80	0.49	-4.85	-9.86	10.35
G	335 – 340	-5.06	-1.34	-2.30	0.85	-1.16	-2.30	-5.25	4.09
H	346 – 350	-6.40	6.28	-11.46	-0.50	6.30	-6.42	-11.46	17.76
I	621 – 624	-0.16	5.08	2.22	-0.06	5.08	2.22	-0.16	5.23
J	635 – 638	-0.14	14.95	2.52	-0.12	14.95	2.52	-0.14	15.08
K	841 – 844	-0.17	18.35	1.15	0.03	18.35	1.15	-0.17	18.51
L	855 – 858	-0.04	34.99	1.94	-0.02	34.99	1.94	-0.04	35.03
M	941 – 944	-0.19	27.29	0.90	0.03	27.29	0.90	-0.19	27.48
N	955 – 958	-0.07	53.54	2.29	0.01	53.54	2.29	-0.07	53.61
O	1101 – 1104	-0.21	31.42	0.56	0.00	31.42	0.56	-0.21	31.63
P	1115 – 1118	-0.10	65.09	2.67	0.00	65.09	2.67	-0.10	65.18
Q	1261 – 1264	-0.17	28.95	1.12	-0.01	28.95	1.12	-0.17	29.12
R	1275 – 1278	-0.09	53.03	2.05	0.00	53.03	2.05	-0.09	53.13
S	1561 – 1564	-0.17	8.21	2.45	0.12	8.22	2.45	-0.17	8.39
T	1575 – 1578	-0.14	24.25	2.83	0.06	24.25	2.83	-0.14	24.39
U	1841 – 1846	0.51	0.49	2.13	-0.18	2.13	0.68	0.32	1.81
V	1852 – 1856	4.77	14.30	-1.86	-2.58	14.95	4.11	-1.86	16.81
W	1969 – 1976	20.74	3.86	-9.26	-3.37	4.32	-9.26	-21.20	25.51
X	2370 – 2570	-3.97	-1.82	0.18	1.06	0.18	-1.38	-4.40	4.59
Y	2305 – 2565	-3.07	-0.06	1.14	0.53	1.14	0.03	-3.16	4.29
Z	2301 – 2561	-2.26	0.16	1.36	2.22	1.48	1.36	-3.58	5.06

* Stresses are taken at 0 degrees (under the load) at each section.

Table 2.10.10-33 Primary Membrane Plus Primary Bending ($P_m + P_b$) Stresses; 30-Foot Side Drop; $\phi = 90^\circ$; 1.20-Inch Outer Shell Thickness; Circumferential Location = 0°

Section	Node to Node	Stresses* (ksi)							
		S_x	S_y	S_z	S_{xy}	S_1	S_2	S_3	SI
A	177 – 327	-16.88	-3.68	0.56	-3.01	0.56	-3.03	-17.54	18.10
B	4 – 104	-10.00	-3.37	-3.11	-1.31	-3.11	-3.12	-10.25	7.14
C	10 – 110	-11.24	-0.89	-5.07	0.01	-0.89	-5.07	-11.24	10.36
D	185 – 335	-13.80	-1.54	-5.90	-0.01	-1.54	-5.90	-13.80	12.26
E	18 – 118	-8.66	2.96	-6.08	-0.84	3.03	-6.08	-8.73	11.75
F	143 – 150	-1.94	7.18	-3.59	-0.80	7.25	-2.01	-3.59	10.85
G	335 – 340	-9.47	-4.30	-4.96	0.85	-4.16	-4.96	-9.61	5.45
H	346 – 350	-5.16	16.66	-5.20	-0.50	16.67	-5.17	-5.20	21.87
I	621 – 624	-0.11	6.23	2.33	-0.06	6.23	2.33	-0.11	6.34
J	635 – 638	-0.03	19.66	2.20	-0.12	19.66	2.20	-0.03	19.69
K	841 – 844	-0.07	19.82	2.32	0.03	19.82	2.32	-0.07	19.88
L	855 – 858	0.04	36.61	1.34	-0.02	36.61	1.34	0.04	36.57
M	941 – 944	-0.11	29.12	2.15	0.03	29.12	2.15	-0.11	29.23
N	955 – 958	0.02	56.00	2.10	0.01	56.00	2.10	0.02	55.98
O	1101 – 1104	-0.15	33.42	1.80	0.00	33.42	1.80	-0.15	33.57
P	1115 – 1118	0.02	68.25	3.06	0.00	68.25	3.06	0.02	68.23
Q	1261 – 1264	-0.08	30.88	2.38	-0.01	30.88	2.38	-0.08	30.96
R	1275 – 1278	0.03	55.93	3.42	0.00	55.93	3.42	0.03	55.91
S	1561 – 1564	-0.15	9.98	3.22	0.12	9.98	3.22	-0.15	10.13
T	1575 – 1578	0.01	28.32	4.68	0.06	28.32	4.68	0.01	28.31
U	1841 – 1846	-0.15	0.09	2.90	-0.18	2.90	0.19	-0.24	3.15
V	1852 – 1856	10.17	18.66	1.89	-2.58	19.39	9.45	1.89	17.50
W	1969 – 1976	-42.95	-14.16	-10.81	-3.37	-10.81	-13.77	-43.34	32.53
X	2370 – 2570	-11.33	-4.07	-1.38	1.72	-1.38	-3.68	-11.72	10.34
Y	2305 – 2565	-2.48	-0.39	1.60	1.55	1.60	0.43	-3.30	4.90
Z	2301 – 2561	-1.60	0.12	1.68	8.10	7.40	1.68	-8.88	16.29

* Stresses are taken at 0 degrees (under the load) at each section.

Table 2.10.10-34 Primary Membrane (P_m) Stresses; 30-Foot Side Drop; $\phi = 90^\circ$; 1.20-Inch Outer Shell Thickness; Circumferential Location = 90°

Section	Node to Node	Stresses* (ksi)									
		S_x	S_y	S_z	S_{xy}	S_{yz}	S_{xz}	S_1	S_2	S_3	SI
A	177 – 327	1.27	-0.03	-4.99	0.02	-2.03	-0.91	1.50	0.56	-5.81	7.32
B	4 – 104	1.13	-0.01	-4.30	0.04	1.07	-0.94	1.30	0.21	-4.69	5.99
C	10 – 110	0.76	0.00	-3.08	0.07	0.23	-2.17	1.74	0.01	-4.07	5.81
D	185 – 335	0.76	0.42	-3.12	0.09	-1.46	-2.31	2.17	0.43	-4.53	6.70
E	18 – 118	0.25	0.18	-1.51	0.05	-1.33	-2.17	2.08	0.15	-3.31	5.39
F	143 – 150	-0.06	0.11	-0.92	0.03	-3.30	0.23	2.94	-0.05	-3.76	6.70
G	335 – 340	0.90	0.62	-2.01	0.18	-1.63	-2.46	2.79	0.54	-3.82	6.62
H	346 – 350	-0.03	0.06	-0.41	0.01	-11.67	-5.75	12.83	-0.02	-13.19	26.02
I	621 – 624	-0.08	0.38	0.35	-0.09	-5.88	-0.06	6.24	-0.07	-5.51	11.75
J	635 – 638	0.00	0.30	0.03	0.00	-15.87	-0.06	16.03	0.00	-15.70	31.73
K	841 – 844	-0.01	-0.08	0.55	0.03	-3.80	-0.01	4.05	-0.01	-3.58	7.63
L	855 – 858	-0.01	0.23	-0.03	0.00	-12.09	-0.03	12.19	-0.01	-11.99	24.18
M	941 – 944	-0.01	0.05	0.54	0.00	-1.33	0.01	1.65	-0.01	-1.06	2.71
N	955 – 958	0.00	0.10	-0.01	0.00	-8.08	-0.01	8.12	0.00	-8.03	16.16
O	1101 – 1104	-0.01	0.06	0.54	0.00	-0.22	0.01	0.63	-0.01	-0.03	0.66
P	1115 – 1118	0.00	0.13	0.02	0.00	0.20	-0.01	0.28	0.00	-0.13	0.42
Q	1261 – 1264	-0.01	0.05	0.54	0.00	1.83	0.00	2.15	-0.01	-1.56	3.70
R	1275 – 1278	0.02	-0.28	0.07	-0.01	8.05	-0.01	7.95	0.02	-8.16	16.11
S	1561 – 1564	-0.04	-0.20	0.26	0.03	6.00	-0.06	6.04	-0.04	-5.98	12.02
T	1575 – 1578	0.01	-2.23	0.26	0.03	15.08	0.00	14.14	0.01	-16.11	30.26
U	1841 – 1846	-0.99	0.32	-1.39	0.10	2.40	0.24	2.03	-0.99	-3.10	5.13
V	1852 – 1856	-0.30	-2.02	0.51	0.15	11.13	-5.20	11.70	-0.50	-13.01	24.71
W	1969 – 1976	3.42	-1.82	-1.43	0.61	3.63	-0.54	3.50	2.01	-5.34	8.84
X	2370 – 2570	1.47	0.99	-1.44	-0.59	0.31	-0.61	2.00	0.60	-1.58	3.58
Y	2305 – 2565	1.32	0.21	-2.02	-0.24	-0.05	-0.33	1.40	0.17	-2.06	3.45
Z	2301 – 2561	1.36	0.16	-2.25	0.00	-2.45	0.00	1.69	1.36	-3.78	5.47

Table 2.10.10-35 Primary Membrane Plus Primary Bending ($P_m + P_b$) Stresses; 30-Foot Side Drop; $\phi = 90^\circ$; 1.20-Inch Outer Shell Thickness; Circumferential Location = 90°

Section	Node to Node	Stresses* (ksi)									
		S_x	S_y	S_z	S_{xy}	S_{yz}	S_{xz}	S_1	S_2	S_3	SI
A	177 – 327	1.36	-0.05	-4.68	0.01	-1.81	-1.81	2.01	0.34	-5.72	7.73
B	4 – 104	1.56	-0.03	-4.19	0.00	1.14	-1.73	2.08	0.17	-4.92	7.00
C	10 – 110	0.79	-0.01	-3.02	0.06	0.38	-3.22	2.63	0.01	-4.89	7.52
D	185 – 335	1.41	1.07	-2.39	0.32	-2.90	-4.10	5.01	0.88	-5.81	10.82
E	18 – 118	0.56	0.41	-1.48	0.11	-2.93	-2.24	3.38	0.40	-4.28	7.66
F	143 – 150	0.01	0.47	-1.63	0.03	-3.30	0.23	2.89	0.02	-4.06	6.95
G	335 – 340	2.47	1.30	-2.16	0.18	-1.63	-2.46	3.83	1.43	-3.64	7.46
H	346 – 350	0.06	0.40	-0.45	0.01	-11.67	-5.75	12.96	0.12	-13.07	26.03
I	621 – 624	-0.07	0.88	0.78	-0.09	-5.88	-0.06	6.70	-0.07	-5.05	11.75
J	635 – 638	0.00	0.53	0.18	0.00	-15.87	-0.06	16.22	0.00	-15.51	31.73
K	841 – 844	-0.05	0.12	1.16	0.03	-3.80	-0.01	4.48	-0.05	-3.20	7.68
L	855 – 858	-0.01	0.08	-0.45	0.00	-12.09	-0.03	11.91	-0.01	-12.28	24.19
M	941 – 944	-0.05	0.24	1.25	0.00	-1.33	0.01	2.17	-0.05	-0.68	2.85
N	955 – 958	0.00	0.18	0.23	0.00	-8.08	-0.01	8.28	0.00	-7.88	16.16
O	1101 – 1104	-0.05	0.24	1.24	0.00	-0.22	0.01	1.28	0.20	-0.05	1.33
P	1115 – 1118	0.00	0.06	-0.29	0.00	0.20	-0.01	0.15	0.00	-0.38	0.54
Q	1261 – 1264	-0.05	0.24	1.25	0.00	1.83	0.00	2.65	-0.05	-1.16	3.81
R	1275 – 1278	0.02	0.11	1.33	-0.01	8.05	-0.01	8.80	0.02	-7.35	16.16
S	1561 – 1564	-0.03	-0.38	0.05	0.03	6.00	-0.06	5.84	-0.03	-6.18	12.02
T	1575 – 1578	0.01	-2.93	-0.46	0.03	15.08	0.00	13.43	0.01	-16.82	30.26
U	1841 – 1846	-0.11	0.72	-1.31	0.10	2.40	0.24	2.33	-0.12	-2.91	5.25
V	1852 – 1856	-0.03	-1.96	0.67	0.15	11.13	-5.20	11.83	-0.26	-12.89	24.72
W	1969 – 1976	9.68	2.99	-0.85	0.61	3.63	-0.54	9.74	5.17	-3.09	12.83
X	2370 – 2570	3.65	2.27	-2.21	-0.89	0.89	-1.63	4.59	1.84	-2.72	7.31
Y	2305 – 2565	1.21	0.23	-2.54	0.06	0.00	-0.55	1.30	0.22	-2.62	3.91
Z	2301 – 2561	1.67	0.12	-1.61	0.00	-9.29	0.00	8.58	1.67	-10.08	18.66

Table 2.10.10-36 Primary Membrane (P_m) Stresses; 30-Foot Side Drop; $\phi = 90^\circ$; 1.20-Inch Outer Shell Thickness; Circumferential Location = 180°

Section	Node to Node	Stresses* (ksi)									
		S_x	S_y	S_z	S_{xy}	S_{yz}	S_{xz}	S_1	S_2	S_3	SI
A	177 – 327	-2.36	1.64	0.62	0.45	0.00	0.00	1.69	0.62	-2.41	4.10
B	4 – 104	-2.77	1.44	2.05	0.76	0.00	0.00	2.05	1.58	-2.91	4.96
C	10 – 110	-1.99	0.44	2.92	-0.68	0.00	0.00	2.92	0.62	-2.16	5.09
D	185 – 335	-1.86	0.13	3.49	0.27	0.00	0.00	3.49	0.17	-1.90	5.39
E	18 – 118	-0.99	-1.22	3.41	-0.43	0.00	0.00	3.41	-0.66	-1.55	4.96
F	143 – 150	-0.70	-1.20	4.44	0.21	0.00	0.00	4.44	-0.63	-1.27	5.71
G	335 – 340	-4.22	-0.41	1.36	-0.02	0.00	0.00	1.36	-0.41	-4.22	5.58
H	346 – 350	-5.62	-7.07	2.37	-2.99	0.00	0.00	2.37	-3.27	-9.42	11.79
I	621 – 624	-0.01	-5.43	-0.64	0.13	0.00	0.00	-0.01	-0.64	-5.43	5.42
J	635 – 638	0.15	-16.16	-3.10	0.11	0.00	0.00	0.15	-3.10	-16.16	16.32
K	841 – 844	-0.07	-18.02	-0.15	0.03	0.00	0.00	-0.07	-0.15	-18.02	17.95
L	855 – 858	0.06	-35.26	-1.88	0.03	0.00	0.00	0.06	-1.88	-35.26	35.32
M	941 – 944	-0.05	-27.22	0.12	-0.03	0.00	0.00	0.12	-0.05	-27.22	27.34
N	955 – 958	0.07	-53.61	-2.26	0.00	0.00	0.00	0.07	-2.26	-53.61	53.68
O	1101 – 1104	-0.02	-31.36	0.46	0.00	0.00	0.00	0.46	-0.02	-31.36	31.82
P	1115 – 1118	0.09	-65.21	-2.71	0.00	0.00	0.00	0.09	-2.71	-65.21	65.30
Q	1261 – 1264	-0.06	-28.88	-0.10	0.00	0.00	0.00	-0.06	-0.10	-28.88	28.81
R	1275 – 1278	0.06	-52.34	-2.20	0.02	0.00	0.00	0.06	-2.20	-52.34	52.40
S	1561 – 1564	0.00	-7.47	-0.83	-0.17	0.00	0.00	0.00	-0.83	-7.47	7.47
T	1575 – 1578	0.11	-19.27	-3.16	-0.09	0.00	0.00	0.11	-3.16	-19.27	19.39
U	1841 – 1846	0.98	-1.06	2.15	0.05	0.00	0.00	2.15	0.98	-1.06	3.22
V	1852 – 1856	-4.17	-9.23	0.78	2.62	0.00	0.00	0.78	-3.06	-10.34	11.12
W	1969 – 1976	-2.02	-0.11	0.97	0.07	0.00	0.00	0.97	-0.11	-2.02	3.00
X	2370 – 2570	-1.53	-1.48	0.89	0.20	0.00	0.00	0.89	-1.30	-1.71	2.60
Y	2305 – 2565	-1.52	0.04	1.21	-0.07	0.00	0.00	1.21	0.04	-1.52	2.73
Z	2301 – 2561	-2.26	0.16	1.36	-2.22	0.00	0.00	1.48	1.36	-3.58	5.06

Table 2.10.10-37 Primary Membrane Plus Primary Bending ($P_m + P_b$) Stresses; 30-Foot Side Drop; $\phi = 90^\circ$; 1.20-Inch Outer Shell Thickness; Circumferential Location = 180°

Section	Node to Node	Stresses* (ksi)									
		S_x	S_y	S_z	S_{xy}	S_{yz}	S_{xz}	S_1	S_2	S_3	SI
A	177 – 327	-10.98	-0.42	-0.59	-2.11	0.00	0.00	-0.02	-0.59	-11.39	11.37
B	4 – 104	-5.81	-0.09	-0.01	0.78	0.00	0.00	0.01	-0.01	-5.91	5.92
C	10 – 110	-3.97	0.010	1.26	-0.62	0.00	0.00	1.26	0.11	-4.07	5.33
D	185 – 335	-6.48	-1.22	0.47	0.03	0.00	0.00	0.47	-1.21	-6.48	6.96
E	18 – 118	-2.52	-2.83	3.24	-0.77	0.00	0.00	3.24	-1.88	-3.46	6.70
F	143 – 150	0.81	-4.81	4.46	0.21	0.00	0.00	4.46	0.82	-4.82	9.27
G	335 – 340	-7.62	-0.86	1.22	-0.02	0.00	0.00	1.22	-0.86	-7.62	8.84
H	346 – 350	-12.20	-16.96	-2.69	-2.99	0.00	0.00	-2.69	-10.76	-18.40	15.71
I	621 – 624	0.03	-6.68	-1.18	0.13	0.00	0.00	0.04	-1.18	-6.68	6.72
J	635 – 638	0.00	-19.78	-4.04	0.11	0.00	0.00	0.00	-4.04	-19.78	19.79
K	841 – 844	-0.07	-18.98	0.27	0.03	0.00	0.00	0.27	-0.07	-18.98	19.25
L	855 – 858	-0.05	-37.16	-2.24	0.03	0.00	0.00	-0.05	-2.24	-37.16	37.11
M	941 – 944	-0.02	-28.54	0.67	-0.03	0.00	0.00	0.67	-0.02	-28.54	29.21
N	955 – 958	-0.02	-56.22	-2.56	0.00	0.00	0.00	-0.02	-2.56	-56.22	56.19
O	1101 – 1104	0.02	-32.86	1.01	0.00	0.00	0.00	1.01	0.02	-32.86	33.88
P	1115 – 1118	-0.01	-68.24	-2.47	0.00	0.00	0.00	-0.01	-2.47	-68.24	68.23
Q	1261 – 1264	-0.05	-30.30	0.44	0.00	0.00	0.00	0.44	-0.05	-30.30	30.74
R	1275 – 1278	0.01	-54.47	-1.05	0.02	0.00	0.00	0.01	-1.05	-54.47	54.48
S	1561 – 1564	0.07	-8.63	-0.90	-0.17	0.00	0.00	0.08	-0.90	-8.63	8.71
T	1575 – 1578	-0.01	-22.01	-3.35	-0.09	0.00	0.00	-0.01	-3.35	-22.01	22.00
U	1841 – 1846	0.02	-3.55	1.48	0.05	0.00	0.00	1.48	0.02	-3.55	5.03
V	1852 – 1856	-8.45	-16.56	-3.18	2.62	0.00	0.00	-3.18	-7.67	-17.33	14.15
W	1969 – 1976	-6.29	-1.31	0.67	0.07	0.00	0.00	0.67	-1.30	-6.29	6.96
X	2370 – 2570	-4.58	-3.65	0.14	0.63	0.00	0.00	0.14	-3.33	-4.90	5.04
Y	2305 – 2565	-2.72	0.03	0.92	-0.17	0.00	0.00	0.92	0.04	-2.73	3.65
Z	2301 – 2561	-1.60	0.12	1.68	-8.10	0.00	0.00	7.40	1.68	-8.88	16.28

Table 2.10.10-38 Primary Membrane (P_m) and Primary Membrane Plus Primary Bending ($P_m + P_b$) Stress Qualification; 30-Foot Side Drop; $\phi = 90^\circ$; 1.20-Inch Outer Shell Thickness; Circumferential Location = 0°

Section	Node to Node	Max. Temp. (°F)	P _m Stresses (ksi)			P _m + P _b Stresses (ksi)		
			Allow. * 0.7 S _u	Calc.	MS	Allow. * 1.0 S _u	Calc.	MS
A	177 – 327	222	48.93	9.64	+Large	69.90	18.10	+2.86
B	4 – 104	215	49.18	6.79	+Large	70.25	7.14	+Large
C	10 – 110	212	49.28	7.61	+Large	70.40	10.35	+Large
D	185 – 335	221	48.96	8.78	+Large	69.95	12.26	+Large
E	18 – 118	208	49.42	10.32	+3.79	70.60	11.75	+Large
F	143 – 150	209	49.38	10.35	+3.77	70.55	10.85	+Large
G	335 – 340	221	48.96	4.09	+Large	69.95	5.45	+Large
H	346 – 350	212	49.28	17.76	+1.77	70.40	21.87	+2.22
I	621 – 624	222	48.93	5.23	+Large	69.90	6.34	+Large
J	635 – 638	199	49.73	15.08	+2.30	71.04	19.69	+2.61
K	841 – 844	232	68.49	18.51	+2.70	97.84	19.88	+3.92
L	855 – 858	204	69.50	35.03	+0.98	99.29	36.57	+1.72
M	941 – 944	247	67.94	27.48	+1.47	97.06	29.23	+2.32
N	955 – 958	211	69.25	53.61	+0.29	98.93	55.98	+0.77
O	1101 – 1104	255	67.65	31.63	+1.14	96.64	33.57	+1.88
P	1115 – 1118	216	69.07	65.18	+0.06	98.67	68.23	+0.45
Q	1261 – 1264	251	67.79	29.12	+0.30	96.85	30.96	+2.13
R	1275 – 1278	216	69.07	53.13	+0.30	98.67	55.91	+0.76
S	1561 – 1564	217	49.10	8.39	+Large	70.15	1013	+Large
T	1575 – 1578	197	49.78	24.39	+1.04	71.12	28.31	+1.51
U	1841 – 1846	212	49.28	1.81	+Large	70.40	3.15	+Large
V	1852 – 1856	205	49.53	16.81	+1.95	70.75	17.50	+3.04
W	1969 – 1976	198	49.76	25.51	+0.95	71.08	32.53	+1.19
X	2370 – 2570	201	49.66	4.59	+Large	70.95	10.34	+Large
Y	2305 – 2565	205	49.53	4.29	+Large	70.75	4.90	+Large
Z	2301 – 2561	204	49.56	5.06	+Large	70.80	16.29	+3.35

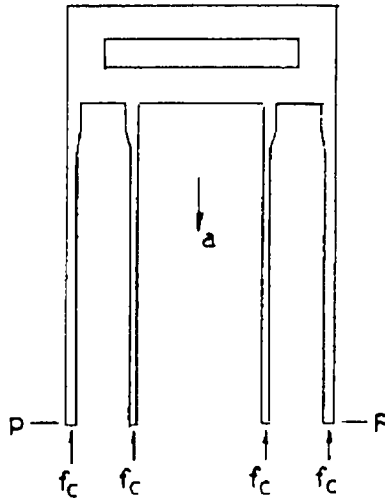
* Allowable stresses for sections “K” through “R” are taken from Type XM-19 stainless steel; all others are from Type 304 stainless steel.

2.10.11 Hand Calculation for the 30-Foot Drop Accident Conditions

2.10.11.1 Top End Drop

The hand-calculation method is used to evaluate the stresses for a 30-foot top end drop condition. Only the stress at the midsection of the cask is evaluated. The hand-calculated stress results can be used to verify the accuracy of the finite element calculations and vice versa.

The NAC-LWT cask is considered as a hollow, circular cylinder, which contains the inner, lead and outer shells, and is subjected to a 30-foot top end impact as shown in Figure 2.10.11-1. A free body diagram (shown below) is provided for the portion of the cask above section “P-P,” which is located 100.5 inches from the cask bottom.



The axial (compressive) stresses developed in the cask at section “P-P” are calculated by using the following formula:

$$f_c = \frac{W}{A}$$

where:

W = cask weight above sections “O-O” and “P-P,” but not including the weight of the lead shell (Figure 2.10.11-1)

= 5,440 lbs

A = cross-sectional areas of the stainless steel inner and outer shells

= $\pi(14.30752 - 13.18752 + 7.43752 - 6.68752)$

= 130.03 in²

W is obtained from the following calculations. Table 2.10.11-1 presents the geometric dimensions of the cask.

$$W = W_9 + W_8 + W_7 + W'_6 + W'_4 \text{ (} W'_4 \text{ through } W_9 \text{ are the weights of components 4 through 9 as shown in Figure 2.10.2-5.)}$$

where:

$$\begin{aligned} W_9 &= \pi \times 10.375^2 \times 3 \times 0.41 \\ &= 416 \text{ lbs} \end{aligned}$$

$$\begin{aligned} W_8 + W_7 &= (\pi \times 14.3075^2 \times 10.5 - \pi \times 10.375^2 \times 3)(0.288) \\ &= 1,653 \text{ lbs} \end{aligned}$$

$$\begin{aligned} W'_6 &= \pi (14.307^2 - 13.1875^2)(100.5 - 10.5)(0.288) \\ &= 2,508 \text{ lbs} \end{aligned}$$

$$\begin{aligned} W'_4 &= \pi (7.4375^2 - 6.6875^2)(100.5 - 10.5)(0.288) \\ &= 863 \text{ lbs} \end{aligned}$$

The compressive stress at the midpoint (\pm) of the cask resulting from its mass is:

$$f_c = \frac{-5440}{130.03} = -41.84 \text{ psi}$$

This compressive stress results from a 1 g cask weight load. To account for a 30-foot top end drop condition, multiply this result by 76.8 g. The 76.8 g is derived from the multiplication of 60 g (Table 2.6.7-34) by the factor 48,000/37,519, where 48,000 lbs is the cask body design weight and 37,519 lbs is the model weight.

$$f_c = 76.8 (-41.84) = -3,213 \text{ psi}$$

The compressive stresses¹ at sections “O-O” and “P-P” calculated by the finite element method are -3,260 psi and -2,990 psi, respectively, with an average of -3,125 psi. The difference between the hand calculation and the finite element stresses is 3 percent, which compares favorably as expected.

2.10.11.2 Side Drop

The hand-calculation method is used to evaluate the stresses for the 30-foot side drop condition. The hand-calculated stress results can be used to verify the accuracy of the finite element

¹ Table 2.10.10-4 documents the compressive stresses, SY, for sections “O-O” and “P-P.”

calculations and vice versa. Because of the limitation of the hand-calculation method, only the stress results at the most critical region (the central portion of the cask outer shell) are evaluated.

The cask structure is considered as a hollow, circular, cross-sectional beam that is simply supported at each end of the cask centerline and is subject to internal pressure and impact and inertial loads. The classical beam theory method is used to calculate the bending stress resulting from impact and inertial loads for a 30-foot side drop condition:

$$\sigma_b = \frac{M_c}{I_{eff}}$$

where:

σ_b = bending stress

M = bending moment in the cask

C = radial distance between the cask centerline and the selected point (location) in the cask

I_{eff} = effective moment of inertia of the cask

The geometric dimensions of the cask are:

Inner Shell (I.S.)	r_i	=	inner radius = 6.6875 inches
	r_o	=	outer radius = 7.4375 inches
	E_s	=	Young's modulus (stainless steel)
		=	27.3×10^6 psi at 250°F
Lead	r_i	=	inner radius = 7.4375 in
	r_o	=	outer radius = 13.133 in
	E_L	=	Young's modulus (lead)
		=	2.0×10^6 psi at 250°F
Outer Shell (O.S.)	r_i	=	inner radius = 13.188 in
	r_o	=	outer radius = 14.387 in
	E_s	=	Young's modulus (stainless steel)
		=	27.3×10^6 psi at 250°F

The effective bending rigidity, $(EI)_{eff}$, of the cask is:

$$(EI)_{eff} = (EI)_{I.S.} + (EI)_{Lead} + (EI)_{O.S.}$$

$$\begin{aligned} & \frac{\pi}{4}[(7.4375^4 - 6.6875^4)(27.3 \times 10^6) \\ & + (13.1334 - 7.43754)(2.0 \times 10^6) \end{aligned}$$

$$+ (14.3874 - 13.1884)(27.3 \times 10^6]$$

$$= 3.347 \times 10^{11} \text{ lb-in}^2$$

The effective moment of inertia for the cask is:

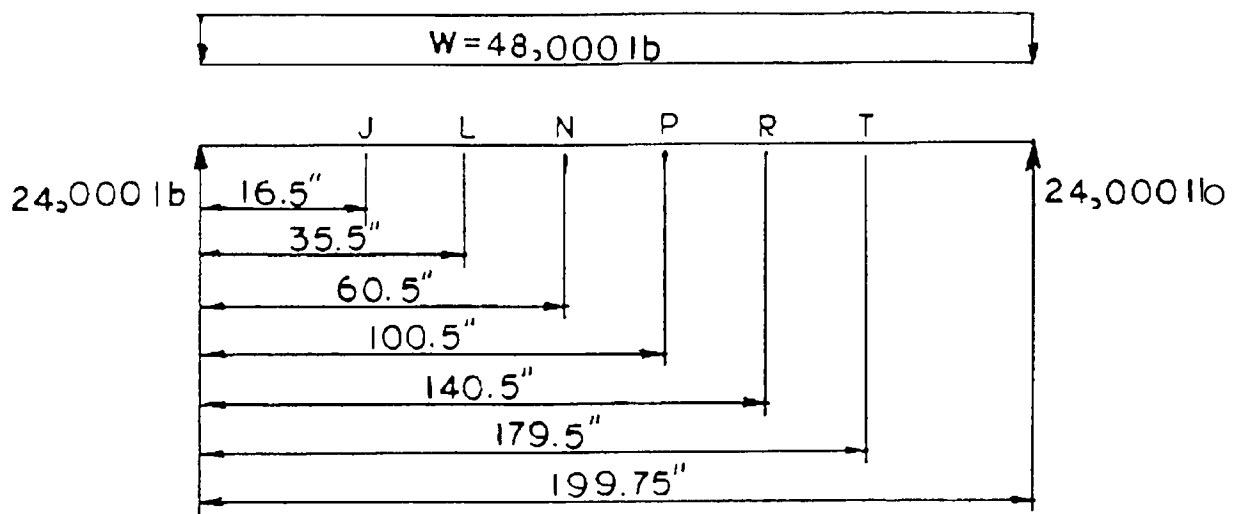
$$I_{\text{eff}} = \frac{(EI)_{\text{eff}}}{E_s} = \frac{3.347 \times 10^{11}}{27.3 \times 10^6} = 12,259 \text{ in}^4$$

The bending moments induced in the cask as a result of the 30-foot side drop condition are calculated by considering the following:

- The cask weight without content (48,000 lbs), which is assumed to be uniformly distributed over the entire cask length of 199.75 inches;
- The content weight (4,000 lbs), which is uniformly distributed over the entire cask cavity length of 178 inches; and
- Impact loads (totaling 52,000 lbs), which are assumed to be uniformly distributed over the 12 inches at each end of the cask.

2.10.11.2.1 Case A

The bending moments at locations “J,” “L,” “N,” “P,” “R” and “T” in the cask are a result of the cask weight due to a 1 g load.¹



$$w = \text{cask weight/total cask length} = \frac{48,000}{199.75} = 240.30 \text{ lb/in}$$

¹ The g load factor for the 30-foot side drop condition is 49.7 g.

$$M_J = 24,000 (16.5) - \frac{w(16.5^2)}{2} = 363,289 \text{ in-lb}$$

$$M_L = 24,000 (33.5) - \frac{w(33.5^2)}{2} = 669,161 \text{ in-lb}$$

$$M_N = 24,000 (60.5) - \frac{w(60.5^2)}{2} = 1,012,220 \text{ in-lb}$$

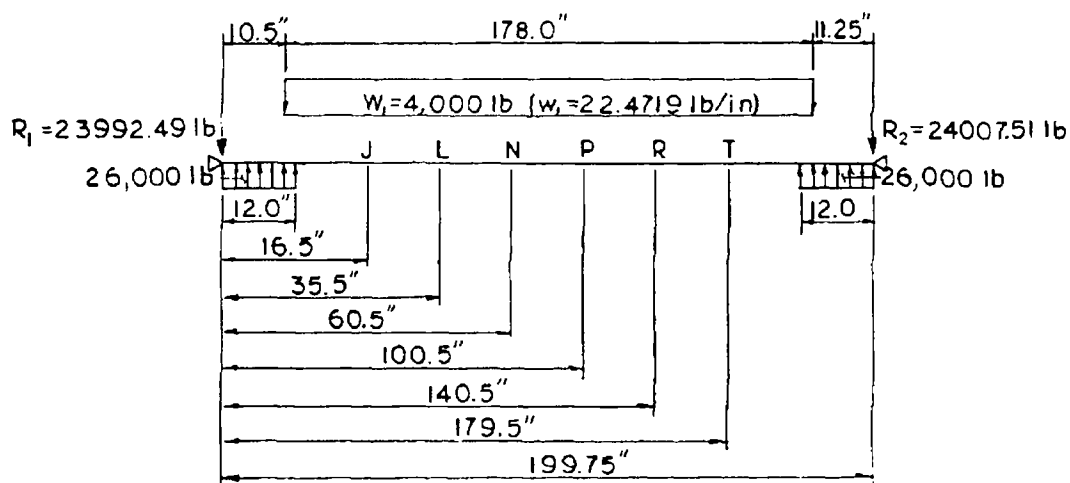
$$M_P = 24,000 (100.5) - \frac{w}{2} (100.5^2) = 1,198,453 \text{ in-lb}$$

$$M_R = 24,000 (140.5) - \frac{w(140.5^2)}{2} = 1,000,205 \text{ in-lb}$$

$$M_T = 24,000 (179.5) - \frac{w(179.5^2)}{2} = 436,731 \text{ in-lb}$$

2.10.11.2.2 Case B

The bending moments at locations “J,” “L,” “N,” “P,” “R” and “T” are a result of the impact and content load due to a 1 g load.¹



$$w_1 = \text{content weight/cask cavity length} = \frac{4000}{178} = 22,472 \text{ lb/in}$$

R_1 = reaction force at cask left end resulting from the impact and content loads

¹ The g load factor for the 30-foot side drop condition is 49.7 g.

$$M_J = 26,000 (10.5) - 23,992.49 (16.5) - \left(\frac{22.472}{2} \right) (6^2) = -123,281 \text{ in-lb}$$

$$M_L = 26,000 (29.5) - 23,992.49 (35.5) - \frac{w_1}{2} (25^2) = -91,756 \text{ in-lb}$$

$$M_N = 26,000 (54.5) - R_1 (60.5) - \frac{w_1}{2} (50^2) = -62,636 \text{ in-lb}$$

$$M_P = 26,000 (94.5) - R_1 (100.5) - \frac{w_1}{2} (90^2) = -45,256 \text{ in-lb}$$

$$M_R = 26,000 (134.5) - R_1 (140.5) - \frac{w_1}{2} (130^2) = -63,832 \text{ in-lb}$$

$$M_T = 26,000 (173.5) - R_1 (179.5) - \frac{w_1}{2} (169^2) = -116,562 \text{ in-lb}$$

The bending stresses in the cask are calculated by adding the bending moments resulting from cases A and B and by using the classical beam theory method:

$$\sigma_b = \frac{M_J C_i}{I_{\text{eff}}}$$

where:

M_J = summation of bending moments at location “J” as a result of Case A and Case B and so forth

C_i = radial distance between the cask centerline and the selected point

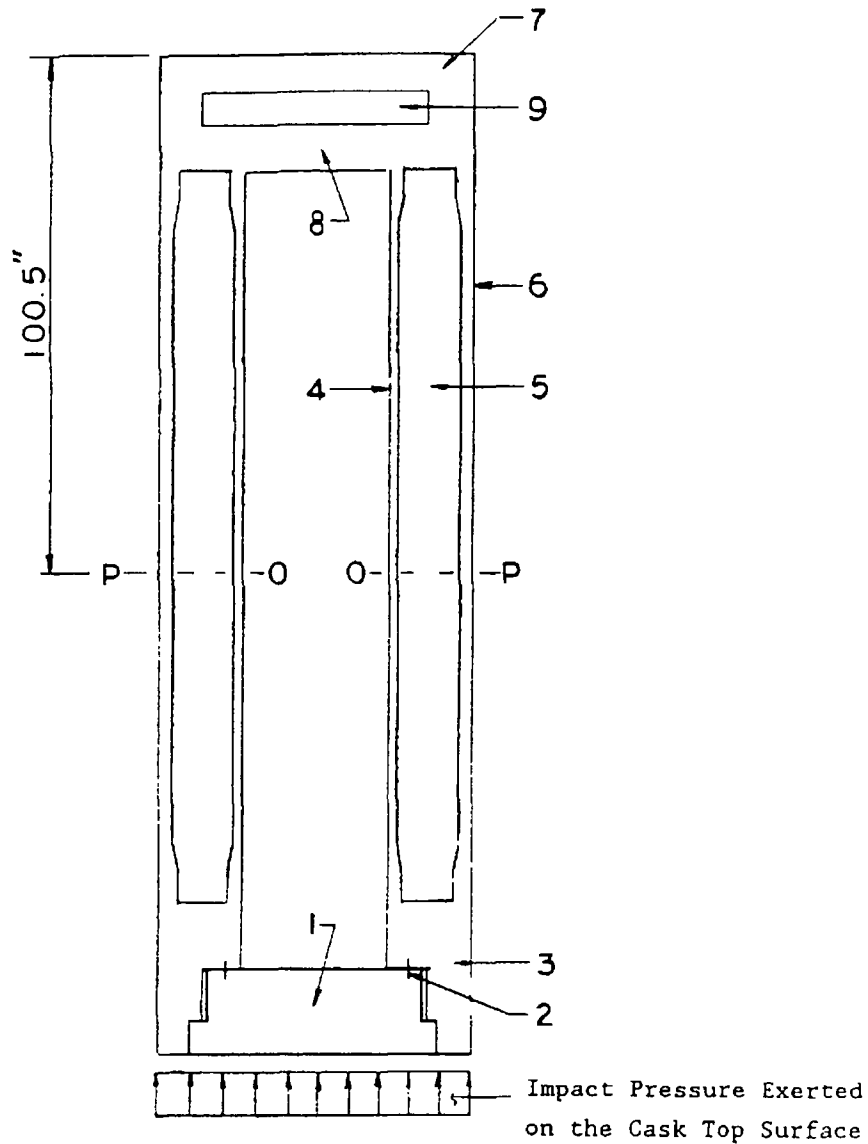
$I_{\text{eff}} = 12,259 \text{ in}^4$

Table 2.10.11-2 gives the bending stresses in the cask, at different locations in the inner and outer shell regions, obtained by the above-mentioned hand-calculation method. Table 2.10.11-2 also provides the comparison of the hand-calculated and finite element stress results. At the midsection of the outer shell (location “P2” in Table 2.10.11-2), the bending stresses are 67,236 psi by the hand-calculation method and 68,230 psi by the finite element method. The difference in the stress results is less than 1.5 percent between these two methods. The stress comparison between these two methods is also provided for other locations, denoted as “K” through “O” and “Q” through “R”. The average difference in the stress results between these two methods is acceptable.

In conclusion, the comparison is extremely favorable and indicates the following results:

- The finite element model was accurately constructed; the use of higher aspect ratio elements in the central portion of the finite element model does produce accurate stresses in the shells.
- The inertial weight of the cask was adequately represented in the finite element model analysis.

Figure 2.10.11-1 Mathematical Model of NAC-LWT Cask (30-Foot Top End Impact)



- | | |
|---|--------------------|
| 1 | Closure Lid |
| 2 | Closure Lid Bolt |
| 3 | Top Ring |
| 4 | Inner Shell |
| 5 | Lead (Gamma) Shell |
| 6 | Outer Shell |
| 7 | Bottom |
| 8 | Bottom Cover Plate |
| 9 | Bottom Lead Plate |

Table 2.10.11-1 Geometric Dimensions of the Cask

	Dimensions
Inner Shell (I.S.)	r_i = inner radius = 6.6875 inches
	r_o = outer radius = 7.4375 inches
	ρ_s = density for stainless steel = 0.288 lb/in ³
Outer Shell (O.S.)	r_i = inner radius = 13.1875 inches
	r_o = outer radius = 14.3075 inches
	ρ_s = density for stainless steel = 0.288 lb/in ³
Lead	ρ_L = density for lead = 0.41 lb/in ³

Table 2.10.11-2 Comparison of the Hand-Calculated and Finite Element Results

Location	C _i	Moments (in-lb)		σ_b (1 g)	Hand-Calculated	Finite ¹ Element
		Case A	Case B		σ_b (49.7 g)	σ_b (49.7 g)
I1	6.6875	363,289	-123.281	130.90	6,504	3,820
I2	7.4375	363,289	-123.281	145.91	7,234	6,110
J1	13.188	363,289	-123.281	258.20	12,827	10,060
J2	14.387	363,289	-123.281	281.67	13,993	19,650
K1	6.6875	669,161	-91,756	314.98	15,648	16,700
K2	7.4375	669,161	-91,756	350.31	17,403	19,710
L1	13.188	669,161	-91,756	621.16	30,859	33,280
L2	14.387	669,161	-91,756	677.63	33,664	36,590
M1	6.6875	1,012,220	-62,636	518.01	25,735	25,270
M2	7.4375	1,012,220	-62,636	576.11	28,621	29,010
N1	13.188	1,012,220	-62,636	1021.54	50,750	50,990
N2	14.387	1,012,220	-62,636	1114.42	55,364	55,990
O1	6.6875	1,198,453	-45,256	629.09	31,253	29,220
O2	7.4375	1,198,453	-45,256	699.64	34,758	33,310
P1	13.188	1,198,453	-45,256	1240.58	61,632	61,810
P2	14.387	1,198,453	-45,256	1353.38	67,236	68,230
Q1	6.6875	1,000,205	-63,832	510.81	25,377	26,830
Q2	7.4375	1,000,205	-63,832	568.09	28,223	30,770
R1	13.188	1,000,205	-63,832	1007.33	50,044	50,030
R2	14.387	1,000,205	-63,832	1098.91	54,594	55,920
S1	6.6875	436,731	-116,562	174.65	8,677	6,330
S2	7.4375	436,731	-116,562	194.25	9,650	9,950
T1	13.188	436,731	-116,562	344.43	17,111	20,030
T2	14.387	436,731	-116,562	375.75	18,667	28,310

¹ The finite element stress values are taken from the SY stress category in Table 2.10.10-38.

2.10.12 Impact Limiter Force-Deflection Curves and Data

2.10.12.1 Potential Energy and Cask Drop Motion

The Code of Federal Regulations, 10 CFR 71, states that analyses must show that a licensed spent-fuel shipping cask is capable of sustaining a normal condition test (a 1-foot free drop) followed by a hypothetical accident test (a 30-foot free drop). This has conservatively been interpreted to mean, impact limiters must be designed to absorb or dissipate no less than the potential energy of the cask if dropped, in any orientation, from 31 feet onto an unyielding surface. When at rest on the unyielding surface (a datum surface), the cask has zero potential energy.

The distance through which the cask free falls is measured from the nearest point on the cask (either impact limiter) to the unyielding surface. This assures that center of gravity will translate a minimum of 31 feet before an impact limiter contacts the unyielding surface. Additionally, it is assumed that the cask will always seek a stable orientation after contacting the unyielding surface on both impact limiters. After an end drop, for example, the cask is assumed to tip over and reach a stable horizontal orientation.

Potential energy is calculated by multiplying the weight of the cask by the height to which the center of gravity of the cask was raised. The design weight of the cask, contents and impact limiters is 52,000 lbs. For these analyses, the NAC-LWT cask is assumed to be symmetric about the three major axes; therefore, the center of gravity is at the midpoint of the longitudinal centerline of the cask. The center of gravity is a datum point at which all the mass (weight) is located.

2.10.12.1.1 Translational Motion – Side Drop

Figure 2.10.12-1 shows the cask in the horizontal or side drop position. When released in this orientation from 31 feet (372 inches), the cask has 1.934×10^7 inch-pounds of potential energy. As shown by the heavy dashed lines in Figure 2.10.12-1, the cask translates vertically on an unyielding surface. The deceleration forces created when crushing the impact limiters opposes the translational motion of the cask. Impact limiter crushing continues until all the potential energy from the cask is absorbed; thereby, decelerating the cask to rest. Both impact limiters crush simultaneously in a side drop; therefore, once at rest, the cask is in a stable orientation.

In a side drop, the cask experiences only vertical, translational motion. Ignoring the energy stored elastically in the impact limiter during deceleration, the dissipated energy equals the initial potential energy of the cask. During the side drop, both impact limiters engage in

simultaneously decelerating the cask; therefore, each impact limiter absorbs the “energy absorbed by the first limiter” (EI) as shown in Table 2.10.12-1.

2.10.12.1.2 Translational and End-Rotational Motion – End Drop

Figure 2.10.12-2 shows the cask in the end drop position. End drops are drop angles that range between 0 degrees (end drop) and 15 degrees (corner drop) and characteristically show translational and end-rotational motion. As in a side drop, a cask in the end drop position translates vertically through 31 feet and decelerates on the unyielding surface. Deceleration forces acting on the bottom of the cask are symmetric and uniform; therefore, the cask remains upright during deceleration and after the cask has come to rest. The energy absorbed by the single impact limiter while decelerating the cask (EI, Table 2.10.12-1), equals the initial potential energy of the cask; however, the center of gravity is approximately 116.4 inches above the unyielding datum surface. The cask is metastable when resting on the crushed impact limiter. The cask has 6.04×10^6 inch-pounds more potential energy (EP) after the cask has come to rest. It has been assumed that the cask will seek a stable state, and a force is applied to the cask causing it to rotate on its end (crushed limiter). By tipping over, the cask will reach a stable orientation. The potential energy will be absorbed by the second impact limiter, as if the cask were in a side drop.

2.10.12.1.3 Translational, End-Rotational, Mid-Point Rotational Motion – Oblique Drops

Figure 2.10.12-3 shows the cask in an oblique drop orientation. Oblique drops are drop angles that range between 15 degrees (corner drop) and 90 degrees (side drop). The cask translates vertically after it is released, to the unyielding surface. The impact limiter, which contacts the unyielding surface first, decelerates the lower end of the cask, and brings its velocity to zero. Energy absorbed by the first limiter (EI) decelerates the lower end of the cask to rest. The cask is now able to rotate or pivot on the stopped lower end. However, the energy absorbed by the first impact limiter is less than the initial energy of the cask, leaving the energy remaining (ER) to be absorbed by the second impact limiter.

Simultaneously during deceleration of the first or lower end of the cask, two other actions are taking place. First, the upper or free end of the cask rotates around the stopped end of the cask and continues to accelerate due to gravity. Second, a component of the deceleration force causes a torque perpendicular to the longitudinal axis of the cask, resulting in the cask beginning to rotate around the center of gravity. Both “actions” increase the energy to be absorbed by the second impact limiter.

During deceleration of the lower end of the cask, the upper end continues to accelerate while translating vertically because no deceleration force is applied to it. Newton’s first law, “Every

body persists in its state of rest or of uniform motion in a straight line unless it is compelled to change that state by forces impressed on it...” (Resnick, page 75) requires the upper end to continue to translate vertically and continue to be accelerated by gravity until the second impact limiter contacts the unyielding surface. However, because the cask body is rigid, when the lower end of the cask stops, the upper end of the cask continues translating and the cask begins to pivot on the crushed impact limiter. This continues until the second impact limiter contacts the unyielding surface and significant deceleration forces are generated.

The second action, occurring while the lower end of the cask is decelerating, is a vector component of the deceleration force that causes the cask to rotate around its center of gravity. The deceleration force is always perpendicular to the unyielding surface. Depending on the cask angle, the deceleration force can be vectorially broken down into a force parallel to the longitudinal axis of the cask and a component perpendicular to the cask longitudinal axis. The perpendicular force component acts at a distance of approximately half the cask length. A torque, equivalent to the perpendicular force multiplied by half the cask length, attempts to spin the cask around the center of gravity. The “spin” or rotational velocity can also be thought of as rotational kinetic energy that must be absorbed by the second impact limiter. A detailed explanation of the torque and rotational kinetic energy is presented in Appendix 2.10.4.

Finally, the third component of energy that must be absorbed by the second impact limiter is the energy stored elastically in the first impact limiter. The elastically stored energy causes a force perpendicular to the unyielding surface to augment the rotational velocity of the cask and “lift” the first impact limiter, which is at rest.

Oblique drops have four distinct quantities of energy that need to be absorbed to bring the cask to rest in a stable, horizontal orientation.

- Potential energy absorbed by the impact limiter to strike the unyielding surface first (EI), which brings the translational velocity of the lower end of the cask to zero. The remaining potential energy (ER), also needs to be absorbed.
- Potential energy (EP), of the center of gravity, which results from its height above the unyielding surface.
- Rotational kinetic energy given to the cask as a result of the deceleration force and elastically stored energy (ES) from the impact that brings the lower end of the cask to rest.

2.10.12.2 Potential to Kinetic Energy Conversion

Just before the release, the cask is at rest and at a given drop angle. The uniform gravitational force constantly acts on the cask and when released, accelerates the cask at a constant rate. Gravitational acceleration (g) equals 32.2 ft/sec². No other forces act on the cask as it falls; therefore, no additional energy is supplied to the cask that must be dissipated by the impact

limiters. Uniform forces acting on the cask mean the drop angle will not change while the cask is falling. Since energy can not be created or destroyed, the initial potential energy of the cask is converted to kinetic energy. To calculate the velocity at the time the impact limiter contacts the unyielding surface, energy conversion is used in the following way:

$$PE = KE$$

or

$$mgh = \frac{1}{2}mv^2$$

Solving for v:

$$v = (2gh)^{0.5}$$

The initial velocity (at the time crushing begins) is a constant and is only a function of drop height. For a drop height of 31 feet, the velocity of the cask at the time an impact limiter contacts the unyielding surface is 44.7 feet/second.

The correlation between potential energy and kinetic energy is the foundation on which the computer program RBCUBED is based. Translational velocity (translational kinetic energy), which the cask gained while free falling or while pivoting on end (oblique drop), is directly attributable to the initial potential energy of the cask. Rotational velocity (rotational kinetic energy) is created during an oblique drop while decelerating the lower end of the cask; elastically stored energy is a small, calculable quantity of energy. When it is shown that the total energy absorbed is at least equal to the initial potential energy, the rotational kinetic energy and the stored energy of the cask, then the cask is at rest.

2.10.12.3 Deceleration Forces and Energy Absorption Calculation

The following quotation describes how an aluminum honeycomb impact limiter works: "...the kinetic energy of a body in motion is equal to the work it can do in being brought to rest..." (Resnick, page 75). The source of kinetic energy in a cask was established in Section 2.10.12.2. Work done by crush force is the magnitude of that force multiplied by the distance (deformation) through which the crush occurs. The units of work are in inch-pounds.

The NAC-LWT cask impact limiters are right cylindrical aluminum shells filled with aluminum honeycomb. Aluminum honeycomb is used to dissipate the kinetic energy of the cask. "Honeycomb" describes cells created when multiple corrugated thin aluminum sheets are bonded together. The honeycomb cells are designed to crush when a nominal force per unit area is applied to the honeycomb. Honeycomb is anisotropic. Honeycomb shows nominal crush strength in the plane, parallel with the corrugations and a greatly reduced crush strength

perpendicular to the corrugations. Aluminum honeycomb is manufactured in batch blocks and tested to ensure that the crush strength is within specified tolerances. Wedges of tested honeycomb are bonded together giving the impact limiter isotropic crush strength for all drop angles between 0 degrees (end drop) and 90 degrees (side drop). A thin aluminum exterior skin is bonded and seal welded to the honeycomb to prevent cosmetic and contamination damage to each impact limiter.

The aluminum honeycomb crushes because it is trapped between the cask and the unyielding surface. The initial energy (PE) of the cask will have an equivalent amount of kinetic energy (KE) just before the impact limiter contacts the unyielding surface. When the limiter contacts the unyielding surface, it immediately comes to rest; however, the cask continues to move into the impact limiter until it is opposed by a force vector. To explain the work done in stopping the cask, an illustrative example of the end drop is presented:

The cask is assumed to have been dropped 8.8 inches; $PE = KE = 456,000$ inch-pounds; cask velocity when the limiter contacts the unyielding surface is 6.9 feet/second (82.5 in/sec).

The cask is a rigid structure and each end has an area of approximately 651 square inches. Nominal crush strength of the honeycomb material is 3,500 psi. The cask is rigid and isolates ("backs") the honeycomb material that effectively stops the cask from that which does not. The force required to crush the backed honeycomb is 2.28×10^6 pounds. When the backed honeycomb crushes 0.1 inch, 228,000 inch-pounds of work is performed:

$$W = (F)(d)$$

where:

$$F = 2.28 \times 10^6 \text{ lbs}$$

$$d = 0.1 \text{ in}$$

Using the definition of work and Newton's second law, $F = ma$, yields the following derivation:

$$W = \frac{1}{2}mv^2 - \frac{1}{2}mv_o^2$$

where:

W = work performed on a particle, in-lb (Work performed on the cask by the honeycomb is negative.)

m = mass of the cask weight of the cask divided by the gravitational constant 32.2 ft/sec², lbf*sec²/ft

v = velocity of the cask after the work is performed, ft/sec

v_o = initial velocity of the cask, ft/sec

Solving for the velocity after an incremental amount of work has been performed:

$$v = \sqrt{\frac{2W}{m} + v_0^2}$$

Substituting for W, m, v_0 and adjusting for correct units, the cask velocity after the first crush increment is 4.91 feet/second. Repeating this analysis for another 0.1-inch increment, shows that the cask velocity diminishes to 0.76 feet/second, and after another fraction of a crush increment, the cask is stopped.

In summary, the force (a vector quantity) that is created by crushing the honeycomb opposes the velocity of the cask, which is also a vector quantity. Crushing an incremental amount of honeycomb is a finite quantity of work performed on the cask, decreasing its velocity and kinetic energy. Once the kinetic energy is completely dissipated, the cask velocity equals zero.

RBCUBED, the impact limiter computer program used to design the aluminum honeycomb impact limiters, functions in exactly the same way as the illustrative example. Cask geometry and weight, drop angle, crush increment, honeycomb crush strengths, honeycomb lock-up stroke and honeycomb geometry are input to the program. The computer calculates an initial velocity (as the limiter touches the unyielding surface), a backed area engaged in crushing, a crush force, the energy absorbed for a crush increment, the elapsed crush time and the cask velocity at the end of the crush increment. The computation cycle is repeated until all the kinetic energy is absorbed and the end of the cask is stopped.

RBCUBED calculates the energy dissipation necessary to stop the translational motion of the end of the cask that first contacts the unyielding surface (both limiters in the side drop). In Table 2.10.12-1, the energy dissipated while reducing the translational velocity of the first end to contact the unyielding surface is the energy absorbed by the first limiter (EI). If EI is less than the initial kinetic energy of the cask, the difference is reported by RBCUBED as “remaining energy,” and shown in Table 2.10.12-1 as energy remaining after first impact (ER).

In oblique drops, at the instant the translational velocity of the first end to contact the unyielding surface is zero, the cask is in position 2 in Figure 2.10.12-3 (Rotation of the cask around its mid-point is addressed in Appendix 2.10.4). The center of gravity of the cask has a calculable potential energy, which is the energy that increases the velocity of the cask as it pivots on the crushed (“first”) impact limiter. In Table 2.10.12-1, the potential energy, which equals the velocity gain as the cask pivots on end, is the potential energy of cask after first impact (EP).

The aluminum honeycomb dissipates energy while crushing, but elastically stores a small amount of the total energy dissipated. The quantity of elastically stored energy was determined by quasi-static testing of the scale model impact limiters (Section 2.10.12.5). The quantity of stored energy ranged between 5.3 percent (side drop) to 9.7 percent (end drop) of the total energy

dissipated by the limiters tested. As stated above, once all the kinetic energy (EI) has been absorbed, the stored energy is released. The force, which the stored energy creates, tends to augment the torque attempting to cause the cask to spin around the center of gravity. This analysis has conservatively ignored the cask spinning and elected to absorb the energy in the second impact limiter. In Table 2.10.12-1, the elastically stored energy is the energy stored in the first limiter and absorbed in the second limiter while in the side drop orientation (ES).

In summary, lower end translational velocity is reduced to zero by absorbing an amount of energy (EI). The cask will pivot over and absorb the remaining potential energy (ER), the potential energy due to rotation to a horizontal orientation (EP) and the elastically stored energy (ES) all in the second limiter in the side drop orientation. Table 2.10.12-1 shows that the four components of energy are absorbed by both impact limiters for drop angles from 0 degrees to 90 degrees.

2.10.12.4 RBCUBED Calculated Force-Deflection Graphs

Figure 2.10.12-4 through Figure 2.10.12-17 show the deceleration force as a function of crush depth, calculated using RBCUBED for the full-scale cask. Each graph is for either the top or bottom limiter, showing the plus and minus tolerance energy absorption profile. Graphs for the top end (0°), oblique (60°) and side (90°) are broken into simple geometric shapes to facilitate checking of the energy absorbed and maximum force. Quasi-static tests substantiate RBCUBED calculated values for the quarter-scale model limiters, as described in Section 2.10.12.5.

2.10.12.5 Quarter-Scale Model Quasi-Static Force-Deflection Tests

Quasi-static force-deflection tests were performed on quarter-scale model impact limiters used in drop testing a model earlier at Oak Ridge National Laboratories. Limiter samples were selected for a particular quasi-static test based on the limiter having no damage for test orientation. Three limiter orientations - 0 degrees, 15 degrees, 90 degrees - were tested. While each limiter tested was being compressed, two calibrated linear variable differential transformers (LVDT) mechanically attached to test fixtures provided data to an X - Y recorder, which plotted crush force as the impact limiter deformed. Deformation of the limiter proceeded well into honeycomb lock-up. As the force on the limiter decreased after the limiter locked up, force and deflection continued to be monitored, revealing the amount of elastically stored energy. Based on the results of the quasi-static tests, the energy absorption capacity of each limiter is presented in Figure 2.10.12-18 through Figure 2.10.12-20. The static force for each data point is multiplied by 1.196, a static to dynamic scaling factor, enabling comparison with RBCUBED computed values. The scaling factor is an average value established by manufacturers' tests. Figure 2.10.12-18 through Figure 2.10.12-20 show for comparison, the dynamically scaled forces and

RBCUBED computed values. These figures also clearly show the energy absorption capacity of each limiter and the potential energy absorption margins.

Figure 2.10.12-18 through Figure 2.10.12-20 also show the maximum deceleration forces that occur for each of the drop angles. RBCUBED calculated force values are higher in all cases except the end drop. Closer examination of the crushed impact limiter, quasi-statically tested in the end drop orientation, revealed a shearing previously unaccounted for, causing 10 percent higher forces than calculated by RBCUBED. The shearing and shear force generation occurs simultaneously with crushing, and is a small force compared with the crush force. Figure 2.10.12-21 shows a cross section of the crushed impact limiter, with the shear plane clearly visible. Table 2.10.12-2 compares the average maximum/peak forces and g-loads calculated using RBCUBED with corresponding values from each of the quasi-static tests. Force margins are also shown in Table 2.10.12-2 along with stress (structural) margins assuring that structural margins are satisfactory.

Figure 2.10.12-1 Side Drop ($\theta = 90^\circ$)

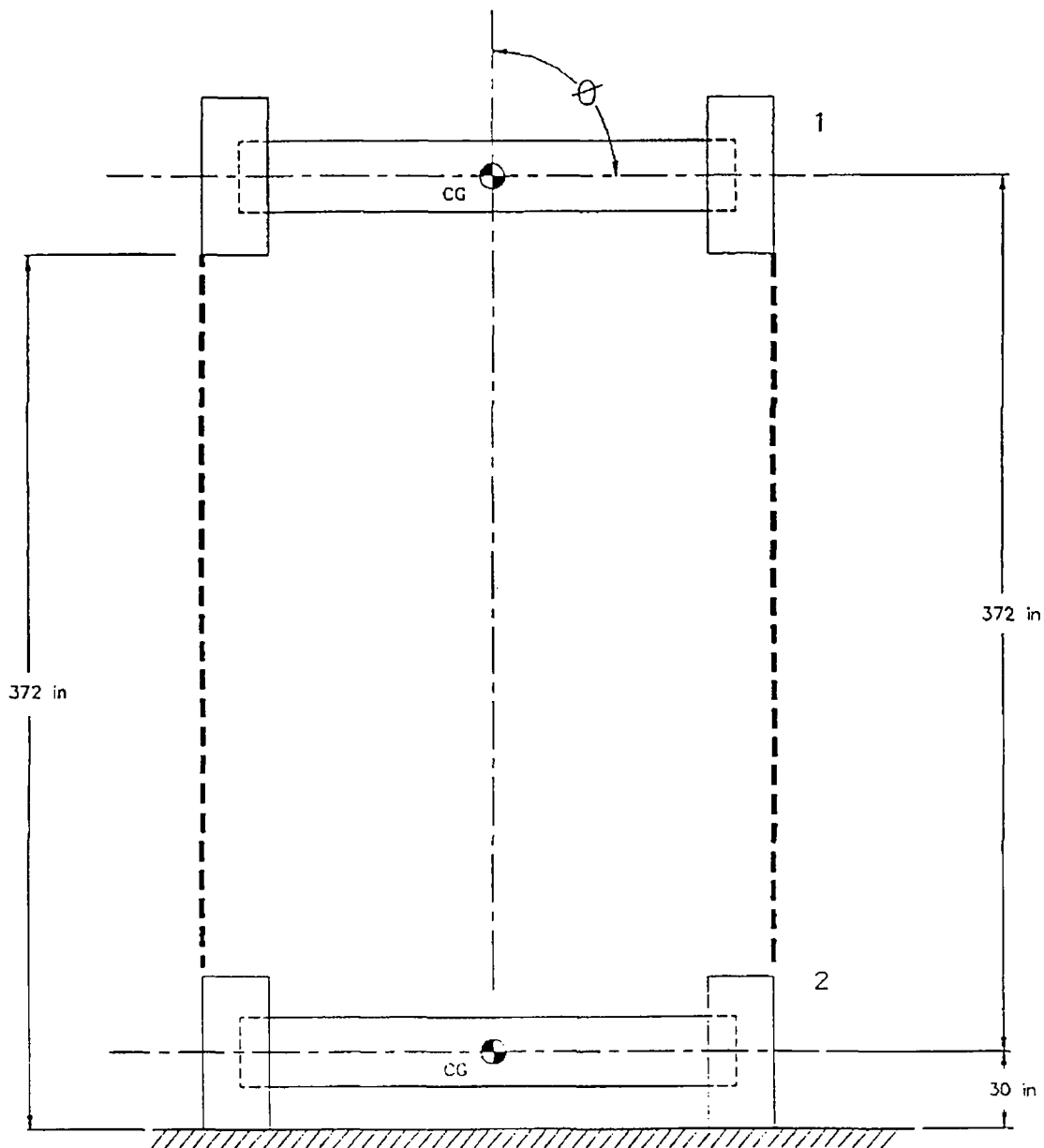


Figure 2.10.12-2 End Drop ($0^\circ \leq \theta < 15^\circ$)

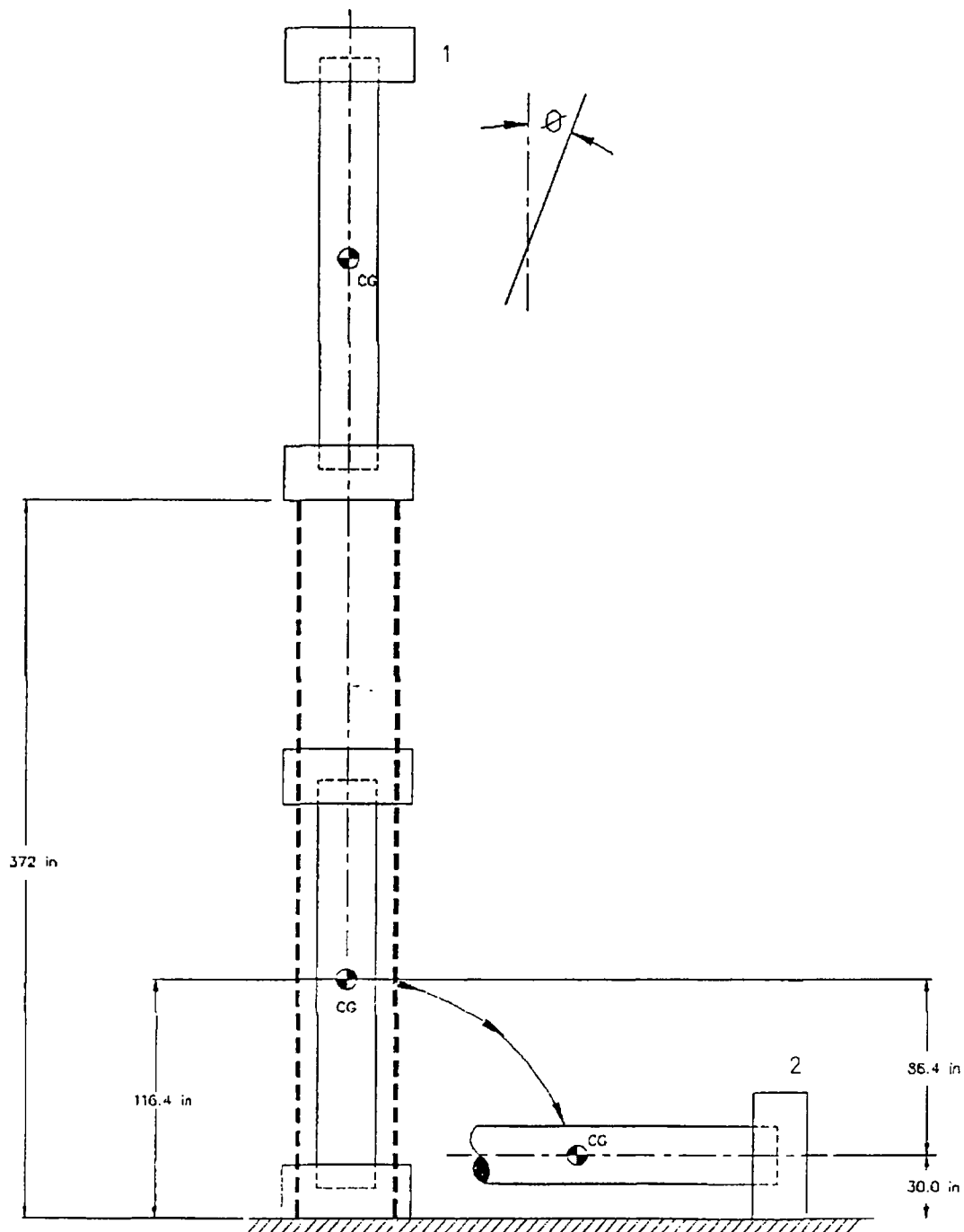


Figure 2.10.12-3 Oblique Drop ($15^\circ \leq \theta < 90^\circ$)

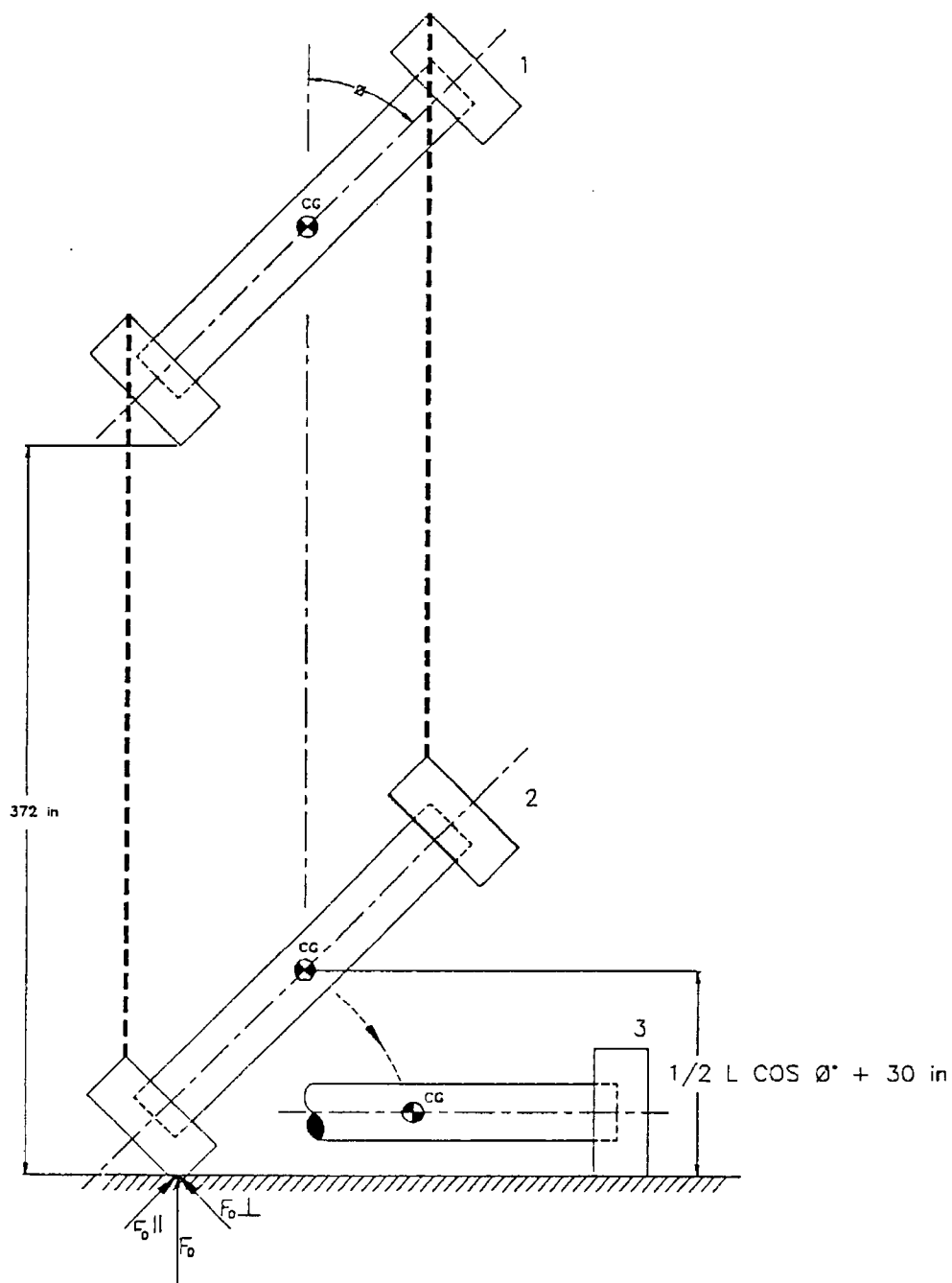


Figure 2.10.12-4 Force Deflection Graph (0-Degree, Top End Drop)

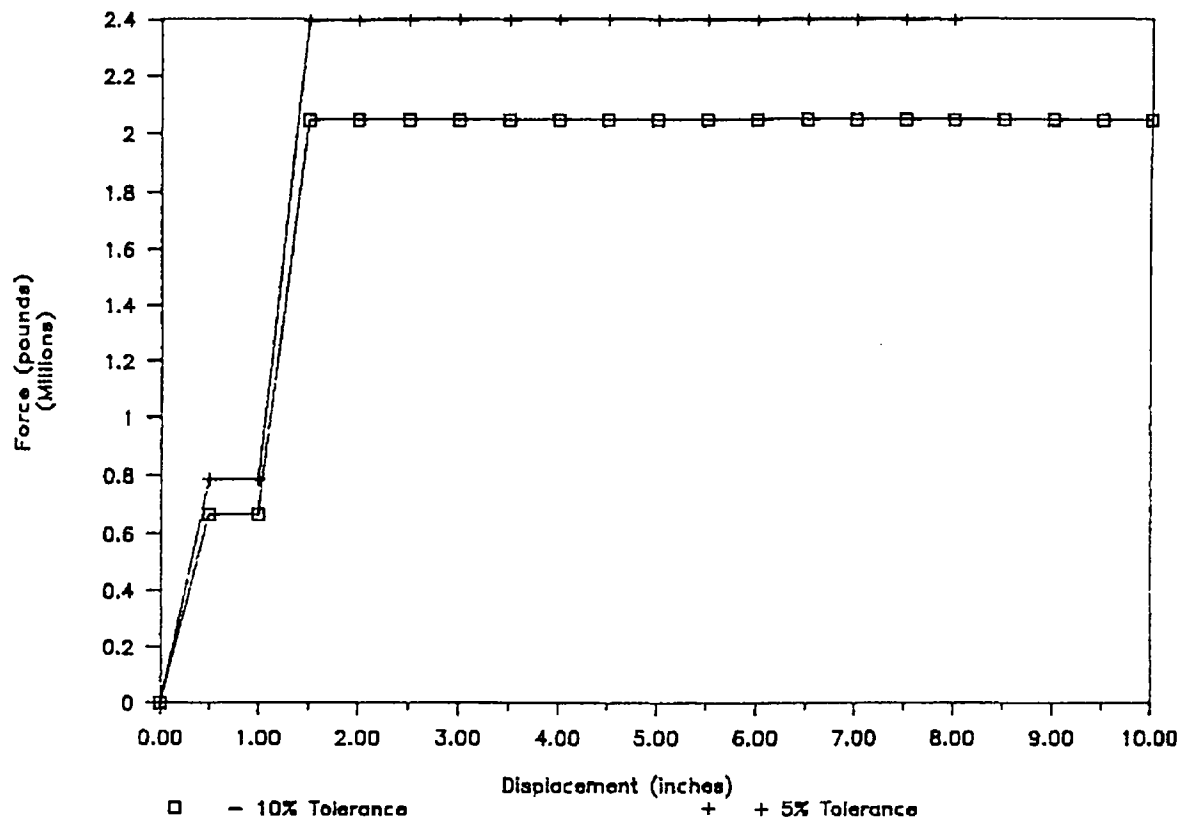


Figure 2.10.12-5 Force-Deflection Graph (0-Degree, Bottom-End Drop)

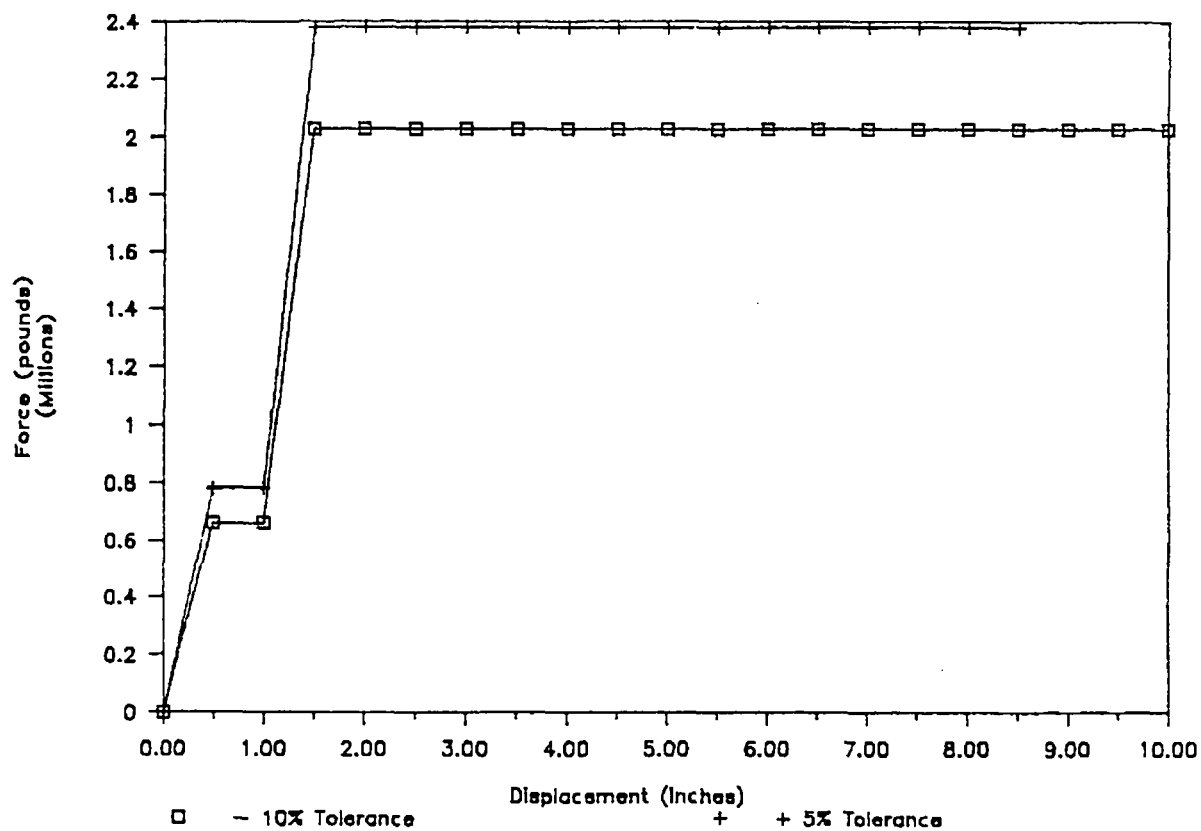


Figure 2.10.12-6 Force-Deflection Graph (15.74-Degree, Top Corner Drop)

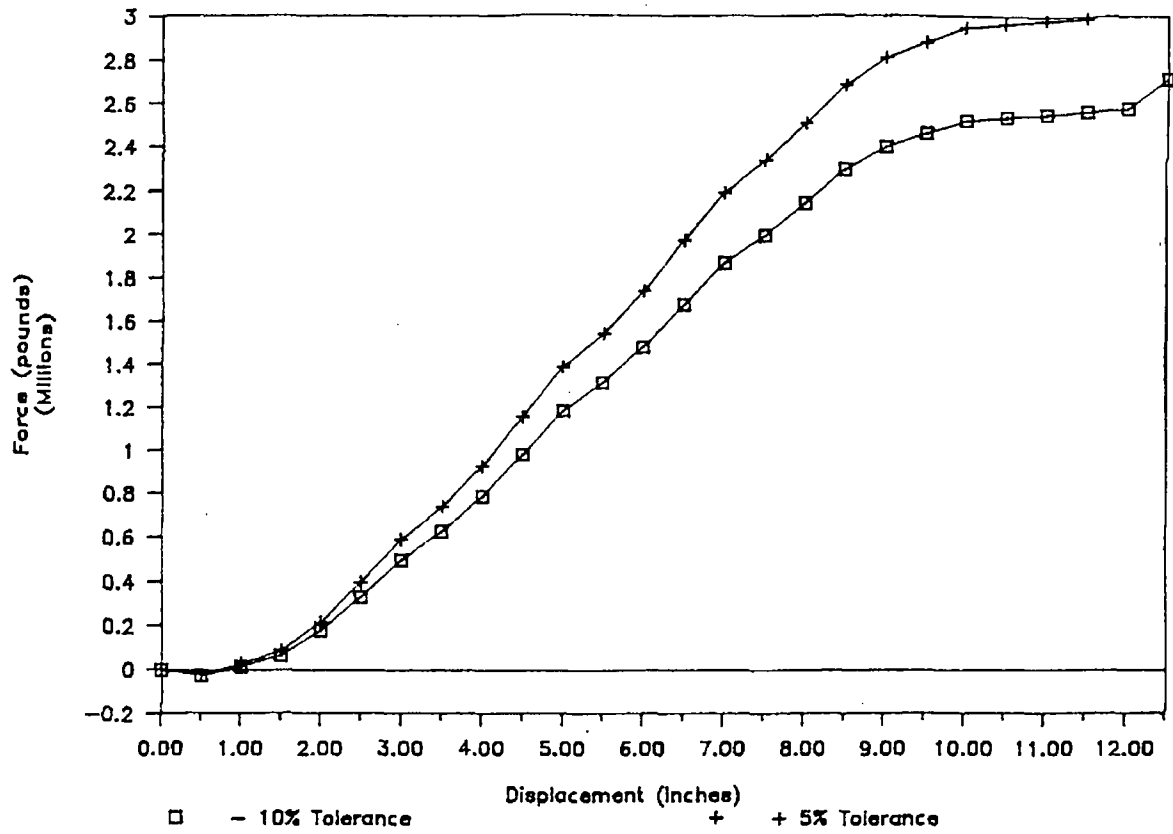


Figure 2.10.12-7 Force-Deflection Graph (14.5-Degree, Bottom Corner Drop)

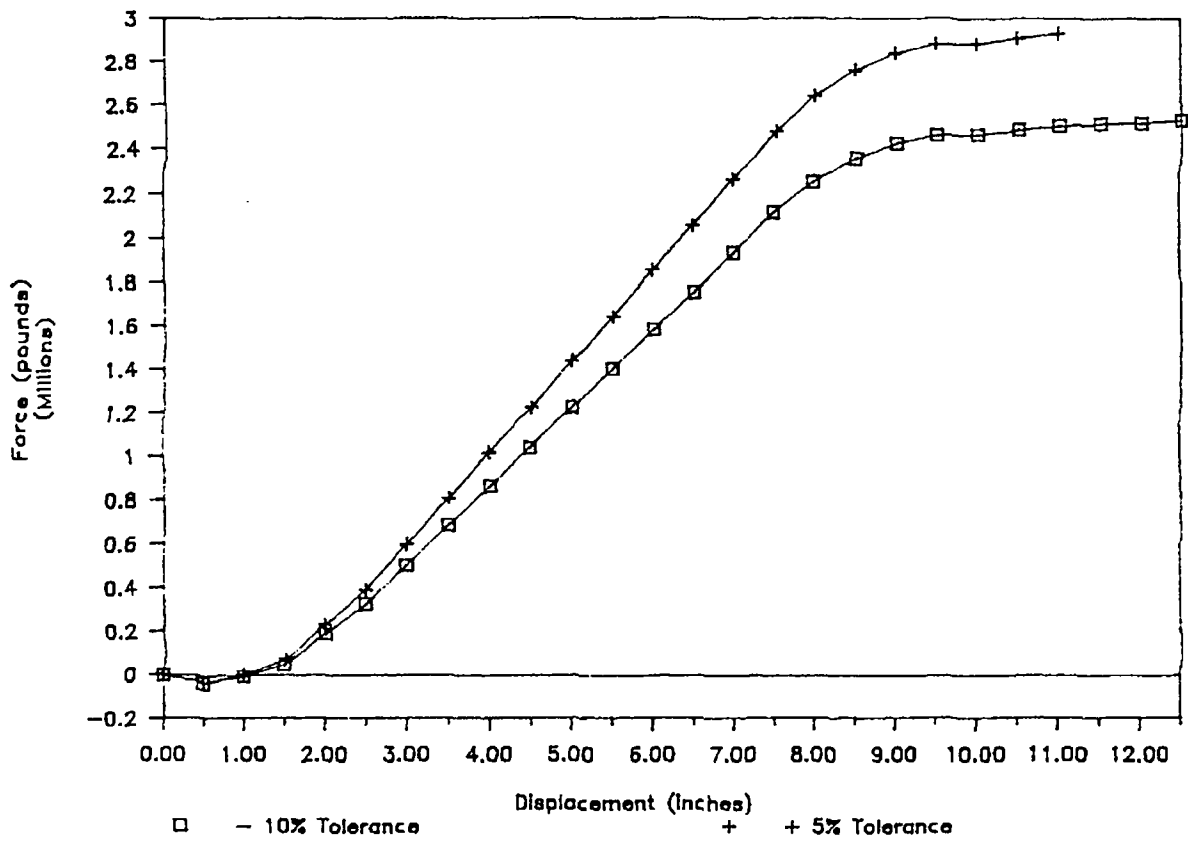


Figure 2.10.12-8 Force-Deflection Graph (30-Degree, Top Oblique Drop)

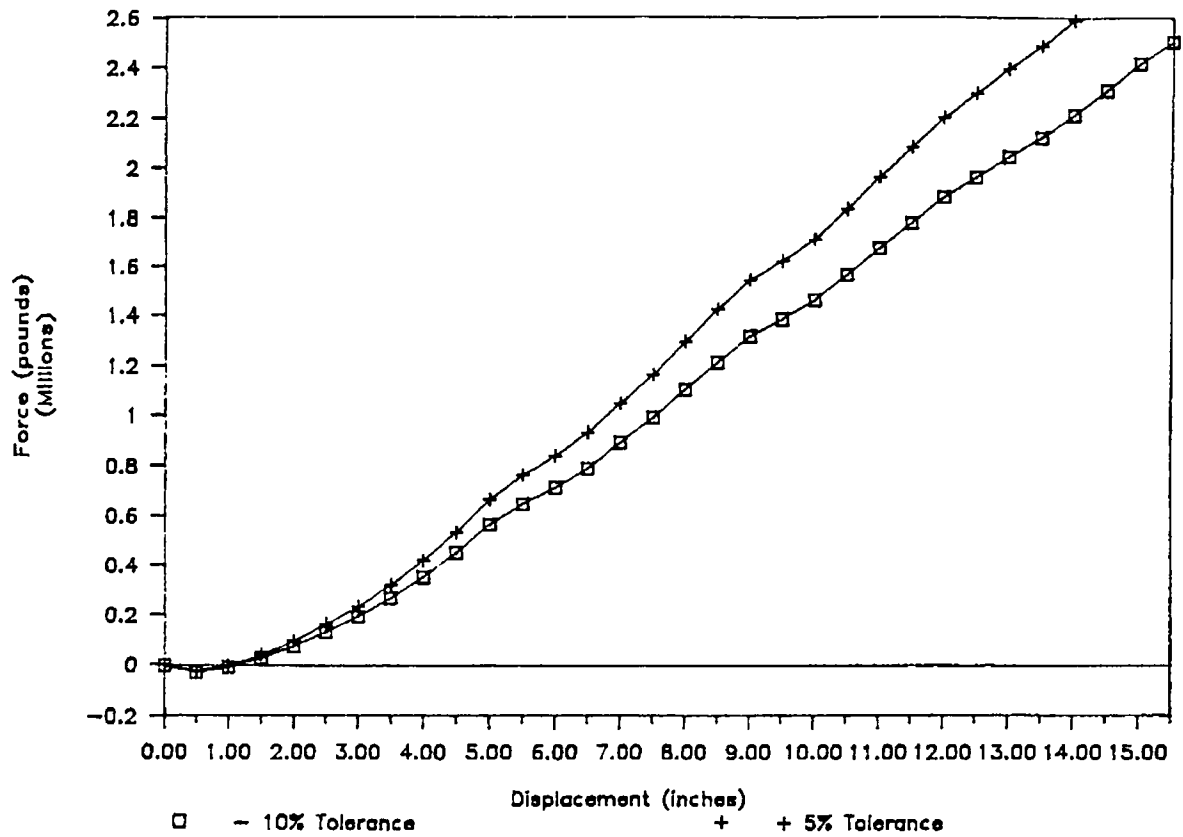


Figure 2.10.12-9 Force-Deflection Graph (30-Degree, Bottom Oblique Drop)

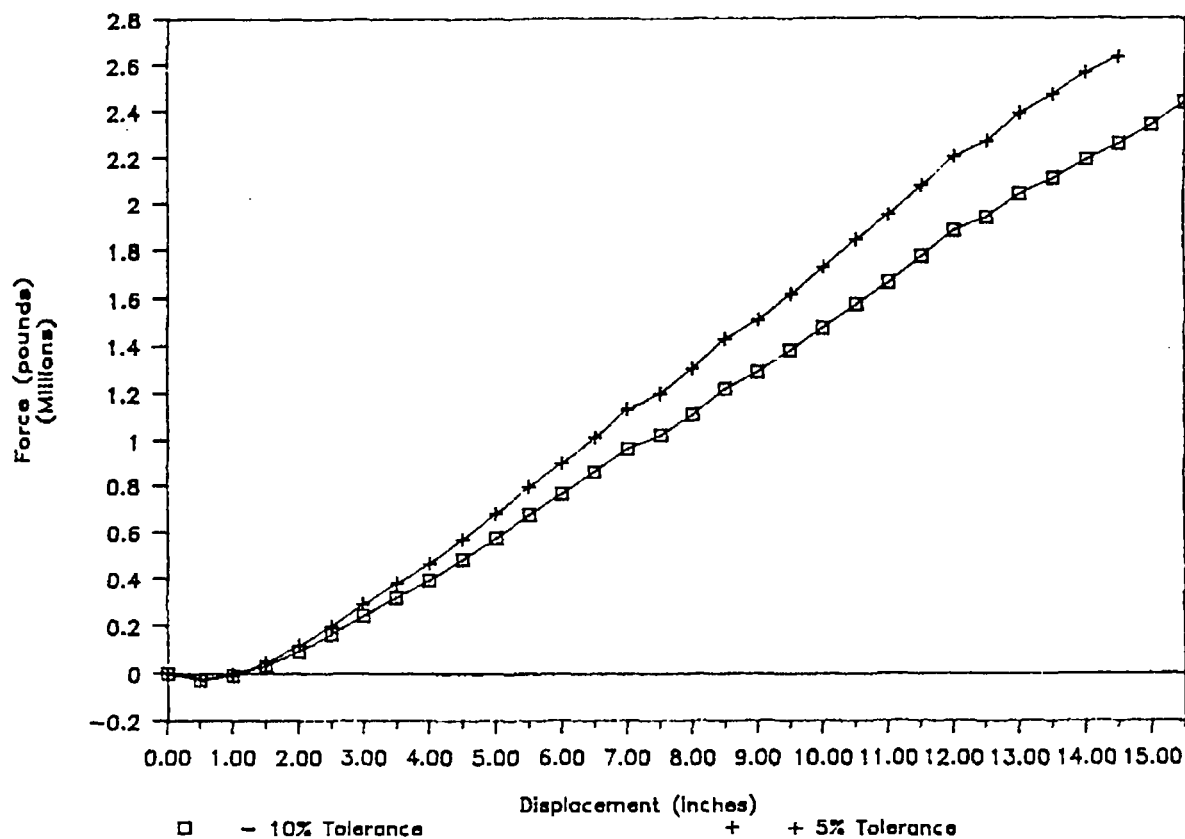


Figure 2.10.12-10 Force-Deflection Graph (45-Degree, Top Oblique Drop)

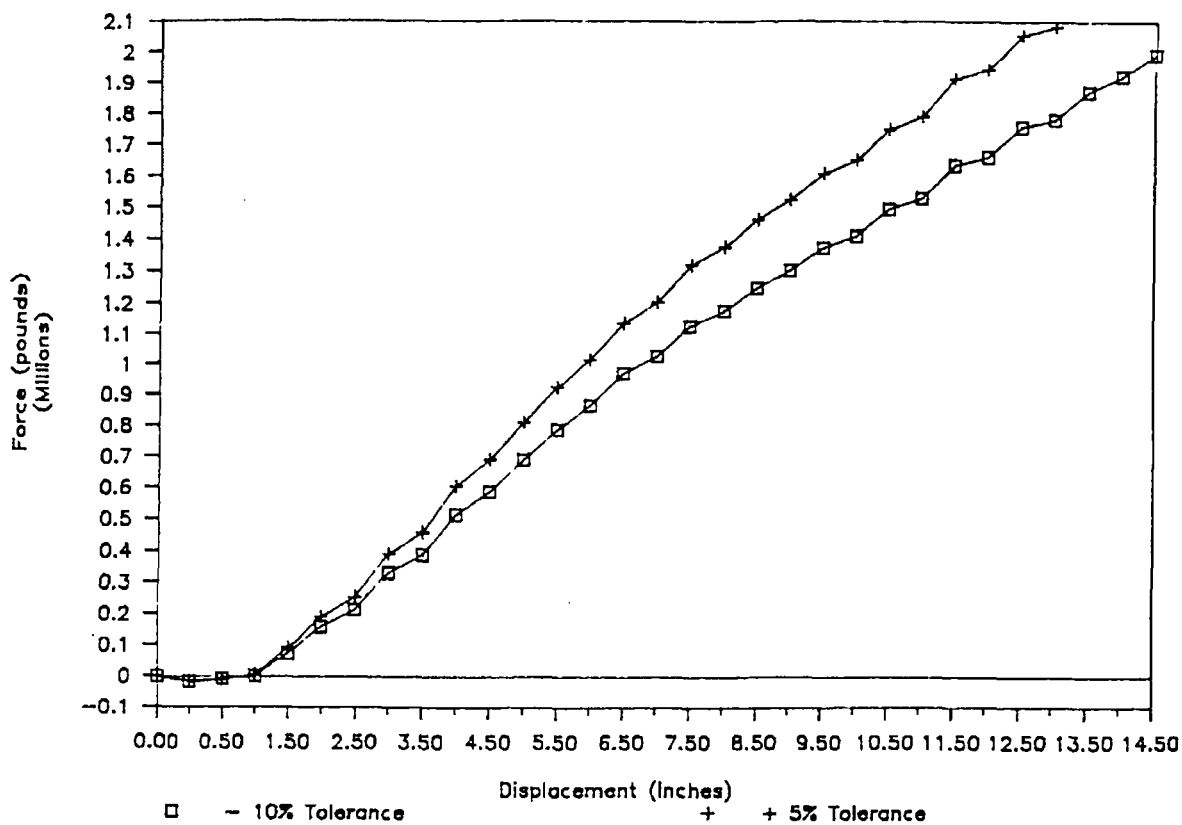


Figure 2.10.12-11 Force-Deflection Graph (45-Degree, Bottom Oblique Drop)

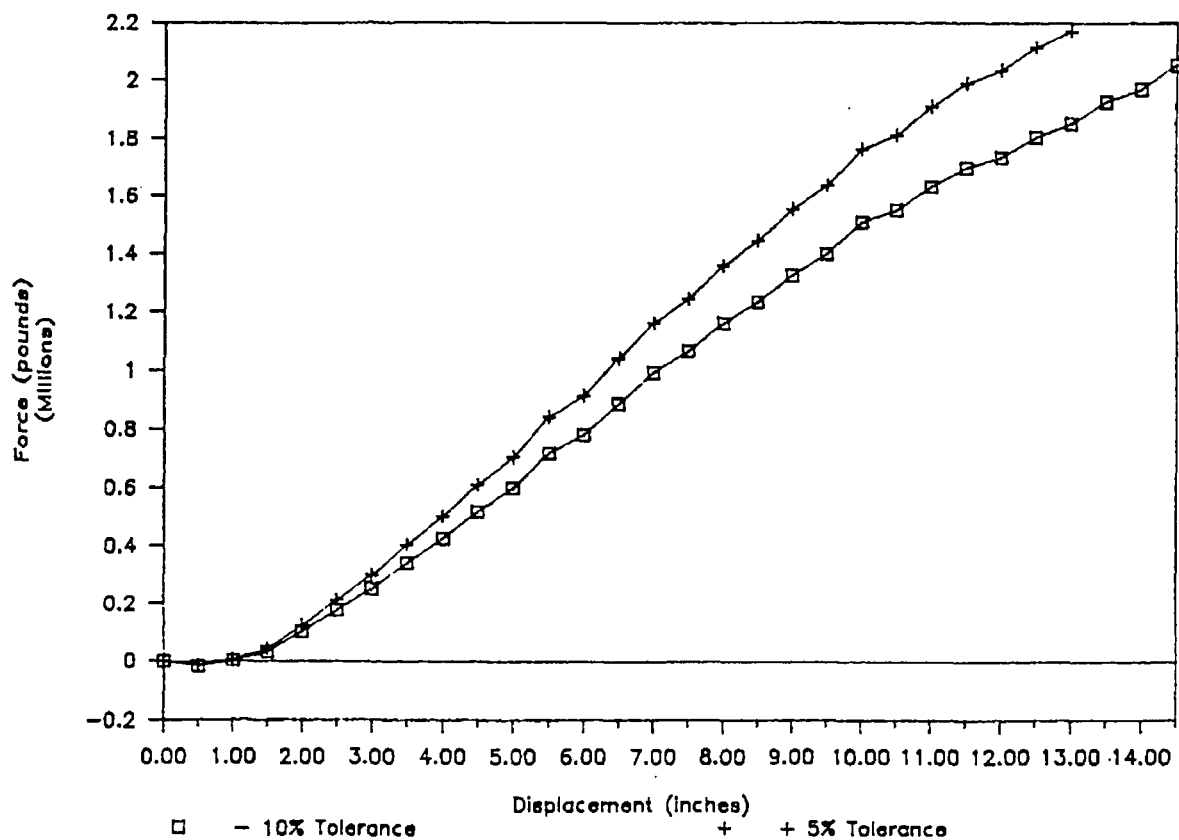


Figure 2.10.12-12 Force-Deflection Graph (60-Degree, Top Oblique Drop)

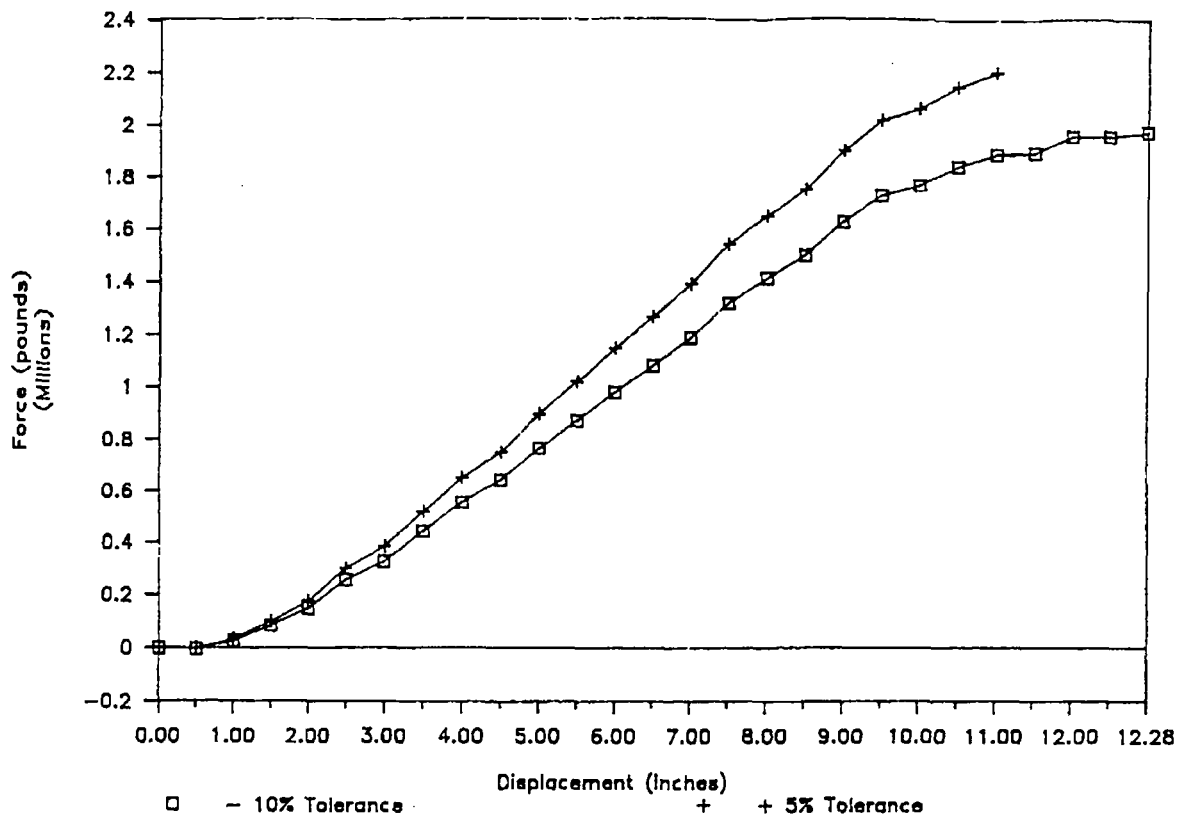


Figure 2.10.12-13 Force-Deflection Graph (60-Degree, Bottom Oblique Drop)

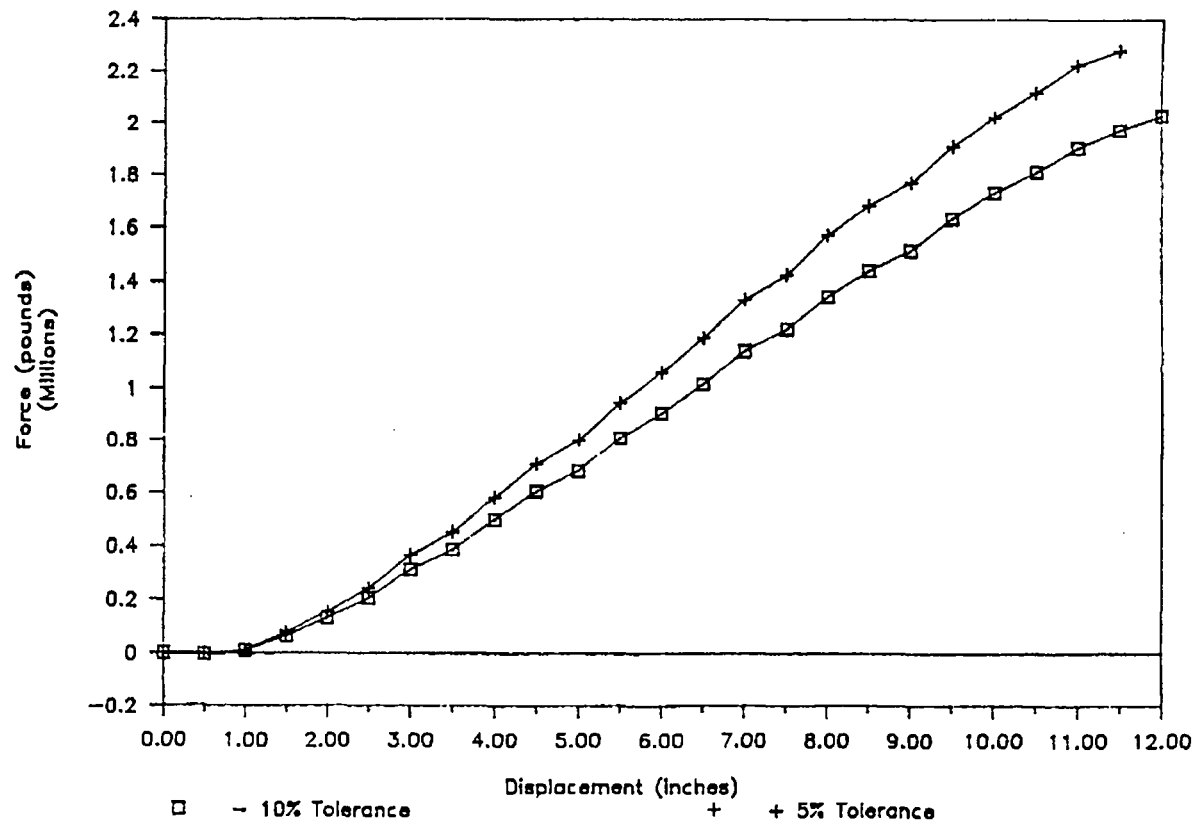


Figure 2.10.12-14 Force-Deflection Graph (75-Degree, Top Oblique Drop)

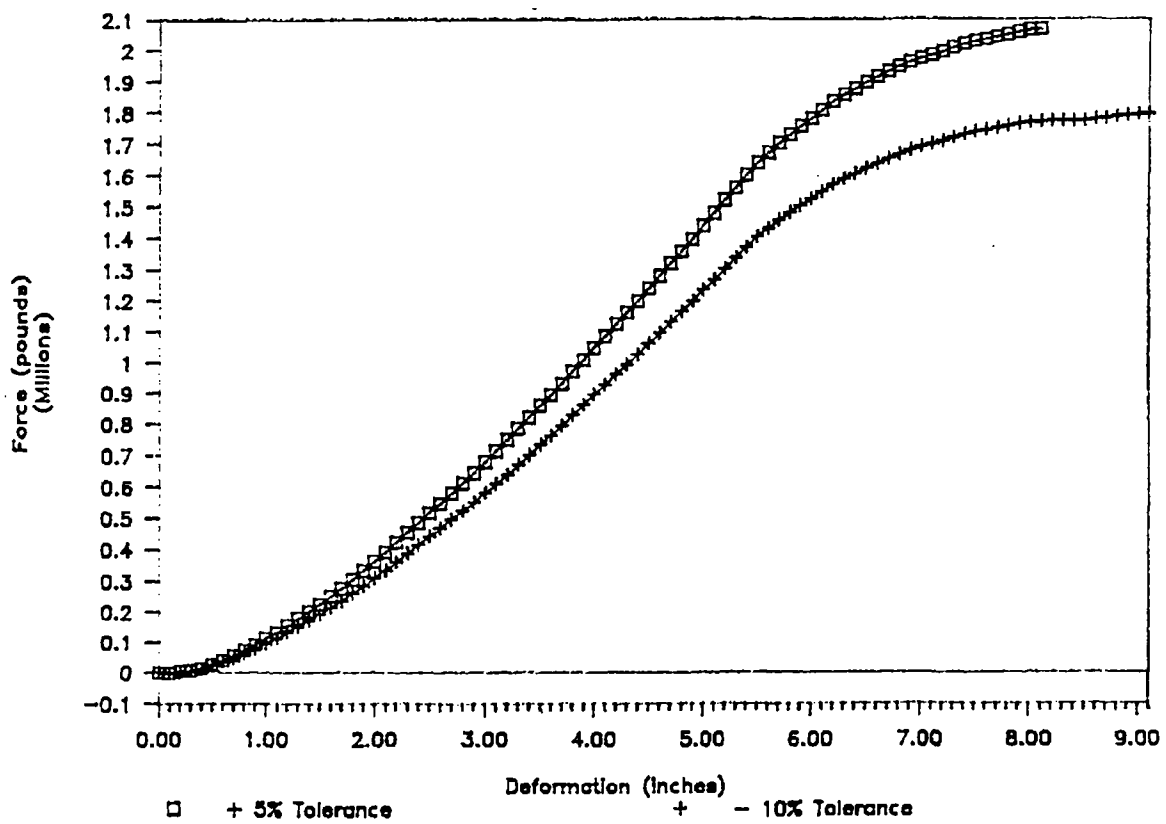


Figure 2.10.12-15 Force-Deflection Graph (75-Degree, Bottom Oblique Drop)

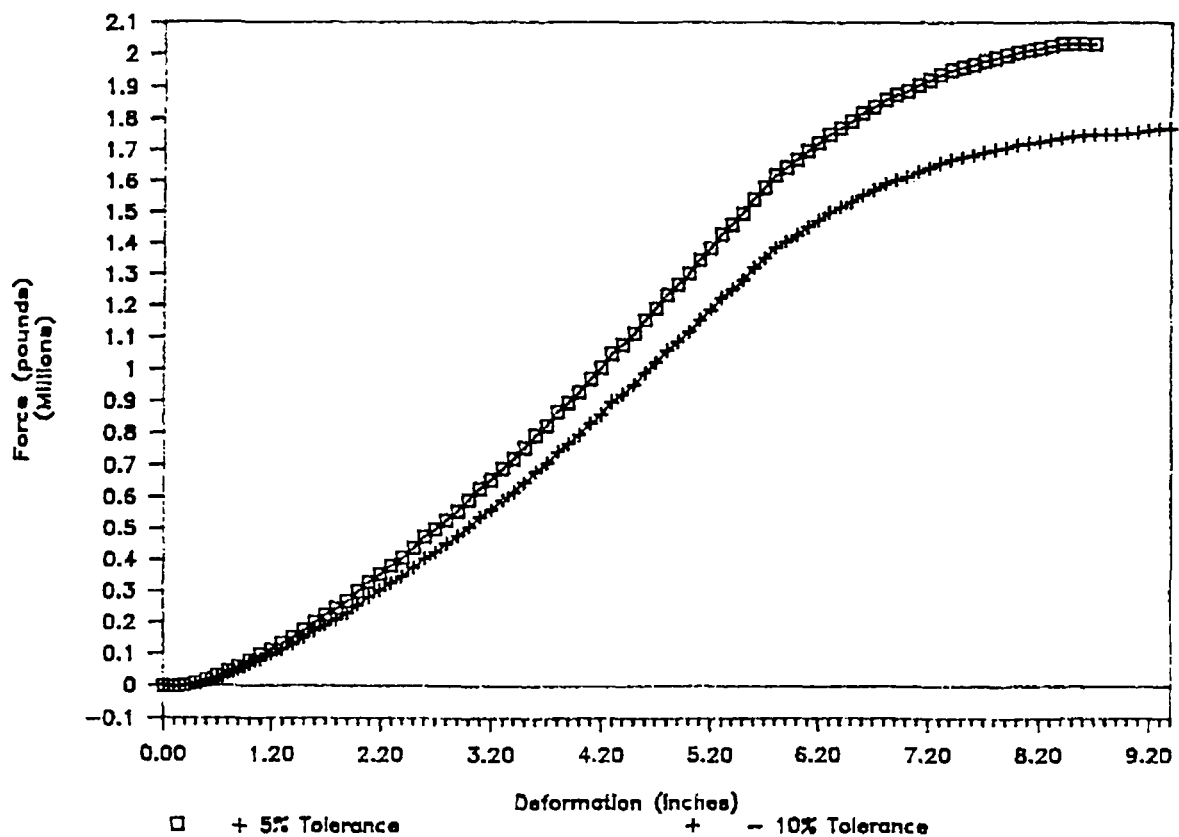


Figure 2.10.12-16 Force-Deflection Graph (90-Degree, Top Side Drop)

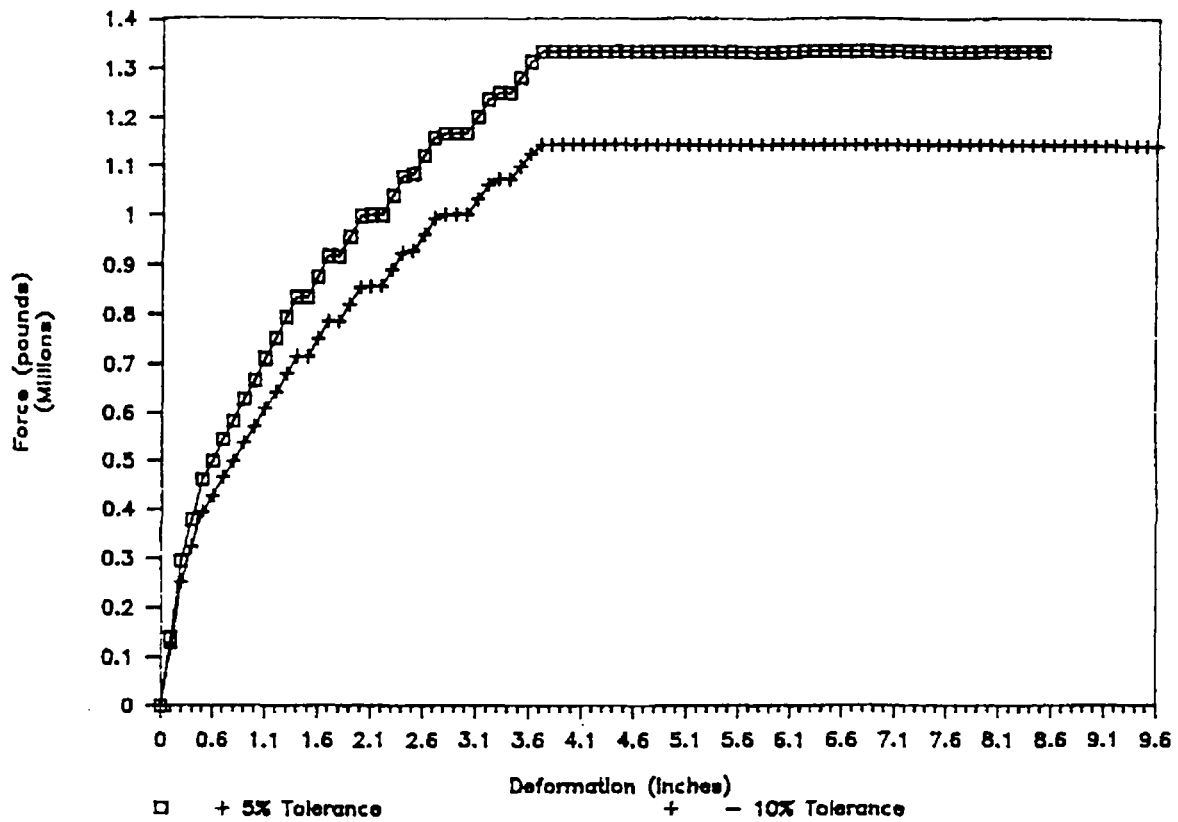


Figure 2.10.12-17 Force-Deflection Graph (90-Degree, Bottom Side Drop)

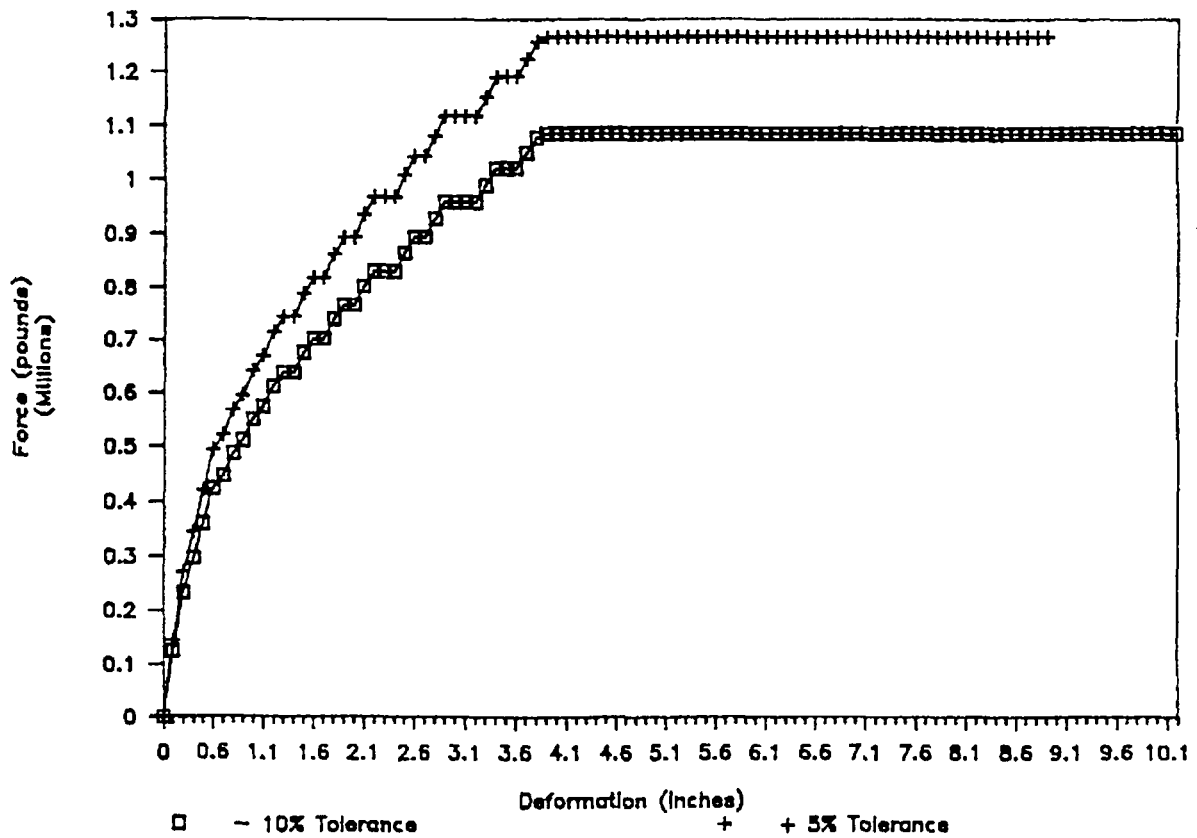


Figure 2.10.12-18 Force-Deflection Curve (0-Degree Impact, Drop Tested Limiter)

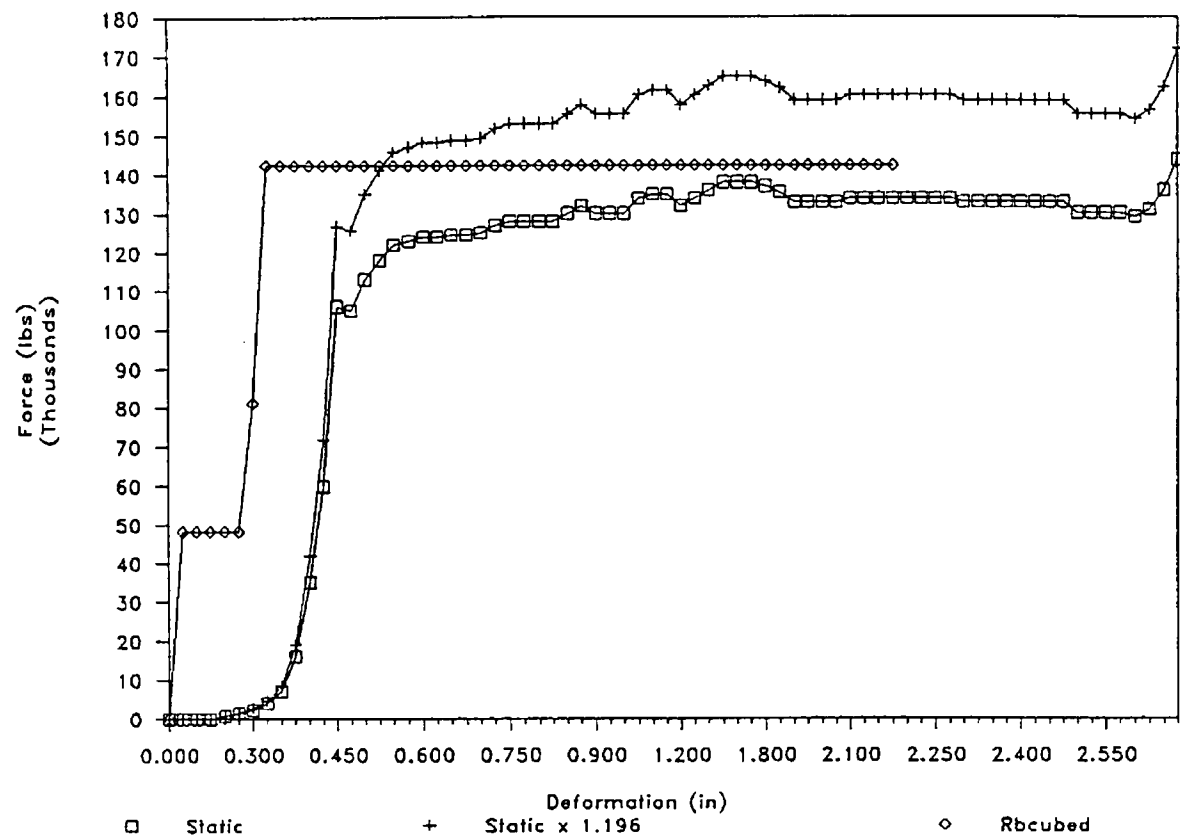


Figure 2.10.12-19 Force-Deflection Curve (14-Degree Impact, Drop Tested Limiter)

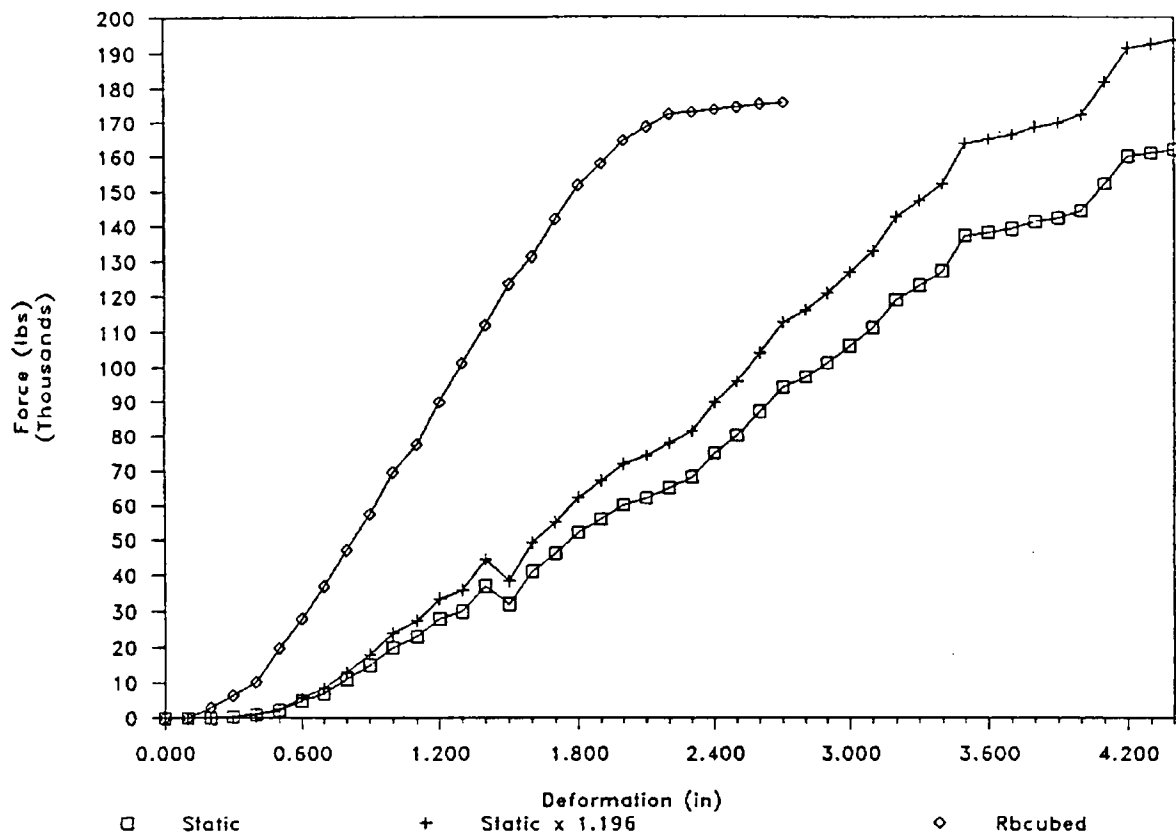


Figure 2.10.12-20 Force-Deflection Curve (90-Degree Impact, Drop Tested Limiter)

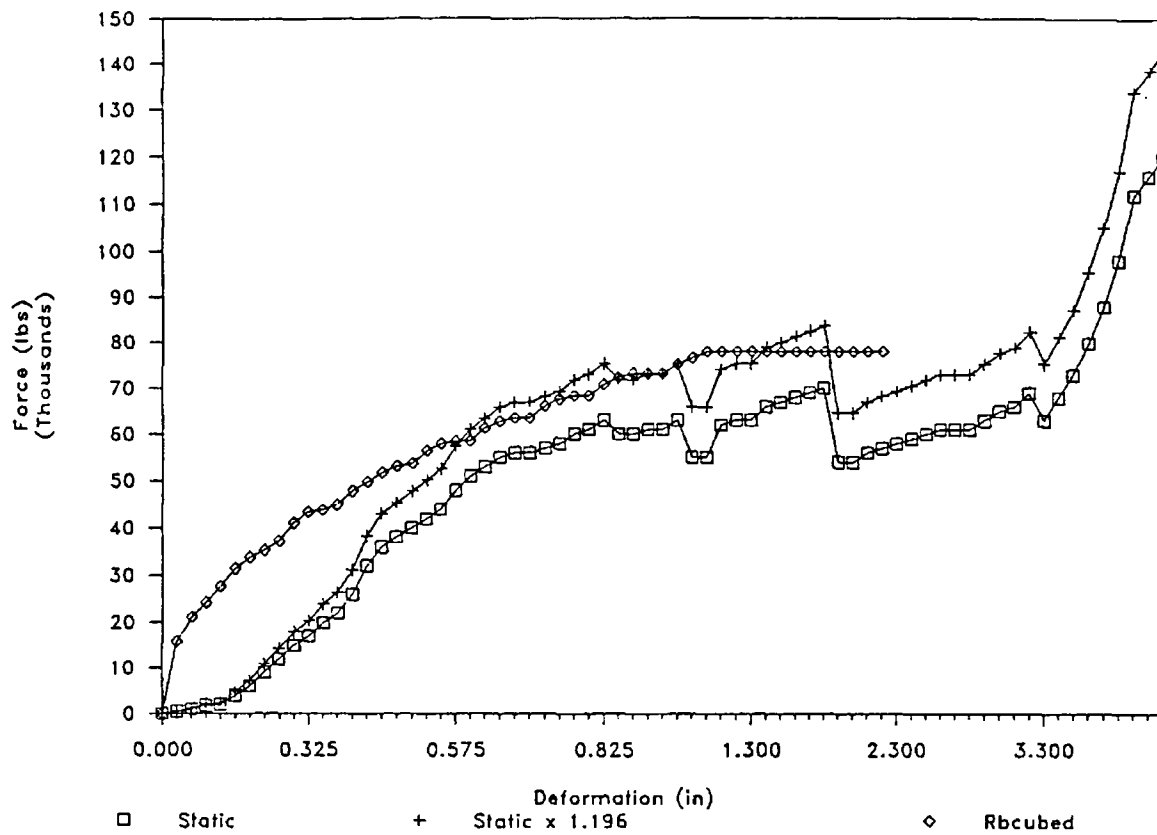


Figure 2.10.12-21 End Drop Impact Limiter Cross Section

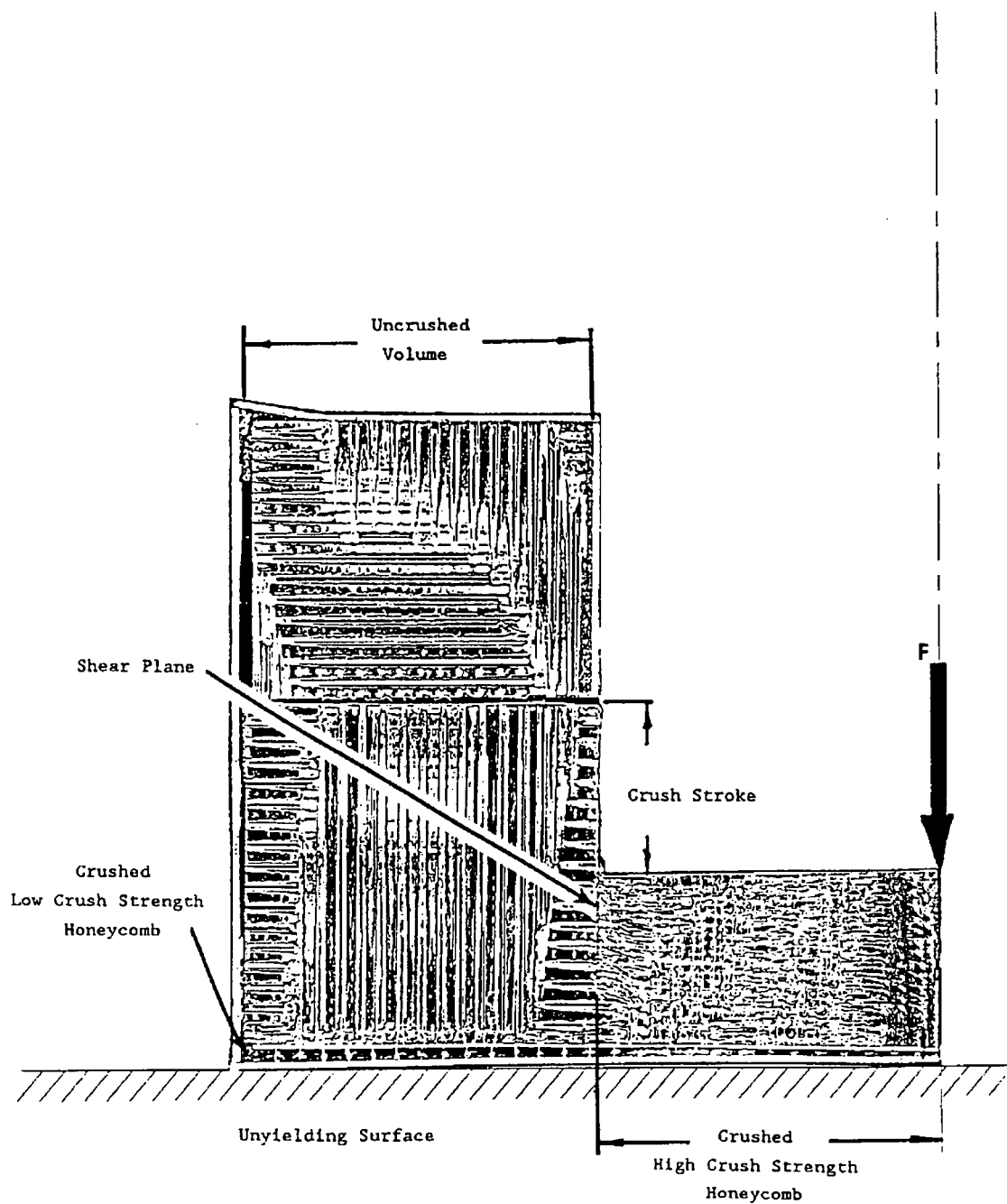


Table 2.10.12-1 Determination of Maximum Energy Remaining for Secondary Impact – Full-Scale Impact Limiter

DROP ANGLE (degrees)	0	15	30	45	60	75	90
E1 Energy absorbed by first limiter (in-lb)	1.93×10^7	1.88×10^7	1.74×10^7	1.52×10^7	1.23×10^7	1.03×10^7	9.67×10^6
ER Energy remaining after first impact (in-lb)	0.00	5.40×10^5	1.94×10^6	4.14×10^6	7.04×10^6	9.02×10^6	9.67×10^6
EP Potential energy of cask after first impact (in-lb)	6.04×10^6 ¹	4.97×10^6	4.40×10^6	3.45×10^6	2.21×10^6	7.68×10^5	0.00
ES Energy stored in first limiter; absorbed in second limiter in side drop orientation (in-lb)	1.87×10^6 (9.7%)	1.24×10^6 (6.6%)	1.04×10^6 (6.0%) ²	8.66×10^5 (5.7%) ²	6.77×10^5 (5.5%) ²	5.56×10^5 (5.4%) ²	5.13×10^5 (5.3%)
E2 Secondary impact total of ER + EP + ES (in-lb)	7.91×10^6	6.75×10^6	7.38×10^6	8.46×10^6	9.93×10^6	1.03×10^7	1.02×10^7
E _{max} – Side Drop Maximum energy absorption capability of impact limiter in side drop orientation (in-lb)	1.49×10^7	1.49×10^7	1.49×10^7	1.49×10^7	1.49×10^7	1.49×10^7	1.49×10^7
Energy Absorption Margin	88.32%	120.71%	101.79%	76.20%	50.10%	44.04%	46.33%

¹ Assumes tip-over of cask onto the second impact limiter.

² Interpolated values.

Table 2.10.12-2 Determination of Extreme Force During Cask Deceleration (First Limiter) – Quarter-Scale Impact Limiter

DROP ANGLE (degrees)	0	15	90
RBCUBED Average Maximum or Peak Force	142,340	175,710	78,070
Equivalent g Load	177.9	219.6	97.6
STATIC TEST – DROP-TESTED LIMITERS Dynamic Average Maximum or Peak Force	158,382	169,000	74,152
Equivalent g Load	198.0	211.3	92.7
FORCE MARGIN	-11.27%	3.82%	5.02%
CALCULATED STRESS MARGIN	200.00%	1.00%	6.00%
REVISED STRESS MARGIN*	188.73%	4.82%	11.02%

* Approximate stress margin, which includes the effect of impact limiter testing. Quarter-scale cask model weight = 800 lbs

2.10.13 Structural Evaluation of Failed Fuel Cans and Liners (Baskets)

This evaluation documents the thermal and structural adequacy of the failed fuel cans (FFCs) and liners (baskets) for a three-hole basket and a six-hole basket to be used for the transport of failed fuel and failed fuel filters in the NAC-LWT spent fuel shipping cask. The maximum normal operating temperature is calculated to be 214°F for the FFC in the six-hole basket, and 229°F for the FFC in the three-hole basket. Each FFC in the six-hole basket has been designed to contain a single failed fuel rod. Each FFC in the three-hole basket has been evaluated for up to three failed fuel rods per FFC (up to nine failed fuel rods per cask) or up to ten failed fuel filters (up to 30 failed fuel filters per cask). The conservatively calculated minimum margin of safety for any component is +0.24. The FFCs and liners are structurally adequate to satisfy all regulatory requirements.

2.10.13.1 Discussion

Nuclear Assurance Corporation has designed an FFC and three-hole basket that will permit up to nine encapsulated failed metallic fuel rods or up to 30 encapsulated failed fuel filters to be shipped in the NAC-LWT cask. A six-hole basket containing six smaller diameter FFCs has been evaluated based on a capacity of six failed fuel rods per cask. With either basket, the FFC is a sealed, dry aluminum canister. Up to three failed metallic fuel rods or up to ten failed fuel filters are placed in each FFC when the three-hole basket is used. Only one failed metallic fuel rod may be placed in each FFC if the six-hole basket is used.

Each metallic fuel rod is assumed to weigh 125 lbs (actual weight is 53 kg or 117 lbs) and is approximately 124 inches long. Each failed fuel filter is assumed to weigh 12 pounds and is approximately 11 inches long. The failed fuel rods have a maximum decay heat load of 5 watts per rod, resulting in a maximum decay heat load of 30 watts for the six-hole basket, and 45 watts for the three-hole basket. Each FFC containing up to 10 failed fuel filters is limited to the amount of fuel in a single metallic fuel rod resulting in a maximum decay heat load of 5 watts, or a total of 15 watts for the three-hole basket.

2.10.13.2 Method of Analysis

Thermal analyses were performed using the one-dimensional SCOPE computer program to determine the maximum normal operating temperature of the FFC and liner. A total decay heat load of 30 watts was used for the six-hole basket, and 45 watts for the three-hole basket. The maximum FFC temperature was 214°F for the six-hole basket, and 229°F for the three-hole

basket. A temperature of 250°F was conservatively used to determine the material properties of the FFCs and liners. The SCOPE inputs and outputs are provided in Section 3.6.

Classical stress analysis methods are used to evaluate the FFCs for buckling during the end impact and for bending during a side impact. The tubes in the liners are also analyzed for bending during a side impact. The impact loadings include the g-factors determined in Section 2.6.7.4. The calculated stresses in the FFCs and the liners are conservatively compared to the material yield strength to demonstrate that containment is maintained by the FFCs and that no permanent deformation of the FFCs or the liners occurs.

2.10.13.3 Input Geometry & Data

1. Total Heat Load = 30 Watts (For 6 Metallic Fuel Rods).
 = 45 Watts (For 9 Metallic Fuel Rods).
 = 15 Watts (For 30 Failed Fuel Filters).

2. Metallic Fuel Rod Weight = 125 lbs/Rod.
 Failed Fuel and Filter Weight = 12 lbs/Filter.

3. NAC-LWT Cask Geometry: (Ref. Section 1.4)
 Inner Shell (Cavity) I.D. = 13.375 inches
 Inner Shell Thickness = 0.75 inch
 Lead Shell Thickness = 5.75 inches
 Outer Shell Thickness = 1.20 inches
 Neutron Shield Thickness = 5.00 inches
 Neutron Shield Shell Thickness = 0.24 inch

4. Free Drop Impact G-Loads: (Ref. Table 2.6.7-33 and Table 2.6.7-34)

 Normal Operation¹
 1-Foot Side Drop 24.3 g

 Accident¹
 30-Foot Top End Drop 48.3 g
 30-Foot Bottom End Drop 48.1 g
 30-Foot Side Drop 49.7 g
 30-Foot Corner Drop 60.4 g

¹ Ref. 10 CFR 71 and Regulatory Guide 7.8.

2.10.13.4 Mechanical Properties of Materials

1. 6061-T6 Aluminum Alloy (Ref. MIL-HDBK-5E)
 $(S_u)_{70} = 42 \text{ ksi } (70^\circ\text{F})$ $(S_y)_{70} = 35 \text{ ksi } (70^\circ\text{F})$ (page 3-222)

At 250°F: $(S_u)_{250} = 0.86$ $(S_u)_{70} = 36.1 \text{ ksi}$ (page 3-227)
 $(S_y)_{250} = 0.88$ $(S_y)_{70} = 30.8 \text{ ksi}$ (page 3-228)
2. 6063-T832 Aluminum Alloy (Ref. ASME B210)
 $(S_u)_{70} = 40 \text{ ksi}$ $(S_y)_{70} = 35 \text{ ksi}$ (page 194)

At 250°F: $(S_u)_{250} = 0.86^1$ $(S_u)_{70} = 34.4 \text{ ksi}$
 $(S_y)_{250} = 0.88^1$ $(S_y)_{70} = 30.8 \text{ ksi}$
3. 6061-T6511 Aluminum Alloy (Ref. MIL-HDBK-5E)
 $(S_u)_{70} = 38 \text{ ksi}$ $(S_y)_{70} = 35 \text{ ksi}$ (page 3-225)

At 250°F: $(S_u)_{250} = 0.86^1$ $(S_u)_{70} = 32.7 \text{ ksi}$
 $(S_y)_{250} = 0.88^1$ $(S_y)_{70} = 30.8 \text{ ksi}$

2.10.13.5 Thermal Evaluation

The SCOPE thermal analysis computer program is used to evaluate the NAC-LWT cask containing the six-hole basket with six 2.75-inch inner diameter (I.D.) FFCs loaded with one metallic fuel rod each, for a total heat load of 30 watts. The maximum temperature for the FFC is 214°F. A similar analysis for the three-hole basket with three 4.00-inch I.D. FFCs loaded with three metallic fuel rods each for a total heat load of 45 watts, resulted in a maximum temperature of 229°F for the FFCs. This is the bounding maximum thermal case for the three-hole basket.

2.10.13.6 Structural Evaluation

The FFCs are evaluated to demonstrate that containment of the failed fuel rod or the failed fuel filters is maintained for all loading conditions. The maximum stress occurs in the shells of the FFCs for the 30-foot side drop load case. Buckling of the shells is evaluated for the 30-foot end drop load case.

¹ The strength variation with temperature is assumed to be the same as that for 6061-T6 Aluminum Alloy.

The liners (baskets) for the failed fuel cans are evaluated to demonstrate that rupture (ultimate failure) does not occur for any loading condition. The maximum stress occurs in the housing (tube) of the liners for the 30-foot side drop load case.

The drawings referenced in these evaluations are included as Figure 2.10.13-1 through Figure 2.10.13-5.

2.10.13.6.1 Failed Fuel Can – 2.75-Inch Inner Diameter

Shell – Bending

Ref. Dwg. 340-108-D2 (Figure 2.10.13-4)

Loading (temperature conservatively assumed - 250°F)

30-Foot Side Drop Acceleration = 49.7 g

Support Spacing = 33.66 inches (Ref. Dwg. 315-40-12)

Weight: Fuel = 125 lbs/124 inches = 1.008 lb/in

Shell = $(\pi/4)[(3.0)^2 - (2.75)^2](1)(0.10)$ = 0.113 lb/in

Total = 1.121 lb/in

Conservatively, assume the shell is simply supported at the support disks; then, the moment during impact is:

$$M = (1/8)(1.121)(33.66)^2 (49.7) = 7,890 \text{ in-lb}$$

Shell Properties:

$$I/C = 0.7791 \text{ in}^3$$

Material Properties: (ASTM B221 Type 6061-T6)

$$(S_y)_{250} = 30.8 \text{ ksi}$$

Stresses:

$$S_b = 7890/0.7791 = 10,127 \text{ psi}$$

$$MS = [(S_y)_{250}/S_b] - 1 = +2.04$$

Shell – Buckling

Estimated Weight of Can Assembly = 20 lbs

The maximum axial acceleration is for the corner drop

Top End Drop Deceleration = 48.3 g

Maximum axial acceleration $[\cos(15.74^\circ)](60.4) = 58.2 \text{ g}$

The compressive stress in the shell due to its weight during impact is:

$$S_c = \frac{(20)(58.2)}{\left[\frac{\pi}{4}\right](3.0)^2 - (2.75)^2} = 1,031 \text{ psi}$$

The margin of safety on yield is:

$$\text{M.S.} = \frac{30.8}{1.03} - 1 = +\underline{\text{Large}}$$

The buckling of the cylindrical shell under the action of uniform axial compression may be evaluated using equation 11-1 on page 458 of Theory of Elastic Stability by Timoshenko and Gere.

$$S_{cr} = \frac{Et}{r[3(1 - \nu^2)]^{0.5}}$$
$$= 267 \text{ ksi}$$

where:

$$E = (0.97)(10.1\text{E}03) = 9.8\text{E}03 \text{ ksi at } 250^\circ\text{F}$$

$$t = 0.125 \text{ in}$$

$$r = 2.81 \text{ inches, env. radius for all tubes in assembly}$$

$$\nu = 0.33$$

The margin of safety on buckling is:

$$\text{MS} = S_{cr}/S_c - 1 = +\underline{\text{Large}}$$

Conclusion

The stress in the cylindrical shell caused by a corner drop with an axial component of 58.2 g deceleration is much lower than the yield stress and the critical buckling stress.

2.10.13.6.2 Liner – Failed Fuel Can – 2.75 Inner Diameter

Housing – Bending

Ref. Dwg. 315-040-43 (Figure 2.10.13-2)

Loading (temperature conservatively assumed - 250°F)

$$30\text{-Foot Side Drop Deceleration} = 49.7 \text{ g}$$

$$\text{Support Spacing} = 33.66 \text{ inches}$$

$$\begin{aligned}
 \text{Weight: Fuel} &= 125 \text{ lbs}/124 \text{ inches} = 1.008 \text{ lb/in} \\
 \text{Aluminum Shell} &= [\pi/4][(3)^2 - (2.75)^2](1)(0.10) = 0.113 \text{ lb/in} \\
 \text{Housing} &= [\pi/4][(3.75)^2 - (3.5)^2](1)(0.10) = \underline{0.142 \text{ lb/in}} \\
 \text{Total} &= 1.263 \text{ lb/in}
 \end{aligned}$$

Conservatively, assume the housing is simply supported at the support disks; then, the moment during impact is:

$$M = (1/8)(1.263) (33.66)^2 (49.7) = 8,890 \text{ in-lb}$$

Housing Properties:

$$\begin{aligned}
 I/C &= (\pi)(d_o^4 - d_i^4) / 32d_o \\
 &= (\pi) [3.75^4 - (3.5)^4] / (32)(3.75) = 1.2485 \text{ in}^3
 \end{aligned}$$

Material Properties: (ASTM B210 Type 6063-T832)

$$(S_y)_{250} = 30.8 \text{ ksi}$$

Stresses:

$$S_b = 8,890 / 1.2485 = 7121 \text{ psi}$$

$$MS = [(S_y)_{250} / S_b] - 1 = +3.32$$

Weld Between Bulkhead and Tubes

Peak Deceleration = 60.0 g (Ref. Table 2.6.7-34, 30-Foot End Drop)

Ref. Dwg. 315-040-43 (Figure 2.10.13-2)

$$\begin{aligned}
 \text{Weight of 1 Bulkhead} &= (\pi/4)[(13)^2 - (6)(2.75)^2](1/4)(0.1) \\
 &= 2.4 \text{ lbs}
 \end{aligned}$$

$$\text{Weight of U-Bolts} = \underline{1.6 \text{ lbs}}$$

$$\text{Total} = 4.0 \text{ lbs}$$

$$\text{Inertial load of bulkhead on welds: } P_{act} = (4)(60) = 240 \text{ lbs}$$

$$\text{Total length of weld per bulkhead: } L_w = (4)(6) + (2)(3) = 30 \text{ inches}$$

$$\text{Size of fillet} = 1/8 \text{ in}$$

$$\text{Assume } F_u \text{ of aluminum weld:} = 4,000 \text{ psi}$$

$$\text{Allowable shear stress} = (0.3)(4,000) = 1,200 \text{ psi}$$

(Ref. AISC Manual of Steel Construction, 8th Ed., Section 1.5.3)

$$\begin{aligned}\text{Working capacity of welds} &= P_{\text{cap}} \\ &= (0.707)(1/8)(30)(1200) \\ &= 3,180 \text{ lbs}\end{aligned}$$

$$\text{M.S.} = [P_{\text{cap}} / P_{\text{act}}] - 1 = 3,180/240 - 1 = +\text{Large}$$

The other accident drop conditions are:

$$30\text{-Foot Top End Drop} \quad a = 48.3 \text{ g}$$

$$30\text{-Foot Bottom End Drop} \quad a = 48.1 \text{ g}$$

$$30\text{-Foot Top Corner Drop} \quad a = 60.4 \text{ g}$$

Compared to a 30-foot side drop accident condition, with $a = 49.7 \text{ g}$, the above accident conditions are less critical. Therefore, neither rupture nor yielding of the liner housing will occur.

2.10.13.6.3 Failed Fuel Rod Can – 4.00 Inner Diameter (3 Failed Fuel Rod Loading)

Shell – Bending

Ref. Dwg. 340-108-DI (Figure 2.10.13-3)

Loading (Temperature conservatively assumed - 250°F)

$$\begin{aligned}30\text{-Foot Side Drop Acceleration} &= 49.7 \text{ g} \\ \text{Support Spacing} &= 50.37 \text{ inches} \\ \text{Weight: Fuel} &= (125 \text{ lbs}/124 \text{ inches})(3) = 3.024 \text{ lb/in} \\ \text{Shell} &= [\pi/4][(4.25)^2 - (4.0)^2](1)(0.10) = 0.162 \text{ lb/in} \\ \text{Total} &= 3.186 \text{ lb/in}\end{aligned}$$

Conservatively, assume the shell is simply supported at the support disks at four locations with the maximum spacing of 50.37 inches. The moment during impact, by Case 36 of the AISC steel manual, is:

$$M = (0.100)(3.186)(50.37)^2(49.7) = 40,174 \text{ in-lb}$$

Shell Properties:

$$I/C = (\pi)[(4.25)^4 - (4)^4]/(32)(4.25) = 1.623 \text{ in}^3$$

Material Properties: (ASTM B210 Type 6061 T6)

$$(S_y)_{250} = 30.8 \text{ ksi}$$

Stresses:

$$S_b = 40,174/1.623 = 24,753 \text{ psi}$$

$$\text{M.S.} = [(S_y)_{250}/S_b] - 1 = +0.24$$

2.10.13.6.4 Liner – 3 Element NAC-LWT Cask (3 Failed Fuel Rods/Can)

Tube - Bending

Ref. Dwg. 315-040-12 (Figure 2.10.13-1)

Loading

$$30\text{-Foot Side Drop Acceleration} = 49.7 \text{ g}$$

$$\text{Support Spacing} = 50.37 \text{ inches}$$

$$\text{Weight: Fuel} = (125 \text{ lbs}/124 \text{ inches})(3) = 3.024 \text{ lb/in}$$

$$\text{Shell} = [\pi/4][(4.25)^2 - (4.0)^2](1)(0.10) = 0.162 \text{ lb/in}$$

$$\text{Tube} = [\pi/4][(5.625)^2 - (5.375)^2](1)(0.1) = 0.216 \text{ lb/in}$$

$$\text{Total} = 3.402 \text{ lb/in}$$

Conservatively, assume the tube is simply supported at the support disks; then, the moment during impact is:

$$M = (1/8)(3.402)(50.37)^2 (49.7) = 53,622 \text{ in-lb}$$

Tube Properties:

$$I/C = (\pi)[(5.625)^4 - (5.375)^4]/(32)(5.625) = 2.9053 \text{ in}^3$$

Material Properties: (ASTM B210 Type 6061-T6)

$$(S_y)_{250} = 30.8 \text{ ksi}$$

Stresses:

$$S_b = 53,622/2.9053 = 18,457 \text{ psi}$$

$$\text{M.S.} = [(S_y)_{250}/S_b] - 1 = +0.67$$

Weld Between Bulkhead and Tubes

Ref. Dwg. 315-40-12 (Figure 2.10.13-1)

$$\text{Peak Deceleration} = 60.0 \text{ g (30-Foot End Drop)}$$

$$\begin{aligned}\text{Weight of Bulkhead} &= [\pi/4][(13)^2 - (3)(5.625)^2](1/4)(0.1) \\ &= 1.5 \text{ lbs}\end{aligned}$$

$$\text{Weight of U-Bolts} = 1.5 \text{ lbs}$$

$$\text{Total} = 3.0 \text{ lbs}$$

$$\text{Inertial load of bulkhead on welds: } P = (3.0)(60) = 180 \text{ lbs}$$

$$\text{Total length of weld per bulkhead: } L_w = (3)(3.0) = 9.0 \text{ in min}$$

$$\text{Size of fillet} = 3/32 \text{ in}$$

$$\begin{aligned}\text{Working capacity of welds: } P_{cap} &= (0.707)(3/32)(9.0)(1200) \\ &= 716 \text{ lbs}\end{aligned}$$

$$\text{M.S.} = [P_{cap}/P_{act}] - 1 = 716/180 - 1 = +2.98$$

2.10.13.6.5 Failed Fuel Rod Can – 4.00 Inner Diameter (Ten Failed Fuel Filter Elements/Can)

Shell - Bending

Ref. Dwg 340-108-DI, (Figure 2.10.13-3)

Ref. Dwg 491-042, (Figure 2.10.13-5)

Loading

$$\text{30-Foot Side Drop Acceleration} = 49.7 \text{ g}$$

$$\text{Support Spacing} = 50.37 \text{ inches}$$

$$\text{Weight: Fuel} = 12 \text{ lbs}/11.2 \text{ inches} = 1.071 \text{ lb/in}$$

(Assumed to be effectively a distributed load; actual loading will occur near the ends of each failed fuel filter element)

$$\text{Shell} = \frac{\pi}{4}((4.25)^2 - (4.0)^2)(1)(0.10) = \underline{0.162 \text{ lb/in}}$$

$$\text{Total} = 1.233 \text{ lb/in}$$

Conservatively, assume the shell is simply supported at the support disks; then, the moment during impact is:

$$\begin{aligned}M &= \frac{1}{8}(1.233)(50.37)^2(49.7) \\ &= 19,435 \text{ in-lb}\end{aligned}$$

Shell Properties: (4.00 I.D., t = 0.125 in)

$$\begin{aligned} I/C &= [\pi][(4.25)^4 - (4)^4]/[(32)(4.25)] \\ &= 1.623 \text{ in}^3 \end{aligned}$$

Material Properties: (ASTM B221 Type 6061 T6)

$$(S_y)_{250} = 30.8 \text{ ksi}$$

Stresses:

$$S_b = 19,435/1.623 = 11,974 \text{ psi}$$

$$\text{M.S.} = [(S_y)_{250} / S_b] - 1 = +1.57$$

2.10.13.6.6 Liner - 3 Element (Ten Failed Fuel Filter Elements/Can)

Tube - Bending

Ref. Dwg 315-040-12, (Figure 2.10.13-1)

Ref. Dwg 491-042, (Figure 2.10.13-5)

Loading

30-Foot Side Drop Acceleration = 49.7 g

Support Spacing = 50.37 inches

$$\text{Weight: Fuel} = 12 \text{ lbs}/11.2 \text{ inches} = 1.071 \text{ lb/in}$$

$$\text{Shell} = \frac{\pi}{4}((4.25)^2 - (4.0)^2)(1)(0.10) = 0.162 \text{ lb/in}$$

$$\text{Tube} = \frac{\pi}{4}((5.625)^2 - (5.375)^2)(1)(0.1) = 0.216 \text{ lb/in}$$

$$\text{Total} = 1.449 \text{ lb/in}$$

Conservatively assume the tube is simply supported at the support disks; then, the moment during impact is:

$$\begin{aligned} M &= \frac{1}{8}(1.449)(50.37)^2(49.7) 8 \\ &= 22,839 \text{ in-lb} \end{aligned}$$

Tube Properties:

$$\begin{aligned} I/C &= [\pi][(5.625)^4 - (5.375)^4]/[(32)(5.625)] \\ &= 2.9053 \text{ in}^3 \end{aligned}$$

(The FFC is conservatively not considered to provide any bending strength for this analysis.)

Material Properties: (ASTM B210 Type 6061-T6)

$$(S_y)_{250} = 30.8 \text{ ksi}$$

Stresses:

$$S_b = 22,839/2.9053 = 7861 \text{ psi}$$

$$\text{M.S.} = [(S_y)_{250} / S_b] - 1 = +2.91$$

2.10.13.7 Results and Conclusion

The maximum normal operating temperature of the failed fuel cans and the liner (basket) is calculated to be 211°F. The structural evaluation conservatively uses material properties at 250°F.

The calculated margins of safety are:

1. Failed Fuel Can - 2.75 Inner Diameter
 - Shell – Bending +2.04
 - Shell – Buckling +Large
2. Liner - Failed Fuel Can - 2.75 Inner Diameter
 - Housing – Bending +3.32
 - Weld - Bulkhead/Tube +Large
3. Failed Fuel Rod Can - 4.00 Inner Diameter (3 Failed Fuel Rod Loading)
 - Shell – Bending +0.24
4. Liner - 3-Element (3 Failed Fuel Rods/Can)
 - Tube – Bending +0.67
 - Weld - Bulkhead/Tube +2.98
5. Failed Fuel Rod Can - 4.00 Inner Diameter (10 Failed Fuel Filter Elements/Can)
 - Shell – Bending +1.57
6. Liner - 3-Element (10 Failed Fuel Filter Elements/Can)
 - Tube - Bending + 2.91

No permanent deformation occurs in the failed fuel cans or the liners for the critical loading conditions. Containment of the failed metallic fuel rods and failed fuel filters is maintained and the liner structure remains intact; therefore, structural adequacy is ensured.

2.10.13.8 Failed Fuel Shipment Component Drawings

The drawings referenced in Section 2.10.13.6 in support of analyses associated with the transport of failed fuel rods or filters containing severely failed fuel are provided in this section.

- NAC Drawing: 340-108-D1, Failed Fuel Rod Can - 4.00 I.D., Fuel Rod Containerization
- NAC Drawing: 340-108-D2, Failed Fuel Rod Can - 2.75 I.D., Fuel Rod Containerization
- NAC Drawing: 315-40-12, LWT Cask Metal Fuel Basket Assembly Safety Analysis Report
- NAC Drawing: 315-040-43, Liner - Failed Fuel Can, 2.75 I.D., LWT Cask, Safety Analysis Report
- NAC Drawing: 491-042, Failed Fuel Filter

Figure 2.10.13-1 LWT Cask, Metal Fuel Basket Assembly Safety Analysis Report, NAC Drawing No. 315-40-12

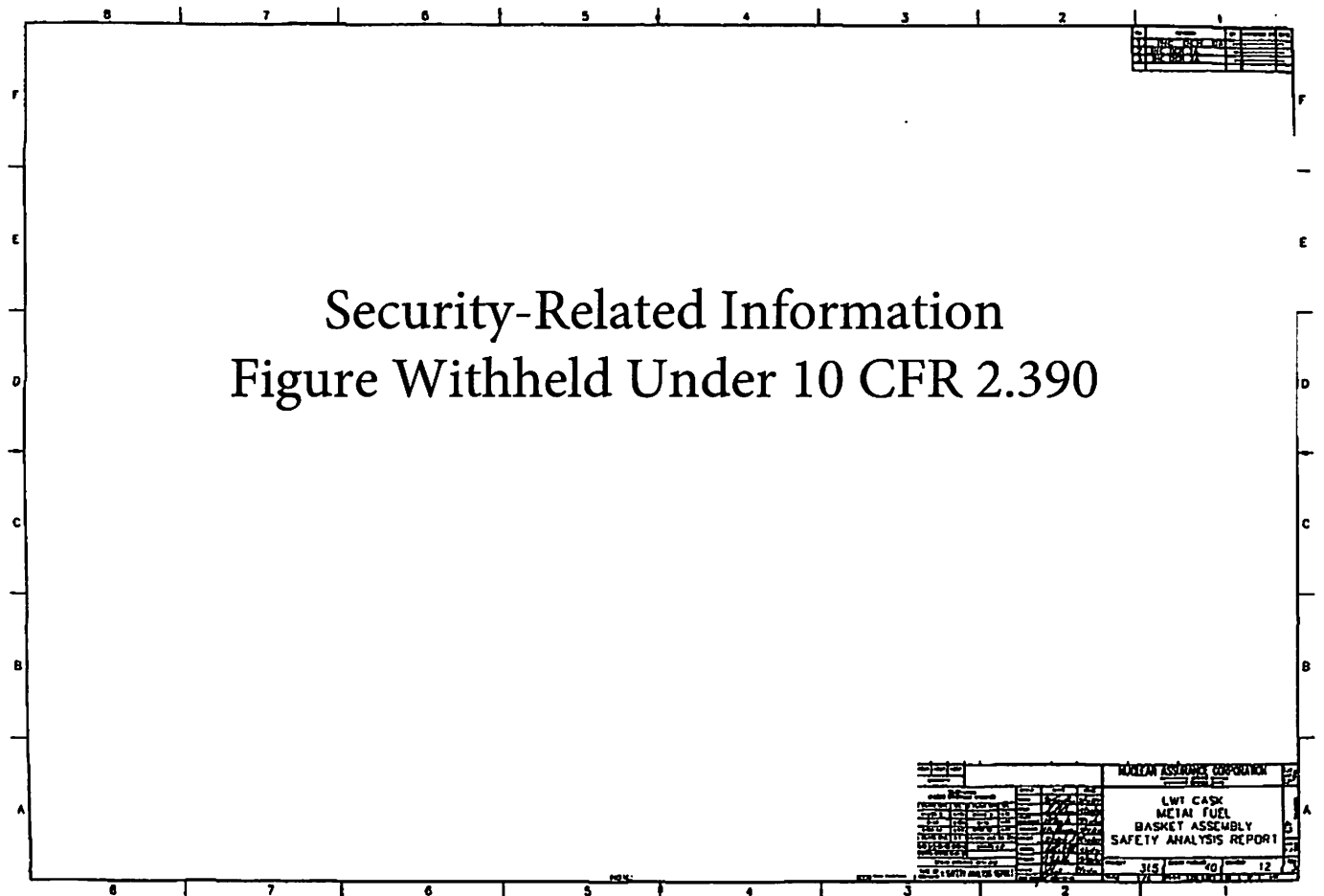
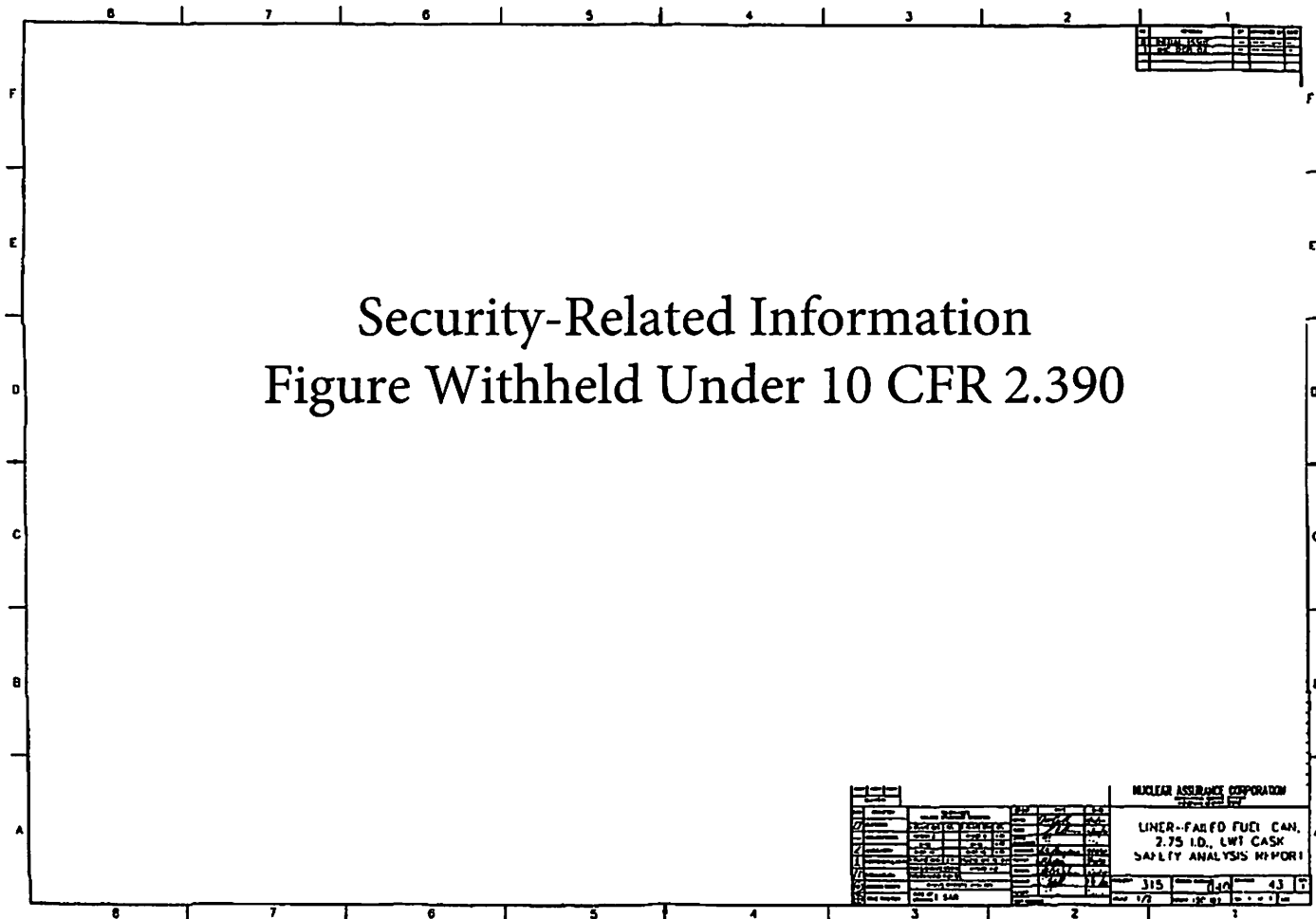


Figure 2.10.13-2 Liner-Failed Fuel Can, 2.75 I.D., LWT Cask, Safety Analysis Report, NAC Drawing No. 315-040-43



Security-Related Information
Figure Withheld Under 10 CFR 2.390

Figure 2.10.13-4 Failed Fuel Rod Can – 2.75 I.D., Fuel Rod Containerization, NAC Drawing No. 340-108-D2

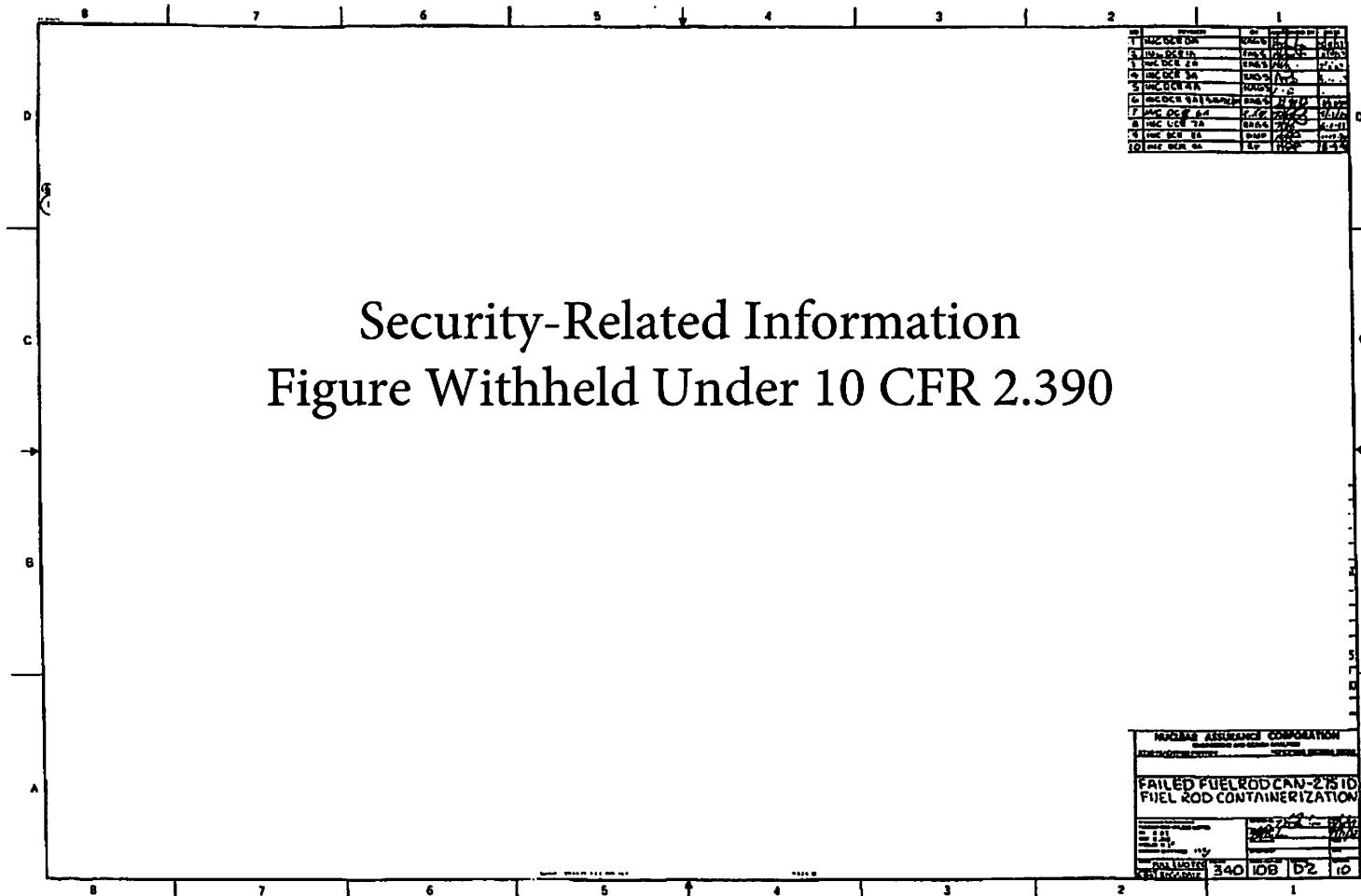
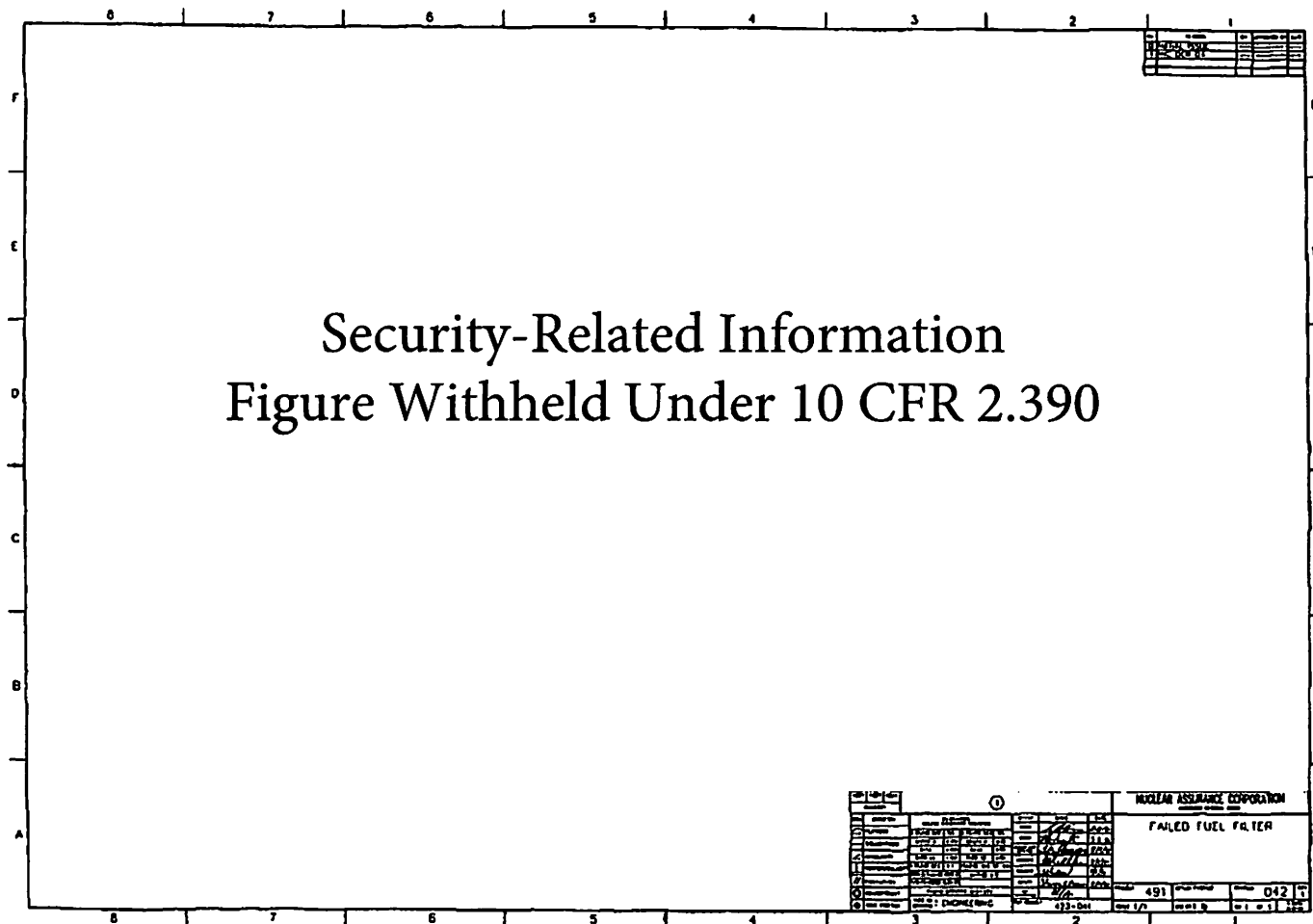


Figure 2.10.13-5 Failed Fuel Filter, NAC Drawing No. 491-042



2.10.14 Structural Evaluation of the NAC-LWT Cask Body with TPBAR Contents

This section presents a structural evaluation of the NAC-LWT cask system with TPBAR contents under normal conditions of transport and hypothetical accident conditions. The NAC-LWT cask system with TPBARs is comprised of four primary components: NAC-LWT cask body, TPBAR basket, basket spacers, and TPBAR contents. The NAC-LWT cask system is structurally evaluated for two TPBAR content conditions: up to 300 production TPBARs loaded into an open (i.e., unsealed) consolidation canister; and up to 55 segmented TPBARs loaded into a welded closed waste container.

The NAC-LWT cask system containing TPBAR contents is required to have the Alternate B port covers installed and tested on the vent and drain ports to assure a leaktight containment boundary during transport. Section 2.10.15 presents the structural evaluation of the Alternate B port cover. Sections 2.6.12.10 and 2.7.7.12 present the structural evaluation for the TPBAR basket and basket spacers for the transport of the TPBAR content conditions under normal conditions of transport and hypothetical accident conditions, respectively.

2.10.14.1 Normal Conditions of Transport for Cask Body with TPBAR Contents

This section provides the cask body structural evaluation for normal conditions of transport. The following sections discuss the governing conditions of hot, cold, and drop conditions for normal transport.

2.10.14.1.1 Hot and Cold Conditions

Hot and cold conditions, as defined in 10CFR 71.71 (c) (1) and (2), are evaluated as part of the normal conditions of transport for a 1-foot free-drop evaluation (see Section 2.10.14.1.2). Since the 1-foot drop evaluations include the inertial loads and a bounding thermal load, the 1-foot drop evaluation bounds the evaluation for hot and cold conditions.

2.10.14.1.2 Free Drop (1 Foot)

The normal conditions drop orientations considered are: side drop, top-end drop, bottom-end drop, top-end CG-over-corner drop, and bottom-end CG-over-corner drop. Corner drops are defined as the CG of the cask over the impact limiter corner (15.74° from vertical).

Finite Element Model Description

A three-dimensional half-symmetry model of the LWT cask body is constructed using ANSYS solid elements (SOLID45). The finite element model contains the top and bottom forgings, cask

sidewalls, lead shielding, cask lid and bolts. The cask shells are modeled using SA-240 Type XM-19 stainless steel material properties. The cask top and bottom forgings and cask lid are modeled using SA182 Type 304 stainless steel forging material properties. The model is shown in Figure 2.10.14-1 through Figure 2.10.14-3.

The neutron shield tank and water inside the neutron shield tanks are represented with ANSYS MASS21 elements (approximately 5,600 lbs for entire cask, 2,000 lbs for tanks, and 3,600 lbs for the water). For the end drops, the MASS21 elements are applied around the outer circumference (0°–180°) of the LWT cask. For the side and corner drops, the MASS21 elements are applied to the lower half of the outer circumference (0°–90°) of the outer shell. As a modeling convenience, a small hole is modeled in the center of the lid and bottom of the cask. Symmetry boundary conditions are applied to the plane of symmetry of the cask body model. The lid bolts are modeled using beam elements (BEAM4). The preload of 35,000 lbs per bolt is modeled by applying an initial strain to the beam elements. The applied strain is 0.00273 in/in.

The lead is considered a soft material when compared with the stainless steel shells. To simulate the interface between lead and the stainless steel shells, a small gap of 0.015 inch is modeled using ANSYS CONTAC52 gap elements. Gap elements are also modeled between the lid and top forging and between the cask and the impact limiters. The interface between the cask and impact limiters simulates the pressure applied by the impact limiters during drop conditions. The gap stiffness is modeled as a cosine distribution from a maximum value of 1.0×10^6 lb/in at the line of impact to a value of 1.31×10^5 lb/in at an angle of 82.5° from the line of impact. A minimal value of 100 lb/in is used from 90° to 180°.

Inertia loads of 25 g for side drop and 20 g for the end and corner drops are used in the cask body evaluation for normal conditions. For all drop cases, a conservative internal pressure of 300 psig is applied on the cask cavity and lid interior surfaces in the outward normal direction. The pressure bounds the MNOP of 289 psig for normal conditions of transport (Section 3.4.4.4). The weight of the contents (basket, consolidation canister, and TPBARs) is also applied as a concentrated pressure loading over a single row of elements (7.5°) for side and corner drops. For end drops, the contents weight is applied to either the cask lid or bottom forging as appropriate. For other drop orientations, pressure is applied on the appropriate surface, depending on the drop angle.

To calculate the thermal stresses in the cask, the temperature results from the design basis PWR fuel configuration are used to derive a conservative temperature gradient for the calculation of thermal stresses. The heat load for the design basis PWR fuel of 2.5 kW is greater than the heat load for the TPBAR configuration (< 0.7 kW) and, therefore, the analysis is conservative. A temperature of 227°F is applied to the cask lid and top forging regions. At the axial center of the inner and outer shells, a temperature of 274°F and 229°F is applied, respectively. For the bottom

of the cask and interface with the inner and outer shells, a temperature of 239°F is used. Using these temperatures as input, a thermal conduction solution is obtained using the finite element model described in this section, with the exception that the ANSYS SOLID45 structural elements are replaced with the equivalent SOLID70 thermal elements. Once calculated, the temperatures from the thermal conduction solution are applied as a boundary condition to the cask body structural model to calculate thermal stresses.

Finite Element Analysis Result Summary

The most crucial sections for each cask component are shown in Figure 2.10.14-4. Table 2.10.14-1 shows the material designation at each section location. The maximum P_m , $P_m + P_b$, and $P+Q$ stresses for each component are reported in Table 2.10.14-2 through 2.10.14-16 for the different drop orientations. Allowable stresses are conservatively reported at a temperature of 250°F. Margins of Safety greater than +10 are reported as “+Large.”

The minimum margin of safety is +0.13, which occurs at section 2 for the condition of P_m stress for 1-foot side-drop conditions. This section is located at the axial center of the cask outer shell. The minimum margins of safety for each stress category for 1-foot drop conditions are as follows.

Stress Category	Section	Drop Orientation	Stress Intensity, ksi	Stress Allowable, ksi	Margin of Safety
P_m	2	Side	28.57	32.3	+0.13
$P_m + P_b$	2	Side	32.87	48.45	+0.47
$P+Q$	18	Side	31.3	60.0	+0.93

2.10.14.2 Hypothetical Accident Conditions for Cask Body with TPBAR Contents

This section provides the cask body structural evaluation for hypothetical accident conditions. The following sections discuss drop conditions and inner shell buckling.

2.10.14.2.1 Free Drop (30-Foot)

The hypothetical accident conditions drop orientations considered are: side drop, top-end drop, bottom-end drop, top-end CG-over-corner drop, and bottom-end CG-over-corner drop. Corner drops are defined as the CG of the cask over the impact limiter corner (15.74° from vertical).

Finite Element Model Description

The finite element model is described in Section 2.10.14.1.2. For accident conditions, an acceleration of 60 g is applied to all drop orientations. The temperature-dependent material properties presented in Section 2.3 are used in the analysis.

Finite Element Analysis Result Summary

The most critical sections for each cask component are shown in Figure 2.10.14-4. Table 2.10.14-1 shows the material at each section location. The maximum P_m and $P_m + P_b$ stresses for each component are reported in Tables 2.10.14-17 through 2.10.14-26 through for different drop conditions. Allowable stresses are reported at a temperature of 250°F. Margins of Safety greater than +10.0 are reported as “+Large.”

The minimum margin of safety is +0.02, which occurs at section 2 for the condition of P_m stress, for 30-foot drop conditions. This section is located at the axial center of the cask outer shell. The minimum Margins of Safety for each stress category for 30-foot drop conditions are as follows.

Stress Category	Section	Drop Orientation	Stress Intensity, Ksi	Stress Allowable, ksi	Margin of Safety
P_m	2	Side	66.5	67.83	+0.02
P_m+P_b	2	Side	74.14	96.9	+0.31

2.10.14.2.2 Fire Accident

A finite element analysis is performed using the three-dimensional model as described in Section 2.10.14.1.2 for the evaluation of the fire accident conditions. The maximum calculated internal pressure for the fire accident is 337 psig (Section 3.5.4.4). A bounding internal pressure of 600 psig is conservatively used in combination with the inertial load in the model. The maximum P_m and P_m+P_b stresses for each cask component are presented in Table 2.10.14-27 and Table 2.10.14-28. The minimum Margin of Safety is +7.38 and +8.32 for the P_m and P_m+P_b stresses, respectively.

2.10.14.3 Inner Shell Buckling

Section 2.10.6 presents a buckling evaluation of the cask inner shell per ASME Code Case N-284 for the design basis cask configuration. The evaluation presented in Section 2.10.6 bounds the TPBAR contents based on the following.

- The maximum weight of the TPBAR contents of 1,000 lbs is enveloped by the weight of the design basis contents, which would reduce the compressive stresses in the cask shells due to less inertia loading for the drop conditions.
- The cask internal pressure for the TPBAR contents is significantly higher than the cask internal pressure for the design basis contents. The increase in the pressure would increase the tensile stresses in the shell that result in stiffening of the inner shell and, consequently, in reducing the compressive stresses associated with buckling.

The interaction summary presented in Table 2.10.6-10, associated with the design basis weight and the design basis pressure, is bounding for the TPBAR content conditions. Therefore, it is

concluded that the cask inner shell will not buckle with the TPBAR contents in the NAC-LWT cask.

2.10.14.4 NAC-LWT Cask Closure Lid and Bolts

The NAC-LWT cask closure lid is bolted to the cask body top forging with twelve 1-8 UNC bolts fabricated from SA-453, Grade 660 high-alloy steel. The threaded portion of the bolt engages the cask body a minimum of 1.875 inches. From Section 2.1.3.2.2, the torque on the cask lid bolts is 260 ± 20 ft-lb and the bolt preload is specified as 34,843 lbs. For the LWT cask configured to ship TPBARs, the maximum internal pressure of 600 psig is conservatively used in the closure lid evaluation. This pressure bounds the maximum pressure during the fire accident contained in Section 3.5.4.4. To ensure that the seal is not unloaded during accident conditions, the preload is calculated to account for the weight of the lid, internal weight of the cask contents, force resulting from internal pressure, force resulting from compression of the TFE O-ring, and force resulting from compression of the metallic O-ring. The load resulting from the weight of the LWT cask contents is

$$F_2 = W_c a = 1,800 \times 60g = 108,000 \text{ lbs}$$

where:

$$W_c = 1,800 \text{ lbs (bounding weight of TPBAR basket and contents)}$$

$$a = 60 g \text{ (maximum accident acceleration)}$$

The load resulting from accident pressure (fire accident) is:

$$F_{ip} = P_{ip} A = 600 \times 171.36 = 102,816 \text{ lbs}$$

where:

$$P_{ip} = 600 \text{ psig (accident internal pressure)}$$

$$A = \frac{\pi}{4} \times 14.771^2 = 171.36 \text{ in}^2$$

The total required bolt preload force (12 bolts) is:

$$\begin{aligned} FT &= F_1 + F_2 + F_{tr} + F_{mr} + F_{ip} \\ &= 56,460 + 108,000 + 2,474 + 79,470 + 102,816 = 349,220 \text{ lbs} \end{aligned}$$

where:

$$F_{tr} = 2,474 \text{ lbs, TFE O-ring load (Section 2.1.3.2.2)}$$

$$F_{mr} = 79,470 \text{ lbs, Metallic O-ring load (Section 2.1.3.2.2)}$$

$$F_l = 56,460 \text{ lbs, Lid load (Section 2.1.3.2.2)}$$

The required bolt preload per bolt is:

$$F_{\text{bolt}} = \frac{F_T}{12} = \frac{349,220}{12} = 29,102 \text{ lbs} < 34,843 \text{ lbs (Section 2.1.3.2.2)}$$

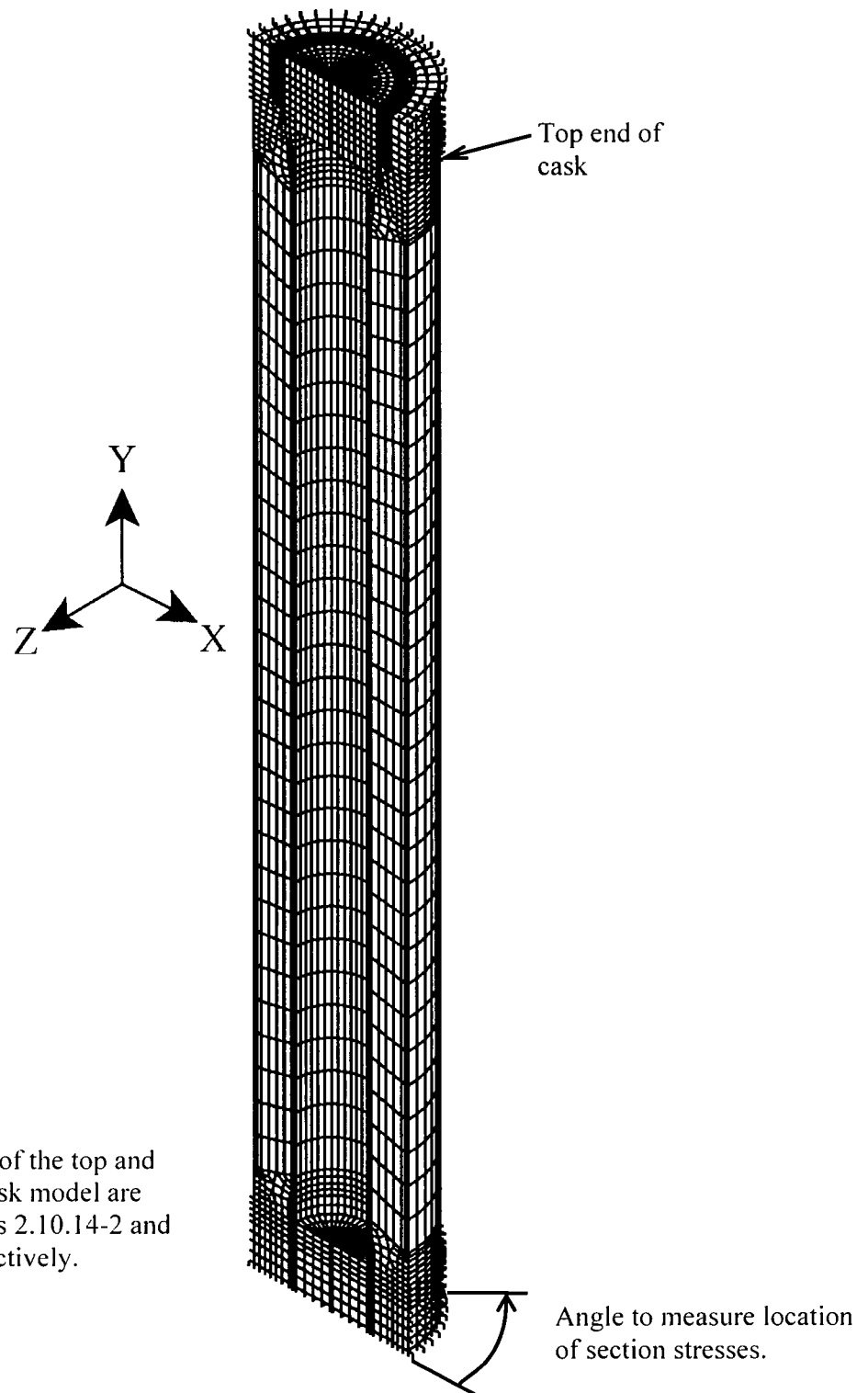
Since the bolt preload presented in Section 2.1.3.2.2 of the NAC-LWT is bounding, no further analysis of the LWT lid bolts is required.

The preload applied to the cask lid bolts is due to the load applied to the lid. The load applied to the lid for the design basis weight and pressure for the PWR fuel bounds the load applied to the lid for the TPBAR contents. Therefore, the stresses in the cask lid due to the design basis weight and pressure also bound the stresses in the cask lid due to the TPBAR content weight and pressure.

2.10.14.5 Conclusion

Based on the evaluations presented in Sections 2.10.14.1 through 2.10.14.4, the NAC-LWT cask with TPBAR contents satisfies the requirements of 10 CFR 71 for the normal conditions of transport and for hypothetical accidents.

Figure 2.10.14-1 ANSYS Finite Element Model of the Cask Body



Note:
A detailed view of the top and
bottom of the cask model are
shown in Figures 2.10.14-2 and
2.10.14-3, respectively.

Figure 2.10.14-2 Detailed View of the Cask Body Finite Element Model Top

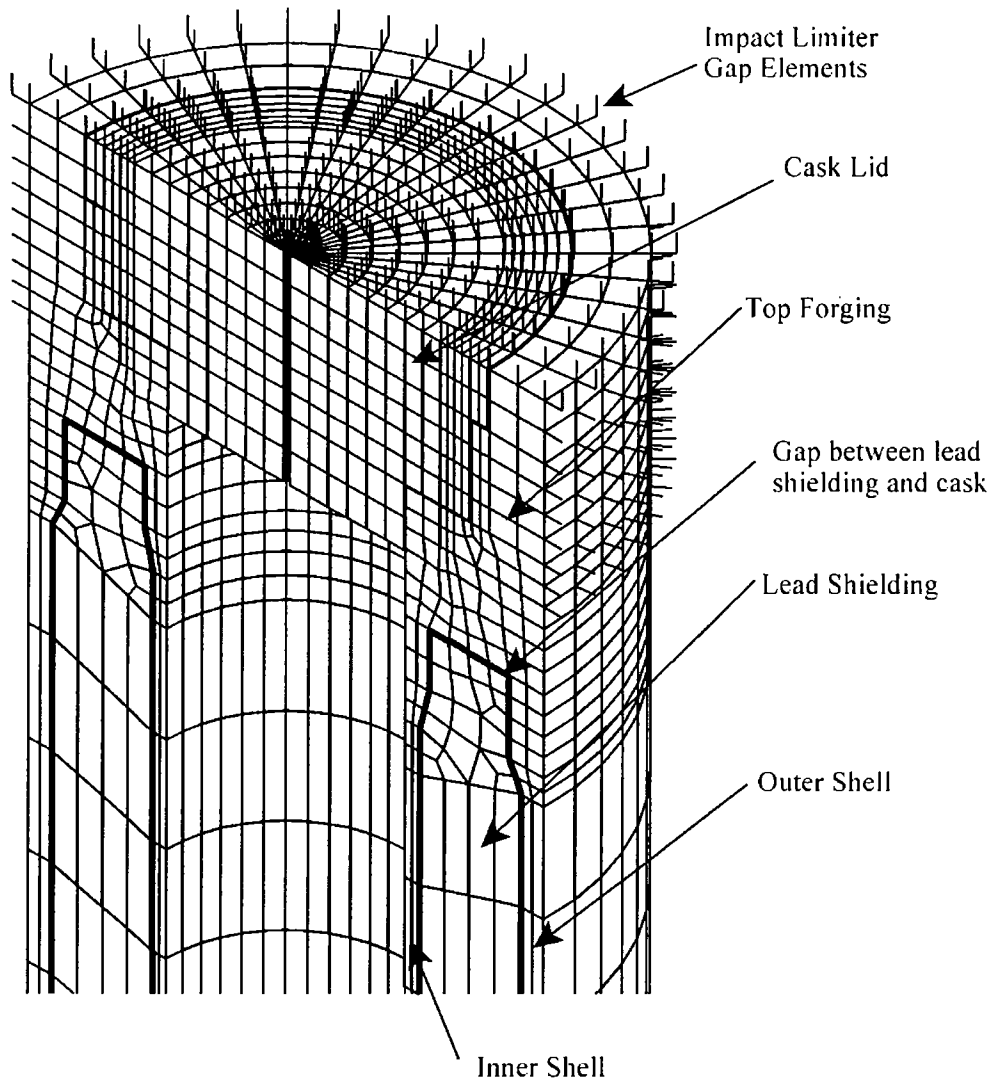


Figure 2.10.14-3 Detailed View of the Cask Body Finite Element Model Bottom

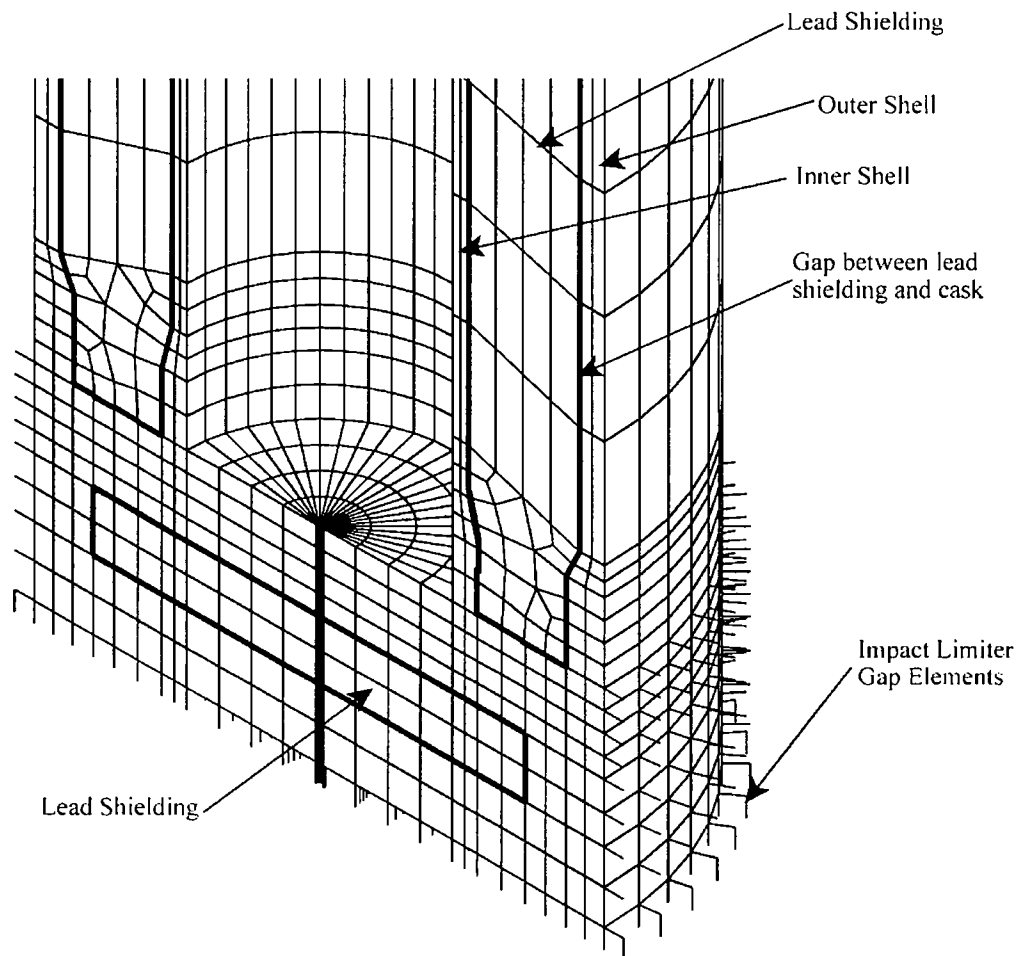


Figure 2.10.14-4 Location of Sections of the NAC-LWT Cask Body Model

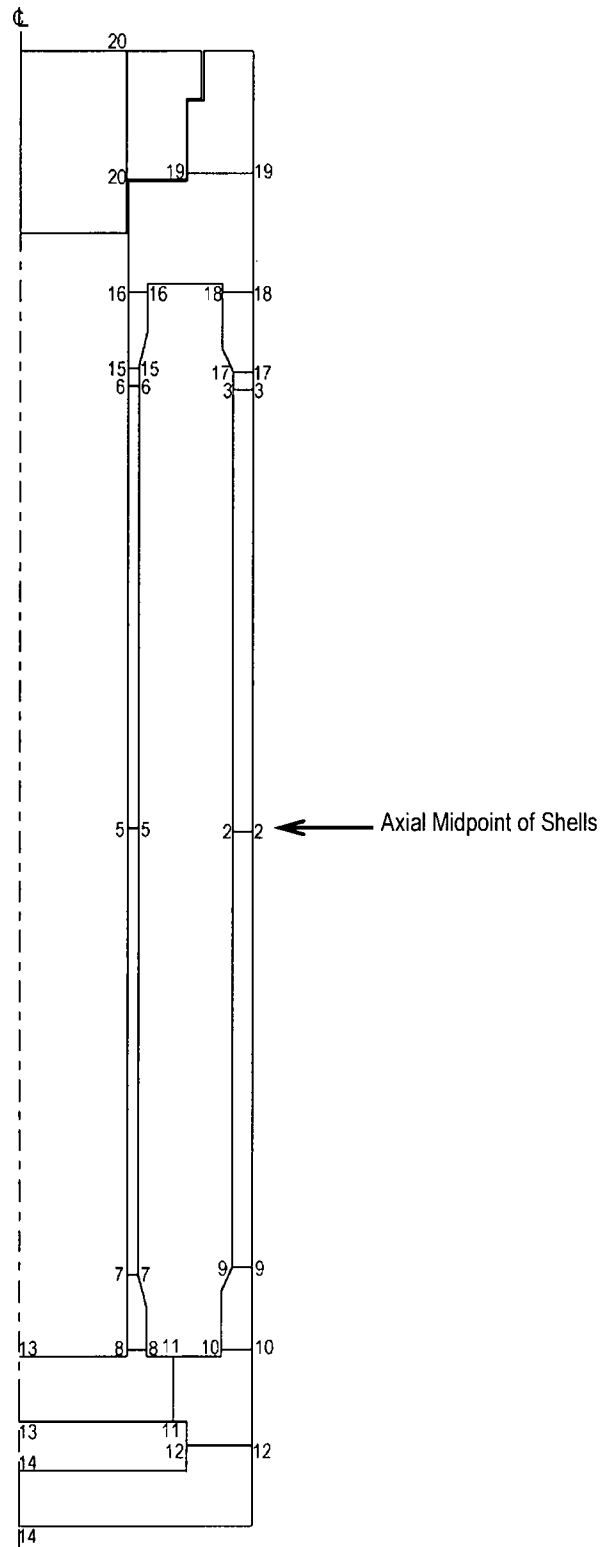


Table 2.10.14-1 Material Designations for Sections

Location	Material	Sections ¹
Outer Shell	SA240 Type XM-19	1-3
Inner Shell	SA240 Type XM-19	4-6
Bottom Forging	SA182 Type 304	7-14
Top Forging	SA182 Type 304	15-19
Lid	SA182 Type 304	20

¹ Sections are shown on Figure 2.10.14-4.

Table 2.10.14-2 1-Foot Side Drop with Internal Pressure, P_m Stresses, ksi

Sec ¹	Location (deg) ²	S_x^3	S_y^3	S_z^3	S_{xy}^3	S_{yz}^3	S_{xz}^3	Stress Intensity	Stress Allow.	MS
1	75	0.03	0.28	2.66	0.08	-6.74	-0.03	13.69	32.30	1.36
2	0	-0.14	1.71	28.41	-0.18	-0.01	0.00	28.57	32.30	0.13
3	67.5	0.04	0.39	3.97	0.05	6.06	0.00	12.64	32.30	1.56
4	97.5	-0.21	2.30	1.31	0.10	-4.21	0.01	8.48	32.30	2.81
5	180	-0.17	2.54	-16.05	0.18	0.00	0.00	18.61	32.30	0.74
6	97.5	-0.22	2.26	1.16	0.10	4.14	-0.01	8.36	32.30	2.86
7	112.5	-0.25	1.92	1.95	0.01	-5.75	-0.01	11.50	20.00	0.74
8	180	-1.99	1.79	6.11	0.06	-0.30	-1.98	9.04	20.00	1.21
9	67.5	0.02	-0.43	2.97	-0.34	-6.56	0.06	13.57	20.00	0.47
10	0	1.78	-4.55	1.05	0.74	-0.43	3.56	9.81	20.00	1.04
11	0	-4.87	-4.05	-0.46	0.11	0.06	0.28	4.45	20.00	3.49
12	0	-0.02	-1.51	-0.31	0.12	0.03	-0.54	1.92	20.00	9.42
13	90	-0.73	-3.26	-0.41	-0.08	0.36	0.04	2.94	20.00	5.80
14	0	-0.26	0.85	-0.41	0.00	-0.18	-0.33	1.56	20.00	+Large
15	112.5	-0.26	1.58	1.55	-0.03	5.90	0.00	11.81	20.00	0.69
16	127.5	-0.18	0.66	1.86	0.03	4.05	0.06	8.18	20.00	1.44
17	67.5	0.04	0.22	3.39	-0.30	6.07	-0.05	12.56	20.00	0.59
18	60	0.04	-0.27	2.57	0.05	4.11	-0.18	8.70	20.00	1.30
19	0	-2.82	-3.44	-1.15	0.41	0.06	1.74	4.04	20.00	3.95
20	105	0.12	-0.10	-0.78	-0.14	0.08	-0.43	1.30	20.00	+Large

- Notes:
1. See Figure 2.10.14-4 for locations of sections.
 2. The location specifies the angle at which the maximum stress intensity occurs. See Figure 2.10.14-1 for definition of angular location.
 3. Stress components correspond to a cylindrical coordinate system.

Table 2.10.14-3 Side Drop with Internal Pressure, $P_m + P_b$ Stresses, ksi

Sec ¹	Location (deg) ²	S_x^3	S_y^3	S_z^3	S_{xy}^3	S_{yz}^3	S_{xz}^3	Stress Intensity	Stress Allow.	MS
1	67.5	0.06	1.96	3.85	0.10	-7.45	-0.02	15.03	48.45	2.22
2	180	-0.06	5.49	-27.35	0.40	-0.01	0.00	32.87	48.45	0.47
3	67.5	0.07	2.32	4.74	0.08	6.85	-0.01	13.91	48.45	2.48
4	105	-0.38	-2.18	-0.40	0.07	-4.49	0.00	9.17	48.45	4.28
5	180	-0.10	3.68	-16.56	0.25	0.00	0.00	20.25	48.45	1.39
6	105	-0.10	6.74	2.59	0.03	3.79	-0.01	9.08	48.45	4.34
7	120	-0.31	-2.74	-0.38	-0.08	-6.52	-0.03	13.25	30.00	1.26
8	180	-3.38	1.06	11.77	0.00	0.00	-2.00	15.66	30.00	0.92
9	60	-0.07	0.46	3.44	-0.65	-7.78	0.24	15.90	30.00	0.89
10	0	4.60	-8.34	-11.23	0.64	-0.03	3.96	17.74	30.00	0.69
11	0	-8.51	-6.19	-0.09	0.09	0.09	0.82	8.59	30.00	2.49
12	0	0.19	-1.60	0.64	0.08	-0.06	-0.26	2.37	30.00	+Large
13	90	-1.43	-4.34	-0.43	-0.03	0.22	0.02	3.93	30.00	6.63
14	0	0.16	1.78	-1.80	0.02	-0.64	-0.30	3.84	30.00	6.81
15	120	-0.31	-3.50	-0.84	-0.15	6.59	0.01	13.45	30.00	1.23
16	180	-1.05	2.38	12.50	0.23	0.12	2.22	14.27	30.00	1.10
17	60	-0.08	1.62	4.85	-0.61	7.18	-0.31	14.78	30.00	1.03
18	37.5	-0.28	-0.47	6.66	0.12	5.17	-1.38	12.88	30.00	1.33
19	0	-1.16	-0.70	2.61	0.02	0.20	1.43	4.74	30.00	5.33
20	15	-2.43	-1.21	-1.48	0.08	-0.17	1.79	3.73	30.00	7.04

- Notes:
1. See Figure 2.10.14-4 for locations of sections.
 2. The location specifies the angle at which the maximum stress intensity occurs. See Figure 2.10.14-1 for definition of angular location.
 3. Stress components correspond to a cylindrical coordinate system.

Table 2.10.14-4 1-Foot Side Drop with Internal Pressure, P + Q Stresses, ksi

Sec ¹	Location (deg) ²	S _x ³	S _y ³	S _z ³	S _{xy} ³	S _{yz} ³	S _{xz} ³	Stress Intensity	Stress Allow.	MS
1	0	-0.55	15.41	23.96	-1.59	-0.42	0.12	24.70	96.90	2.92
2	0	-0.71	19.69	44.57	-1.80	-0.01	0.00	45.44	96.90	1.13
3	0	-0.54	13.83	26.27	-1.43	0.36	-0.13	26.97	96.90	2.59
4	105	-0.36	-2.17	3.28	0.07	-4.50	0.01	10.53	96.90	8.20
5	0	-0.18	6.18	23.65	-0.50	0.00	0.00	23.86	96.90	3.06
6	105	-0.38	-2.53	2.98	0.06	4.39	0.01	10.37	96.90	8.34
7	127.5	-0.28	-1.89	5.19	-0.29	-6.44	-0.03	14.72	60.00	3.08
8	180	-3.32	7.25	20.14	0.56	-0.01	-3.12	24.31	60.00	1.47
9	60	-0.93	8.89	16.68	-0.64	-7.74	1.26	22.56	60.00	1.66
10	0	0.34	6.19	26.82	0.50	-0.65	3.58	27.50	60.00	1.18
11	180	4.69	4.56	-9.20	0.03	-0.55	-3.99	16.06	60.00	2.74
12	180	-9.18	5.30	19.13	0.72	-0.15	1.68	28.54	60.00	1.10
13	90	-5.07	-10.02	0.47	-0.13	0.49	0.28	10.56	60.00	4.68
14	0	13.71	21.20	-4.61	-0.29	-0.83	-0.40	25.89	60.00	1.32
15	120	-0.32	-3.25	1.66	-0.15	6.60	0.17	14.09	60.00	3.26
16	180	-6.25	-4.80	8.34	-0.53	0.72	5.04	17.92	60.00	2.35
17	52.5	-0.81	9.24	19.43	-0.69	6.98	-1.50	24.02	60.00	1.50
18	0	-10.55	1.90	17.33	-1.49	-0.70	-6.67	31.10	60.00	0.93
19	0	-4.67	-5.23	-4.44	0.73	-0.11	2.00	4.31	60.00	+Large
20	45	-0.64	0.39	-1.81	0.39	-0.15	-3.41	7.01	60.00	7.56

- Notes:
1. See Figure 2.10.14-4 for locations of sections.
 2. The location specifies the angle at which the maximum stress intensity occurs. See Figure 2.10.14-1 for definition of angular location.
 3. Stress components correspond to a cylindrical coordinate system.

Table 2.10.14-5 1-Foot Top-End Drop with Normal Internal Pressure, P_m Stresses, ksi

Sec ¹	S_x^2	S_y^2	S_z^2	S_{xy}^2	S_{yz}^2	S_{xz}^2	Stress Intensity	Stress Allow.	MS
1	0.00	-0.01	0.02	0.00	0.00	0.00	0.03	32.30	+Large
2	0.00	0.00	-0.42	0.00	0.00	0.00	0.42	32.30	+Large
3	0.00	-0.05	-0.95	0.00	0.00	0.00	0.96	32.30	+Large
4	-0.13	2.65	0.80	-0.18	0.00	0.00	2.81	32.30	+Large
5	-0.13	2.66	0.36	-0.18	0.00	0.00	2.82	32.30	+Large
6	-0.13	2.69	-0.15	-0.19	0.00	0.00	2.85	32.30	+Large
7	-0.14	2.75	0.82	-0.19	0.00	-0.05	2.92	20.00	5.85
8	-0.18	0.63	0.50	-0.05	0.01	0.14	0.84	20.00	+Large
9	0.00	-0.01	0.04	0.00	0.00	0.00	0.05	20.00	+Large
10	0.00	0.01	0.04	0.00	0.00	0.00	0.04	20.00	+Large
11	-0.04	0.01	-0.02	0.00	0.00	0.02	0.06	20.00	+Large
12	0.00	0.02	0.01	0.00	0.00	0.02	0.04	20.00	+Large
13	0.02	0.02	-0.21	0.00	0.00	0.03	0.24	20.00	+Large
14	0.04	0.05	-0.02	0.00	0.00	0.01	0.07	20.00	+Large
15	-0.15	2.63	-0.25	-0.18	0.01	0.04	2.91	20.00	5.87
16	-2.27	-1.66	-1.13	-0.24	0.10	0.88	2.16	20.00	8.26
17	0.02	0.35	-0.94	0.00	0.00	0.02	1.29	20.00	+Large
18	-2.14	0.67	-1.27	0.34	0.14	-0.50	3.12	20.00	5.41
19	-0.25	0.73	-1.44	0.10	-0.06	0.34	2.27	20.00	7.81
20	-0.27	-0.52	-2.01	-0.01	-0.01	0.31	1.85	20.00	9.81

- Notes: 1. See Figure 2.10.14-4 for locations of sections.
2. Stress components correspond to a cylindrical coordinate system.

Table 2.10.14-6 1-Foot Top-End Drop with Internal Pressure, $P_m + P_b$ Stresses, ksi

Sec ¹	S_x^2	S_y^2	S_z^2	S_{xy}^2	S_{yz}^2	S_{xz}^2	Stress Intensity	Stress Allow.	MS
1	0.00	-0.01	0.03	0.00	0.00	0.00	0.03	48.45	+Large
2	0.00	0.00	-0.42	0.00	0.00	0.00	0.43	48.45	+Large
3	0.00	-0.11	-1.10	0.01	0.00	0.00	1.10	48.45	+Large
4	-0.21	2.84	0.84	-0.20	0.00	0.00	3.07	48.45	+Large
5	-0.20	2.85	0.39	-0.20	0.00	0.00	3.07	48.45	+Large
6	-0.21	2.94	-0.09	-0.21	0.01	0.01	3.18	48.45	+Large
7	-0.20	2.80	0.36	-0.20	0.00	-0.05	3.02	30.00	8.93
8	-0.33	0.92	1.28	-0.08	0.01	0.16	1.65	30.00	+Large
9	0.00	0.00	0.06	0.00	0.00	0.01	0.06	30.00	+Large
10	0.00	0.01	0.04	0.00	0.00	0.00	0.04	30.00	+Large
11	-0.06	0.02	-0.04	0.00	0.00	0.00	0.08	30.00	+Large
12	-0.01	0.02	0.00	0.00	0.00	0.02	0.05	30.00	+Large
13	0.33	0.48	-0.15	-0.01	0.00	0.03	0.63	30.00	+Large
14	0.08	0.13	-0.02	0.00	0.00	0.01	0.16	30.00	+Large
15	-0.19	2.70	-0.94	-0.19	0.01	0.05	3.65	30.00	7.22
16	-3.18	-3.36	-4.31	0.43	-0.36	1.53	3.42	30.00	7.77
17	0.00	0.22	-1.23	-0.02	0.01	0.02	1.45	30.00	+Large
18	-3.50	-0.35	-3.43	-0.47	-0.39	-1.04	4.34	30.00	5.91
19	-0.49	0.68	-1.77	0.14	-0.13	0.47	2.64	30.00	+Large
20	0.13	-0.14	-1.72	0.00	-0.01	1.83	4.10	30.00	6.32

¹ See Figure 2.10.14-4 for locations of sections.

² Stress components correspond to a cylindrical coordinate system.

Table 2.10.14-7 1-Foot Top-End Drop with Internal Pressure, P + Q Stresses, ksi

Sec ¹	S _x ²	S _y ²	S _z ²	S _{xy} ²	S _{yz} ²	S _{xz} ²	Stress Intensity	Stress Allow.	MS
1	-0.52	12.95	15.18	-1.32	0.04	0.04	15.83	96.90	5.12
2	-0.64	15.83	13.76	-1.49	0.00	0.00	16.74	96.90	4.79
3	-0.52	10.70	13.97	-1.14	-0.10	-0.08	14.61	96.90	5.63
4	-0.20	3.10	4.88	0.00	-0.21	0.02	5.10	96.90	+Large
5	-0.20	2.83	3.76	-0.20	0.00	0.00	3.97	96.90	+Large
6	-0.21	3.31	4.56	0.02	0.48	-0.01	4.93	96.90	+Large
7	-0.28	5.22	5.61	-0.18	-1.18	-0.12	6.91	60.00	7.68
8	-0.81	6.85	8.05	-0.38	-0.88	-0.76	9.45	60.00	5.35
9	-0.51	7.65	14.92	-0.65	0.20	0.33	15.50	60.00	2.87
10	2.39	4.05	20.04	1.25	-0.57	2.66	19.10	60.00	2.14
11	-2.18	-14.93	-8.39	2.15	0.03	-3.63	15.09	60.00	2.98
12	-11.68	-3.17	20.44	0.95	0.25	0.86	32.27	60.00	0.86
13	-12.94	-27.36	-3.27	2.41	1.70	0.18	24.72	60.00	1.43
14	14.78	25.68	0.00	0.43	2.99	0.07	26.38	60.00	1.27
15	-0.51	6.64	6.70	-0.24	1.89	0.26	9.09	60.00	5.60
16	-2.24	-10.97	2.01	-0.21	3.30	0.34	14.59	60.00	3.11
17	-1.28	7.78	13.30	-0.79	0.05	-1.06	14.80	60.00	3.05
18	-13.49	2.32	3.59	1.97	1.52	-5.23	20.64	60.00	1.91
19	-0.33	-21.42	-6.90	1.77	2.11	-0.54	21.71	60.00	1.76
20	-4.38	-1.14	-3.50	-0.08	-0.46	6.65	13.37	60.00	3.49

¹ See Figure 2.10.14-4 for locations of sections.

² Stress components correspond to a cylindrical coordinate system.

Table 2.10.14-8 1-Foot Top-Corner Drop with Internal Pressure, P_m Stresses, ksi

Sec ¹	Location (deg) ²	S_x^3	S_y^3	S_z^3	S_{xy}^3	S_{yz}^3	S_{xz}^3	Stress Intensity	Stress Allow.	MS
1	180	0.00	0.10	-1.84	0.00	-0.03	-0.01	1.95	32.30	+Large
2	180	-0.03	-0.13	-3.67	0.00	0.02	0.00	3.65	32.30	7.85
3	0	0.02	0.11	-2.83	0.00	0.07	0.00	2.94	32.30	9.99
4	90	-0.14	2.66	0.59	0.04	-0.87	0.01	3.12	32.30	9.35
5	180	-0.15	2.63	-2.37	0.17	0.01	0.00	5.01	32.30	5.45
6	0	-0.14	2.80	-2.49	-0.22	0.05	0.00	5.31	32.30	5.08
7	120	-0.17	2.54	1.01	0.03	-1.26	-0.02	3.42	20.00	4.85
8	180	-0.75	1.14	2.00	0.05	-0.09	-0.55	2.97	20.00	5.73
9	60	0.00	-0.06	0.42	-0.04	-0.95	-0.01	1.96	20.00	9.20
10	0	0.10	-0.78	-0.21	0.09	-0.07	0.72	1.58	20.00	+Large
11	180	0.18	0.23	0.19	-0.01	0.04	-0.42	0.85	20.00	+Large
12	0	0.00	-0.23	-0.17	0.02	0.02	-0.19	0.43	20.00	+Large
13	82.5	-0.04	-0.25	0.00	0.02	0.07	0.00	0.30	20.00	+Large
14	90	0.03	-0.30	0.00	-0.01	0.08	-0.01	0.36	20.00	+Large
15	0	-0.13	2.29	-3.27	-0.17	0.05	-0.05	5.57	20.00	2.59
16	180	-2.14	-1.54	0.38	-0.23	0.09	0.87	3.12	20.00	5.41
17	0	0.03	0.55	-3.01	-0.03	0.07	0.07	3.57	20.00	4.60
18	0	-2.92	0.34	-3.47	-0.43	-0.12	-0.68	4.35	20.00	3.60
19	0	-1.02	-0.31	-3.45	0.01	0.12	0.47	3.24	20.00	5.17
20	0	-0.56	-0.65	-2.69	0.03	0.04	0.38	2.27	20.00	7.81

¹ See Figure 2.10.14-4 for locations of sections.

² The location specifies the angle at which the maximum stress intensity occurs. See Figure 2.10.14-1 for definition of angular location.

³ Stress components correspond to a cylindrical coordinate system.

Table 2.10.14-9 1-Foot Top-Corner Drop with Internal Pressure, $P_m + P_b$ Stresses, ksi

Sec ¹	Location (deg) ²	S_x^3	S_y^3	S_z^3	S_{xy}^3	S_{yz}^3	S_{xz}^3	Stress Intensity	Stress Allow.	MS
1	52.5	0.02	0.75	0.68	0.02	-1.19	-0.01	2.38	48.45	+Large
2	180	-0.02	1.88	-3.16	0.14	0.02	0.00	5.06	48.45	8.58
3	0	0.03	0.19	-2.96	-0.01	0.07	0.00	3.15	48.45	+Large
4	180	-0.21	5.36	1.54	0.29	-0.06	0.00	5.60	48.45	7.65
5	180	-0.22	2.93	-2.17	0.19	0.01	0.00	5.11	48.45	8.48
6	0	-0.04	3.07	-2.44	-0.23	0.04	-0.01	5.53	48.45	7.76
7	180	-0.30	4.86	3.07	0.23	-0.18	-0.03	5.20	30.00	4.77
8	180	-1.05	0.29	3.37	-0.02	0.08	-0.57	4.56	30.00	5.58
9	45	-0.02	0.29	0.44	-0.12	-1.30	0.03	2.62	30.00	+Large
10	0	0.63	-1.09	-2.46	0.08	0.07	0.74	3.44	30.00	7.72
11	180	0.85	0.60	0.02	-0.01	0.05	-0.55	1.37	30.00	+Large
12	180	0.06	0.13	0.24	0.00	0.01	-0.25	0.54	30.00	+Large
13	90	-0.13	-0.39	0.03	-0.02	0.10	0.01	0.47	30.00	+Large
14	105	-0.05	-0.48	0.02	-0.13	0.07	0.00	0.56	30.00	+Large
15	15	-0.16	2.38	-3.36	-0.02	0.29	-0.04	5.77	30.00	4.20
16	7.5	-1.53	-2.80	-6.23	0.11	-0.21	0.48	4.81	30.00	5.24
17	0	-0.03	0.52	-3.23	-0.03	0.06	-0.02	3.75	30.00	7.00
18	0	-4.71	-0.82	-5.65	-0.61	-0.44	-1.37	6.00	30.00	4.00
19	7.5	-0.55	-0.93	-4.50	0.09	0.07	0.29	4.02	30.00	6.46
20	15	0.53	-0.15	-1.96	0.03	0.01	1.82	4.41	30.00	5.80

¹ See Figure 2.10.14-4 for locations of sections.

² The location specifies the angle at which the maximum stress intensity occurs. See Figure 2.10.14-1 for definition of angular location.

³ Stress components correspond to a cylindrical coordinate system.

Table 2.10.14-10 1-Foot Top-Corner Drop with Internal Pressure, P + Q Stresses, ksi

Sec ¹	Location (deg) ²	S _x ³	S _y ³	S _z ³	S _{xy} ³	S _{yz} ³	S _{xz} ³	Stress Intensity	Stress Allow.	MS
1	0	-0.61	13.84	16.03	-1.45	0.00	0.09	16.78	96.90	4.77
2	0	-0.68	17.69	17.49	-1.62	0.02	0.00	18.65	96.90	4.20
3	180	-0.58	10.62	13.95	1.13	0.13	-0.09	14.65	96.90	5.61
4	180	-0.20	5.24	5.22	0.28	-0.07	0.01	5.52	96.90	+Large
5	0	-0.08	3.13	6.51	-0.23	0.01	0.00	6.61	96.90	+Large
6	180	-0.23	2.64	5.39	0.20	0.04	0.00	5.63	96.90	+Large
7	180	-0.31	5.20	7.56	0.25	-0.19	0.00	7.90	60.00	6.59
8	180	-1.00	6.47	11.74	0.54	0.07	-1.69	13.22	60.00	3.54
9	30	-0.89	8.92	13.67	-0.16	-1.38	1.06	15.09	60.00	2.98
10	0	0.94	6.46	15.53	-0.24	-0.04	1.11	14.77	60.00	3.06
11	7.5	5.44	-0.93	-7.47	0.03	-0.02	-3.90	15.09	60.00	2.98
12	180	-9.30	4.39	18.60	0.70	-0.13	1.85	28.18	60.00	1.13
13	75	7.18	10.40	-0.43	-0.01	0.04	-0.03	10.83	60.00	4.54
14	0	13.27	19.46	-2.77	-0.31	-0.19	-0.14	22.25	60.00	1.70
15	180	-0.25	3.87	8.31	0.26	0.03	0.26	8.59	60.00	5.98
16	165	-2.03	-4.30	7.35	-0.10	0.25	0.62	11.71	60.00	4.12
17	180	-1.17	7.04	14.41	0.73	0.03	-1.36	15.88	60.00	2.78
18	180	-12.10	2.59	6.12	1.79	1.42	-4.91	21.15	60.00	1.84
19	0	-1.40	0.01	-4.32	0.09	-0.01	0.22	4.36	60.00	+Large
20	15	1.69	0.13	-2.70	0.02	0.00	3.18	7.73	60.00	6.76

¹ See Figure 2.10.14-4 for locations of sections.

² The location specifies the angle at which the maximum stress intensity occurs. See Figure 2.10.14-1 for definition of angular location.

³ Stress components correspond to a cylindrical coordinate system.

Table 2.10.14-11 1-Foot Bottom-End Drop with Internal Pressure, P_m Stresses, ksi

Sec ¹	S_x^2	S_y^2	S_z^2	S_{xy}^2	S_{yz}^2	S_{xz}^2	Stress Intensity	Stress Allow.	MS
1	0.01	0.08	-1.34	0.00	0.00	-0.01	1.42	32.30	+Large
2	0.00	0.00	-0.78	0.00	0.00	0.00	0.78	32.30	+Large
3	0.00	0.02	-0.34	0.00	0.00	0.00	0.36	32.30	+Large
4	-0.13	2.69	-0.49	-0.18	0.00	0.00	3.19	32.30	9.13
5	-0.13	2.66	0.00	-0.18	0.00	0.00	2.82	32.30	+Large
6	-0.13	2.67	0.43	-0.18	0.00	0.00	2.82	32.30	+Large
7	-0.12	2.58	-0.57	-0.18	0.00	0.00	3.16	20.00	5.33
8	0.07	1.33	-0.38	-0.01	-0.01	0.04	1.71	20.00	+Large
9	0.01	0.09	-1.30	-0.01	0.00	-0.03	1.39	20.00	+Large
10	0.09	0.29	-0.98	0.01	0.00	-0.08	1.28	20.00	+Large
11	0.62	0.06	-3.56	-0.04	-0.22	0.14	4.20	20.00	3.76
12	-0.35	0.34	-1.66	0.04	0.03	-0.17	2.03	20.00	8.85
13	0.69	0.93	-0.79	0.02	0.00	-0.13	1.73	20.00	+Large
14	-0.40	-0.68	-4.05	0.02	-0.05	-0.60	3.85	20.00	4.19
15	-0.14	2.68	0.45	-0.18	0.00	0.03	2.84	20.00	6.04
16	-0.08	1.08	0.29	-0.08	0.00	-0.06	1.18	20.00	+Large
17	0.00	0.02	-0.29	0.00	0.00	0.01	0.32	20.00	+Large
18	0.00	0.06	-0.18	0.00	0.00	0.02	0.25	20.00	+Large
19	-0.04	0.22	-0.22	0.00	0.00	0.03	0.45	20.00	+Large
20	-0.15	0.08	-0.90	0.00	0.00	-0.25	1.06	20.00	+Large

¹ See Figure 2.10.14-4 for locations of sections.

² Stress components correspond to a cylindrical coordinate system.

Table 2.10.14-12 1-Foot Bottom-End Drop with Internal Pressure, $P_m + P_b$ Stresses, ksi

Sec ¹	S_x^2	S_y^2	S_z^2	S_{xy}^2	S_{yz}^2	S_{xz}^2	Stress Intensity	Stress Allow.	MS
1	0.01	0.12	-1.35	-0.01	0.00	-0.01	1.47	48.45	+Large
2	0.00	0.01	-0.78	0.00	0.00	0.00	0.79	48.45	+Large
3	0.00	0.02	-0.34	0.00	0.00	0.00	0.36	48.45	+Large
4	-0.20	2.92	-0.45	-0.20	0.00	0.00	3.38	48.45	+Large
5	-0.20	2.85	0.03	-0.20	0.00	0.00	3.07	48.45	+Large
6	-0.21	2.85	0.47	-0.20	0.00	0.00	3.09	48.45	+Large
7	-0.19	2.75	-0.71	-0.19	0.00	0.00	3.47	30.00	7.65
8	-0.08	1.45	-0.52	0.10	-0.01	0.01	1.98	30.00	+Large
9	0.03	0.11	-1.36	-0.01	-0.01	-0.07	1.47	30.00	+Large
10	0.07	0.21	-1.16	-0.03	-0.03	-0.06	1.38	30.00	+Large
11	-0.32	-1.37	-7.60	-0.07	-0.62	0.23	7.37	30.00	3.07
12	-0.63	-0.07	-3.13	0.04	0.03	-0.26	3.09	30.00	8.71
13	1.89	2.83	-0.47	0.01	-0.01	-0.11	3.31	30.00	8.06
14	1.41	3.02	-2.90	0.00	0.05	-0.70	6.03	30.00	3.98
15	-0.20	2.77	0.13	-0.19	0.00	0.03	2.99	30.00	9.03
16	-0.18	1.29	0.63	-0.10	-0.01	-0.06	1.49	30.00	+Large
17	0.01	0.02	-0.31	0.00	0.00	0.02	0.34	30.00	+Large
18	0.01	0.07	-0.18	0.00	0.00	0.02	0.26	30.00	+Large
19	-0.06	0.22	-0.45	0.00	0.01	0.02	0.67	30.00	+Large
20	-0.31	0.33	-0.88	0.01	0.00	-1.66	3.37	30.00	7.90

¹ See Figure 2.10.14-4 for locations of sections.

² Stress components correspond to a cylindrical coordinate system.

Table 2.10.14-13 1-Foot Bottom-End Drop with Internal Pressure, P + Q Stresses, ksi

Sec ¹	S _x ²	S _y ²	S _z ²	S _{xy} ²	S _{yz} ²	S _{xz} ²	Stress Intensity	Stress Allow.	MS
1	-0.51	12.99	13.84	-1.32	0.03	0.04	14.48	96.90	5.69
2	-0.64	15.83	13.40	-1.49	0.00	0.00	16.74	96.90	4.79
3	-0.53	10.82	14.75	-1.15	-0.10	-0.07	15.40	96.90	5.29
4	-0.16	3.34	3.35	-0.07	-0.56	-0.01	4.06	96.90	+Large
5	-0.20	2.83	3.40	-0.20	0.00	0.00	3.61	96.90	+Large
6	-0.21	3.26	5.02	0.02	0.46	-0.01	5.34	96.90	+Large
7	-0.28	5.08	4.11	-0.19	-1.24	-0.08	6.22	60.00	8.65
8	-0.61	7.94	8.34	-0.39	-0.92	-0.87	9.81	60.00	5.12
9	-0.52	7.71	13.65	-0.66	0.20	0.36	14.24	60.00	3.21
10	2.70	4.55	19.44	1.26	-0.54	2.56	18.13	60.00	2.31
11	1.52	0.70	-16.74	-0.02	-1.30	-1.91	18.76	60.00	2.20
12	-12.30	-3.34	17.50	0.96	0.22	0.72	29.94	60.00	1.00
13	-13.81	-28.99	-4.35	2.43	1.73	0.00	25.26	60.00	1.38
14	11.85	19.76	-7.14	0.45	1.90	-0.81	27.22	60.00	1.20
15	-0.46	6.38	6.77	-0.23	1.81	0.24	8.88	60.00	5.76
16	-1.29	-7.82	1.82	-0.45	3.42	0.31	11.86	60.00	4.06
17	-1.31	7.38	13.67	-0.76	0.05	-1.07	15.20	60.00	2.95
18	-10.04	2.68	6.68	1.51	1.13	-4.19	19.03	60.00	2.15
19	-0.21	-22.47	-6.98	1.67	2.23	-0.70	22.88	60.00	1.62
20	-5.62	-2.02	-2.52	-0.04	-0.44	5.39	11.25	60.00	4.33

¹ See Figure 2.10.14-4 for locations of sections.

² Stress components correspond to a cylindrical coordinate system.

Table 2.10.14-14 1-Foot Bottom-Corner Drop with Internal Pressure, P_m Stresses, ksi

Sec ¹	Location (deg) ²	S_x^3	S_y^3	S_z^3	S_{xy}^3	S_{yz}^3	S_{xz}^3	Stress Intensity	Stress Allow.	MS
1	0	0.03	0.29	-3.53	-0.01	-0.09	-0.02	3.83	32.30	7.43
2	180	-0.03	-0.13	-3.65	0.00	-0.02	0.00	3.62	32.30	7.92
3	180	0.00	0.13	-2.21	0.01	0.03	0.01	2.34	32.30	+Large
4	0	-0.14	2.80	-2.63	-0.21	-0.05	0.00	5.44	32.30	4.94
5	180	-0.15	2.63	-2.35	0.17	-0.01	0.00	4.99	32.30	5.47
6	82.5	-0.14	2.69	0.54	0.04	0.82	0.00	3.11	32.30	9.39
7	0	-0.11	2.28	-3.40	-0.17	-0.05	0.08	5.70	20.00	2.51
8	7.5	0.17	0.97	-2.24	-0.02	-0.04	0.23	3.23	20.00	5.19
9	0	0.02	0.09	-3.75	0.00	-0.08	-0.07	3.84	20.00	4.21
10	0	0.50	-0.14	-2.88	0.07	-0.06	0.08	3.39	20.00	4.90
11	0	-0.04	-0.24	-4.08	0.05	0.26	0.53	4.22	20.00	3.74
12	0	-0.96	-0.25	-3.79	0.03	-0.07	-0.25	3.56	20.00	4.62
13	180	0.12	0.71	-0.73	0.01	0.00	-0.24	1.51	20.00	+Large
14	180	-0.38	-0.52	-3.79	-0.02	0.06	-0.75	3.73	20.00	4.36
15	112.5	-0.16	2.56	0.76	0.04	1.25	0.01	3.36	20.00	4.95
16	165	-0.16	1.58	1.85	-0.01	0.53	0.46	2.59	20.00	6.72
17	180	0.00	0.16	-1.95	-0.01	0.02	0.05	2.12	20.00	8.43
18	180	-0.01	0.04	-1.25	0.00	0.01	0.08	1.29	20.00	+Large
19	180	-0.09	0.20	-0.32	0.02	-0.03	0.17	0.61	20.00	+Large
20	82.5	0.02	-0.38	-0.99	0.10	0.02	-0.16	1.08	20.00	+Large

¹ See Figure 2.10.14-4 for locations of sections.

² The location specifies the angle at which the maximum stress intensity occurs. See Figure 2.10.14-1 for definition of angular location.

³ Stress components correspond to a cylindrical coordinate system.

Table 2.10.14-15 1-Foot Bottom-Corner Drop with Internal Pressure, $P_m + P_b$ Stresses, ksi

Sec ¹	Location (deg) ²	S_x ³	S_y ³	S_z ³	S_{xy} ³	S_{yz} ³	S_{xz} ³	Stress Intensity	Stress Allow.	MS
1	0	0.04	0.39	-3.44	-0.02	-0.08	0.00	3.84	48.45	+Large
2	180	-0.02	1.88	-3.13	0.14	-0.03	0.00	5.03	48.45	8.63
3	180	0.01	0.38	-2.18	0.02	0.04	0.00	2.56	48.45	+Large
4	0	-0.05	3.09	-2.58	-0.23	-0.04	0.01	5.69	48.45	7.51
5	180	-0.22	2.87	-2.17	0.19	-0.01	0.00	5.06	48.45	8.58
6	180	-0.21	5.48	1.33	0.30	0.06	0.00	5.72	48.45	7.47
7	0	-0.03	2.32	-3.59	-0.17	-0.03	0.08	5.92	30.00	4.07
8	7.5	0.41	0.83	-2.60	-0.03	0.02	0.22	3.45	30.00	7.70
9	0	0.09	0.04	-3.99	0.00	-0.11	-0.22	4.11	30.00	6.30
10	0	0.50	-0.74	-4.57	0.03	-0.07	0.18	5.08	30.00	4.91
11	0	-0.70	-1.66	-8.28	0.10	0.70	0.77	7.82	30.00	2.84
12	0	-0.96	-0.45	-4.83	-0.01	-0.06	-0.34	4.41	30.00	5.80
13	7.5	1.23	2.32	-0.47	0.06	0.00	-0.02	2.79	30.00	9.75
14	7.5	1.46	2.91	-2.86	0.01	-0.01	-0.44	5.81	30.00	4.16
15	180	-0.28	4.86	3.14	0.23	0.18	-0.02	5.19	30.00	4.78
16	180	-0.09	1.16	4.05	0.13	-0.08	0.62	4.34	30.00	5.91
17	37.5	-0.01	0.54	0.81	-0.14	1.21	-0.06	2.45	30.00	+Large
18	22.5	-0.07	0.01	1.28	0.02	1.01	-0.28	2.46	30.00	+Large
19	180	-0.21	0.31	-0.27	0.05	-0.08	0.25	0.83	30.00	+Large
20	45	-0.23	0.33	-0.87	0.11	-0.03	-1.67	3.41	30.00	7.80

¹ Figure 2.10.14-4 for locations of sections.

² The location specifies the angle at which the maximum stress intensity occurs. See Figure 2.10.14-1 for definition of angular location.

³ Stress components correspond to a cylindrical coordinate system.

Table 2.10.14-16 1-Foot Bottom-Corner Drop with Internal Pressure, P + Q Stresses, ksi

Sec ¹	Location (deg) ²	S _x ³	S _y ³	S _z ³	S _{xy} ³	S _{yz} ³	S _{xz} ³	Stress Intensity	Stress Allow.	MS
1	180	-0.62	12.07	14.85	1.27	-0.13	0.07	15.60	96.90	5.21
2	0	-0.68	17.69	17.35	-1.62	-0.02	0.00	18.65	96.90	4.20
3	0	-0.57	12.42	16.02	-1.31	-0.01	-0.10	16.72	96.90	4.80
4	180	-0.08	2.46	5.51	0.17	-0.04	0.00	5.60	96.90	+Large
5	0	-0.09	3.16	6.42	-0.23	-0.01	0.00	6.52	96.90	+Large
6	180	-0.22	5.33	5.05	0.30	0.06	0.00	5.59	96.90	+Large
7	180	-0.22	3.33	6.15	0.24	-0.04	-0.04	6.39	60.00	8.39
8	0	0.29	4.73	-5.70	-0.27	-0.09	-0.99	10.61	60.00	4.66
9	180	-1.36	7.51	13.74	0.81	0.02	1.25	15.38	60.00	2.90
10	180	1.51	7.41	13.95	0.36	-0.24	0.37	12.49	60.00	3.80
11	0	1.43	0.66	-17.49	0.04	1.40	-1.33	19.21	60.00	2.12
12	180	-9.62	4.51	17.43	0.73	-0.17	2.15	27.43	60.00	1.19
13	7.5	8.54	12.54	-0.89	0.03	0.00	-0.04	13.43	60.00	3.47
14	0	11.05	15.72	-8.54	-0.22	-0.32	-0.43	24.29	60.00	1.47
15	127.5	-0.23	4.70	7.10	0.00	1.04	0.17	7.72	60.00	6.77
16	180	-5.29	-6.02	-0.11	-0.63	0.52	3.45	9.07	60.00	5.62
17	30	-0.79	8.41	14.78	-0.16	1.26	-1.19	15.99	60.00	2.75
18	0	-10.18	2.24	9.24	-1.50	-0.97	-4.88	21.99	60.00	1.73
19	165	-0.10	1.23	-1.27	-0.02	-0.02	-0.22	2.54	60.00	+Large
20	75	-0.96	0.43	-1.89	0.03	-0.01	-3.39	6.84	60.00	7.77

¹ See Figure 2.10.14-4 for locations of sections.

² The location specifies the angle at which the maximum stress intensity occurs. See Figure 2.10.14-1 for definition of angular location.

³ Stress components correspond to a cylindrical coordinate system.

Table 2.10.14-17 30-Foot Side Drop with Internal Pressure, P_m Stresses, ksi

Sec ¹	Location (deg) ²	S_x^3	S_y^3	S_z^3	S_{xy}^3	S_{yz}^3	S_{xz}^3	Stress Intensity	Stress Allow.	MS
1	75	0.04	0.89	5.89	0.11	-15.69	-0.04	31.78	67.83	1.13
2	0	-0.30	4.10	66.15	-0.43	-0.03	0.00	66.50	67.83	0.02
3	75	0.08	0.97	6.23	0.07	14.38	0.01	29.24	67.83	1.32
4	97.5	-0.31	1.59	1.21	0.02	-9.10	0.02	18.20	67.83	2.73
5	180	-0.12	2.40	-36.71	0.12	-0.01	0.00	39.12	67.83	0.73
6	97.5	-0.31	1.50	0.66	-0.02	9.07	-0.01	18.16	67.83	2.74
7	112.5	-0.37	0.56	2.52	-0.23	-12.30	-0.04	24.67	48.00	0.95
8	180	-3.13	3.13	10.63	0.08	-0.56	-3.64	15.61	48.00	2.07
9	75	0.02	-0.55	5.28	-0.81	-15.37	0.09	31.32	48.00	0.53
10	0	4.62	-9.90	3.03	1.72	-0.95	7.57	21.90	48.00	1.19
11	0	-11.37	-9.00	-0.92	0.29	0.10	0.26	10.50	48.00	3.57
12	0	-0.01	-3.58	-0.50	0.28	0.02	-1.20	4.59	48.00	9.46
13	90	-1.53	-7.84	-0.72	-0.20	0.73	0.06	7.28	48.00	5.59
14	127.5	0.31	-0.09	-0.05	-1.20	0.67	0.35	2.83	48.00	+Large
15	112.5	-0.29	-0.22	1.50	-0.43	12.67	0.02	25.41	48.00	0.89
16	120	-0.16	-0.93	1.93	-0.02	8.29	-0.07	16.83	48.00	1.85
17	75	0.05	0.84	5.35	-0.73	14.28	-0.05	28.95	48.00	0.66
18	67.5	0.05	-0.15	4.57	0.03	9.72	-0.32	20.02	48.00	1.40
19	0	-6.41	-8.47	-2.13	1.01	0.16	3.99	9.76	48.00	3.92
20	15	-2.56	-0.62	-1.27	0.41	-0.29	0.45	2.32	48.00	+Large

¹ See Figure 2.10.14-4 for locations of sections.

² The location specifies the angle at which the maximum stress intensity occurs. See Figure 2.10.14-1 for definition of angular location.

³ Stress components correspond to a cylindrical coordinate system.

Table 2.10.14-18 30-Foot Side Drop with Internal Pressure, $P_m + P_b$ Stresses, ksi

Sec ¹	Location (deg) ²	S_x^3	S_y^3	S_z^3	S_{xy}^3	S_{yz}^3	S_{xz}^3	Stress Intensity	Stress Allow.	MS
1	75	0.07	3.30	6.47	0.19	-17.17	-0.04	34.49	96.90	1.81
2	180	-0.09	8.89	-65.21	0.65	-0.03	0.00	74.14	96.90	0.31
3	75	0.13	3.98	7.54	0.14	15.84	0.00	31.88	96.90	2.04
4	97.5	-0.50	-6.43	-1.73	0.03	-9.93	0.01	20.41	96.90	3.75
5	0	-0.26	3.65	40.86	-0.45	-0.01	0.00	41.17	96.90	1.35
6	97.5	-0.46	-6.87	-2.30	-0.02	9.80	0.01	20.13	96.90	3.81
7	112.5	-0.37	-6.53	-2.00	-0.19	-13.83	-0.04	28.04	68.50	1.44
8	180	-5.70	2.96	22.06	0.07	-0.15	-3.64	28.71	68.50	1.39
9	67.5	-0.15	0.45	6.24	-1.51	-17.91	0.42	36.41	68.50	0.88
10	0	10.64	-18.81	-23.45	1.44	-0.18	8.60	38.28	68.50	0.79
11	0	-19.75	-13.55	-0.19	0.25	0.16	1.39	19.77	68.50	2.46
12	0	0.45	-3.78	1.86	0.18	-0.19	-0.51	5.83	68.50	+Large
13	90	-2.66	-9.71	-0.67	-0.11	0.43	0.01	9.08	68.50	6.54
14	0	0.61	3.47	-1.97	0.02	-0.65	-0.53	5.69	68.50	+Large
15	112.5	-0.33	-7.35	-2.50	-0.44	13.99	0.02	28.41	68.50	1.41
16	127.5	-0.11	-2.45	-0.26	0.04	12.99	0.54	26.10	68.50	1.62
17	67.5	-0.07	2.89	8.46	-1.40	16.45	-0.51	33.50	68.50	1.04
18	52.5	-0.37	-0.58	10.45	0.23	12.54	-1.93	27.69	68.50	1.47
19	22.5	-0.91	-4.63	6.48	0.55	0.46	1.91	11.68	68.50	4.86
20	15	-5.76	-2.35	-2.16	0.25	-0.35	2.61	6.40	68.50	9.70

¹ See Figure 2.10.14-4 for locations of sections.

² The location specifies the angle at which the maximum stress intensity occurs. See Figure 2.10.14-1 for definition of angular location.

³ Stress components correspond to a cylindrical coordinate system.

Table 2.10.14-19 30-Foot Top-End Drop with Internal Pressure, P_m Stresses, ksi

Sec ¹	S_x^2	S_y^2	S_z^2	S_{xy}^2	S_{yz}^2	S_{xz}^2	Stress Intensity	Stress Allow.	MS
1	0.00	0.00	-0.16	0.00	0.00	0.00	0.16	67.83	+Large
2	0.00	0.00	-1.49	0.00	0.00	0.00	1.50	67.83	+Large
3	0.02	-0.11	-3.07	0.01	0.00	-0.01	3.08	67.83	+Large
4	-0.13	2.65	0.60	-0.18	0.00	0.00	2.81	67.83	+Large
5	-0.13	2.66	-0.71	-0.18	0.00	0.00	3.39	67.83	+Large
6	-0.12	2.76	-2.20	-0.19	0.01	0.00	4.97	67.83	+Large
7	-0.14	2.74	0.68	-0.19	0.00	-0.04	2.90	48.00	+Large
8	-0.18	0.67	0.42	0.06	-0.01	0.13	0.89	48.00	+Large
9	0.00	0.01	-0.09	0.00	0.00	0.00	0.09	48.00	+Large
10	0.00	0.02	-0.04	0.00	0.00	-0.01	0.07	48.00	+Large
11	-0.02	0.03	-0.03	0.00	0.00	0.00	0.07	48.00	+Large
12	-0.01	0.01	-0.01	0.00	0.00	-0.01	0.03	48.00	+Large
13	0.04	0.06	-0.22	0.00	0.00	0.02	0.28	48.00	+Large
14	0.01	0.01	-0.02	0.00	0.00	0.00	0.03	48.00	+Large
15	-0.17	2.42	-2.51	0.01	0.08	0.05	4.94	48.00	8.72
16	-6.61	-6.94	-4.45	-0.87	0.30	2.74	6.31	48.00	6.61
17	0.05	1.10	-3.01	0.00	0.05	0.07	4.11	48.00	+Large
18	-6.44	1.95	-3.98	1.02	0.41	-1.48	9.35	48.00	4.13
19	-0.66	1.84	-3.89	0.26	-0.17	0.99	6.04	48.00	6.95
20	-1.11	-1.22	-4.78	-0.08	-0.11	1.01	4.23	48.00	+Large

¹ See Figure 2.10.14-4 for locations of sections.

² Stress components correspond to a cylindrical coordinate system.

Table 2.10.14-20 30-Foot Top-End Drop with Internal Pressure, $P_m + P_b$ Stresses, ksi

Sec ¹	S_x^2	S_y^2	S_z^2	S_{xy}^2	S_{yz}^2	S_{xz}^2	Stress Intensity	Stress Allow.	MS
1	0.00	0.00	-0.16	0.00	0.00	0.00	0.16	96.90	+Large
2	0.00	0.01	-1.50	0.00	0.00	0.00	1.51	96.90	+Large
3	0.02	-0.30	-3.47	0.02	0.01	0.00	3.49	96.90	+Large
4	-0.21	2.84	0.64	-0.20	0.00	0.00	3.07	96.90	+Large
5	-0.20	2.84	-0.68	-0.20	0.00	0.00	3.53	96.90	+Large
6	-0.22	3.12	-2.13	-0.22	0.01	0.01	5.26	96.90	+Large
7	-0.20	2.78	0.25	-0.19	0.00	-0.04	3.01	68.50	+Large
8	-0.33	0.94	1.15	-0.08	0.01	0.16	1.52	68.50	+Large
9	0.00	0.01	-0.09	0.00	0.00	0.00	0.10	68.50	+Large
10	0.00	0.02	-0.07	0.00	0.00	-0.01	0.09	68.50	+Large
11	-0.04	0.01	-0.07	0.00	0.00	-0.03	0.10	68.50	+Large
12	-0.01	0.01	-0.02	0.00	0.00	-0.01	0.04	68.50	+Large
13	0.27	0.40	-0.17	-0.01	0.00	0.03	0.57	68.50	+Large
14	0.02	0.02	-0.03	0.00	0.00	0.01	0.05	68.50	+Large
15	-0.18	2.46	-3.79	-0.17	0.01	0.06	6.25	68.50	9.96
16	-9.52	-11.56	-13.10	1.37	-1.07	4.69	10.62	68.50	5.45
17	0.00	0.75	-3.79	-0.06	0.02	0.06	4.54	68.50	+Large
18	-10.51	-1.13	-10.56	-1.41	-1.16	-3.09	13.02	68.50	4.26
19	-1.35	1.80	-4.42	0.40	-0.31	1.41	6.85	68.50	9.00
20	0.31	-0.29	-3.55	0.00	-0.02	3.23	7.52	68.50	8.11

¹ See Figure 2.10.14-4 for locations of sections.

² Stress components correspond to a cylindrical coordinate system.

Table 2.10.14-21 30-Foot Top-Corner Drop with Internal Pressure, P_m Stresses, ksi

Sec ¹	Location (deg) ²	S_x^3	S_y^3	S_z^3	S_{xy}^3	S_{yz}^3	S_{xz}^3	Stress Intensity	Stress Allow.	MS
1	67.5	0.02	0.20	0.80	0.04	-2.72	-0.02	5.48	67.83	+Large
2	180	-0.04	-0.28	-10.37	0.00	0.04	0.00	10.33	67.83	5.57
3	52.5	0.07	0.30	-5.70	0.02	3.53	0.00	9.26	67.83	6.33
4	120	-0.19	2.32	-0.33	-0.06	-1.41	0.00	3.87	67.83	+Large
5	180	-0.08	2.48	-6.10	0.14	0.02	0.00	8.59	67.83	6.90
6	0	-0.17	2.59	-5.85	-0.24	0.04	0.02	8.46	67.83	7.02
7	120	-0.19	1.96	-0.08	0.00	-2.50	0.03	5.40	48.00	7.89
8	180	-1.22	1.17	2.55	0.05	-0.18	-1.09	4.37	48.00	9.98
9	60	0.01	-0.12	0.86	-0.14	-2.70	0.00	5.50	48.00	7.73
10	0	0.44	-1.90	-0.39	0.26	-0.20	1.58	3.77	48.00	+Large
11	0	-1.54	-1.53	-0.01	0.05	-0.02	-0.23	1.63	48.00	+Large
12	0	0.03	-0.75	-0.27	0.07	0.01	-0.48	1.16	48.00	+Large
13	90	-0.17	-1.05	-0.06	-0.03	0.10	0.00	1.01	48.00	+Large
14	97.5	0.11	-0.49	-0.02	-0.10	0.11	-0.01	0.66	48.00	+Large
15	0	-0.22	1.61	-6.24	-0.20	-0.02	-0.04	7.88	48.00	5.09
16	180	-6.31	-7.41	-1.56	-0.90	0.29	2.61	7.97	48.00	5.02
17	30	0.08	1.49	-7.98	-0.13	2.34	0.18	10.58	48.00	3.54
18	0	-7.62	0.50	-10.26	-1.09	-0.25	-1.78	11.84	48.00	3.05
19	0	-2.63	-1.19	-8.95	0.04	0.32	1.43	8.09	48.00	4.93
20	0	-1.82	-1.55	-6.33	0.14	0.20	1.14	5.25	48.00	8.14

¹ See Figure 2.10.14-4 for locations of sections.

² The location specifies the angle at which the maximum stress intensity occurs. See Figure 2.10.14-1 for definition of angular location.

³ Stress components correspond to a cylindrical coordinate system.

Table 2.10.14-22 30-Foot Top-Corner Drop with Internal Pressure, $P_m + P_b$ Stresses, ksi

Sec ¹	Location (deg) ²	S_x^3	S_y^3	S_z^3	S_{xy}^3	S_{yz}^3	S_{xz}^3	Stress Intensity	Stress Allow.	MS
1	60	0.04	1.44	1.37	0.04	-3.16	-0.02	6.33	96.90	+Large
2	180	-0.03	3.04	-9.78	0.22	0.04	0.00	12.83	96.90	6.55
3	60	0.04	0.53	-4.64	0.05	4.17	0.01	9.82	96.90	8.87
4	180	-0.16	6.38	0.28	0.33	-0.14	-0.02	6.58	96.90	+Large
5	180	-0.12	7.50	-4.28	0.48	0.02	0.00	11.80	96.90	7.21
6	0	-0.27	4.85	-5.03	-0.40	0.01	0.04	9.91	96.90	8.78
7	127.5	-0.25	-0.78	-1.40	-0.07	-3.30	0.01	6.64	68.50	9.32
8	180	-1.96	0.27	5.70	-0.03	0.07	-1.09	7.97	68.50	7.59
9	52.5	-0.03	0.56	0.96	-0.30	-3.42	0.05	6.88	68.50	8.96
10	0	1.66	-3.19	-5.62	0.24	0.03	1.68	8.03	68.50	7.53
11	180	1.34	1.11	0.01	-0.01	0.08	-0.94	2.30	68.50	+Large
12	0	-0.10	-0.60	-0.13	0.09	0.02	-0.67	1.36	68.50	+Large
13	105	-0.03	-0.98	-0.06	-0.26	0.03	0.01	1.09	68.50	+Large
14	105	0.08	-0.63	-0.01	-0.23	0.09	0.00	0.86	68.50	+Large
15	15	-0.02	2.92	-6.20	0.08	-0.25	-0.03	9.13	68.50	6.50
16	0	-9.28	-10.03	-13.27	1.18	-0.98	4.68	10.55	68.50	5.49
17	45	0.17	1.62	-6.23	-0.33	3.87	0.37	11.06	68.50	5.19
18	0	-12.28	-2.39	-15.48	-1.58	-1.06	-3.57	15.87	68.50	3.32
19	7.5	-1.31	-2.99	-12.42	0.24	0.21	0.86	11.28	68.50	5.07
20	15	1.26	-0.32	-4.05	0.08	0.04	3.14	8.23	68.50	7.32

¹ See Figure 2.10.14-4 for locations of sections.

² The location specifies the angle at which the maximum stress intensity occurs. See Figure 2.10.14-1 for definition of angular location.

³ Stress components correspond to a cylindrical coordinate system.

Table 2.10.14-23 30-Foot Bottom-End Drop with Internal Pressure, P_m Stresses, ksi

Sec ¹	S_x^2	S_y^2	S_z^2	S_{xy}^2	S_{yz}^2	S_{xz}^2	Stress Intensity	Stress Allow.	MS
1	0.02	0.24	-4.22	-0.01	-0.01	-0.02	4.46	67.83	+Large
2	0.00	0.00	-2.55	0.00	0.00	0.00	2.55	67.83	+Large
3	0.00	0.09	-1.21	0.00	0.00	0.01	1.30	67.83	+Large
4	-0.12	2.77	-3.26	-0.18	-0.01	0.00	6.04	67.83	+Large
5	-0.13	2.66	-1.79	-0.18	0.00	0.00	4.47	67.83	+Large
6	-0.13	2.68	-0.49	-0.18	0.00	0.00	3.19	67.83	+Large
7	-0.10	2.23	-3.48	-0.15	0.00	0.10	5.72	48.00	7.39
8	0.80	2.85	-2.23	-0.01	-0.02	-0.17	5.09	48.00	8.43
9	0.03	0.34	-4.10	-0.03	-0.01	-0.08	4.45	48.00	9.79
10	0.34	1.15	-3.10	0.03	-0.01	-0.29	4.27	48.00	+Large
11	2.86	1.32	-7.84	-0.10	-0.48	0.34	10.75	48.00	+Large
12	-1.00	0.93	-5.08	0.12	0.10	-0.67	6.13	48.00	6.83
13	2.20	2.97	-1.94	0.05	0.01	-0.46	4.96	48.00	8.68
14	-1.32	-2.22	-11.77	0.07	-0.15	-1.74	11.02	48.00	3.36
15	-0.13	2.58	-0.39	-0.18	0.00	0.00	2.98	48.00	+Large
16	-0.08	1.10	-0.16	-0.08	0.00	-0.09	1.33	48.00	+Large
17	0.00	0.10	-1.08	0.00	0.00	0.03	1.18	48.00	+Large
18	-0.01	0.07	-0.68	0.00	0.00	0.06	0.76	48.00	+Large
19	-0.05	0.22	-0.32	0.00	0.00	0.06	0.56	48.00	+Large
20	-0.18	0.05	-0.93	0.00	0.00	-0.20	1.03	48.00	+Large

¹ See Figure 2.10.14-4 for locations of sections.

² Stress components correspond to a cylindrical coordinate system.

Table 2.10.14-24 30-Foot Bottom-End Drop with Internal Pressure, $P_m + P_b$ Stresses, ksi

Sec ¹	S_x^2	S_y^2	S_z^2	S_{xy}^2	S_{yz}^2	S_{xz}^2	Stress Intensity	Stress Allow.	MS
1	0.02	0.36	-4.25	-0.02	-0.01	-0.04	4.61	96.90	+Large
2	0.00	0.01	-2.55	0.00	0.00	0.00	2.56	96.90	+Large
3	0.00	0.08	-1.26	0.00	0.00	0.01	1.34	96.90	+Large
4	-0.20	3.09	-3.22	-0.21	-0.01	-0.01	6.33	96.90	+Large
5	-0.20	2.84	-1.76	-0.20	0.00	0.00	4.62	96.90	+Large
6	-0.21	2.87	-0.46	-0.20	0.00	0.00	3.35	96.90	+Large
7	-0.01	1.77	-4.01	-0.12	-0.01	0.10	5.79	68.50	+Large
8	0.68	2.56	-4.53	0.12	-0.02	-0.29	7.12	68.50	8.62
9	0.10	0.42	-4.24	-0.03	-0.02	-0.24	4.68	68.50	+Large
10	0.64	1.84	-2.82	0.01	-0.04	-0.35	4.69	68.50	+Large
11	2.16	-1.09	-16.04	-0.20	-1.32	0.68	18.38	68.50	2.73
12	-1.81	-0.19	-9.08	0.10	0.11	-1.00	9.03	68.50	6.59
13	6.29	9.44	-0.86	0.02	-0.04	-0.38	10.32	68.50	5.64
14	4.12	8.84	-8.49	0.01	0.15	-2.03	17.65	68.50	2.88
15	-0.19	2.69	-0.63	-0.19	0.00	0.00	3.33	68.50	+Large
16	-0.19	1.32	0.18	-0.10	-0.01	-0.09	1.54	68.50	+Large
17	0.01	0.06	-1.24	0.00	0.00	0.09	1.30	68.50	+Large
18	0.01	0.07	-0.73	0.00	0.01	0.07	0.80	68.50	+Large
19	-0.08	0.24	-0.49	0.00	0.01	0.06	0.74	68.50	+Large
20	-0.36	0.25	-0.89	0.01	0.00	-1.65	3.34	68.50	+Large

¹ See Figure 2.10.14-4 for locations of sections.

² Stress components correspond to a cylindrical coordinate system.

Table 2.10.14-25 30-Foot Bottom-Corner Drop with Internal Pressure, P_m Stresses, ksi

Sec ¹	Location (deg) ²	S_x^3	S_y^3	S_z^3	S_{xy}^3	S_{yz}^3	S_{xz}^3	Stress Intensity	Stress Allow.	MS
1	0	-0.04	1.75	-10.25	-0.18	-0.35	-0.03	12.04	67.83	4.63
2	180	-0.04	-0.28	-10.82	0.00	-0.05	0.00	10.78	67.83	5.29
3	180	-0.01	0.31	-5.34	0.01	0.09	0.03	5.66	67.83	+Large
4	0	-0.17	2.59	-6.85	-0.23	-0.03	-0.02	9.46	67.83	6.17
5	180	-0.08	2.48	-6.68	0.14	-0.02	0.00	9.17	67.83	6.40
6	142.5	-0.18	2.20	-1.87	-0.20	1.02	0.03	4.57	67.83	+Large
7	0	-0.16	1.50	-7.19	-0.19	0.02	0.15	8.71	48.00	4.51
8	15	0.95	2.55	-4.19	-0.02	0.02	-0.09	6.74	48.00	6.12
9	0	0.13	0.48	-11.26	0.00	-0.34	-0.18	11.76	48.00	3.08
10	0	1.33	-0.73	-9.11	0.22	-0.24	0.19	10.47	48.00	3.58
11	0	1.26	0.32	-8.62	0.15	0.51	0.82	10.09	48.00	3.76
12	0	-2.47	-1.01	-10.59	0.09	-0.23	-1.08	9.73	48.00	3.93
13	180	0.74	2.35	-1.83	0.03	-0.01	-0.80	4.41	48.00	9.88
14	180	-1.31	-1.79	-11.13	-0.07	0.15	-2.16	10.74	48.00	3.47
15	112.5	-0.18	1.91	-1.13	0.04	2.48	-0.07	5.83	48.00	7.23
16	127.5	-0.06	0.49	-0.50	0.07	2.06	-0.26	4.26	48.00	+Large
17	180	0.01	0.40	-4.57	-0.01	0.08	0.14	4.97	48.00	8.66
18	60	0.02	0.09	0.45	0.02	1.74	0.07	3.50	48.00	+Large
19	0	-1.44	-1.46	-0.82	0.18	0.05	0.74	1.66	48.00	+Large
20	97.5	0.07	-0.46	-1.01	-0.13	0.00	-0.15	1.15	48.00	+Large

¹ See Figure 2.10.14-4 for locations of sections.

² The location specifies the angle at which the maximum stress intensity occurs. See Figure 2.10.14-1 for definition of angular location.

³ Stress components correspond to a cylindrical coordinate system.

Table 2.10.14-26 30-Foot Bottom-Corner Drop with Internal Pressure, $P_m + P_b$ Stresses, ksi

Sec ¹	Location (deg) ²	S_x^3	S_y^3	S_z^3	S_{xy}^3	S_{yz}^3	S_{xz}^3	Stress Intensity	Stress Allow.	MS
1	15	-0.01	1.27	-10.61	0.02	-1.51	-0.06	12.27	96.90	6.90
2	180	-0.03	3.04	-10.21	0.22	-0.05	0.00	13.27	96.90	6.30
3	180	0.01	0.82	-5.25	0.05	0.11	0.01	6.08	96.90	+Large
4	0	-0.26	4.74	-6.06	-0.38	-0.01	-0.03	10.83	96.90	7.95
5	180	-0.12	7.49	-4.87	0.48	-0.02	0.00	12.39	96.90	6.82
6	180	-0.17	6.47	-0.89	0.35	0.13	0.03	7.38	96.90	+Large
7	37.5	0.01	1.65	-7.51	0.03	-0.35	0.19	9.20	68.50	6.45
8	0	0.63	2.19	-7.06	-0.18	0.06	-0.14	9.27	68.50	6.39
9	52.5	0.22	0.18	-8.01	-0.42	-4.78	-0.44	12.63	68.50	4.42
10	0	1.30	-2.45	-14.17	0.11	-0.25	0.46	15.51	68.50	3.42
11	0	1.99	-1.54	-16.99	0.28	1.42	1.39	19.35	68.50	2.54
12	0	-2.54	-1.43	-12.80	0.00	-0.22	-1.52	11.59	68.50	4.91
13	7.5	4.62	8.13	-0.86	0.17	-0.01	-0.10	9.00	68.50	6.61
14	7.5	4.26	8.58	-8.38	0.03	0.00	-1.33	17.10	68.50	3.01
15	127.5	-0.25	-1.48	-2.34	-0.11	3.37	-0.04	6.79	68.50	9.09
16	142.5	-0.17	0.45	-0.67	0.06	4.05	0.17	8.19	68.50	7.36
17	52.5	-0.04	1.06	0.90	-0.28	3.14	-0.03	6.31	68.50	9.86
18	37.5	-0.10	0.08	1.60	0.06	2.68	-0.36	5.63	68.50	+Large
19	0	-0.66	-0.19	1.04	-0.02	0.15	0.74	2.28	68.50	+Large
20	45	-0.20	0.21	-0.85	0.23	-0.06	-1.66	3.42	68.50	+Large

¹ See Figure 2.10.14-4 for locations of sections.

² The location specifies the angle at which the maximum stress intensity occurs. See Figure 2.10.14-1 for definition of angular location.

³ Stress components correspond to a cylindrical coordinate system.

Table 2.10.14-27 Accident Internal Pressure with Inertia Load, P_m Stresses, ksi

Sec ¹	Location (deg) ²	S_x^3	S_y^3	S_z^3	S_{xy}^3	S_{yz}^3	S_{xz}^3	Stress Intensity	Stress Allow.	MS
1	0	0.01	0.07	-1.22	0.00	0.00	-0.01	1.29	67.83	+Large
2	30	0.00	0.00	-0.67	0.00	0.00	0.00	0.67	67.83	+Large
3	180	0.00	0.00	-0.23	0.00	0.00	0.00	0.23	67.83	+Large
4	0	-0.26	5.34	0.37	-0.37	0.00	0.00	5.65	67.83	+Large
5	0	-0.26	5.33	0.86	-0.37	0.00	0.00	5.63	67.83	+Large
6	0	-0.26	5.32	1.29	-0.37	0.00	0.00	5.63	67.83	+Large
7	0	-0.26	5.33	0.29	-0.36	-0.01	-0.04	5.64	48.00	7.51
8	97.5	-0.16	2.06	0.30	-0.01	-0.07	0.16	2.27	48.00	+Large
9	0	0.01	0.08	-1.19	-0.01	0.00	-0.02	1.27	48.00	+Large
10	7.5	0.09	0.31	-0.90	0.01	0.00	-0.07	1.22	48.00	+Large
11	180	0.58	0.06	-3.57	-0.04	-0.22	0.16	4.18	48.00	+Large
12	180	-0.35	0.37	-1.64	0.05	0.03	-0.15	2.03	48.00	+Large
13	180	0.71	0.95	-0.99	0.02	0.01	-0.10	1.95	48.00	+Large
14	0	-0.36	-0.63	-4.17	0.02	-0.06	-0.61	4.00	48.00	+Large
15	0	-0.27	5.41	1.31	-0.37	0.00	0.06	5.73	48.00	7.38
16	0	-0.17	2.25	0.80	-0.16	0.00	-0.09	2.45	48.00	+Large
17	157.5	0.00	0.05	-0.19	0.00	0.00	0.00	0.24	48.00	+Large
18	180	0.01	0.20	-0.11	0.01	0.00	0.04	0.33	48.00	+Large
19	105	-0.03	0.20	-0.20	0.00	0.00	0.04	0.41	48.00	+Large
20	105	-0.15	0.13	-0.88	0.00	0.00	-0.33	1.14	48.00	+Large

¹ See Figure 2.10.14-4 for locations of sections.

² The location specifies the angle at which the maximum stress intensity occurs. See Figure 2.10.14-1 for definition of angular location.

³ Stress components correspond to a cylindrical coordinate system.

Table 2.10.14-28 Accident Internal Pressure with Inertia Load , $P_m + P_b$ Stresses, ksi

Sec ¹	Location (deg) ²	S_x^3	S_y^3	S_z^3	S_{xy}^3	S_{yz}^3	S_{xz}^3	Stress Intensity	Stress Allow.	MS
1	0	0.01	0.11	-1.23	0.00	0.00	-0.01	1.34	96.90	+Large
2	0	0.00	0.01	-0.66	0.00	0.00	0.00	0.67	96.90	+Large
3	0	0.00	-0.01	-0.24	0.00	0.00	0.00	0.24	96.90	+Large
4	0	-0.41	5.76	0.46	-0.41	0.00	0.00	6.22	96.90	+Large
5	0	-0.41	5.69	0.93	-0.40	0.00	0.00	6.15	96.90	+Large
6	0	-0.41	5.69	1.38	-0.40	0.00	0.00	6.16	96.90	+Large
7	0	-0.39	5.55	-0.31	-0.39	-0.01	-0.05	6.01	68.50	+Large
8	105	-0.47	2.39	0.87	0.00	-0.09	0.19	2.89	68.50	+Large
9	0	0.03	0.11	-1.22	-0.01	-0.01	-0.06	1.33	68.50	+Large
10	0	0.07	0.22	-1.09	-0.03	-0.03	-0.06	1.33	68.50	+Large
11	180	-0.34	-1.37	-7.60	-0.07	-0.62	0.27	7.35	68.50	8.32
12	180	-0.63	-0.04	-3.13	0.04	0.03	-0.22	3.11	68.50	+Large
13	172.5	1.58	2.37	-0.74	0.01	-0.01	-0.09	3.11	68.50	+Large
14	7.5	1.42	3.06	-2.98	0.00	0.05	-0.71	6.15	68.50	+Large
15	0	-0.39	5.57	0.65	-0.39	0.00	0.06	6.02	68.50	+Large
16	0	-0.36	2.64	1.34	-0.20	-0.01	-0.09	3.03	68.50	+Large
17	150	0.00	0.03	-0.22	0.00	0.00	0.00	0.26	68.50	+Large
18	0	0.03	0.17	-0.26	-0.01	0.00	0.05	0.44	68.50	+Large
19	105	-0.05	0.22	-0.33	0.00	0.01	0.03	0.55	68.50	+Large
20	45	-0.25	0.42	-0.89	0.01	0.00	-1.68	3.42	68.50	+Large

¹ See Figure 2.10.14-4 for locations of sections.

² The location specifies the angle at which the maximum stress intensity occurs. See Figure 2.10.14-1 for definition of angular location.

³ Stress components correspond to a cylindrical coordinate system.

2.10.15 NAC-LWT Alternate B Port Cover

The Alternate B port cover has two face seals on the inner end of the port cover. The primary containment seal is provided by an inner metal face seal located in a groove on the face (towards the inner edge) of the barrel of the port cover body. The metal face seal is used to maintain a leaktight containment boundary per the requirements of ANSI N14.5-1997. The secondary (test annulus) face seal is a single Viton[®] O-ring located in a groove on the face (towards the outer edge) of the barrel of the port cover body. The Alternate B port cover is fabricated from Type XM-19 stainless steel and is fastened to the cask top forging using high-strength SB-637 Grade N07718 bolts (3/8-16 UNC).

2.10.15.1 Alternate B Port Cover Bolt Analysis

2.10.15.1.1 Port Cover Bolt Preload

The Alternate B port cover uses a metallic O-ring for containment and Viton[®] O-ring face seal for leakage rate testing. The metallic O-ring requires a 1,725 lb/in sealing force and the Viton[®] O-ring requires a sealing force of 120 lb/in (based on manufacturers' data).

The force required to compress the metallic O-ring seal is:

$$P1 = Y2 \times C = 1,898 \times (\pi \times 1.86) = 11,090 \text{ lbs}$$

where:

$$Y2 = Km \times Kd \times Y1 = 1 \times 1.1 \times 1,725 = 1,898 \text{ lb/in}$$

$$C = \pi \times d, \text{ Circumference of the O-ring}$$

$$d = 1.86 \text{ inches, The average diameter of the seal groove}$$

$$Km = 1.0, \text{ Material Factor}$$

$$Kd = 1.1, \text{ Diameter Factor}$$

$$Y1 = 1,725 \text{ lbs, Ideal compressive load}$$

The load due to internal pressure is:

$$P2 = P \times \frac{\pi \times d}{4} = 600 \times \frac{\pi \times 1.86^2}{4} = 1,630 \text{ lbs}$$

where:

$$P = 600 \text{ psig, which bounds the maximum pressure in the LWT cask during the fire accident (Section 3.5.4.4)}$$

The force due to the port cover weight is:

$$P3 = W_{pc} \times 60g = 600 \text{ lbs}$$

where:

$$W_{pc} = 10 \text{ lbs, The approximate weight of the port cover}$$

The force required to compress the Viton[®] O-ring is:

$$P4 = 120 \times \pi \times dp = 955 \text{ lbs}$$

where:

$$dp = 2.534 \text{ in, diameter of the Viton[®] seal}$$

The required bolt preload per bolt is:

$$F = \frac{P1 + P2 + P3 + P4}{3} = \frac{11,090 + 1,630 + 600 + 955}{3} = 4,758 \text{ lb/bolt}$$

Therefore, the required bolt torque is:

$$T = 0.2Fd = 0.2 \times 4758 \times 0.281 = 267 \text{ in-lb}$$

where:

$$d = 0.281 \text{ in, the mean bolt diameter}$$

The recommended torque is 285 ± 15 in-lb, which corresponds to a maximum bolt preload of 5,340 lbs.

The port cover is attached to the cask body with three bolts. The bolts are threaded into the SA182 Type-304 stainless steel top forging of the cask using Helicoils. The tensile stress in the bolt when the maximum bolt preload is applied is:

$$S = \frac{P}{A} = \frac{5,340}{0.06158} = 86.7 \text{ ksi}$$

where:

$$P = 5,340 \text{ lbs, the bolt preload}$$

$$A = \pi d^2/4, \text{ bolt cross-sectional area}$$

$$d = 0.28 \text{ in, the bolt shank diameter}$$

The margin of safety is:

$$MS = \frac{S_y}{S} - 1 = \frac{142.35}{86.7} - 1 = +0.64$$

where:

$$S_y = 142.35 \text{ ksi, yield strength of SB-637, Grade N07718 @ 250°F}$$

The tensile stress in the 3/8-16UNC bolt is:

$$S = \frac{P}{A_t} = \frac{5,340}{0.074} = 72.2 \text{ ksi}$$

where:

$$P = 5,340 \text{ lbs, the bolt preload}$$

$$A_t = 3.1416 \left(\frac{E_{s_{\min}}}{2} - \frac{0.16238}{n} \right)^2 = 3.1416 \left(\frac{0.3266}{2} - \frac{0.16238}{16} \right)^2 = 0.074 \text{ in}^2$$

$$= 0.074 \text{ in}^2, \text{ tensile area of the bolt}$$

For the 3/8-16UNC bolts (Machinery's Handbook)

$$n = 16, \text{ number of threads per inch}$$

$$D = 0.375 \text{ in, bolt diameter}$$

$$K_{n_{\max}} = 0.321 \text{ in, maximum minor diameter of internal thread}$$

$$E_{s_{\min}} = 0.3266 \text{ in, minimum major diameter of external thread}$$

$$E_{n_{\max}} = 0.3429 \text{ in, maximum pitch diameter of internal thread}$$

$$D_{s_{\min}} = 0.3595 \text{ in, minimum major diameter of external thread}$$

$$L_e = 0.75 \text{ in, thread engagement}$$

The margin of safety is:

$$MS = \frac{S_y}{S} - 1 = \frac{142.35}{72.2} - 1 = +0.97 @ 250°F$$

where:

$$S_y = 142.35 \text{ ksi, yield strength of SB-637, Grade N07718 @ 250°F}$$

The shear stress in the bolt thread is:

$$\tau = \frac{P}{A_s} = \frac{5,340}{0.348} = 15.3 \text{ ksi}$$

where:

$$P = 5,340 \text{ lbs, the bolt preload}$$

$$A_s = 3.1416nL_eKn_{max}\left[\frac{1}{2n} + 0.57735(Es_{min} - Kn_{max})\right]$$

$$= 0.348 \text{ in}^2, \text{ shear area of the bolt threads}$$

The margin of safety is:

$$MS = \frac{0.6S_m}{t} - 1 = \frac{0.6 \times 47.5}{15.3} - 1 = +0.86$$

where:

$$S_m = 47.5 \text{ ksi, stress intensity of SB-637, Grade N07718 @250°F}$$

Conservatively ignoring the strength of the Helicoil, the shear stress of the threads in the top forging is:

$$S = \frac{5,340}{0.461} = 11.6 \text{ ksi}$$

where:

$$P = 5,340 \text{ lbs, the bolt preload}$$

$$A_n = 3.1416nL_eDs_{min}\left[\frac{1}{2n} + 0.57735(Ds_{min} - En_{max})\right]$$

$$= 0.461 \text{ in}^2, \text{ shear area of the bolt threads}$$

The margin of safety is:

$$MS = \frac{0.6S_m}{S} - 1 = \frac{0.6 \times 20.0}{11.6} - 1 = +0.03$$

where:

$$S_m = 20.0 \text{ ksi, stress intensity of Type 304 stainless steel @ 250°F}$$

2.10.15.1.2 Port Cover Bolt Thermal Stress Evaluation

Thermal stresses generated in the port cover are due to the difference in thermal expansion of the port cover bolts and adjacent components.

Cold

During the cold condition (−40°F), the port cover will contract at a faster rate than the port cover bolt. The change in length due to thermal expansion/contraction for the components is calculated using the following equation.

$$\Delta L = \Delta T \alpha L$$

At -40°F , the changes in length of the port cover and port cover bolt due to a temperature differential of -110°F ($-40 - 70$) as follows.

Component	Material	Coefficient of Thermal Expansion, α (in/in- $^{\circ}\text{F}$)	Component Length, L (in)	Change in Length, ΔL (in)
Port Cover	SA-479 Type XM-19	8.16×10^{-6}	1.0	-9.0×10^{-4}
Bolt	SB-637 Grade N07718	7.05×10^{-6}	1.0	-7.8×10^{-4}

The net change in bolt length is:

$$\Delta L = (-9.0 \times 10^{-4}) - (-7.8 \times 10^{-4}) = -0.0001 \text{ in}$$

The bolt strain associated with this change in length is 0.0001 ($0.0001/1.0$). Since the port cover contracts more than the bolts, no additional load is applied to the port cover bolts during a -40°F condition.

To maintain the seal in the cold condition, the bolt strain must be less than the strain due to the bolt preload. From Section 2.10.15.1.1, the bolt preload (F) is 5,340 lbs. The strain associated with the preload is:

$$\epsilon = \frac{F}{AE} = \frac{5,340}{0.0616 \times 29.6 \times 10^6} = 0.00293$$

where:

$$E = 29.6 \times 10^6 \text{ psi, modulus of elasticity for SB-637 Grade N07718 @ } -40^{\circ}\text{F}$$

$$A = \frac{\pi d^2}{4} = 0.0616 \text{ in}^2, \text{ bolt cross-sectional area}$$

$$d = 0.28 \text{ in, diameter of the bolt}$$

Since the preload strain is significantly larger than the strain due to cold conditions, the seal is maintained.

Fire Accident

For the fire accident, a peak temperature of 845°F (Section 2.7.2.4.3) is used for the evaluation of the thermal stress in the port cover bolts. At 845°F , the changes in length of the port cover and port cover bolt due to a temperature differential of 775°F ($845 - 70$) are as follows.

Component	Material	Coefficient of Thermal Expansion, α (in/in- $^{\circ}\text{F}$)	Component Length, L (in)	Change in Length, ΔL (in)
Port Cover	SA-479 Type XM-19	9.26×10^{-6}	1.0	7.18×10^{-3}
Bolt	SB-637 Grade N07718	7.92×10^{-6}	1.0	6.14×10^{-3}

The net change in length of the port cover bolt is:

$$\Delta L_{\text{bolt}} = (7.18 \times 10^{-3}) - (6.14 \times 10^{-3}) = 1.0 \times 10^{-3} \text{ in}$$

The change in length of the bolt results in a uniform strain of:

$$\epsilon_b = \frac{\Delta L}{L} = \frac{1.0 \times 10^{-3}}{1.0} = 0.0010 \text{ in/in}$$

where:

$$L = \text{bolt length (shank)} = 1.0 \text{ in}$$

The thermal stress in the bolt is:

$$S = \epsilon_b E = 0.0010 \times (25.7 \times 10^6) = 25,700 \text{ psi} = 25.7 \text{ ksi}$$

where:

$$E = 25.7 \times 10^6 \text{ psi, modulus of elasticity for SB-637 Grade N07718 @845°F}$$

Combining the thermal stress and preload stress (Section 2.10.15.1.1), the total stress in the bolt is:

$$S = 25.7 + 86.7 = 112.4 \text{ ksi}$$

The margin of safety is:

$$MS = \frac{S_y}{S} - 1 = \frac{132.7}{112.4} - 1 = +0.18 @ 845^\circ\text{F}$$

where:

$$S_y = 132.7 \text{ ksi, the yield strength of SB-637 Grade N077/8@845°F}$$

To determine the sealing capacity of the metallic seal during the fire accident, the thermal expansion of each component is calculated. The following gives the thermal expansion of each component.

Component	Length for Expansion, L (in)	Average Temperature (°F)	Change in Temperature, ΔT (°F)	Coefficient of Thermal Expansion, α (in/in-F)	Change in Length, ΔL (in)
Cask	2.255 (3.255-1.0)	640	570	9.59×10^{-6}	0.01233
Bolt	1.000	826	756	7.90×10^{-6}	0.00597
Port Cover	3.255 (3.63-0.375)	659	589	9.10×10^{-6}	0.01745

The displacement that tends to lift the port cover off the seals is:

$$\begin{aligned}\Delta L_{\text{seal}} &= 0.01233 + 0.00597 - 0.01745 \\ &= 0.00085 \text{ in}\end{aligned}$$

This corresponds to a strain in the bolt shank of 0.00085. Since the preload strain is 0.00293 inch and is larger than the strain due to fire accident conditions, the seal is maintained.

2.10.15.1.3 Port Cover Bolt Side-Drop Evaluation

The governing cask drop orientation that would result in reducing the force applied to the metal face seal is the side-drop condition. The side-drop condition is evaluated with the cask body in the orientation, which results in the inertia load of the port cover reducing the force applied to the port cover metal face seal.

A three-dimensional ANSYS finite element model representing one-sixth of the port cover is used to evaluate the LWT port cover during side-drop conditions (see Figure 2.10.15-1). The model is constructed using ANSYS SOLID45, CONTAC52, and BEAM4 elements. CONTAC52 elements are used to model the sealing surface of the port cover to evaluate the sealing force. Beam (BEAM4) elements are used to model the port cover bolts. An initial strain is specified in the BEAM4 elements to generate the initial preload force. Since the bolts are located at a symmetry plane in the model, the applied strain is based on one-half of the total bolt force.

Symmetry boundary conditions are applied to the model on the 0° and 60° surfaces. To prevent axial motion of the port cover, the lower node of the bolt is restrained axially. The CONTAC52 elements on the sealing surface represent the interface with the cask body. The following presents the results for the side-drop analyses for the SB-637 Grade N07718 port cover bolts.

Load Case	Seal Force (lb)	Load per Bolt (lb)	Bolt Stress (psi)	MS
Preload only	2,679	5,357	86,388	0.65
Preload + Normal Pressure	2,759	5,365	86,516	0.65
Preload + Normal Pressure + 60 g	2,501	5,377	86,698	0.64
Preload + Accident Pressure	2,172	4,762	76,788	0.85

Where the reported seal force is one-sixth of the actual port cover seal force. The material allowables during normal conditions are at 250°F; for accident conditions, allowables are at 850°F.

The required force to compress the seals is 12,045 lbs (11,090 + 955) as shown in Section 2.10.15.1.1. For a one-sixth model, the force is 2,008 lbs (12,045/6). Since the sealing forces presented above are greater than 2,008 lbs, the seal is maintained.

2.10.15.1.4 Penetration Evaluation

Using the methodology presented in Section 2.6.10.5, a finite element analysis of the port cover is performed for the penetration event for the normal conditions of transport. The finite element model described in Section 2.10.15.1.3 (Figure 2.10.15-1) is used.

The equivalent dynamic loading, from Ugural and Fenster, is calculated using the following relation.

$$P_{\text{dyn}} = W (1 + (1 + 2h / \delta_{\text{st}})^{1/2})$$

where:

P_{dyn} = dynamic load resulting from weight (W) free falling a height (h), lb

W = weight, 13 lbs

h = drop height, 40 inches

δ_{st} = static deflection resulting from weight (W) on plate, inches

The dynamic loading is calculated to be 6,799 lbs, resulting from the 13-lb, 1.25-inch diameter projectile dropped through a distance of 40 inches onto the port cover. The sealing surface bearing stress is calculated to be 2.61 ksi, which results in a margin of safety of +8.0 compared with yield strength of the upper forging. The dynamic load on the port cover is applied as a bearing load, which will pass through the port cover body to the top forging. Also, the dynamic load increases the compressive force on the inner end O-ring, trapped in an O-ring groove at the bottom of the port cover body. Thus, the primary seal is not affected.

2.10.15.1.5 Puncture Evaluation

The puncture accident follows the 30-foot drop that the cask must sustain. The impact limiters remain attached subsequent to the 30-foot free drop, as shown in Section 2.6.7.4. It is concluded in Section 2.7.1.6 that the hypothetical crush accident does not apply to the NAC-LWT cask. Therefore, the impact limiters are attached to the cask prior to the cask dropping onto the mild steel pin. The port covers are located near the top of the cask, underneath the impact limiter.

When the top impact limiter strikes the mild steel pin, it will support the top end of the cask, while the bottom of the cask continues to translate, then begins to rotate about the mild steel pin as a pivot point, until the bottom impact limiter contacts the unyielding surface. During the time in which the cask is rotating about the pin-impact limiter contact, the maximum force, which can be applied to the port cover surface, is limited by the crush strength of the impact limiter material. The force is calculated from the product of the crush strength of the impact limiter (3,500 psi) and the common area of contact between the impact limiter and the port cover (12.3 in²). The maximum load applied to the port cover by the impact limiter is:

$$\begin{aligned}P_b &= 3,500 \times 12.3 \\&= 43,050 \text{ lbs}\end{aligned}$$

The stress in the Alternate B port cover at the cask body interface is:

$$\begin{aligned}\frac{P_b}{A_s} &= \frac{43,050}{A_s} \text{ psi} \\&= 43,050/2.07 \text{ psi} \\&= 20.8 \text{ ksi}\end{aligned}$$

where:

$$A_s = \text{Total concentric ring bearing area at inner face of port cover} = 2.07 \text{ in}^2$$

The maximum port cover temperature is less than 250°F. For the Alternate B port cover, the margin of safety is:

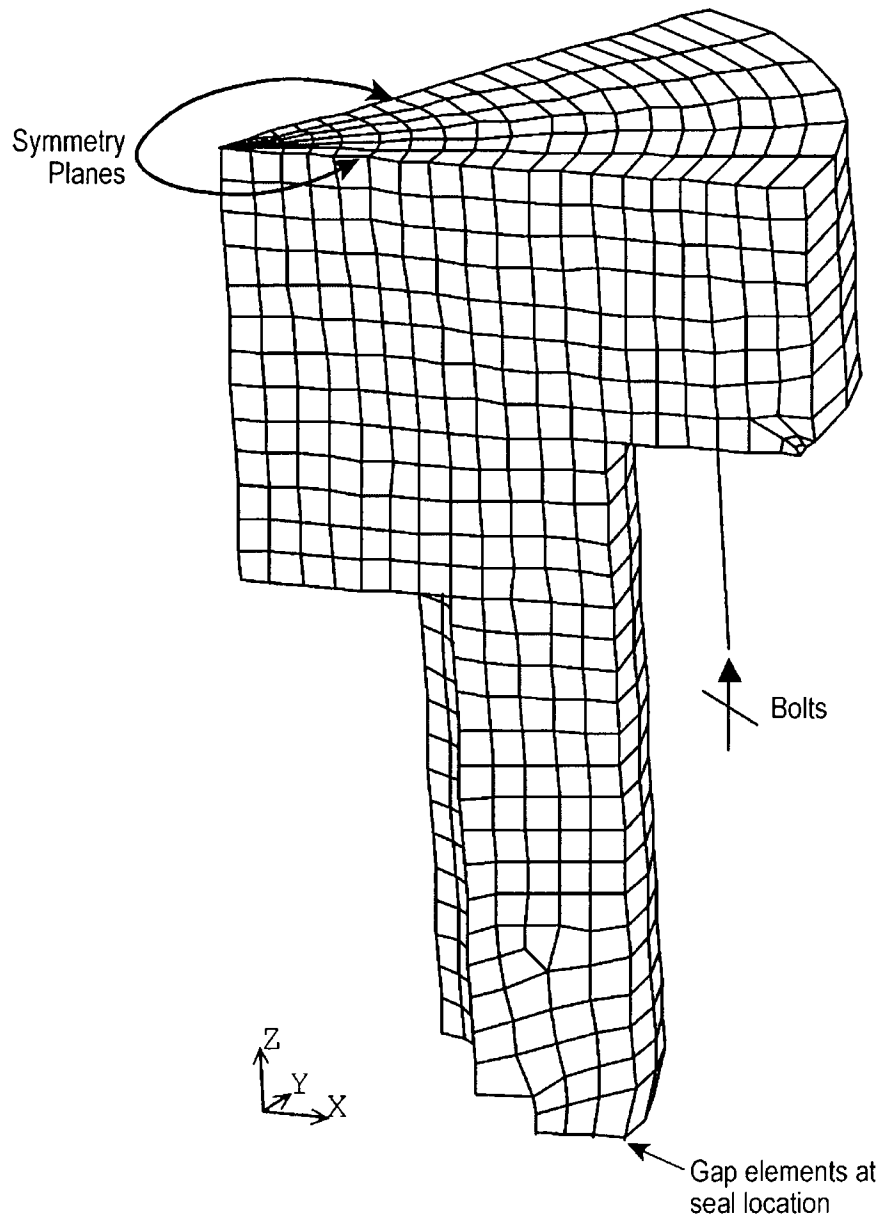
$$MS = \frac{2.4 \times S_m}{20.8} - 1 = +2.7$$

where:

$$S_m = 32.3 \text{ ksi @ } 250^\circ\text{F}$$

The controlling stress in the port cover has a significant margin for the pin puncture event. Therefore, the bolt preload and the Alternate B port cover will maintain the necessary load on the metal face seal to maintain containment.

Figure 2.10.15-1 Alternate B Port Cover Finite Element Model



2.10.16 Structural Evaluation of the NAC-LWT Cask Body with TPBARs in the PWR/BWR Rod Transport Canister

This section presents a structural evaluation of the NAC-LWT cask system for the shipment of up to 25 individual TPBARs in the PWR/BWR Rod Transport Canister, the PWR insert and the TPBAR basket under normal conditions of transport and hypothetical accident conditions. Section 2.10.14 presents the structural evaluation of the NAC-LWT cask system for two TPBAR content conditions: up to 300 production TPBARs loaded into an open (i.e., unsealed) consolidation canister; and up to 55 segmented TPBARs loaded into a welded closed waste container. Although the analysis provided in Section 2.10.14 uses a slightly lower contents weight than the TPBARs in the PWR/BWR Rod Transport Canister configuration, the applied contents load is comparable as conservative accelerations are used. As such, the evaluation of TPBARs in the PWR/BWR Rod Transport Canister uses the results of Section 2.10.14, appropriately scaled to account for any increase in total applied contents load.

2.10.16.1 Normal Conditions of Transport for Cask Body and TPBARs in the PWR/BWR Rod Transport Canister

This section provides the cask body structural evaluation for normal conditions of transport for the shipment of TPBARs in the PWR/BWR Rod Transport Canister, the PWR insert and the TPBAR basket. Section 2.10.14 provides the critical stress intensity results of the NAC-LWT cask system for two TPBAR content conditions: up to 300 production TPBARs loaded into an open (i.e., unsealed) consolidation canister; and up to 55 segmented TPBARs loaded into a welded closed waste container. The Section 2.10.14 analysis used a three-dimensional half-symmetry model of the LWT cask body constructed using ANSYS. A detailed description of the implemented finite element model can be found in Section 2.10.14.1.2. Both the pressure and component temperatures considered in Section 2.10.14 bound the TPBARs in the PWR/BWR Rod Transport Canister configuration.

For the side drop, the cask is loaded by both the contents weight and the weight of the cask body surrounding the cask cavity. The weight of the cask body surrounding the cavity is 34,400 lbs, which includes the lead for shielding, the inner and outer shells, as well as portions of the top and bottom forgings. The evaluation in Section 2.10.14 uses a cask contents weight of 1800 lbs, which is 101 lbs less than the TPBAR in the PWR/BWR Rod Transport Canister contents weight of 1901 lbs. The normal conditions evaluation of Section 2.10.14 uses a conservative inertial load of 25 g for the side drop, which is 0.7 g greater than the required inertial load of 24.3 g (Table 2.6.7-34). Section 2.10.14 provides the minimum margins of safety for each stress category for 1-foot drop conditions. For the analysis of the TPBARs in the PWR/BWR Rod

Transport Canister configuration, the stress-intensity results of critical sections, listed in Section 2.10.14, are scaled by the ratio of the contents weight and cask body weight surrounding the cavity, using the following scale factor.

$$SF_{sd} = \frac{W_{TPBAR / PWR} + W_{cavity \text{ cask body}}}{W_{TPBAR} + W_{cavity \text{ cask body}}} = \frac{1,901 + 34,400}{1,800 + 34,400} = 1.003$$

where:

SF_{sd} = side drop stress intensity scale factor

$W_{TPBAR/PWR}$ = the contents weight for the 25 TPBARs in the PWR/BWR Rod Transport Canister

W_{TPBAR} = the contents weight analyzed in Section 2.10.14.

$W_{cavity \text{ cask body}}$ = the weight of the cask body radially surrounding the cask cavity

The minimum margin of safety is +0.13, which occurs at section 2 for the condition of P_m stress for 1-foot side-drop condition. This section is located at the axial center of the cask outer shell. The minimum margins of safety for each stress category for 1-foot drop conditions are as follows.

Stress Category	Section	Drop Orientation	Stress Intensity, ksi	Stress Allowable, ksi	Margin of Safety
P_m	2	Side	28.66	32.3	+0.13
$P_m + P_b$	2	Side	32.97	48.45	+0.47
$P+Q$	18	Side	31.39	60.0	+0.91

2.10.16.2 Hypothetical Accident Conditions for Cask Body with TPABARs and the PWR/BWR Rod Transport Canister

This section provides the cask body structural evaluation for hypothetical accident conditions. The following sections discuss drop conditions and inner shell buckling.

2.10.16.2.1 Free Drop (30-Foot)

This section provides the cask body structural evaluation for the 30-foot drop accident conditions of transport for the shipment of TPBARs in the PWR/BWR Rod Transport Canister, the PWR insert and the TPBAR basket. Section 2.10.14 provides the critical stress intensity results of the NAC-LWT cask system for two TPBAR content conditions: up to 300 production TPBARs loaded into an open (i.e., unsealed) consolidation canister; and up to 55 segmented TPBARs loaded into a welded closed waste container. The Section 2.10.14 analysis used a three-dimensional half-symmetry model of the LWT cask body constructed using ANSYS. A detailed description of the implemented finite element model can be found in Section 2.10.14.1.2. Both

the pressure and component temperatures considered in Section 2.10.14 bound the TPBARs in the PWR/BWR Rod Transport Canister configuration.

Section 2.10.14.2.1 provides the results of the critical section stresses for the 30-foot drop accident conditions. As listed in Section 2.10.14.2.1, the minimum margins of safety resulted from the 30-foot side drop condition. The evaluation of Section 2.10.14 uses a cask contents weight of 1800 lbs, which is 101 lbs less than the TPBAR in the PWR/BWR Rod Transport Canister contents weight of 1901 lbs. The accident conditions evaluation of Section 2.10.14 uses a conservative inertial load of 60 g for side drop, which is 10.3 g greater than the required inertial load of 49.7 g (Table 2.6.7-34). As a result, the 30-foot drop evaluation of Section 2.10.14.2 uses a contents inertial load of 108,000 lb (1800 lbs \times 60 g). Assuming a conservative acceleration of 55 g for the side drop inertial load, the contents inertial load for the TPBARs in the PWR/BWR Rod Transport Canister is calculated as 104,555 lbs (1901 lbs \times 55 g). The total applied contents load for the critical stresses of Section 2.10.14.2.1 is greater than that for the TPBARs in the PWR/BWR Rod Transport Canister. Therefore, it is concluded that the NAC-LWT cask is structurally adequate for the shipment of TPBARs in the PWR/BWR Rod Transport Canister under the 30-foot drop accident conditions of transport.

2.10.16.2.2 Fire Accident

The pressure and component temperatures for the TPBARs in the PWR/BWR Rod Transport Canister for the fire accident conditions are bounded by the fire accident evaluation of the NAC-LWT cask body with TPBARs in a consolidation canister in Section 2.10.14.2.2. Therefore, based on the results of Section 2.10.14.2.2, presented in Table 2.10.14-27 and Table 2.10.14-28, the NAC-LWT cask is structurally adequate for the shipment of TPBARs in the PWR/BWR Rod Transport Canister under fire accident conditions.

2.10.16.3 Inner Shell Buckling

Section 2.10.6 presents a buckling evaluation of the cask inner shell per ASME Code Case N-284 for the design basis cask configuration. The evaluation presented in Section 2.10.6 bounds the TPBAR contents (up to 25 TPBARs in a rod holder in the PWR/BWR Rod Transport Canister) based on the following.

- The maximum weight of the TPBAR contents (up to 25 TPBARs in a rod holder) in the PWR/BWR Rod Transport Canister of 1901 lbs is enveloped by the weight of the design basis contents, which would reduce the compressive stresses in the cask shells due to less inertia loading for the drop conditions.
- The cask internal pressure for the TPBAR contents (up to 25 TPBARs in a rod holder in the PWR/BWR Rod Transport Canister) is significantly higher than the cask internal pressure for the design basis contents. The increase in the pressure would increase the

tensile stresses in the shell that result in stiffening of the inner shell and, consequently, in reducing the compressive stresses associated with buckling.

The interaction summary presented in Table 2.10.6-10, associated with the design basis weight and the design basis pressure, is bounding for the TPBAR content (up to 25 TPBARs in a rod holder in the PWR/BWR Rod Transport Canister) conditions. Therefore, it is concluded that the cask inner shell will not buckle with the TPBAR contents (up to 25 TPBARs in a rod holder in the PWR/BWR Rod Transport Canister) in the NAC-LWT cask.

2.10.16.4 NAC-LWT Cask Closure Lid and Bolts

The NAC-LWT cask closure lid is bolted to the cask body top forging with twelve 1-8 UNC bolts fabricated from SA-453, Grade 660 high-alloy steel. The threaded portion of the bolt engages the cask body a minimum of 1.875 inches. From Section 2.1.3.2.2, the torque on the cask lid bolts is 260 ± 20 ft-lb and the bolt preload is specified as 34,843 lbs. For the LWT cask configured to ship TPBARs in the PWR/BWR Rod Transport Canister, the maximum internal pressure of 600 psig is conservatively used in the closure lid evaluation. This pressure bounds the maximum pressure during the fire accident contained in Section 3.5.4.4. To ensure that the seal is not unloaded during accident conditions, the preload is calculated to account for the weight of the lid, internal weight of the cask contents, force resulting from internal pressure, force resulting from compression of the TFE O-ring, and force resulting from compression of the metallic O-ring. The load resulting from the weight of the LWT cask contents is:

$$F_2 = W_c a = 1,901 \times 60g = 114,060 \text{ lbs}$$

where:

$$W_c = 1,901 \text{ lbs (weight of TPBAR basket and contents for TPBARs in the PWR/BWR rod transport canister)}$$

$$a = 60 \text{ g (maximum accident acceleration)}$$

The load resulting from accident pressure (fire accident) is:

$$F_{ip} = P_{ip} A = 600 \times 171.36 = 102,816 \text{ lbs}$$

where:

$$P_{ip} = 600 \text{ psig (accident internal pressure)}$$

$$A = \frac{\pi}{4} \times 14.771^2 = 171.36 \text{ in}^2$$

The total required bolt preload force (12 bolts) is:

$$F_T = F_l + F_2 + F_r + F_{mr} + F_{ip}$$

$$= 56,460 + 114,060 + 2,474 + 79,470 + 102,816 = 355,280 \text{ lbs}$$

where:

$$F_{tr} = 2,474 \text{ lbs, TFE O-ring load (Section 2.1.3.2.2)}$$

$$F_{mr} = 79,470 \text{ lbs, Metallic O-ring load (Section 2.1.3.2.2)}$$

$$F_l = 56,460 \text{ lbs, Lid load (Section 2.1.3.2.2)}$$

The required bolt preload per bolt is:

$$F_{bolt} = \frac{F_T}{12} = \frac{355,280}{12} = 29,607 \text{ lbs} < 34,843 \text{ lbs (Section 2.1.3.2.2)}$$

Since the bolt preload presented in Section 2.1.3.2.2 of the NAC-LWT is bounding, no further analysis of the LWT lid bolts is required.

The preload applied to the cask lid bolts is due to the load applied to the lid. The load applied to the lid for the design basis weight and pressure for the PWR fuel bounds the load applied to the lid for the TPBARs in the PWR/BWR Rod Transport Canister contents. Therefore, the stresses in the cask lid due to the design basis weight and pressure also bound the stresses in the cask lid due to the TPBARs in the PWR/BWR Rod Transport Canister content weight and pressure.

2.10.16.5 Conclusion

Based on the evaluations presented in Sections 2.10.14.1 through 2.10.14.4, the NAC-LWT cask with TPBAR contents in the PWR/BWR Rod Transport Canister satisfies the requirements of 10 CFR 71 for the normal conditions of transport and for hypothetical accident conditions.